



Universidade do Minho
Escola de Ciências

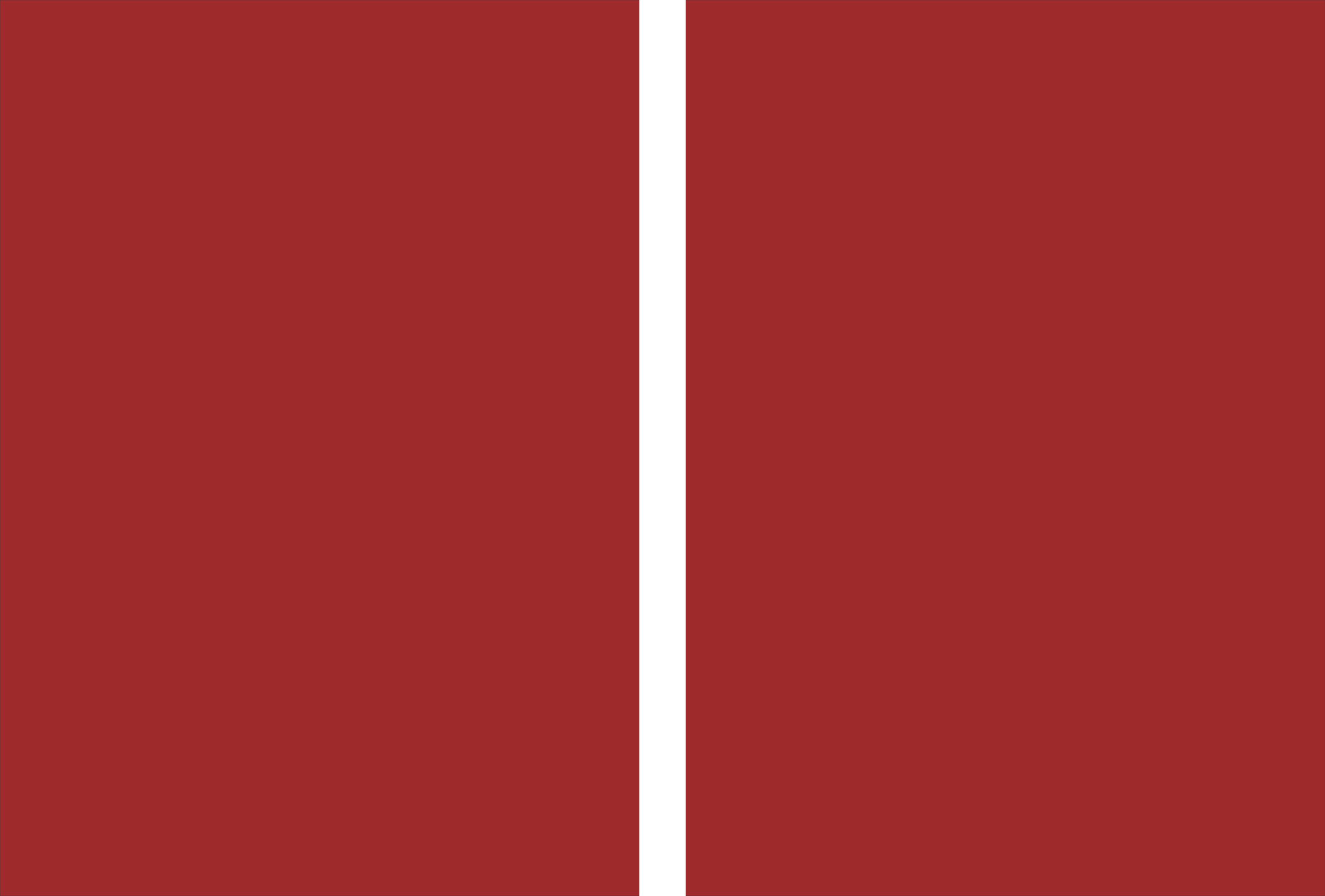
Joana Margarida Sá Pessoa da Graça Santos

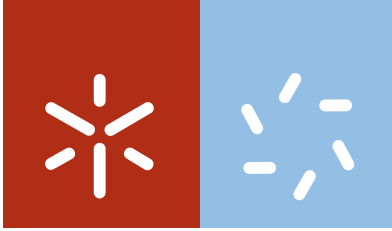
**Structural-functional studies of plasma
membrane carboxylate transporters in yeast**

Joana Margarida Sá Pessoa da Graça Santos
**Structural-functional studies of plasma
membrane carboxylate transporters in yeast**

UMinho | 2013

outubro de 2013





Universidade do Minho

Escola de Ciências

Joana Margarida Sá Pessoa da Graça Santos

**Structural-functional studies of plasma
membrane carboxylate transporters in yeast**

Tese de Doutoramento
Programa Doutoral em Biologia Molecular e Ambiental
Especialidade em Biotecnologia Molecular

Trabalho realizado sob a orientação da
Professora Doutora Margarida Casal
e da
Professora Doutora Sandra Paiva
e do
Professor Doutor George Diallinas

outubro de 2013

DECLARAÇÃO

Nome: Joana Margarida Sá Pessoa da Graça Santos

Endereço eletrónico: joanapessoa@bio.uminho.pt

Número do Bilhete de Identidade: 12121916

Título dissertação: Structural-functional studies of plasma membrane carboxylate transporters in yeast

Orientadores:

Professora Doutora Margarida Casal

Co – Orientadores:

Professora Doutora Sandra Paiva e Professor Doutor George Diallinas

Ano de conclusão: 2013

Designação Ramo de Conhecimento do Doutoramento:

Doutoramento em Biologia Molecular e Ambiental, Especialidade em Biotecnologia Molecular

É AUTORIZADA A REPRODUÇÃO INTEGRAL DESTA TESE APENAS PARA EFEITOS DE INVESTIGAÇÃO, MEDIANTE DECLARAÇÃO ESCRITA DO INTERESSADO, QUE A TAL SE COMPROMETE

Universidade do Minho, 29 de Outubro de 2013

Assinatura: _____

Aos meus...

Cada um é seus caminhos.

Onde Sancho vê moinhos

D. Quixote vê gigantes.

António Gedeão

The work presented in this dissertation was done in the Centre of Molecular and Environmental Biology (CBMA), Department of Biology, University of Minho and in the *Aspergillus* Genetics & Molecular Biology Laboratory in the Faculty of Biology, University of Athens, Athens, Greece. The financial support was given by Fundação para a Ciência e Tecnologia by means of a grant, SFRH/BD/61530/2009, funded by Fundação para a Ciência e a Tecnologia (FCT) and co-funded by Fundo Social Europeu (FSE) and Programa Operacional Potencial Humano (POPH). Financial support for part of the work was received by project PEst-C/BIA/UI4050/2011, supported by FEDER (Fundo Europeu de Desenvolvimento Regional), through POFC (Programa Operacional Factores de Competitividade) - COMPETE, and by Portuguese National Funds from FCT.

Acknowledgements/Agradecimentos

Para ser grande, sê inteiro:

nada teu exagera ou exclui.

Sê todo em cada coisa.

Põe quanto és no mínimo que fazes.

Fernando Pessoa

Somos para os outros e com os outros e somos inteiros naquilo que vamos partilhando. Muito foi partilhado nestes quatro anos e muitos bocadinhos deste e daquele ficaram gravados neste percurso que não é só meu e por isso agradeço.

Em primeiro lugar, gostaria de agradecer à Prof. Margarida Casal por me ter acolhido “debaixo da sua asa” científica, pelos ensinamentos, pela orientação, pelo encorajamento e o espírito e ideias científicas passadas ao longo destes tão rápidos quatro anos. À Prof. Sandra Paiva pelo encorajamento e pelas longas conversas no gabinete, científicas ou de outro tipo. To Prof. George Diallinas for showing me the Greek passion in the form of a love for science in whatever subjects (mainly transporters). I’ve grown immensely as a scientist thanks to my three supervisors.

I am also very grateful to Professor Peter Henderson and his team for welcoming me so well in his laboratory in Leeds and for showing the beauty of the Yorkshire Dales.

To my lab friends in Greece with whom things would not be the same. When I think of Athens, of course I think about the amazing food and culture, but it’s my wonderful friends that give me will to return to Athens even though things are not always easy and you have to struggle just to be able to go to work. (Minoas and Aimilia, we’re not done yet with our weekends out)

A todo o Departamento de Biologia, especialmente o pessoal técnico, por tão bem me terem recebido sempre e pela partilha de experiências. Aos que estão e aos que foram passando pelos corredores do Departamento e foram parte dos ensinamentos que levo comigo o meu muito obrigado, principalmente à Isabel João por me ter iniciado nas artes das leveduras.

Não poderia deixar de agradecer aos meus colegas e amigos do LGM e do LBM que são e foram parte integrante deste percurso, sem os quais o laboratório era muito menos divertido e parte do trabalho não seria possível. A eles agradeço por partilharem os dias

bons e os menos bons, aqueles dias em que entro logo a reclamar e usam o meu nome para por medo nos caloirinhos. By the way, estou de volta, temos de fazer limpeza ao laboratório!

Aos meus amigos aqui e acolá que fazem parte de mim e tantas vezes tiveram as ausências típicas de quem passou a viver longe, especialmente à Pri que deu aquele empurrãozinho de que tanto precisava para arrancar do meu estancado lugar.

Às minhas Bios porque parece que o tempo não passa por nós e sejam três ou seis meses parece que foi ontem que estava convosco em mais um jantar, ou a iniciar-me nas lides académicas. São parte integrante do meu sorriso e do meu orgulho e um pedacinho muito importante do meu coração. Claro que não podia deixar de agradecer assim de uma forma especial à minha Mary que foi parte integrante desta minha vida em Braga e com quem tanto partilhei...

Por último mas não em último tenho de agradecer à minha família que é simplesmente espectacular, que tanto me aturam e que tanto me dão, têm um papel fundamental na minha vida. O núcleo duro da família: avós Mariazinha e Rui, a minha mamã adorada e os meus manos Diana e João, vocês complementam-me e dão-me a sanidade de um abraço que sabe a casa e não se encontra igual em mais lado nenhum!

Passou mais uma etapa e comigo vão todos os que nela se cruzaram, antes e durante, e fizeram destes quatro anos o realizar de um sonho...

Resumo

Os ácidos carboxílicos são um grupo heterogéneo de compostos de grande relevância bioquímica uma vez que podem ser usados como única fonte de carbono e energia por vários seres vivos ou constituir sub-produtos do metabolismo celular. O trabalho descrito na presente tese pretendeu aprofundar o conhecimento sobre a estrutura e a funcionalidade de proteínas membranares transportadoras de ácidos monocarboxílicos em células de microrganismos.

Numa primeira abordagem realizaram-se estudos moleculares sobre a permease de lactato/piruvato de *Saccharomyces cerevisiae* Jen1 e seus homólogos. Foram analisadas mutações em resíduos de aminoácidos potencialmente envolvidos na definição da especificidade para o substrato (ácidos mono- ou dicarboxílicos), localizados nos domínios transmembranares II, V e XI. Este estudo revelou que os aminoácidos F270 (TMS-V) e Q498 (TMS-XI) são cruciais para a especificidade deste transportador e determinam a distinção entre ácidos mono- e dicarboxílicos. Verificou-se igualmente que os resíduos N501 (TMS-XI) e R188 (TMS-II) são essenciais para estrutura da proteína Jen1, e determinam a sua funcionalidade. Foi construído um modelo da estrutura 3D desta proteína usando as similaridades estruturais com a permease GlpT. Neste modelo os aminoácidos críticos para a função encontravam-se alinhados num eixo paralelo ao poro da proteína validando os resultados obtidos *in vivo* com os respetivos mutantes. A modelação da proteína com lactato revelou uma possível rota de translocação do ácido, que inclui resíduos polares identificados experimentalmente como funcionalmente importantes (R188, H383, N501 and Q498).

Abordou-se ainda o papel biotecnológico das permeases de ácidos carboxílicos de *S. cerevisiae* (Jen1 e Ady2) na bioprodução de ácido láctico. Para tal, a enzima L-lactato desidrogenase (L-LDH) de *Lactobacillus casei* foi expressa em células da levedura *S. cerevisiae* W303-1A, incluindo as estirpes mutantes *jen1* Δ , *ady2* Δ e *jen1* Δ *ady2* Δ . Estes estudos comprovaram o papel destas permeases no exporte de ácido láctico. Os resultados obtidos permitiram ainda identificar o papel da permease Ady2 no transporte de lactato. No âmbito desta tese estudou-se ainda o homólogo da proteína Ady2 na bactéria *Escherichia coli*, codificado pelo gene *yaaH*, ambos membros da família de transportadores AceTr. Os resultados demonstraram que o transportador YaaH (SatP) é específico para succinato (um ácido dicarboxílico) e para acetato (um ácido monocarboxílico) com as seguintes constantes de afinidade a pH 6.0: 1.24 ± 0.13 mM

para o ácido acético e 1.18 ± 0.10 mM para o ácido succínico. O mutante $\Delta yaaH$ apresenta menor capacidade de transporte de ácido acético e succínico em células crescidas em glucose. Para além disso, o transportador SatP, juntamente com o transportador anteriormente descrito ActP, afetaram a utilização de ácido acético como única fonte de carbono e energia. Em SatP os aminoácidos L131 e A164 revelaram-se fundamentais para a capacidade de transportar ácido láctico.

Os estudos foram ainda estendidos ao transportador AcpA do fungo filamentosso *Aspergillus nidulans*, também um membro da família AceTr. O seu perfil de especificidade foi analisado revelando que esta permease para além de mediar o transporte de acetato, medeia o transporte de propionato bem como de outros ácidos monocarboxílicos de cadeia curta (benzoato, formato e butirato). Observou-se que esta permease é expressa na germinação dos conidiósporos, atingindo um máximo de expressão aquando do aparecimento do tubo germinativo, mantendo-se a um nível basal no aparecimento do micélio. Para além disso, demonstrou-se que apesar de a amónia aumentar moderadamente o transporte de acetato mediado por AcpA, esta proteína não está envolvida no exporste de amónia.

Abstract

Carboxylic acids comprise a heterogeneous group of compounds that are important in overall cell functionality. They can be both carbon sources and waste products from cell metabolism. This thesis aimed at deepening the current knowledge on microbial monocarboxylate permeases through structural-functional approaches.

A first approach was to investigate molecular determinants in Jen1p, a *Saccharomyces cerevisiae* lactate/proton symporter and its homologues. We have rationally designed and analysed several mutations in TMS-II, TMS-V and TMS-XI, predicted to be involved in substrate specificity and function. From the residues analysed we verified that F270 (TMS-V) and Q498 (TMS-XI) are critical specificity determinants for the distinction of mono- from dicarboxylates, while R188 (TMS-II) and N501 (TMS-XI) were essential residues for function. Using a model based on Jen1p overall structural similarity with the GlpT permease, we showed that all polar residues critical for function in TMS-VII and TMS-XI are aligned in an imaginary axis that lies parallel to the protein pore. Furthermore, substrate docking studies revealed a potential substrate translocation trajectory consisting mostly of the polar residues genetically identified as important for function (R188, H383, N501 and Q498).

Aiming at obtaining a lactic acid producer strain of *S. cerevisiae* the *l-LDH* gene from *Lactobacillus casei* was expressed in *S. cerevisiae* W303-1A and in the isogenic mutants *jen1Δ*, *ady2Δ* and *jen1Δ ady2Δ*. The monocarboxylate permeases Jen1 and Ady2 were shown to be modulators of lactic acid production. In this work, an additional role in lactate uptake was demonstrated for Ady2.

The Ady2 *Escherichia coli* homologue SatP (YaaH) from the AceTr family of acetate transporters was also characterized in the scope of this work. This transporter is highly specific for acetic acid (a monocarboxylate) and for succinic acid (a dicarboxylate), with affinity constants at pH 6.0 of 1.24 ± 0.13 mM for acetic acid and 1.18 ± 0.10 mM for succinic acid. In glucose-grown cells the $\Delta yaaH$ mutant is compromised for the uptake of both labelled acetic and succinic acids. SatP, together with ActP, described previously as an acetate transporter, affect the use of acetic acid as sole carbon and energy source. We have also demonstrated the critical role of SatP amino acid residues L131 and A164 on the enhanced ability to transport lactate.

Additionally, AcpA from the filamentous fungus *Aspergillus nidulans*, also from the AceTr family of transporters, was shown to mediate the uptake of propionate, as well as,

of other short-chain monocarboxylic acids (benzoate, formate and butyrate). We have shown that the expression of this permease is activated upon conidiospore germination, reaching its maximum at the time of germ tube emergence, and is present at basal levels in germlings and young mycelium. Furthermore, we showed that although ammonia increases moderately AcpA-mediated acetate uptake, AcpA is not involved in ammonia export.

Table of contents

Acknowledgements / Agradecimientos.....	v
Resumo.....	vii
Abstract.....	ix
Table of contents.....	xi
List of Figures.....	xiii
List of Tables.....	xv
List of Common Abbreviations.....	xvii

Chapter I - Introduction

1. Transport across the plasma membrane.....	3
2. Classifying transporters – the Transporter Classification Database	4
3. Carboxylic acids	6
4. Carboxylic acid permeases in the yeast <i>Saccharomyces cerevisiae</i>	7
4.1 The lactate/pyruvate permease Jen1 from <i>S. cerevisiae</i>	9
4.2 Structures within the MFS superfamily – a common fold	12
4.3 Homologues of Jen1 in fungi.....	15
4.4 The acetate permease Ady2 from <i>S. cerevisiae</i>	17
4.5 The AceTr family of transporters.....	18
5. Carboxylic acid permeases in bacteria	20
5.1 <i>Escherichia coli</i>	24
5.1.1 Monocarboxylate transporters.....	24
5.1.2 Di- and tri-carboxylate transporters.....	34
5.2 A gram-positive bacterium: <i>Corynebacterium glutamicum</i>	41
5.2.1 Monocarboxylate uptake	41
5.2.2 Dicarboxylate uptake and export	43
5.2.3 Citrate uptake – CitH and TctABC.....	45
5.3 An aerobic bacterium: <i>Bacillus subtilis</i>	46
5.3.1 Monocarboxylate uptake	46
5.3.2 Dicarboxylate uptake	47
5.3.3 Citrate transporters	48
5.4 Nonsulfur purple photosynthetic bacteria – <i>Rhodobacter capsulatus</i>	50
5.4.1 Acetate and other monocarboxylates.....	50
5.4.2 Dicarboxylate uptake	51
5.5 Lactic acid and Acetic acid bacteria.....	52
5.5.1 Acetic acid bacteria	52
5.5.2 Lactic acid bacteria	53
Outline of the present thesis	57
References.....	59

Chapter II - A substrate translocation trajectory in a cytoplasm-facing topological model of the monocarboxylate/H⁺ symporter Jen1p

Abstract	75
Introduction	76
Experimental Procedures.....	78
Results.....	81
Discussion	94
References.....	96

Chapter III - The monocarboxylate transporters Jen1 and Ady2 as modulators of lactic acid production in *Saccharomyces cerevisiae*

Abstract	101
Introduction	102
Experimental Procedures.....	103
Results and Discussion.....	105
References.....	110
Additional data not published.....	113

Chapter IV - SatP (YaaH), a succinate-acetate transporter protein in *Escherichia coli*

Abstract	117
Introduction	118
Experimental Procedures.....	120
Results.....	126
Discussion	141
References.....	145

Chapter V - The fungal Ady2 homologue AcpA from *Aspergillus nidulans*

Abstract	153
Introduction	154
Experimental Procedures.....	158
Results and Discussion.....	160
Conclusions	173
Future perspectives	175
References.....	178

Chapter VI - Final remarks and Future Perspectives

Final Remarks	185
Future perspectives	189
References.....	191

List of Figures

Chapter I

Figure 1 – Various mechanisms for the transport of substrates.....	4
Figure 2 - The main metabolic pathways of oxidative and gluconeogenic metabolism in <i>S. cerevisiae</i>	8
Figure 3 – Model for the regulation of Jen1 endocytosis.	10
Figure 4 - Multiple sequence alignment of Jen1p homologues.....	11
Figure 5 - Model of Jen1p topology.....	12
Figure 6 – The MFS fold.	13
Figure 7 – The inverted topology repeat in LacY.	14
Figure 8 – Distinct conformational states of the MFS structures depicting the alternating access mechanism.	15
Figure 9 - Phylogenetic tree of ScJen1p homologues.	16
Figure 10 – Alignment of the protein sequences of <i>Y. lipolytica</i> Gpr1p and the <i>S. cerevisiae</i> proteins Ady2 and Fun34.....	19
Figure 11 – Monocarboxylate transporters in <i>E. coli</i>	24
Figure 12 – Topology of vSGLT.	26
Figure 13 – Transport cycle based on an alternating-access-type mechanism	27
Figure 14 – Topology diagram of FocA.	31
Figure 15 – Structure of the formate transporter FocA.....	31
Figure 16 – Representation of the concerted movement of the N-terminal helices of protomers A and B in FocA.....	33
Figure 17 – Di- and tricarboxylates transporters in <i>E. coli</i>	34
Figure 18 – Carboxylate transporters in <i>C. glutamicum</i>	41
Figure 19 – Carboxylate transporters in <i>B. subtilis</i>	46

Chapter II

Figure 1 – Multiple sequence alignment of TMS-II, TMS-V and TMS-XI of Jen1 homologues	82
Figure 2 – Relative % of Jen1p-mediated [¹⁴ C]-lactic acid transport in mutants.	83
Figure 3 – Epifluorescent microscopy of GFP-tagged version of Jen1p in a control strain and mutants.....	84
Figure 4 – Growth test of control and mutant strains.	86
Figure 5 – Overall structure of the Jen-1 model.	90
Figure 6 – Illustration of the F270-S271 residue pair location.	91
Figure 7 – The stepwise translocation pathway of lactate across the Jen1p pore.....	92
Figure 8 – The translocation pathway followed by the substrate along the pore of Jen1p transporter.	93

Chapter III

Figure 1 – Growth profile and glucose, lactic acid and ethanol concentration in the medium, for the strains <i>S. cerevisiae</i> W303-1A-LDH, <i>jen1Δ</i> -LDH, <i>ady2Δ</i> -LDH and <i>jen1Δ ady2Δ</i> -LDH	106
Figure 2 – Eadie-Hofstee plots of the initial uptake rates of labeled lactic acid as a function of the acid concentration, at pH 5.0, in <i>S. cerevisiae</i> <i>jen1Δ ady2Δ</i> -p416-GPD and <i>jen1Δ ady2Δ</i> -ADY2.	107
Figure 3 – Eadie-Hofstee plots of the initial uptake rates of labeled acetic acid, pH 6.0, as a function of its concentration, in <i>S. cerevisiae</i> <i>jen1Δ ady2Δ</i> -ADY2 cells.	108
Figure 4 – Effect of Jen1 and Ady2 constitutive expression on lactic acid production and on glucose consumption over time in <i>S. cerevisiae</i> strains expressing constitutively LDH.....	109

Figure 5 – Specificity profile of Ady2.	114
--	-----

Chapter IV

Figure 1 – The functional role of <i>yaaH</i> and <i>actP</i> genes as acetate transporters in <i>E. coli</i>	127
Figure 2 – Energetics of the YaaH transporter.	128
Figure 3 – Acetic acid kinetics of the YaaH transporter.	129
Figure 4 – Acetate uptake profiles of cells grown on acetic acid.	130
Figure 5 – The physiological role of YaaH and ActP on acetate assimilation.	132
Figure 6 – Acetate uptake profiles of cells grown on glucose.	133
Figure 7 – Distinct physiological roles of the two <i>E. coli</i> acetate transporters.	135
Figure 8 – Substrate specificity of the YaaH transporter.	137
Figure 9 – Succinic acid kinetics of the YaaH transporter.	138
Figure 10 – Site-directed mutagenesis of the <i>yaaH</i> gene.	140

Chapter V

Figure 1 – <i>A. nidulans</i> life cycle.	155
Figure 2 – Central carbon metabolism of <i>A. nidulans</i>	156
Figure 3 – Evaluation of the uptake of labelled acetate (30 μ M final concentration) in <i>A. nidulans</i> <i>acpA</i> and <i>acpA</i> Δ strains.	160
Figure 4 – Relative percentage uptake of labelled acetate in <i>A. nidulans</i> spores grown in different conditions.	161
Figure 5 – Evaluation of the uptake of labelled acetate in <i>A. nidulans</i> <i>acpA</i> ⁺ and <i>acpA</i> Δ upon addition of acetate.	162
Figure 6 – Initial uptake rates of [¹⁴ C]-acetic acid as a function of the acid concentration in <i>A. nidulans</i> <i>acpA</i> and <i>acpA</i> Δ cells.	163
Figure 7 - Evaluation of the uptake of labelled acetate in <i>A. nidulans</i> <i>acpA</i> ⁺ and <i>acpA</i> Δ grown at the pH values indicated.	164
Figure 8 – Evaluation of the uptake of labelled acetate in both <i>A. nidulans</i> <i>acpA</i> ⁺ and <i>acpA</i> Δ strains.	165
Figure 9 – The effect of acetate as a carbon source.	166
Figure 10 – Growth test of <i>acpA</i> ⁺ and <i>acpA</i> Δ in minimal media supplemented with several mono- and dicarboxylic acids as carbon sources.	167
Figure 11 - Relative transport percentage of labelled acetate in the presence of unlabelled inhibitors 1000-fold concentrated in <i>A. nidulans</i> <i>acpA</i> ⁺	168
Figure 12 – Eadie-Hofstee plots of the initial uptake rates of [1- ¹⁴ C]-acetic acid, pH 6.0, in the absence and in the presence of non-labelled propionic acid 1 and 5 mM.	169
Figure 13 – Relative transport of labelled acetate in the presence of unlabelled ammonium tartrate.	170
Figure 14 - Evaluation of the uptake of labelled acetate in <i>A. nidulans</i> <i>acpA</i> after pre-loading with ammonium tartrate (NH ₄) or acetate.	171
Figure 15 – Growth test of <i>acpA</i> and <i>acpA</i> Δ on methyl-ammonium hydrochloride.	172
Figure 16 – Efflux assay of labelled methyl ammonium (20 μ M).	172
Figure 17 – Molecular Phylogenetic analysis by Maximum Likelihood method of the AceTr family.	176
Figure 18 – Multiple sequence alignment of AceTr family members of characterized function.	178

List of Tables

Chapter I

Table 1 – Carboxylic acids and representation of their structure.	7
Table 2 - MFS proteins of known crystallographic structure.	12
Table 3 – Overview of the characterized bacterial carboxylate transporters.	21

Chapter II

Table 1 – Sequence of the forward primers used in the <i>Jen1</i> mutagenesis.	79
Table 2 – Relative capacity (%) of ¹⁴ C-lactic acid uptake in the presence of non-labelled carboxylic acids.	87
Table 3 – Kinetic parameters of ¹⁴ C-lactic acid transport (maximum velocity, V_{max} , and affinity constant, K_m) for some mutants, compared to the wild-type protein.	88
Table 4 – Inhibition constant (K_i) of ¹⁴ C-lactic acid uptake for succinic and malic acids of the mutants able to grow in dicarboxylates	89

Chapter III

Table 1 – <i>S. cerevisiae</i> strains used in this study.	103
---	-----

Chapter IV

Table 1 – List of strains used in this work.	121
Table 2 – List of plasmids used in this work.	121
Table 3 – List of oligos used in this work.	122

Chapter V

Table 1 – K_i values (mM) of AcpA for benzoate, butyrate, formate and propionate.	169
--	-----

List of Common Abbreviations

AMP – Adenosine monophosphate	min – Minute
AMS – Membrane-impermeable alkylating agent	MM – Minimal media
ATP – Adenosine triphosphate	mRNA – Messenger ribonucleic acid
BLAST – Basic Local Alignment Research Tool	NADH – Nicotinamide adenine dinucleotide
bp – Base pairs	NCBI – National Center for Biotechnology Information
CCCP – Carbonyl cyanide m-chlorophenyl hydrazone	°C – Degrees Celsius
Ci – Curie	OD – Optical density
Clustal – Cluster analysis of pairwise alignments	PCR – Polymerase chain reaction
CM – Complete media	PDB – Protein Database
C _T – Threshold cycle	Pi – Inorganic phosphate
DNA – Deoxyribonucleic acid	p <i>K</i> _a – Acid dissociation constant
Dpm – Disintegrations per minute	RMS – Root-mean-square
dry wt – Dry weight	RNA – Ribonucleic acid
EC – Enzyme commission	rpm – Revolutions per minute
FLIM – Fluorescence-lifetime imaging microscopy	RT-PCR – Reverse transcription polymerase chain reaction
FRET – Förster resonance energy transfer	s – second
g – Gram	SD – Standard deviation
<i>g</i> – Gravity acceleration	TC – Transporter classification system
GFP – Green fluorescence protein	TCA – Tricarboxylic acid
h – Hour	TCDB – Transporter Classification Database
HPLC – High performance liquid chromatography	TM – Transmembrane domain
IUBMB – International Union of Biochemistry and Molecular Biology	TMHMM – Tied Mixture Hidden Markov Model
K _{0.5} – Apparent substrate affinity	TMS – Transmembrane segment
K _i – Inhibition constant	v; vol. – Volume
K _m – Michaelis Menten constant	VIC – Voltage-gated Ion Channel
L – Litre	V _{max} – Maximum velocity
M – Molar	w – Weight
MD – Molecular dynamics	WT – Wild type
MFS – Major Facilitator Superfamily	YNB – Yeast Nitrogen Base

Families of Transporters

2-HCT – 2-Hydroxycarboxylate Transporter

AAEx – Aspartate:Alanine Exchanger

ABC – ATB-binding cassette superfamily

AceTr – Acetate Uptake Transporter

CitMHS – Citrate-Mg²⁺:H⁺ (CitM) Citrate-Ca²⁺:H⁺ (CitH) Symporter

DAACS – Dicarboxylate/Amino Acid:Cation (Na⁺ or H⁺) Symporter

DASS – Divalent Anion:Na⁺ Symporter

Dcu – C₄-Dicarboxylate Uptake

DcuC – C₄-dicarboxylate Uptake C

FNT – Formate-Nitrite Transporter

LctP – Lactate Permease

MCT – Monocarboxylate transporter

MCT – Monocarboxylate Transporter

MFS – Major Facilitator Superfamily

NhaC – NhaC Na⁺:H⁺ Antiporter

SSS – Solute:Sodium Symporter

SulP – Sulfate Permease

TRAP-T – Tripartite ATP-independent Periplasmic Transporter

TTT – Tripartite Tricarboxylate Transporter

Amino Acids

A	Ala	Alanine	M	Met	Methionine
C	Cys	Cysteine	N	Asn	Asparagine
D	Asp	Aspartic acid	P	Pro	Proline
E	Glu	Glutamic acid	Q	Gln	Glutamine
F	Phe	Phenylalanine	R	Arg	Arginine
G	Gly	Glycine	S	Ser	Serine
H	His	Histidine	T	Thr	Threonine
I	Ile	Isoleucine	V	Val	Valine
K	Lys	Lysine	W	Trp	Tryptophan
L	Leu	Leucine	Y	Tyr	Tyrosine

Chapter I

General Introduction

CHAPTER 1

GENERAL INTRODUCTION

1. Transport across the plasma membrane

Biological membranes are the barriers that keep a cell isolated from the outside. The maintenance of intracellular equilibrium depends on the transport of molecules across the membrane. Transport systems are crucial for cells allowing nutrient uptake, regulation of metabolites and excretion of toxic compounds playing a role in metabolism, sensing and communication (Saier, 2000).

Some molecules are believed to be able to cross the hydrophobic phospholipid bilayer by simple or passive diffusion. In this process small neutral molecules such as O_2 , NH_3 , CO_2 or ethanol, are translocated across the membrane down their electrochemical gradient. Simple diffusion follows Fick's law where the velocity of translocation depends on the permeability coefficient of the solute, the surface area of the membrane and the concentration difference of the solute across the two sides of the membrane (reviewed in Henderson, 2012). Mediated transport may occur by facilitated diffusion through carriers (facilitators) or channels or by primary or secondary active transport (reviewed in Saier, 2000). Facilitated diffusion is the translocation of a molecule mediated by a transport protein down its electrochemical gradient. This process is not coupled to metabolic energy and follows Michaelis-Menten equation kinetics (reviewed in Saier, 2000; Henderson, 2012). Channels or facilitators serve as ion-conducting pores, gated or not, moving ions, hydrophilic or hydrophobic molecules (with the appropriate residues lining the conducting pore) working at very fast rates (Saier, 2000; Henderson, 2012). Facilitators or carriers have lower transport rates than channels and have stereospecific substrate specificities (Saier, 2000). Furthermore carriers are usually monomeric while most channels are oligomeric (Saier, 2000). Active transport is the translocation of molecules against their electrochemical concentration requiring metabolic energy (Henderson, 2012). According to the type of energy supplied, active transporters can be divided into primary or secondary active transporters. In primary active transporters there

is a primary source of energy such as respiration, photosynthesis or ATP hydrolysis, while secondary active transporters use the electrochemical gradient to drive transport, either the proton gradient or an ion gradient (Na^+ in most cases) (Henderson, 2012). Secondary active transporters can be further divided according to the movement of substrates being considered as symporters, if both substrates (or substrate and ion) move in the same direction, or antiporters, if the movement is in opposite directions (Saier, 2000). The various mechanisms for the transport of substrates are summarized in Figure 1. Membrane transport can also follow some atypical routes with channels allowing high-affinity uptake, with transporters displaying multiphasic kinetics and transporters being able to function as channels (reviewed in Conde *et al.*, 2010).

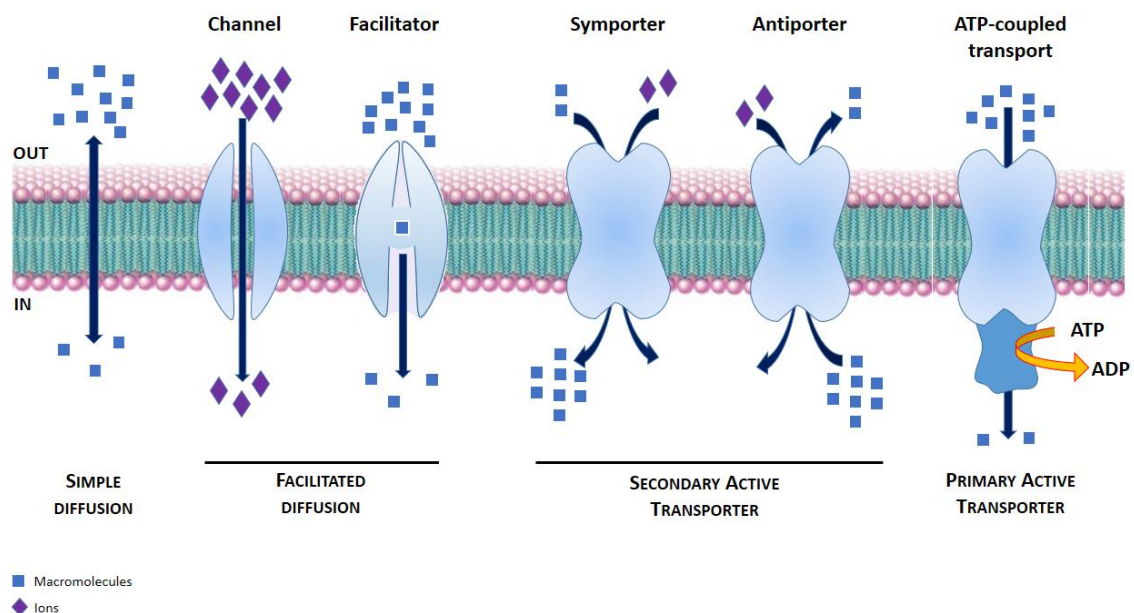


Figure 1 – Schematic diagram of the various mechanisms for the transport of substrates. Substrates are depicted by rhombus or squares representing concentration in either side of the membrane. IN – intracellular space; OUT – extracellular space.

2. Classifying transporters – the Transporter Classification Database

The immense data available on the biological important transporter proteins, allied with the constant progress in the availability of genomic information and computational biology, has led to the development of the Transporter Classification Database (TCDB, www.tcdb.org). This database gives a structural, functional and evolutionary view on

transporter proteins on a free accessible web resource (Saier *et al.*, 2006). The database compiles information for about 5600 protein sequences classified into more than 600 families based on the Transporter Classification (TC) system, approved by the International Union of Biochemistry and Molecular Biology (IUBMB) (www.tcdb.org, data from September 2013).

The TC system was adopted based on the principle that molecular phylogeny is a guide for protein structure and mechanism, providing also some information on the process catalysed and the substrate (function). Transporters are classified in five components with a number V.W.X.Y.Z, whereby V represents the transporter class (channel, primary active transporter and so on) and W the subclass (energy source), X corresponds to the family (or superfamily) and Y to the subfamily while Z corresponds to the substrate. Whenever two transporter proteins share the same TC classification they are likely to have the same mechanism of solute transport, whether being orthologs or paralogs, with mechanistic variations appearing when there is high sequence divergence (Saier, 2000; Saier *et al.*, 2009).

There are 9 classes of transporters defined in TCDB (Busch and Saier, 2004; Saier *et al.*, 2009). Class 1 consists of channel-type facilitators that catalyse facilitated diffusion through a pore or channel and that may exhibit some specificity for a class of molecules. Class 2 includes electrochemical potential-driven transporters that usually are stereospecific. Class 3 transporters are primary active transporters which can be driven by P-P-bond hydrolysis, decarboxylation, methyl transfer, oxidoreduction or light absorption. Class 4 is composed of group translocators that chemically alter the substrate during transport. Class 5 is the one of transmembrane electron carriers that catalyse electron flow across the membrane influencing cell energetics. Auxiliary transport proteins form class 8 that groups proteins that function or are coupled to known transport proteins. Transport proteins with insufficient information for classification are grouped in class 9 including proteins for which the transport mechanism is unknown or putative transporters. Class 6 and 7 are not assigned being reserved for the expansion of the TC system (Busch and Saier, 2004; Saier *et al.*, 2009).

To assign a family homology criteria must be satisfied, namely the presence of sequence similarity in comparable portions of the protein. Families provide a phylogenetic classification while classes distinguish the functionality of transporters, being the TC classification a functional/phylogenetic system (Saier, 2000; Busch and Saier, 2004). Some families are actually superfamilies with the Voltage-gated Ion Channel (VIC), the

Major Facilitator (MFS) and the ATP-binding cassette (ABC) superfamilies being the largest and most diverse (Busch and Saier, 2004).

This phylogenetic classification allows to infer also on three-dimensional structural features since two homologous proteins in terms of mechanism are expected to have similar structures (Busch and Saier, 2004). Furthermore the phylogenetic classification of the TC system is also correlated to the organisms' evolutionary history being linked to their overall physiology, habitat and lifestyle (Ren and Paulsen, 2005).

3. Carboxylic acids

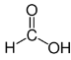
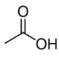
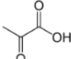
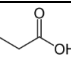
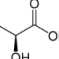
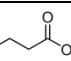
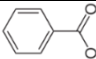
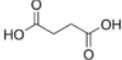
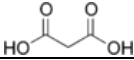
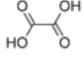
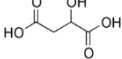
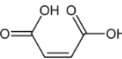
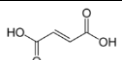
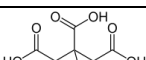
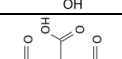
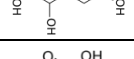
Carboxylic acids are organic acids characterized by the presence of a carboxyl group with the general formula R-COOH, with R being the monovalent functional group. Acids with more than one carboxyl group are called dicarboxylics (2 -COOH), tricarboxylics (3 -COOH) and so forth. When a carboxyl group is deprotonated its conjugate base is a carboxylate anion. Examples of carboxylic acids are represented in table 1 with their respective structure.

Carboxylic acids are weak acids that only partially dissociate into protons and carboxylates in neutral solutions. The degree of dissociation depends on the acid pK_a and on the pH of the medium. At low pH carboxylic acids are mostly in the undissociated form (R-COOH), which is lipid soluble, being able to cross the membrane by simple diffusion (Salmond *et al.*, 1984; Piper *et al.*, 2001). These acids are usually used as food preservatives because once inside the cell they dissociate due to the near neutral intracellular pH, generating intracellular acidification and anion accumulation (Salmond *et al.*, 1984; Russell, 1992). The dissociation of carboxylic acids can also lead to severe oxidative stress by free radical production (Piper *et al.*, 2001). To cross a biological membrane the dissociated acid requires a plasma membrane transporter protein (Piper *et al.*, 2001).

Carboxylic acids have always been present in industry as precursors for many applications, being used as food preservatives, in soaps, in pharmaceuticals and in cosmetics (Royce *et al.*, 2013). Furthermore, the interest in these compounds has increased in the last years due to the demand of biological fuel alternatives being

carboxylic acids important building blocks in the polymer industry and in diesel fuel applications (Sauer *et al.*, 2008; Royce *et al.*, 2013).

Table 1 – Carboxylic acids and representation of their structure.

	Common name	Structure
Monocarboxylic acids	Formic acid	
	Acetic acid	
	Pyruvic acid	
	Propionic acid	
	Lactic acid	
	Butyric acid	
	Benzoic acid	
Dicarboxylic acids	Succinic acid	
	Malonic acid	
	Oxalic acid	
	Malic acid	
	Maleic acid	
	Fumaric acid	
Tricarboxylic acids	Citric acid	
	Isocitric acid	
	Aconitic acid	

4. Carboxylic acid permeases in the yeast *Saccharomyces cerevisiae*

The yeast *S. cerevisiae* is able to thrive in a variety of carbon substrates, being glucose and fructose among the preferred substrates. Furthermore, this yeast species can also grow in several non-fermentable carbon sources as glycerol, ethanol and in the short-chain

carboxylic acids lactate and acetate, but not on di- or tricarboxylate intermediates of the Tricarboxylic Acid (TCA) Cycle (Barnett and Kornberg, 1960). Utilization of carbon sources depends on nutrient translocation across the plasma membrane and metabolic degradation of substrates. The translocation of carboxylic acids across the plasma membrane requires mediated transport systems (Cássio *et al.*, 1987; Casal *et al.*, 1996). In terms of metabolism the utilization of these alternative non-fermentable carbon sources requires activity of gluconeogenesis, the glyoxylate shunt, the TCA cycle and the respiratory chain. Acetate is converted to acetyl-coA which is then used to generate TCA cycle intermediates (Figure 2). Lactate is first oxidized to pyruvate which is then decarboxylated to acetyl-coA (Figure 2). When glucose is present, the expression of genes of these metabolic pathways are repressed, a phenomenon named yeast catabolite repression (reviewed in Gancedo, 1998).

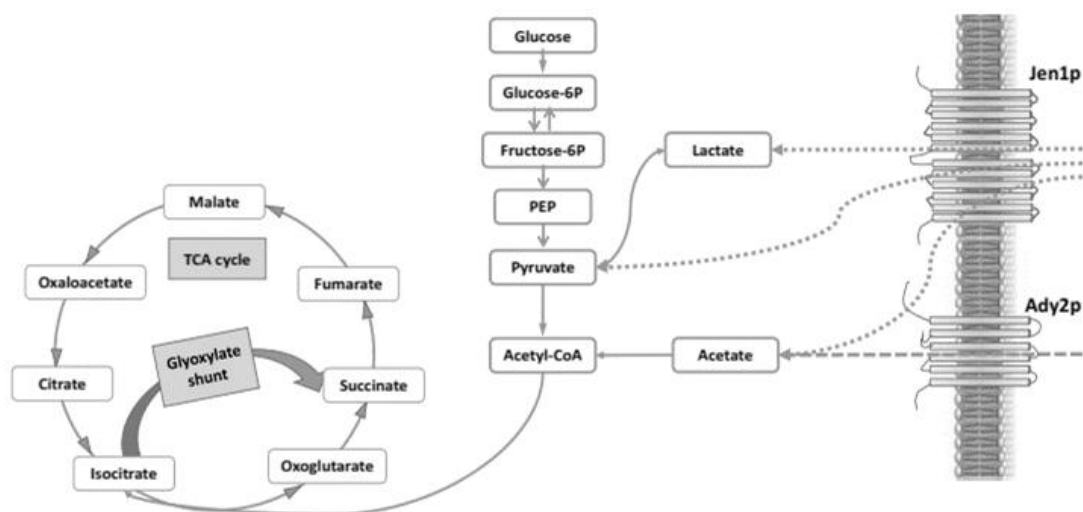


Figure 2 - The main metabolic pathways of oxidative and gluconeogenic metabolism in *Saccharomyces cerevisiae* (adapted from Casal *et al.*, 2008). The genes involved in the uptake of carboxylic acids are indicated: Jen1 (lactate transporter) and Ady2 (acetate transporter).

The ability to grow in TCA cycle intermediates such as succinic or malic acids is not equal among yeasts. While the Krebs-positive species *Candida utilis*, *Kluyveromyces lactis* or *Hansenula anomala* can grow on intermediates of the TCA cycle as sole carbon sources, consuming citric, succinic, fumaric and malic acids (Barnett and Kornberg, 1960; Zmijewski and MacQuillan, 1975; Cássio and Leão, 1993), Krebs-negative species such as *S. cerevisiae*, *Zygosaccharomyces bailii* or *Schizosaccharomyces pombe* can only consume TCA intermediates in the presence of other metabolizable carbon source (Baranowski and Radler, 1984; Osothsilp and Subden, 1986; Rodriguez and Thornton,

1990). Many fungi are known for their capacity to produce large amounts of a particular organic acid such as citric acid (*Aspergillus niger*) or lactic acid (from the phylum Zygomycota) and are used as microbial factories in industrial settings (Magnuson and Lasure, 2004).

Carboxylic acid transporters have long been an object of study with the first identified transport system reported in *Kluyveromyces lactis* for succinic acid (Zmijewski and MacQuillan, 1975) having passed almost thirty years before the gene encoding a succinic acid transporter was identified as KIJen2 (Lodi *et al.*, 2004). In *S. cerevisiae* only two carboxylate permeases have been described: Jen1 (Casal *et al.*, 1999) and Ady2 (Paiva *et al.*, 2004).

4.1 The lactate/pyruvate permease Jen1 from *S. cerevisiae*

Jen1 is a monocarboxylate permease from *S. cerevisiae* that is specific for lactate, pyruvate, acetate and propionate, dependent on the proton motive force and is required for an efficient growth in lactate (Cássio *et al.*, 1987; Casal *et al.*, 1999; Akita *et al.*, 2000). Jen1 lactate uptake measurements revealed a saturable transport system with a K_m of 0.69 mM lactic acid and a V_{max} of 0.40 nmol lactate s^{-1} mg dry weight $^{-1}$ (Casal *et al.*, 1999). Only upon the heterologous expression of *JEN1* from *S. cerevisiae* in *Pichia pastoris* and its reconstitution in hybrid vesicles, the role of this lactate permease was fully elucidated (Soares-Silva *et al.*, 2003). Jen1 is also involved in the uptake of the micronutrient selenite in a proton-coupled manner, with a K_m of 0.91 ± 0.13 mM sodium selenite and a V_{max} of 1.3 nmol 10^9 cells $^{-1}$ min $^{-1}$. The recognition of selenite by Jen1 is probably due to the fact that this molecule is an inorganic molecular mimic of monocarboxylates (McDermott *et al.*, 2010).

The Jen1 permease is repressed in the presence of glucose (Casal *et al.*, 1999) and induced in the presence of non-fermentable carbon sources, especially lactate, pyruvate and ethanol (Cássio *et al.*, 1987; Andrade and Casal, 2001). Repression by glucose occurs both at the mRNA level with down-regulation of *JEN1* when grown in glucose, and accelerated mRNA degradation when glucose is added to *JEN1*-expressing cells (Andrade and Casal, 2001; Andrade *et al.*, 2005), and at the protein level with internalization of the protein after addition of glucose (Paiva *et al.*, 2002). Upon addition of glucose to lactic acid derepressed-cells, Jen1p is removed from the membrane,

internalized by endocytosis following an ubiquitylation signal and accumulated in the vacuole for degradation (Paiva *et al.*, 2002). Degradation through this pathway is dependent on phosphorylation by the yeast casein kinase 1 (Yck1/Yck2) and ubiquitylation by the ubiquitin ligase Rsp5 (Paiva *et al.*, 2009). In Jen1 two lysine residues were identified as potential ubiquitylation targets (Peng *et al.*, 2003), with K338 in fact being a target for oligo-ubiquitylation with ubiquitin-Lys63 chains (Paiva *et al.*, 2009). This transporter endocytosis in response to glucose is mediated by the arrestin-related protein Rod1/Art4, which is dephosphorylated in response to glucose, allowing its ubiquitylation by Rsp5, and subsequent ubiquitylation and internalization of Jen1 (Becuwe *et al.*, 2012). Rod1 serves as a link between glucose availability and endocytosis (Figure 3). When cells are in lactate, Rod1 is phosphorylated by the Snf1 kinase and bound to 14-3-3 proteins preventing Rod1's ubiquitylation. When glucose becomes available the enzyme PP1 inhibits Snf1 and dephosphorylates Rod1, displacing the 14-3-3 protein and allowing ubiquitylation by Rsp5. Only the ubiquitylated Rod1 is functional and can ubiquitylate Jen1 and target this permease for degradation by endocytosis (Becuwe *et al.*, 2012).

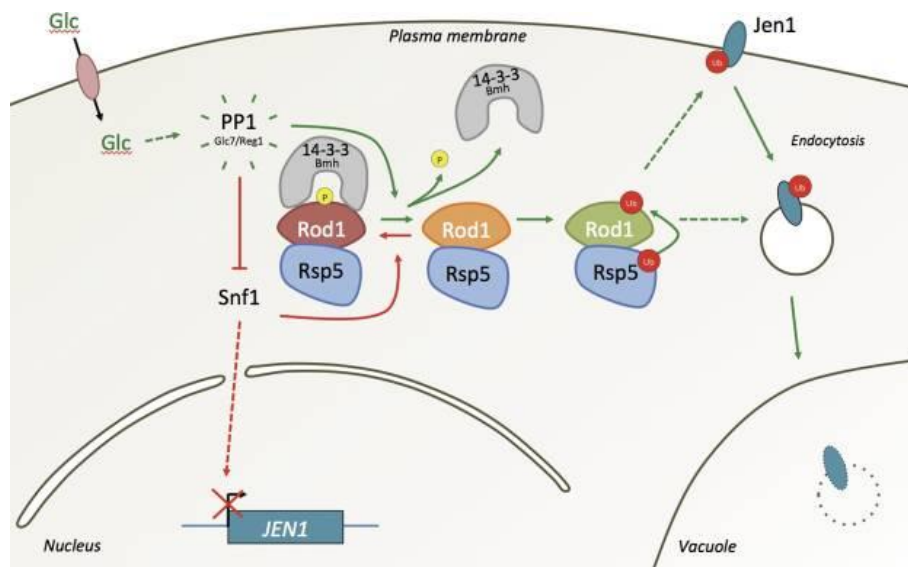


Figure 3 – Model for the regulation of Jen1 endocytosis. When yeast cells are grown in lactate medium, Snf1 is active and phosphorylates Rod1 to inactivate it (red arrows). Glucose addition triggers Jen1 endocytosis, which depends on Rod1 activation through its PP1-mediated dephosphorylation and subsequent Rsp5-mediated ubiquitylation, which are coordinated by 14-3-3 proteins (green arrows). The subcellular compartment at which Rod1 acts on Jen1 endocytosis may be the plasma membrane, or internal compartments (dashed lines). The Snf1/PP1 pathway also controls the expression of *JEN1* in response to glucose. (Bekuwe *et al.*, 2012).

Jen1 has 616 amino acids arranged in 12 putative α -helical transmembrane domains and is classified in TCDB as a part of the Sialate:H⁺ Symporter (SHS) Family which is included in the Major Facilitator Superfamily (TCDB # 2.A.1.12.2). A multiple alignment of several Jen1 homologues (Figure 4) revealed the presence of a highly conserved motif ³⁷⁹NXX[S/T]HX[S/T]QDXXX³⁹¹, with all the conserved amino acids being polar or charged and with X representing hydrophobic residues, that is considered to be the signature motif of the lactate/pyruvate:H⁺ symporter family (Soares-Silva *et al.*, 2007). Substitution of these polar or charged amino acids, even conserved substitutions, results in reduced transport activities and/or altered binding affinities therefore this motif is critical in substrate binding and translocation (Soares-Silva *et al.*, 2007).

Accession		365	379	383	386	387	391	424
CAA53556	ScJEN1	WLLFAYLVVL	LVGPNYLTHA	SQDLLPTMLR	AQL----	GLS	KDAVTVIVVV	TNIGAICGGM
CAG99769	KlJEN1	WLLFGYLILL	LVGPNYLTHA	SQDLFPTMLR	AQL----	RFS	EDAVTVIVVV	VCLGSIAGGM
AABY01000094	S. par	WLLFAYLVVL	LVGPNYLTHA	SQDLLPTMLR	AQL----	GLS	KDAVTVIVVV	TNIGAICGGM
AACI02000093	S. kud	WLLFTYLVIL	LVGPNYLTHA	SQDLLPTMLR	AQL----	GLS	KDAVTVIVVV	TNIGAICGGM
AABZ01000004	S. mik	WLLFAYLVIL	LVGPNYLTHA	SQDLLPTMLR	AQL----	GLS	KDAVTVIVVV	TNIGAICGGM
AACG02000104	S. bay	WLLFAYLVIM	LVGPNYLTHA	SQDLLPTMLR	AQL----	GLS	KDAVTVIVVV	TNIGAICGGM
AACE02000220	S. klu	WLLFTYLVLL	LVGPNYLTHA	SQDLLPTMLR	KQL----	EFs	EDAITVITV	VNLGAICGGM
CAG98245	KlJEN2	WLSMIYLVLL	MAGFNFSHG	SQDLFPTMLT	SQY----	QFS	ADASTXTNSV	ANLGAIAAGGI
XP_716108	CaJEN1	WLIFSylvLL	YAGWNFTTHG	SQDLYVTMIT	KQY----	HVG	LDKKTVIIVV	SNIGGIIGGI
EAA33605	NcJEN1	WKMCVYCCIL	MTWFNC-NHT	SQDNYTTFVL	RAK----	EMD	NSAASRASII	MKAGACVGGT
AAO33826	BbJEN1	WKMCVYCIFL	MTWFNFYSHT	SQDSYTFML	TEK----	ELS	NKGASRASIM	MKVGACVGGT
AAM77971	MaJEN1	WKMRVYCIIL	MTWFNYSHT	SQDSYTFML	TQK----	GLD	NAGASRASIL	MKAGACVGGT
XP_664307	Asp. nid	WLLLYLVLL	MAGFNFSHG	SQDLYPTLVQ	RQY----	GFS	RDAVTVTQVV	ANLGALTGGT
EAA73530	G. zea	WLLLYLVLL	MAGFNFSHG	SQDLYPTMLE	NQL----	NFS	KNKVTVTQVV	ANLGAMTGGs
CAC11721	TaJEN1	WKLfVYLSIL	LVGMNFVSHS	TQDLYPTFLE	HQL----	HFS	PTYVASTAIA	YNAAAIIGGI
AAL19310	S. typhi	WKLClyLVLV	MAFFNFFSHG	TQDLYPTFLK	MQH----	GFD	PHLISIIAIF	YNIAAMLGGI
ZP_00284297	B fun	VKLSLYAIIl	MTAFNFFSHG	SQDLYPTFLR	VQH----	QFD	AHTVSWITIT	LNVAICGGGL
AAQ60088	Chr. viola	WRLSLYAIIl	MTCFNFFSHG	TQDMYPTFLR	VQH----	KFD	PHTVQLIAIC	LNVAIVGGL
CAB10058	M. tuber	VRRFVYLVLL	MTAFNWMShG	TQDVYPTFLT	ATTDHGAGLS	SLTARWIVVI	YNIGAIIGGL	
BAB50041	Mes. loti	WGIALYAVVL	MMFFNFFSHG	TQDLYPTFLK	KQH----	GFD	PHTVSWITIV	ANLGAIVGGL
AAA86827	NanT	WPTGVMLMVV	VLFAFLYSWP	IQALLPTYLK	TDL----	AYN	PHTVANVLFF	SGFGAAVGCC
	Consensus	w.l..Ylv.l	m..fNf.sHg	sQDlypT.l.	.q.	.fs	...v..i...	.n.gai.GG.
	Conserved residues		N	H	QD	T		

Figure 4 - Identification of the conserved sequence ³⁷⁹NXX[S/T]HX[S/T]QDXXX³⁹¹ (numbering refers to Jen1p) in the lactate/pyruvate:H⁺ symporter subfamily (TC#2.A.1.12.2). Multiple sequence alignment of Jen1p homologues was built by the Multalin (INRA) bioinformatics tool. (Soares-Silva *et al.*, 2007).

Other residues involved in both function and specificity have been identified (Soares-Silva *et al.*, 2011) and are discussed in Chapter II of the present thesis. Homology threading of the Jen1 protein sequence revealed a high probability of a common topology with the LacY permease (Soares-Silva *et al.*, 2007). The location of the important residues for function and degradation in the predicted topology of Jen1 is depicted in Figure 5.

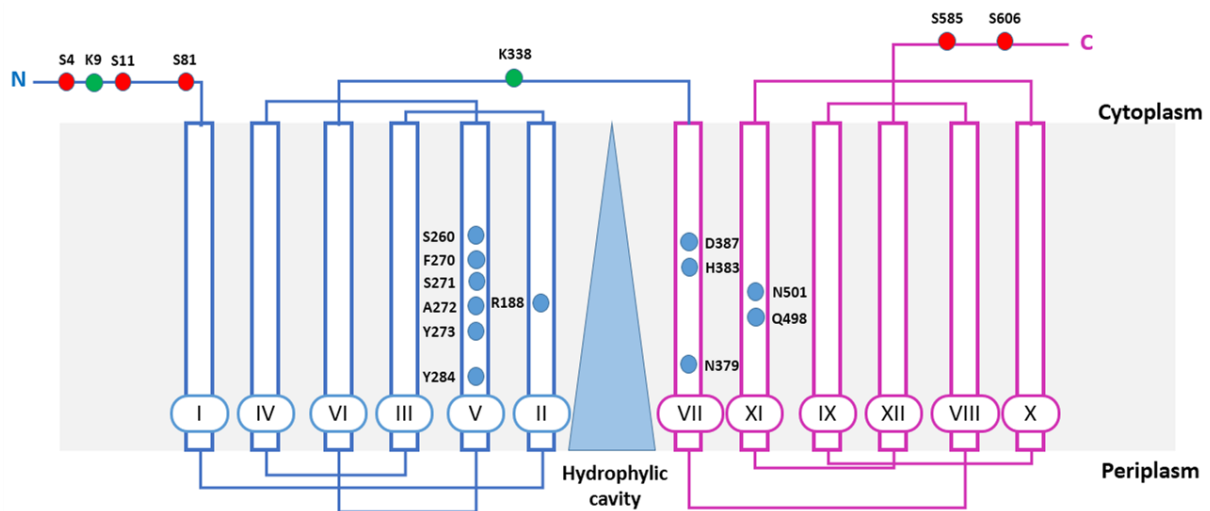


Figure 5 - Model of Jen1p topology. The location of residues involved in substrate translocation (blue), phosphorylation (red) and ubiquitination (green) is depicted in circles.

4.2 Structures within the MFS superfamily – a common fold

The MFS superfamily comprises more than 10,000 sequenced members (including Jen1) but only a handful have their three dimensional structure determined by crystallography (reviewed in Table 2). The MFS proteins usually comprise 12 transmembrane domains (TM) with N- and C- termini facing the cytoplasm. Despite having low sequence similarity, and having different transport mechanisms and specificities, MFS members are believed to share a common structural fold, the MFS fold (Yan, 2013).

Table 2 - MFS proteins of known crystallographic structure (adapted from Yan, 2013).

Protein	Function	TCDB number	Organism	PDB code	Publication
LacY	Lactose:proton symporter	2.A.1.5.1	<i>Escherichia coli</i>	1PV6, 1PV7, 2CFP, 2CFQ, 2V8N, 2Y5Y	Abramson <i>et al</i> , 2003
GlpT	Glycerol-3-phosphate:Pi antiporter	2.A.1.4.3	<i>Escherichia coli</i>	1P24	Huang <i>et al</i> , 2003
EmrD	Multidrug transporter	2.A.1.2.9	<i>Escherichia coli</i>	2GFP	Yin <i>et al</i> , 2006
FucP	L-Fucose:proton symporter	2.A.1.7.1	<i>Escherichia coli</i>	3O7Q, 3O7P	Dang <i>et al</i> , 2010
PepT_{so}	Peptide:proton symporter	2.A.17.4.7	<i>Shewanella oneidensis</i>	2XUT	Newstead <i>et al</i> , 2011
PepT_{st}	Peptide:proton symporter	2.A.17.1.6	<i>Streptococcus thermophilus</i>	4APS	Solcan <i>et al</i> , 2012
XylE	D-Xylose:proton symporter	2.A.1.1.3	<i>Escherichia coli</i>	4GBY, 4GBZ, 4GC0	Sun <i>et al</i> , 2012
YajR	Potential drug efflux protein	2.A.1.2.60	<i>Escherichia coli</i>	3WDO	Jiang <i>et al</i> , 2013

The MFS fold comprises 12 TMs organized into two inverted 3 + 3 TM repeats and displaying a pseudo-symmetry related by an axis perpendicular to the membrane plane depicted in Figure 6 (Yan, 2013).

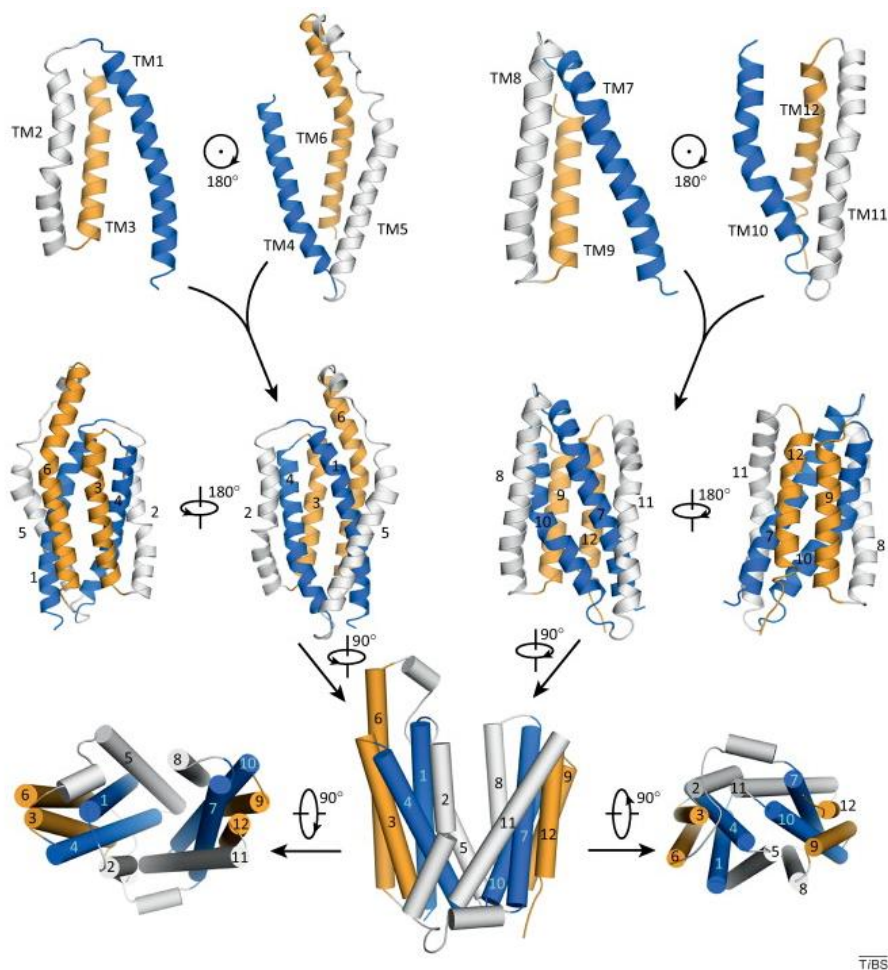


Figure 6 – The MFS fold. A MFS contains four 3-TM repeats (top row). Each two inverted 3-TM repeats form one domain (middle row). The two domains form the MFS fold (bottom row) that is perpendicular to the plane of the membrane. Corresponding TMs in each 3-TM repeat are coloured the same. (Yan, 2013).

In LacY the N- and the C-domains can be superimposed showing this inverted topology repeat depicted in Figure 7 (Radestock and Forrest, 2011). Corresponding TMs in each 3-TM repeat play similar roles, with TMs 1, 4, 7 and 10 in the centre of the protein coordinating substrate binding and coupling of the co-transported molecule, TMs 2, 5, 8 and 11 in the side of the structure mediating interdomain contacts, and with TMs 3, 6, 9 and 12 on the outside of the protein allowing structure integrity (reviewed in Yan, 2013). This inverted topology repeat model allows the functioning of the alternating-access mechanism of MFS transporters. Application of this principle to model the outward-facing conformation of LacY revealed information consistent with data obtained

biochemically during several years, namely salt-bridge formation (Radestock and Forrest, 2011).

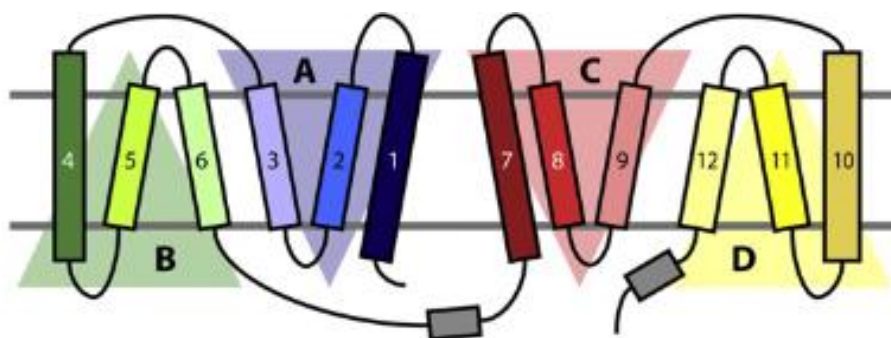


Figure 7 – Schematic representation of the inverted topology repeat in LacY. (Radestock and Forrest, 2011).

In the alternating-access mechanism model, the transporter is never exposed to both sides of the membrane. Upon substrate binding in the outward-facing state there is a conformational change to the inward-facing conformation due to a domain movement that allows the N- and C- portions of the transporter to move back and forth against each other (rocker-switch mechanism) (reviewed in Law *et al.*, 2008). This mechanism was elucidated by the existing MFS structures depicted in Figure 8 since they represent several steps of the alternating access cycle namely ligand-free and outward-open FucP, ligand-bound and outward-facing XyleE, occluded EmrD, inward-occluded PepT and inward open LacY, GlpT and PepT (reviewed in Yan, 2013).

MFS proteins contain a single binding site between the two pseudo-symmetrical N- and C- domains located halfway into the membrane (Kaback *et al.*, 2001). In LacY the substrate is hydrogen-bonded to two positively charged residues, R144 (TM 5) and K358 (TM 11) (Kaback *et al.*, 2001). Furthermore, some residues have been identified as critical in determining the affinity and specificity of the transporter, namely E126 (TM4) and R144/W151 (TM5) (Kaback *et al.*, 2001). In other MFS transporters other amino acid residues have been identified as crucial in substrate binding. For instance, in FucP substrate binding is mediated by E135 (TM4) and Q162 (TM5), while in GlpT R45 (TM1) and R269 (TM7) fill this role (Abramson *et al.*, 2004; Dang *et al.*, 2010).

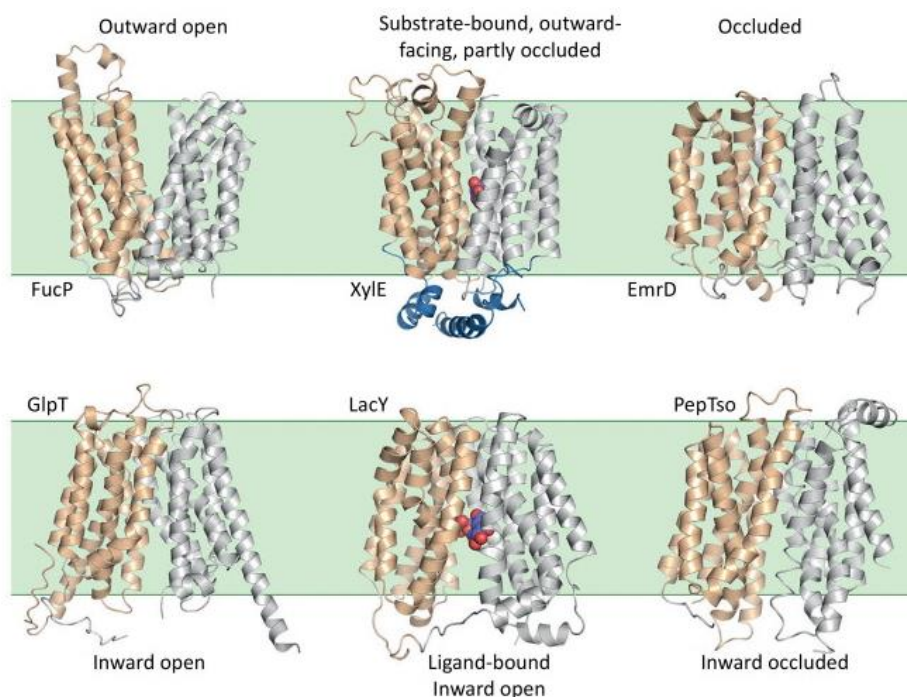


Figure 8 – Distinct conformational states of the MFS structures depicting the alternating access mechanism. N and C domains are colored wheat and silver, respectively. The intracellular helix domain unique to XylE is colored blue. The bound ligands in XylE and LacY are shown as spheres. The PDB accession codes for these structures are 3O7Q for FucP, 4GBY for XylE, 2GFP for EmrD, 2XUT for PepTso, 1PV7 for LacY, and 1PW4 for GlpT (Yan, 2013).

LacY has been the paradigm of the MFS transporters due to the wealth of biochemical information originated from the work of Kaback's group. The crystallization of more MFS transporters revealed a basic architecture that can be applied in the creation of structural models for other proteins, identifying the key residues in the substrate binding site that define specificity as applied in chapter III of the present thesis.

4.3 Homologues of Jen1 in fungi

Jen1 homologous genes have been described for several yeast species namely *Candida albicans* (Vieira *et al.*, 2010), *Beauveria bassiana* (Jin *et al.*, 2010) and *Kluyveromyces lactis* (Lodi *et al.*, 2004). An *in silico* study combining synteny analysis, sequence similarity and Jen1 amino acid motif analysis revealed two main phylogenetic clusters with different substrate specificities, a Jen1 cluster that comprises monocarboxylate transporters and a Jen2 cluster that comprises dicarboxylate transporters, represented in Figure 9 (Lodi *et al.*, 2007; Casal *et al.*, 2008).

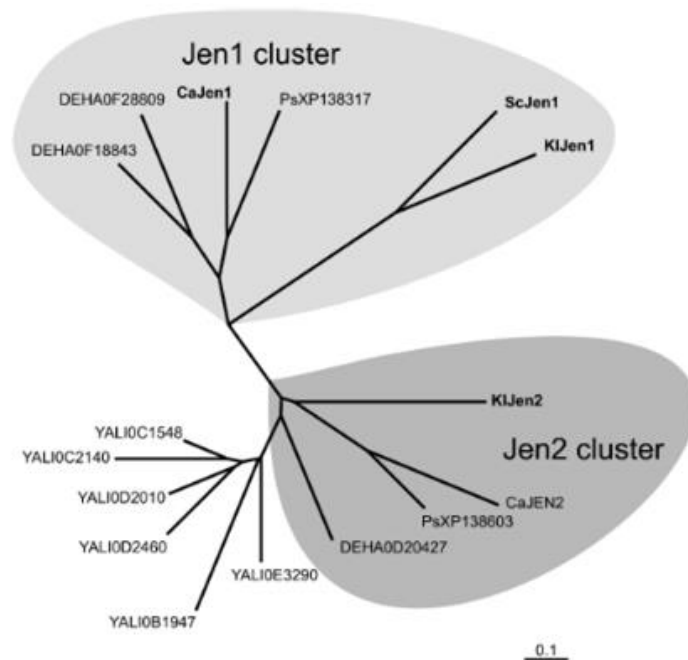


Figure 9 - Phylogenetic tree of ScJen1p homologues. The permeases with characterized function are highlighted in bold. (Casal *et al.*, 2008).

In *K. lactis*, two Jen1 homologue proteins exist (KIJen1 and KIJen2) which share 39 % identity (Lodi *et al.*, 2004). *KIJEN1* shows higher expression in lactate while *KIJEN2* shows high expression in lactate, dicarboxylic acids, glycerol and ethanol (Lodi *et al.*, 2004; Queirós *et al.*, 2007). Deletion of *KIJEN1* impairs growth of *K. lactis* in lactate and pyruvate (Lodi *et al.*, 2004) and inhibits lactate uptake, while inactivation of *KIJEN2* affects growth in the dicarboxylates succinate, fumarate and malate, with uptake of these compounds being strongly reduced (Queirós *et al.*, 2007). *K. lactis* cells derepressed in DL-lactic acid show a saturable uptake system for lactate with a K_m of 2.08 ± 0.50 mM lactic acid, which is competitively inhibited by pyruvic acid. Malic or succinic acid grown-cells show a mediated transport system for labelled malic and succinic acids with a K_m of 0.15 ± 0.03 mM for malic acid and of 0.11 ± 0.03 mM for succinic acid with malic acid uptake being competitively inhibited by succinic acid and vice-versa (Queirós *et al.*, 2007). Heterologous expression of these genes in *S. cerevisiae* confirmed that KIJen1 is a monocarboxylate transporter while KIJen2 is a dicarboxylate transporter.

In *C. albicans* *JEN1* encodes a monocarboxylate transporter and *JEN2* a dicarboxylate transporter, subjected to glucose repression (Soares-Silva *et al.*, 2004; Vieira *et al.*, 2010). Lactic acid-grown-cells show only one mediated transport system for labelled DL-lactic acid, the plasma membrane permease CaJen1, with a K_m of 0.33 ± 0.09 mM dependent on the proton motive force and competitively inhibited by propionic and pyruvic acids

(Soares-Silva *et al.*, 2004). Disruption of *CaJEN2* affects growth in the dicarboxylates succinate and malate when grown as sole carbon and energy sources (Vieira *et al.*, 2010). Uptake assays with whole *C. albicans* cells revealed a mediated transport of these acids through CaJen2 with a K_m of 0.49 ± 0.27 mM for succinic acid and 0.12 ± 0.019 mM for malic acid (Vieira *et al.*, 2010). Both CaJen1 and CaJen2 are expressed during growth in both mono- and dicarboxylates but with a stronger induction of CaJen1 in the monocarboxylates lactic and pyruvic acids and of CaJen2 in the dicarboxylates succinic and malic acids (Vieira *et al.*, 2010).

Carboxylate transport through Jen1 has not been investigated in detail in filamentous fungi. In the entomopathogenic fungus *B. bassiana*, Jen1 was shown to transport monocarboxylates into cells and to be a virulence factor by initiating fungal pathogenesis in insects (Jin *et al.*, 2010). *Aspergillus nidulans* has homologues of both Jen1 and Jen2 although with no functional characterization.

4.4 The acetate permease *Ady2* from *S. cerevisiae*

In acetic acid or ethanol grown cells, *S. cerevisiae* was shown to possess a proton symporter system for acetic, propionic and formic acids and to be impermeable to lactic and pyruvic acids. In lactic acid grown cells, both this system as well as Jen1 are active (Casal *et al.*, 1996). The identification of the gene encoding this permease was achieved latter resorting to a genome-wide analyses of yeast adaptation to acetic acid (Paiva *et al.*, 2004). A comparison between the gene expression profile of glucose-grown cells versus cells shifted from glucose to acetic acid as the sole carbon and energy source revealed the derepression of gluconeogenic genes and the induction of the glyoxylate and TCA cycles as well as the induction of several transporters. Among these transporters, three genes were strongly activated: *YCR010c/ADY2*, *YNR002c/FUN34* and *YDR384c* (Paiva *et al.*, 2004). Deletion of these genes revealed that only inactivation of *Ady2* impaired acetate transport activity (Paiva *et al.*, 2004). *Ady2* is a protein with 283 amino acids arranged in 6 putative transmembrane domains that belongs to the YaaH family (TCDB 2.A.96) which has recently been renamed as the Acetate Uptake Transporter (AceTr) Family.

The *Ady2* protein is also believed to be involved in ammonia production during colony development in *S. cerevisiae* (Palková *et al.*, 2002). The three genes *YCR010c/ADY2*, *YNR002c/FUN34* and *YDR384c* are strongly expressed during the first 12 h of ammonia

production in yeast colonies, the alkali phase of colony growth, and their deletion decreases ammonia production in cells and colonies (Palková *et al.*, 2002). Furthermore, these proteins seem to have their production induced by external ammonia (Rídicová *et al.*, 2007). Analysis of Ady2 by GFP tagging revealed its localization in patches in the plasma membrane, being the formation of patches pH dependent (Rídicová *et al.*, 2007). A more recent study using FRET and FLIM revealed that Ady2 can form homodimers or oligomers (Strachotová *et al.*, 2012). Doubts regarding the true function of Ady2 still remain and structural-functional studies are necessary to clarify this question as analysed in chapter VI of the present thesis.

4.5 The AceTr family of transporters

The AceTr (former YaaH) family members display a predicted topology arranged in six transmembrane segments, containing a conserved motif (N-P-[AV]-P-[LF]-G-L-x-[GSA]-F) located at the first putative transmembrane region of the N-terminus of the protein. Members of the AceTr family are found in archaea, eukaryotes and bacteria, with some members experimentally demonstrated as acetate transporters, such as Ady2 in *S. cerevisiae* described in the previous section and AcpA in the filamentous fungus *A. nidulans* (Robellet *et al.*, 2008). An *acpA* deletion mutant of *A. nidulans* displays reduced growth on acetate as a sole carbon source, at low concentration and in a high pH medium, which is fully restored upon reintroduction of the *acpA* gene. This gene is also required for the induction of the acetate assimilation pathways and direct measurement of acetate incorporation into germinating conidia confirmed that AcpA is fundamental for acetate uptake, especially at low substrate concentrations (Robellet *et al.*, 2008). The *acpA* transcript level increases as the demand for acetate uptake increases and its expression is induced in the presence of several weak monocarboxylic acids such as glyoxylate, propionate, lactate, pyruvate and formate (Robellet *et al.*, 2008). Further characterization of this permease is among the aims of this study, described in chapter VI of the present dissertation.

Other members have not been shown to be directly implicated in acetate uptake, but rather have been linked to acetic acid adaptation, such as Gpr1 in the yeast *Yarrowia lipolytica* (Augstein *et al.*, 2003; Gentsch *et al.*, 2007) and MA4008 in the archaea species *Methanosarcina acetivorans*. In *Y. lipolytica* *GPR1* mRNA expression is induced

threefold in acetic acid or ethanol medium, but deletion of this gene does not impair utilization of acetic acid as sole carbon source (Augstein *et al.*, 2003). Three mutations in the N-terminal motif AFGGTLNPG of Gpr1, a motif conserved in other eukaryotic homologues including Ady2 (depicted in Figure 10), as well as one in the C-terminus of Gpr1 induce sensitivity to acetic acid (Augstein *et al.*, 2003). Substitutions in this motif in Ady2 also induce acetic acid sensitivity (Gentsch *et al.*, 2007). Truncations in the C-terminal of Gpr1 or deletion of the yeast conserved motif YANYA in this region abolish this sensitivity phenotype revealing its role in determining acetic acid sensitivity (Gentsch *et al.*, 2007). The Gpr1 was proposed to be a protein involved in acetic acid adaptation, but not directly involved in resistance to acetic acid toxicity (Augstein *et al.*, 2003; Gentsch *et al.*, 2007). In *M. acetivorans* quantitative transcription analysis of acetic acid versus methanol-grown cells revealed a 125 fold induction of *MA4008* expression. Expression at these high levels is only achieved in the presence of acetate as the only carbon source since growth in methanol plus acetic acid lowers the values of expression to those found in the preferred carbon source methanol. The expression of this gene was similar to acetate kinase (*ack*) and acetyl-CoA phosphotransferase (*pta*), two of the enzymes required for acetate utilization. All these evidence point to a role of MA4008 in acetate uptake (Rohlin and Gunsalus, 2010).

Other AceTr family members are not functionally related with acetate. For instance *S. cerevisiae* *FUN34* and *ATO3* have been described as involved in ammonia export (Guaragnella and Butow, 2003; Ricicová *et al.*, 2007) and *A. nidulans* AlcS is of unknown function being induced by ethanol (Flipphi *et al.*, 2006).

Gpr1p	KFHRDDFYRA	FGGTLN PGGA	PQPSRKFGNP	<u>APLGLSAFAL</u>	<u>TTLVFS</u> LCTV	<u>QARGVP</u> NP ^{SI}	110
Ycr010cp	KFLKSDLYCA	FGGTLN PGLA	PAPVHKF ^{EN} P	<u>APLGLSAFAL</u>	<u>TFVLSM</u> FNA	<u>RAQG</u> ITV ^{PNV}	120
Ynr002cp	KFLRRDLFEA	FGGTLN PGLA	PAPVHKF ^{AN} P	<u>APLGLSGFAL</u>	<u>TFVLSM</u> FNA	<u>RAQG</u> ITV ^{PNV}	119
Gpr1p	<u>AVGLAL</u> FYGG	<u>VCQFA</u> AGMWE	<u>FVQENT</u> FGAA	<u>ALTSY</u> GGFWM	<u>SWAAI</u> EMNAF	<u>GIKDS</u> YNDP-	169
Ycr010cp	<u>VVGCAM</u> FYGG	<u>LVQLI</u> AGIWE	<u>IALENT</u> FGGT	<u>ALCSY</u> GGFWL	<u>SFAAI</u> YIPWF	<u>GILEA</u> YEDNE	180
Ynr002cp	<u>VVGCAM</u> FYGG	<u>LVQLI</u> AGIWE	<u>IALENT</u> FGGT	<u>ALCSF</u> GGFWL	<u>SFGAI</u> YIPWF	<u>GILDA</u> YKDE	179
Gpr1p	<u>IEVQNA</u> VG ^{IY}	<u>LFGWF</u> I ^{FTLM}	<u>LTLCT</u> LK ^{STV}	<u>AFFGL</u> FFMLM	<u>MTFLV</u> LACAN	<u>VTQHH</u> GTAIG	229
Ycr010cp	<u>SDLNNA</u> LG ^{FY}	<u>LLGWAI</u> FTFG	<u>LTVCT</u> MK ^{STV}	<u>MFFLL</u> FFLLA	<u>LTFL</u> LLSIGH	<u>FANRL</u> GVTRA	240
Ynr002cp	<u>SDLGNA</u> LG ^{FY}	<u>LLGWAL</u> FTFG	<u>LSVCT</u> MK ^{STI}	<u>MFFAL</u> FFLLA	<u>VTFL</u> LLSIAN	<u>FTGEV</u> GVTRA	239
Gpr1p	<u>GGWLG</u> IITAF	<u>FGFYN</u> AYAGL	<u>ANPGN</u> SYIVP	<u>VPLDM</u> PFVKK	D--		270
Ycr010cp	<u>GGVLG</u> VVVA ^F	<u>IAWYN</u> AYAGV	<u>ATKQN</u> SYVLA	<u>RPFPL</u> PSTER	VIF		283
Ynr002cp	<u>GGVLG</u> VIVAF	<u>IAWYN</u> AYAGI	<u>ATRON</u> SYIMV	<u>HPFAL</u> PSNDK	VFF		282

Figure 10 – Alignment of the protein sequences of *Y. lipolytica* Gpr1p and the *S. cerevisiae* proteins Ady2 and Fun34. Conserved amino acids are in bold. Amino acids whose substitution resulted in acetic acid sensitivity are white on black background. The family motif NPAPLGL and the YNAYA motif are highlighted on a grey background. Sequences that form putative transmembrane domains are underlined. The less conserved N-terminus was omitted. (Gentsch *et al.*, 2007).

5. Carboxylic acid permeases in bacteria

Carboxylic acids in bacteria are both carbon sources and products of sugar metabolism (metabolic intermediates or end-products) with active transporters playing a detrimental role in their use and excretion. Since bacteria constantly face times of feast or famine of different substrates, they have a plethora of transporter systems to face this variation in resource concentration, nutrients and habitats (Koch, 2005). Different bacterial species have different uptake efficacy and different selection of the substrates from the environment, mostly due to their different uptake systems and intermediate metabolism (Koch, 2005). An overview of the different carboxylic acid transporters found in the industrial important bacteria *Escherichia coli*, *Bacillus subtilis*, *Corynebacterium glutamicum*, *Rhodobacter capsulatus* and acetic and lactic acid bacteria is given in this section. The different carboxylate transporters that have characterized in these bacterial species are summarized in Table 3. Knowledge on the mechanisms underlying the transport of carboxylic acids is crucial towards an efficient biological production of these carboxylates in industry.

Table 3 – Overview of the bacterial carboxylate transporters reviewed herein. The table includes the transporters in each species, the transporter family (www.tcdb.org), number of predicted TM domains, specificity and affinity (when available) and the corresponding bibliographic reference.

Bacterial species	Transporter	Transporter Family	Predicted TM	Specificity / Affinity	Reference
<i>Escherichia coli</i>	ActP	SSS	14	Acetate (K_m 5.4 μ M) and Glyoxylate Proton symporter	Gimenez <i>et al</i> , 2003
	SatP	AceTr	6	Acetate (K_m 1.24 mM) and Succinate (K_m 1.18 mM) coupling ion: proton	Sá-Pessoa <i>et al</i> , 2013
	FocA	FNT	6 in pentameric channels (PDB 3KCU)	Preference for formate uptake/efflux (K 11.7 mM) Exports products of mixed acid fermentation: Acetate (K 23.9 mM), Lactate (K 96 mM), Pyruvate (K 11.6 mM)	Falke <i>et al</i> , 2009; Wang <i>et al</i> , 2009; Lü <i>et al</i> , 2012
	LldP	LctP	12	L-lactate, D-lactate and glycolate	Núñez <i>et al</i> , 2001; Núñez <i>et al</i> , 2002
	GlcA	LctP	12	L-lactate, D-lactate and glycolate	Núñez <i>et al</i> , 2001; Núñez <i>et al</i> , 2002
	DcuA	Dcu	10	Anaerobic antiporter of aspartate, malate, fumarate and succinate Uptake and efflux of fumarate	Six <i>et al</i> ., 1994; Zientz <i>et al</i> , 1996
	DcuB	Dcu	12	Anaerobic antiporter of aspartate, malate, fumarate and succinate Uptake and efflux of fumarate	Six <i>et al</i> ., 1994; Zientz <i>et al</i> , 1996
	DcuC	DcuC	14	Anaerobic electroneutral C4-dicarboxylate exchanger Dicarboxylate-proton symporter (lower activity)	Zientz <i>et al</i> ., 1999
	TtdT	DASS	11	L-tartrate:succinate antiporter L-tartrate uptake (K_m 700 μ M) and Succinate efflux (K_m 400 μ M)	Kim and Uden, 2007
	CitT	DASS	12	Citrate:succinate antiporter	Pos <i>et al</i> , 1998
	DctA	DAACS	14	Aerobic dicarboxylate transporter: Succinate (K_m 25 μ M), Orotate and Fumarate – inhibited by fumarate, malate, aspartate and tartrate	Kay and Kornberg, 1971; Baker <i>et al</i> , 1996; Karinou <i>et al</i> , 2013
	DauA	SulP	10	Aerobic succinate transporter Succinate (K_m 0.56 mM), aspartate and fumarate	Karinou <i>et al</i> , 2013

<i>Corynebacterium glutamicum</i>	MctC	SSS	12-13	Acetate/propionate: H ⁺ symporter Pyruvate is an additional substrate Pyruvate ($K_{0.5}$ 250 μ M), Acetate ($K_{0.5}$ 31 μ M), Propionate ($K_{0.5}$ 9 μ M)	Jolkver <i>et al.</i> , 2009
	NCgl2816	MFS	12	Putative L-lactate transporter Evidences from transcript analysis only	Stansen <i>et al.</i> , 2005
	DccT (DcsT)	DASS	14-15	Aerobic sodium dicarboxylate transporter for: succinate (K_m 30 μ M), fumarate (K_m 79 μ M), malate (K_m 360 μ M) and oxaloacetate with low affinity	Ebbighausen <i>et al.</i> , 1991; Teramoto <i>et al.</i> , 2008; Youn <i>et al.</i> , 2008
	DctA	DAACS	7-8	Proton motive force-dependent uptake for the dicarboxylates l-malate (K_m 736 μ M), fumarate (K_m 232 μ M), succinate (K_m 218 μ M) and likely also for oxaloacetate and glyoxylate	Youn <i>et al.</i> , 2009
	SucE	AAEx	10-12	Succinate exporter Exhibits succinate self-exchange	Fukui <i>et al.</i> , 2011
	CitH	CitMHS	10-11	Transports citrate in complex with Ca ²⁺ or Sr ²⁺	Brocker <i>et al.</i> , 2009
	TctABC	TTT	12(TctA) + 4(TctB) + 1(TctC)	Transports citrate in complex with Ca ²⁺ or Mg ²⁺	Brocker <i>et al.</i> , 2009
<i>Bacillus subtilis</i>	CitM	CitMHS	12	[Citrate or D-isocitrate]•divalent metal : H ⁺ symporter (K_m 35-63 μ M) Metal (in order of preference): Mg ²⁺ , Mn ²⁺ , Ni ²⁺ , Zn ²⁺ and Co ²⁺	Krom <i>et al.</i> , 2009
	CitH	CitMHS	12	[Citrate]•divalent metal : H ⁺ symporter (K_m 35-63 μ M) Metal (in order of preference): Ca ²⁺ , Ba ²⁺ and Sr ²⁺	Krom <i>et al.</i> , 2009
	CimH	2-HCT	11	Electroneutral L-malate/citrate:H ⁺ symporter Citrate (K_m 10 μ M, low capacity), L-malate (K_m 1.5 mM, high capacity)	Krom <i>et al.</i> , 2001
	MleN	NhaC	12	Malate:lactate antiporter coupled with proton uptake and sodium efflux Malic ²⁻ -2H ⁺ : Na ⁺ -lactate ¹⁻	Wei <i>et al.</i> , 2000
	MaeN	2-HCT	11	Malate:Na ⁺ symporter	Tanaka, 2003
	DctA	DAACS	10	Dicarboxylate:H ⁺ symporter for succinate (K_m 2.6 μ M) inhibited by fumarate, malate and oxaloacetate	Groeneveld <i>et al.</i> , 2010

<i>Rhodobacter capsulatus</i>	ActP	SSS	14	Acetate uptake permease, ActP1 (K_m 1.89 mM), inhibited by pyruvate and lactate. Also takes up tellurite (K_m 163 μ M)	Borghese <i>et al.</i> , 2008; Borghese <i>et al.</i> , 2011
	RRC01191	TRAP-T	--	Monocarboxylate 2-oxoacids transporter Binds pyruvate (K_d 3.4 μ M) and 2-oxobutyrate (K_d 0.32 μ M)	Thomas <i>et al.</i> , 2006
	DctPQM	TRAP-T	12 (DctM) + 4 (DctQ) + receptor	Tripartite dicarboxylate:H ⁺ symporter Substrates: malate (K_d 8.4 μ M) competitively inhibited by fumarate (K_i 2 μ M) and succinate (K_i 8 μ M)	Forward <i>et al.</i> , 1997
<i>Acetobacter aceti</i>	AatA	ABC	--	Acetate exporter Mediates resistance to acetic, propionic, formic and lactic acids	Nankano <i>et al.</i> , 2006
<i>Lactococcus lactis</i>	MleP	2-HCT	13	Electrogenic malate:lactate exchanger Substrates: S-malate (K_m 0.46 mM), S-lactate (K_m 4.6 mM), R-lactate and R-malate with lower affinity	Poolman <i>et al.</i> , 1991; Pudlik and Lolkema 2012
	CitP	2-HCT	13	Electrogenic citrate:L-lactate exchanger Citrate (K_m 56 μ M), S-malate (K_m 0.1 mM), S-lactate (K_m 26 mM), R-lactate and R-malate with lower affinity	Pudlik and Lolkema 2012

TCDB Families: 2-HCT – 2-Hydroxycarboxylate Transporter; AAEx – Aspartate:Alanine Exchanger; ABC – ATB-binding cassette superfamily; AceTr – Acetate Uptake Transporter; CitMHS – Citrate-Mg²⁺:H⁺ (CitM) Citrate-Ca²⁺:H⁺ (CitH) Symporter; DAACS – Dicarboxylate/Amino Acid:Cation (Na⁺ or H⁺) Symporter; DASS – Divalent Anion:Na⁺ Symporter; Dcu – C₄-Dicarboxylate Uptake; DcuC – C₄-dicarboxylate Uptake C; FNT – Formate-Nitrite Transporter; LctP – Lactate Permease; MFS – Major Facilitator Superfamily; NhaC – NhaC Na⁺:H⁺ Antiporter; SSS – Solute:Sodium Symporter; SulP – Sulfate Permease; TRAP-T – Tripartite ATP-independent Periplasmic Transporter; TTT – Tripartite Tricarboxylate Transporter

5.1 *Escherichia coli*

E. coli, a Gram-negative bacterium, is the most widely studied microorganism used in industry for protein and metabolite production. The ease of manipulation due to the availability of genetic tools and the vast knowledge on genomic, metabolic, and physiological traits of this organism make it the prime bacterial model. *E. coli* can use a variety of carbon sources from the preferred carbohydrate glucose to other carbon sources such as carboxylic acids and can grow aerobically or anaerobically by respiration (reviewed in Wolfe, 2005). The mixed acid fermentation in *E. coli* starts with glucose which enters through the phosphotransferase pathway and suffers glycolysis yielding ATP and NADH, which is then re-oxidized, and pyruvate which is reduced into a mixture of end products such as lactate, acetate, ethanol, succinate, formate, carbon dioxide and hydrogen, by one or more alternative pathways (reviewed in Wolfe, 2005). Interconnected metabolic pathways in this organism include glycolysis, gluconeogenesis, the Entner-Dudoroff pathway, the TCA cycle with the glyoxylate bypass, anaplerotic reactions and acetate production and assimilation (Papagianni, 2012a).

5.1.1 Monocarboxylate transporters

Monocarboxylates can be used as a source of carbon and energy by *E. coli*. Transport of acetate occurs through ActP (Gimenez *et al.*, 2003) and SatP (Sá-Pessoa *et al.*, 2013) and transport of lactate occurs through LldP and GlcA (Núñez *et al.*, 2001). The products of mixed acid fermentation lactate, acetate, formate and pyruvate are exported by FocA (Lü *et al.*, 2012) (Figure 11).

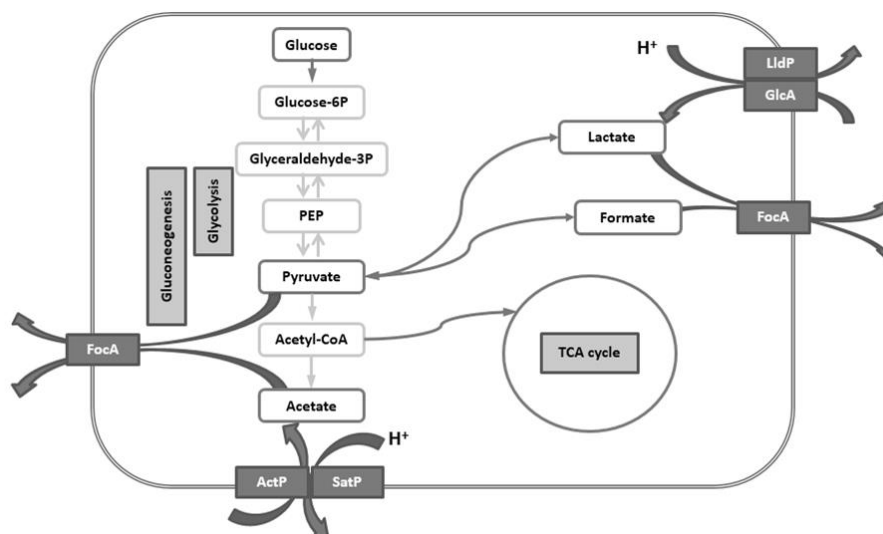


Figure 11 – Monocarboxylate transporters in *E. coli*. Main metabolic pathways involved in monocarboxylic acids utilization with indication of the characterized transporters for these acids in *E. coli*.

5.1.1.1. The acetate transporter ActP

ActP is a member of the Sodium:Solute Symporter (SSS) Family (TCDB # 2.A.21) with 14 putative transmembrane segments (TMS). It is encoded by the gene *yjcG*, which is cotranscribed with the genes *acs* and *yjcH*. While the *yjcH* gene is of unknown function, *acs* codes for acetyl-CoA synthetase that scavenges extracellular acetate and activates its conversion to acetyl coenzyme A, which is then used in the tricarboxylic acid cycle (TCA) or in the glyoxylate shunt (Gimenez *et al.*, 2003).

The *acs-yjcH-actP* operon is correlated with acetate utilization and its expression increases with aerobic acetate formation upon glucose limiting concentrations (Veit *et al.*, 2007; Valgepea *et al.*, 2010). The regulation of the transcription of this operon is complex, involving several transcription factors, two promoters and two sigma factors (Kumari *et al.*, 2000). The expression of *acs* depends on the cyclic AMP receptor protein (CRP) that activates the *acsP2* promoter region but also on the decrease of oxygen availability through the oxygen regulator FNR (Beatty *et al.*, 2003). It also depends indirectly on the flux of carbon through acetate pathways due to interaction with the glyoxylate shunt repressor IclR and its activator FadR as well as enzymes involved in acetate metabolism (Kumari *et al.*, 2000).

ActP mediates the transport of acetate and glycolate driven by the transmembrane electrochemical potential. In a strain lacking isocitrate lyase, therefore with no acetate metabolism, there is a 10-fold higher accumulation of intracellular acetate than in ActP-deficient cells, showing its role in acetate uptake in *E. coli*. The kinetics of accumulation showed an apparent K_m for acetate of 5.4 μM and a V_{max} of 19.6 $\text{nmol}\cdot\text{mg}^{-1}\cdot\text{min}^{-1}$ obtained by subtracting the values obtained for the ActP deficient strain (Gimenez *et al.*, 2003). The specificity of this transporter was accessed by measuring radiolabeled acetate in the presence of a 50-fold higher concentrated non-labelled compound. ActP is strongly inhibited by propionate, whereas butyrate and other two or carbon α -hydroxy acids like glycolate, L-lactate and oxalate cause only weak inhibition and the dicarboxylates succinate and malate cause no inhibition. Growth in acetate (2.5 to 50 mM) is not affected in the absence of ActP revealing that this transporter is not essential to obtain an acetate utilization phenotype (Gimenez *et al.*, 2003). Characterized members of the SSS family couple the transport of solutes to an electrochemical sodium gradient. Acetate transport assays with ActP in a sodium-free buffer showed that the addition of sodium had no effect on the uptake and that the process was sensitive to CCCP, suggesting the involvement of protons as the coupling ion (Gimenez *et al.*, 2003).

The SSS family is spread amongst bacteria, archaea and eukaryotes including animals and its members vary in size possessing between 11 to 15 transmembrane domains (TM). PutP, the proline transporter of *E. coli* is arranged in 13 TMs with the N-terminal in the periplasm and the C-terminal in the cytoplasm determined by gene fusion, Cys-accessibility, gene fusion studies and EPR spectroscopy. Site-directed mutagenesis and biochemical studies have identified several residues involved both in sodium and proline binding. Another member of this family, vSGLT, the sodium/galactose symporter from *Vibrio parahaemolyticus*, has had its structure resolved to 3 Å resolution showing 14 TMD in an inward-facing occluded conformation. The structure revealed a core group of 10 helices with two additional helices at the N- and at the C- terminus arranged in an inverted topology repeat motif (Faham *et al.*, 2008). The structure revealed two discontinuous helices in the centre of the structure, TM 2 and TM 7, which might be involved in the substrate transport mechanism (Figure 12).

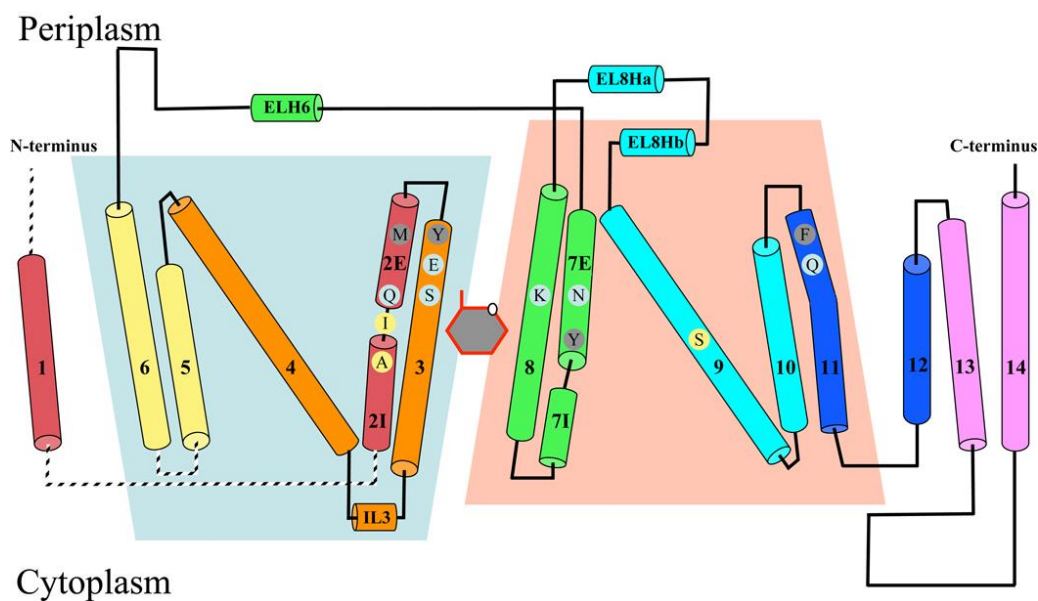


Figure 12 – Topology of vSGLT. The structure is colored as a rainbow from the N terminus (red) to the C terminus (purple). The green and orange trapeziums represent the inverted topology of TM2 to TM6 and TM7 to TM11. The gray hexagon with red trim represents galactose. Residues involved in sugar recognition, gate residues, and a proposed Na⁺ site are shown in cyan, gray, and yellow circles. (Faham *et al.*, 2008)

Galactose is bound in the center of the protomer sandwiched between two hydrophobic gates. There is a break in the first domain of each repeat (TM 1 and TM 6) with backbone polar groups presumed to interact with either the substrate or the sodium ions. The core architecture of the vSGLT is similar to the bacterial leucine/sodium symporter LeuT from

the Neurotransmitter:Sodium Symporter (NSS) Family (Krishnamurthy *et al.*, 2009; Watanabe *et al.*, 2010). This common core architecture is known as the LeuT fold and implies common features in the transport mechanism and substrate and ion binding (Krishnamurthy *et al.*, 2009; Watanabe *et al.*, 2010). During the translocation cycle in the alternating access mechanism, transporters adopt different conformations to allow movement of substrates across the membrane (Figure 13). In an outward facing conformation (T^{OUT}) the transporter binds substrate and ions and isomerizes to an inward facing conformation (T^{IN}) releasing the substrate and the ion via substrate- and ion-bound intermediate states ($T^{\text{MS}^{\text{IN}}}$ and $T^{\text{MS}^{\text{OUT}}}$) and then recycles back to the outward facing conformation (Faham *et al.*, 2008; Watanabe *et al.*, 2010).

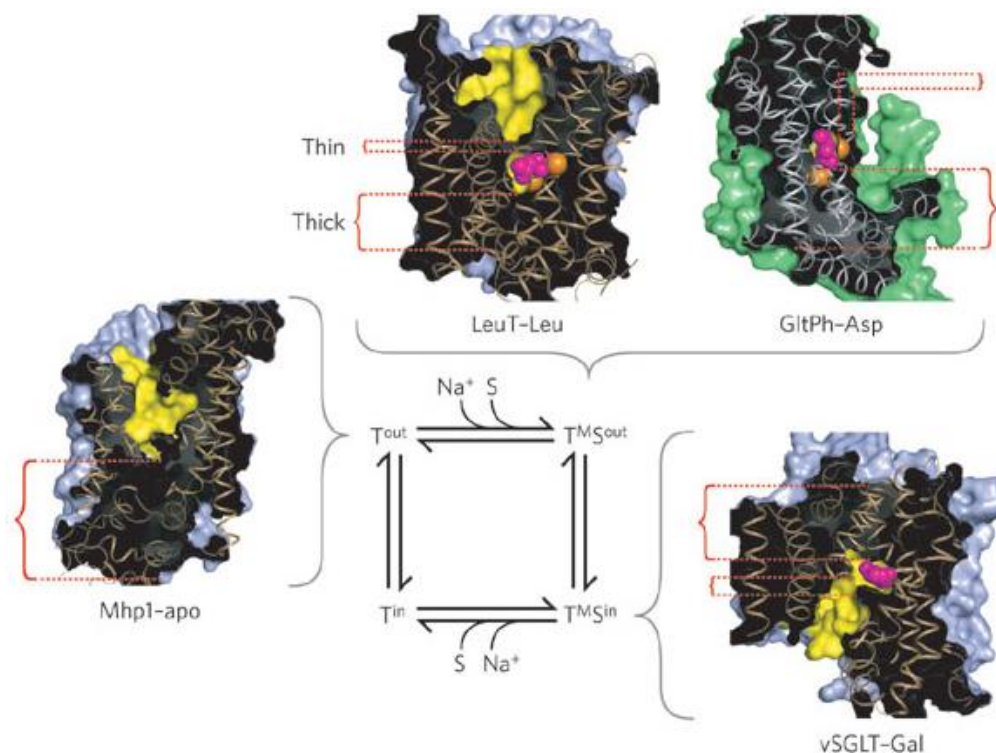


Figure 13 – Transport cycle based on an alternating-access-type mechanism together with insights from crystallographic studies. Clockwise from the T^{out} state: Mhp1-apo (PDB code 2JLN), LeuT-Leu (PDB code 2A65), GltPh-Asp (PDB code 2NWX) and vSGLT-Gal (PDB code 3DH4). Cross-sectional illustrations of the crystal structures of each transporter are shown associated with the states of the cycle they represent. The positions of the 'thin' gates and 'thick' gates are highlighted by red dashed lines. Yellow regions highlight the surfaces of the binding site and cavities that penetrate the structures. Bound ligands, shown as van der Waals spheres, are coloured magenta, with sodium ions in orange. The view of each transporter is approximately parallel to the membrane plane, with the extracellular side at the top of each figure. (Krishnamurthy *et al.*, 2009).

In the crystal structure of vSGLT TM1 is absent (Faham *et al.*, 2008). Computational modelling of the vSGLT structure with TM1 revealed the importance of a conserved residue, Tyr-19, associated with sodium binding. Replacement of this tyrosine residue in PutP by a glutamic acid or a phenylalanine revealed sodium independent binding of the substrate (Mazier *et al.*, 2011). In ActP the conserved tyrosine is replaced by a phenylalanine which might account for the observed sodium independence of this protein.

5.1.1.2 The acetate transporter SatP

The transporter SatP (or YaaH) belongs to the Acetate Uptake Transporter (AceTr) family (TCDB # 2.A.96) and is arranged in 6 putative TMDs. This family is characterized by the presence of the conserved motif N-P-[AV]-P-[LF]-G-L-x-[GSA]-F at the N-terminal part of the first potential transmembrane region being present in bacteria, archaea, fungi and protozoa. In glucose grown cells, deletion of this transporter leads to decreased uptake rates for acetic and succinic acids which is restored when *yaaH* is expressed in a strain (*E. coli* MG1693 $\Delta yaaH \Delta actP$) with residual acetate transporter activity (Sá-Pessoa *et al.*, 2013). Kinetic analysis of this transporter revealed a narrow specificity for acetic and succinic acids with affinity constants at pH 6.0 of 1.24 ± 0.13 mM for acetic acid and 1.18 ± 0.10 mM for succinic acid. This transporter is dependent on ΔpH and inhibited by the addition of CCCP suggesting that it works as a proton symporter, energetically dependent on the proton-motive force (Sá-Pessoa *et al.*, 2013). Analysis of acetate transport activity for $\Delta yaaH$ and $\Delta actP$ mutants revealed distinct physiological roles of the two acetate transporters with YaaH being more active at the exponential growth phase and ActP at the entry to stationary growth phase in high glucose concentrations (Gimenez *et al.*, 2003; Sá-Pessoa *et al.*, 2013). Furthermore, both acetate transporters ActP and SatP are relevant for acetic acid utilization with their expression increasing over time when cells are grown in acetic acid and with their deletion altering the growth pattern at high acetate concentrations (Sá-Pessoa *et al.*, 2013). Site-directed mutagenesis of this protein allowed the identification of two residues, L131 and A164, that when mutated generate an enhanced ability to transport lactate (Sá-Pessoa *et al.*, 2013) as in its yeast homologue (Kok *et al.*, 2012).

5.1.1.3 The lactate transporters LldP and GlcA

LldP and GlcA are members of the Lactate Permease (LctP) Family (TCDB # 2.A.14), a family of lactate transporters present in bacteria and archaea, with proteins composed of twelve putative transmembrane segments (Saier *et al.*, 2009).

LldP (also named LctP) is a lactate permease encoded by the *lct* locus which is involved in L-lactate utilization and contains three genes: the L-lactate dehydrogenase *lctD*, a regulatory protein *lctR* that acts both as a repressor or an activator of this *lct* locus, and the lactate permease *lctP* (Aguilera *et al.*, 2008). Aerobic growth on L-lactate induces threefold the rate of labelled L-lactate uptake and more than threefold the level of L-lactate dehydrogenase activity (Dong *et al.*, 1993).

GlcA is a glycolate permease encoded by the *glc* locus which is associated to glycolate utilization. This locus is composed of a malate synthase *glcB*, genes involved in glycolate oxidase activity *glcDEF*, a gene of unknown function *glcG* and *glcA*, the glycolate permease, organized as an operon induced by growth on glycolate (Pellicer *et al.*, 1999; Núñez *et al.*, 2001). Disruption of *glcA* leads to a reduced growth on glycolate. The uptake of glycolate is also reduced to one third of the value of the wildtype suggesting the existence of another permease for glycolate. Since GlcA and LldP share amino acid sequences with 65 % identity and 80 % similarity and belong to the same family of transporter proteins they were presumed to share substrates. In fact, in a strain disrupted in *glcA* L-lactate uptake is inhibited by glycolate in increasing concentrations. Furthermore, disruption of *lldP* leads to reduced growth and uptake of glycolate and a double mutant for *lldP* and *glcA* is unable to grow in glycolate and uptake of this acid is negligible being this phenotype reverted by introducing either LldP or GlcA (Núñez *et al.*, 2002).

Both proteins are specific for the 2-hydroxymonocarboxylates D-lactate, L-lactate and glycolate with high apparent affinities (Núñez *et al.*, 2001; Núñez *et al.*, 2002) however LldP is more efficient in concentrating L-lactate while GlcA is more efficient in concentrating glycolate (Núñez *et al.*, 2002). Both proteins are inhibited by CCCP and the co-substrate is most likely protons (Núñez *et al.*, 2002). Search for a specific D-lactate permease (Kang, 1978) revealed no specific permease other than LldP which disruption inhibits growth in D-lactate (Núñez *et al.*, 2002).

5.1.1.4 The formate transporter FocA

FocA is a member of the Formate-Nitrite Transporter (FNT) Family (TCDB # 1.A.16) that transports short-chain acids in bacteria, archaea, fungi, algae and parasites. The FocA protein was first identified by Suppmann and Sawers (1994) as an integral membrane protein with six transmembrane domains homologous to the Nitrite Uptake Permease (NirC) protein of *E. coli*. The *focA* gene is co-transcribed with *pfl* (pyruvate-formate lyase), an enzyme which is abundant in anaerobically grown *E. coli* cells and catalyses the cleavage of pyruvate to acetyl CoA and formate. *focA* is induced upon formate production by pyruvate formate lyase (PFL) during anaerobic mixed acid fermentation (Suppmann and Sawers, 1994). It is also activated upon overproduction of the fumarate nitrate regulator (FNR) aerobically (Reyes-Ramírez and Sawers, 2006). The transcription of this operon is regulated by three promoters located at the 5' prime of the operon and from four operon-internal transcripts located at the *focA* sequence and one at the intergenic region between *focA* and *pfl*. Formate is an uncoupler of the trans-membrane potential therefore its levels have to be tightly controlled by the cell. However, the levels of FocA protein are low and overproduction is lethal in *E. coli*. A tight regulation and/or processing of this operon allow differential levels of FocA and Pfl regulating the amount of formate at a given time (Sawers, 2005). Inactivation of FocA leads to resistance to hypophosphite (a toxic analogue of formate). Fermenting *E. coli* cells first export passively formate which accumulates in the culture supernatants, but once the medium pH drops below 6.8, formate is actively imported. A FocA mutant excretes approximately 50 % less formate compared to the wild type and has increased intracellular levels of formate (Suppmann and Sawers, 1994).

Crystal structures of FocA from *E. coli*, *Salmonella typhimurium* and *Vibrio cholera* revealed that FocA is organized in homopentamers. Each monomer has 6 transmembrane segments organized in two internal structural repeats, with a pseudo two fold symmetry between TM1-3 and TM4-6 as shown in Figure 14 (Wang *et al.*, 2009; Waight *et al.*, 2010).

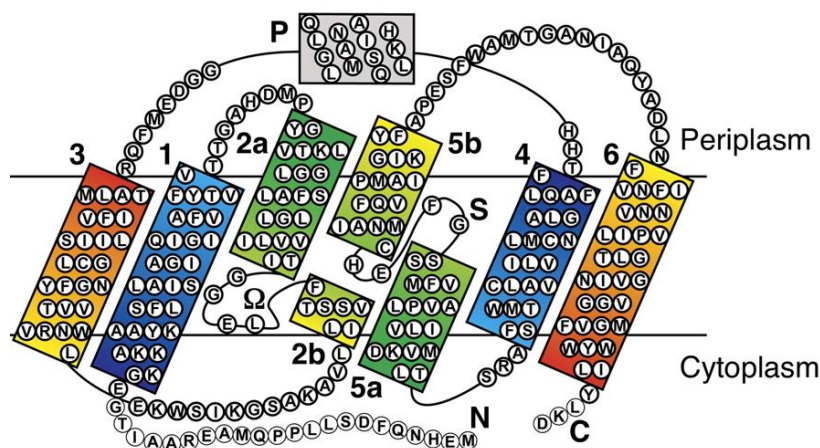


Figure 14 – Topology diagram of FocA. Transmembrane helices (TM) are numbered from TM1 to TM6. TMs in each half of the protein, TM1-3 and TM4-6, are coloured from blue to green to red sequentially, highlighting the structurally inverted repeats. The segment that connects TM2a and TM3 is designated as the Ω loop. The short helix with loop L3-4 on the periplasmic side is designated as the P helix. (Waight *et al.*, 2010)

Each protomer has an amphipathic axial passage perpendicular to the lipid membrane pane and the pentamer has a central hydrophobic pore with an acidic stem and positive charges at the cytoplasmic side. The channel is lined by highly conserved residues, L89, V175 and H209 in the hydrophilic side and F75 and F202 in the hydrophobic side, which might act as the selectivity filter (Wang *et al.*, 2009). The structure of FocA depicted in Figure 15A resembles the ones for the aquaporin family of proteins although aquaporins are structurally organized in tetramers. Reconstitution in proteoliposomes revealed that FocA is relatively impermeable to water and is permeable to formate, being only structurally but not functionally related to aquaporins (Wang *et al.*, 2009).

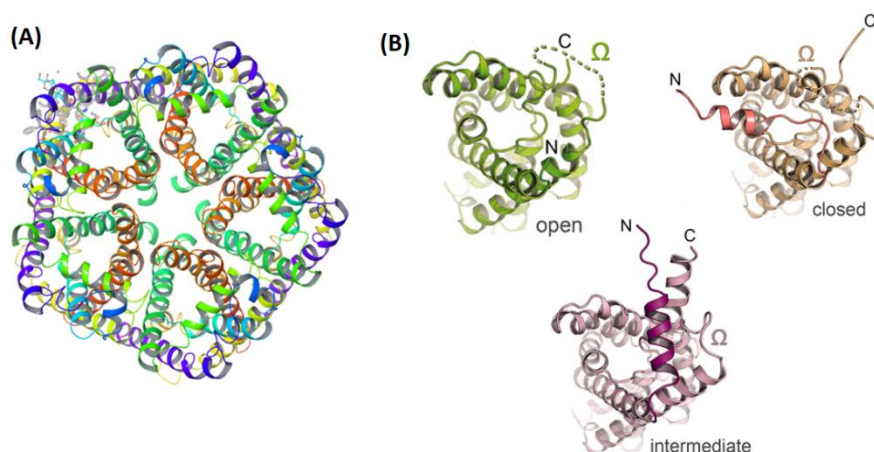


Figure 15 – Structure of the formate transporter FocA. (A) Pentameric structure of the FocA channel (DOI:10.2210/pdb3kcu/pdb) treated with PyMol. (B) Conformational changes in FocA. The three states observed in the protomers of the pentameric channel in the open, intermediate, and closed forms. Structural

changes are restricted to the N-terminal helix, the C-terminus and the Ω loop. In the open state the 3 segments are disordered, in the intermediate state the Ω loop is ordered and in the closed state the N-helix covers the substrate channel while the Ω loop and the C terminus are disordered (Adapted from Lü *et al.*, 2011).

Electrophysiological studies revealed that FocA is pH dependent, acting as a specific channel for anionic formate at high pH. The N-terminus of the protein acts as gate dependent on pH reorienting to allow the passage of the substrate. If the N-terminus is disordered, the channel acquires an open conformation and is completely accessible to the substrate. The N-terminus can form a helix that narrows the channel (intermediate conformation) or completely cross the entrance of the channel blocking the accessibility of the substrate (closed conformation). The conformation of the N-terminus influences the order state of a loop that connects TM2 and TM3, termed the Ω -loop, which structural flexibility allows the rearrangement of the channel allowing the gating of the substrate (Figure 15B). In the open conformation the N-terminus and the Ω -loop are in the disordered state allowing the passage of the substrate but interactions of the N-terminus lead to the ordering of this loop, narrowing the channel (intermediate state). Movement of the N-terminus to cover the channel breaks this interaction and the loop is disordered closing the channel as depicted in Figure 15B (Lü *et al.*, 2011). Molecular simulations of the structures of FocA from *E. coli* and *S. typhimurium* showed that the highly conserved residue His209, with its side chain aligned with the channel passage and pointing to the cytoplasmic side, could be easily protonated and therefore important in channel activity (Feng *et al.*, 2012). In fact, when this residue is unprotonated (high pH), the channel is open through the movement of a pair of protomers, while when it is protonated (low pH), His209 interacts with Asn262 and the channel narrows diminishing formate movements across FocA (Feng *et al.*, 2012). Molecular simulations also revealed that there is a concerted movement of the N-helix of pairs of protomers (Figure 16) with the other pair of protomers maintaining their conformations (Feng *et al.*, 2012). This cooperative mode of action is consistent with the studies of the gating mechanism in aquaporins (Feng *et al.*, 2012). Electrophysiological studies at different pH values showed that the permeability of FocA for formate dropped at pH 5.6, showing that in fact gating occurs at specific pH values, supporting the cooperativity between protomers and the role of His 209 in this event with a H209F mutant showing no current (Lü *et al.*, 2012).

The electrophysiological recordings at high pH showed that FocA is able to export the products of mixed-acid fermentation, with an affinity (K) for formate of 11.7 ± 0.1 mM, for acetate of 23.9 ± 1.7 mM and lactate of 96.0 ± 14.4 mM. Pyruvate, a product of glycolysis, was also recognized by FocA with an affinity close to the one obtained for formate (K of 11.6 ± 1.9 mM) but with a lower conductance (Lü *et al.*, 2012). In vivo studies showed that FocA has a strong preference for formate rather than the other products of mixed-acid fermentation. Increasing the levels of FocA does not alter the export of acetate, succinate or formate (the only reimported acid). On the other hand, the absence of FocA leads to reduction on the excretion of acetate and to accumulation of lactate since the excess pyruvate is exported as lactate (Beyer *et al.*, 2013).

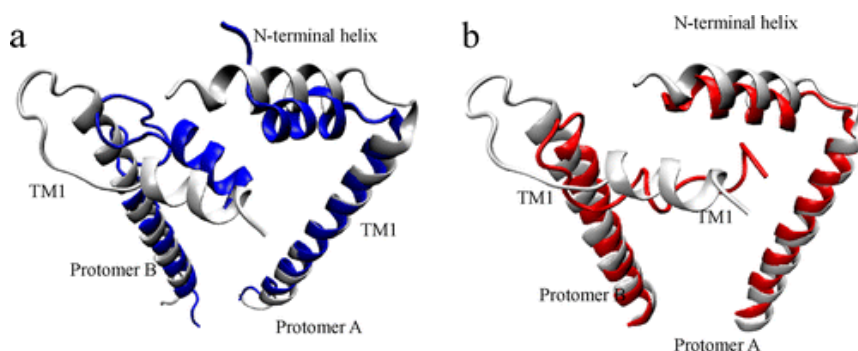


Figure 16 – Representation of the concerted movement of the N-terminal helices of protomers A and B, which eventually opens the transport channel of protomer B at neutral/high pH. Crystal structure of StFocA at pH 4.0 (gray) and structures of StFocA equilibrated by molecular dynamics at (a) neutral/high pH, unprotonated His209 (blue) and (b) low pH, protonated His209 (red). (Feng *et al.*, 2012)

5.1.1.5 Other monocarboxylate transporters

Specific transport systems have also been identified for other monocarboxylates such as pyruvate (Lang *et al.*, 1987) and propionate (Kay, 1972) although the proteins accomplishing these functions have not been identified.

Propionate is taken up by *E. coli* cells by a saturable transport system with an affinity constant of 0.22 mM, being competitively inhibited by acetate (Kay, 1972).

E. coli cells lacking the two main routes for pyruvate metabolism are able to accumulate pyruvate against a concentration gradient. The uptake of pyruvate is strongly inhibited upon treatment of these cells with CCCP and other uncouplers, suggesting that the uptake of pyruvate is dependent on metabolic energy. Pyruvate transport has an affinity constant (K_m) of 18-19 μ M being non-competitively inhibited by acetate, succinate and malate and competitively inhibited by alanine, lactate and 3-bromopyruvate with inhibition constants

of 8.0 mM, 7.5 mM and 0.025 mM, respectively, indicating that only 3-bromopyruvate is a physiological inhibitor of the pyruvate transport system (Lang *et al.*, 1987). Recently, Kreth and co-workers (2013) further characterized the transport of pyruvate using the toxic analog 3-fluoropyruvate. They have isolated a pyruvate transport negative mutant, showing a constitutive transport system (PrvT) as previously described by Lang and co-workers (1987). A revertant of this mutant showed an inducible pyruvate transport system (Usp). The double mutant still accumulated pyruvate in the growth medium suggesting the presence of a pyruvate excretion system. None of these systems were further identified and characterized (Kreth *et al.*, 2013).

5.1.2 Di- and tri-carboxylate transporters

Dicarboxylate transport occurs through exchange, uptake or efflux and depending on aerobic or anaerobic growth conditions different transporters are expressed (Figure 17). In aerobiosis DctA and DauA are the carriers responsible for dicarboxylates uptake (Davies *et al.*, 1999; Karinou *et al.*, 2013) while in anaerobiosis exchange of dicarboxylates occurs through DcuAB (Six *et al.*, 1994; Zientz *et al.*, 1996). Succinate efflux is carried out through DcuC (Zientz *et al.*, 1996; Zientz *et al.*, 1999) and CitT catalyses citrate: succinate antiport (Pos *et al.*, 1998).

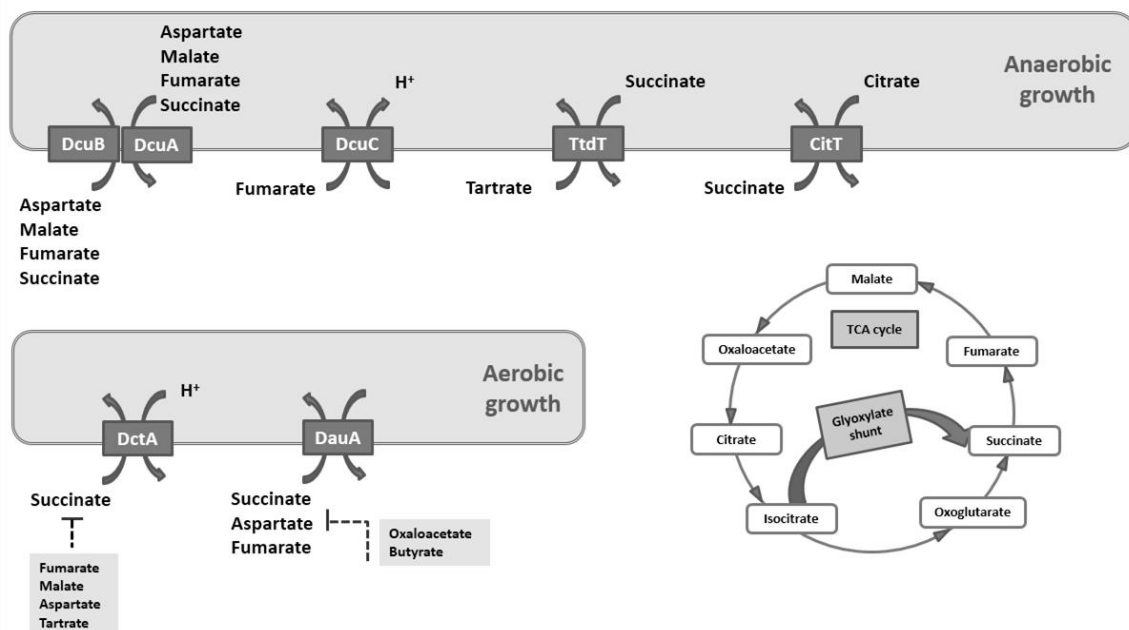


Figure 17 – Dicarboxylic acid transporters in *E. coli*. Depiction of the tricarboxylic acid cycle and of the transporters of di- and tricarboxylates expressed in both aerobic and anaerobic growth in *E. coli*.

5.1.2.1 DctA

DctA is an aerobic dicarboxylate transporter belonging to the Dicarboxylate/Amino Acid:Cation (Na⁺ or H⁺) Symporter (DAACS) Family (TCDB # 2.A.23) with 14 putative transmembrane segments.

E. coli cells accumulate succinate against a concentration gradient dependent on the electrochemical proton gradient through DctA with a K_m of $25 \pm 5 \mu\text{M}$ being competitively inhibited by fumarate, malate, aspartate and tartrate (Kay and Kornberg, 1971; Lo *et al.*, 1972; Karinou *et al.*, 2013). The cyclic monocarboxylate orotate is also a substrate of DctA (Baker *et al.*, 1996). The system is induced by succinate and repressed by glucose (Kay and Kornberg, 1971; Lo *et al.*, 1972). This aerobic succinate transport system is composed of 3 genes: *cbt*, a periplasmic binding protein and *dctA* and *dctB*, integral membrane proteins (Six *et al.*, 1994). Mutations in the *dct* system impair the ability to uptake, oxidise or grow in succinate although the mutants still use succinate at a reduced rate (Kay and Kornberg, 1969). The deletion of *dctA* impairs growth of *E. coli* on malate and fumarate which is restored upon complementation with a plasmid expressing *dctA*. The growth on succinate by this mutant is only reduced but not impaired since there is another succinate transport system with lower affinity in *E. coli* (Davies *et al.*, 1999). The deficiencies in fumarate growth are due to a reduced transport activity with a *dctA* mutant having no uptake activity for fumarate, being this activity restored upon *dctA* complementation in a plasmid. The wild type strain shows high level of fumarate transport activity being inhibited by unlabelled fumarate but not lactate, pyruvate or acetate. Furthermore, succinate transport activity is reduced 10-fold in a *dctA* mutant, explaining the reduced growth in this carbon source (Davies *et al.*, 1999).

The *dctA* gene is regulated in a growth-dependent manner having higher expression in the stationary growth phase, induced by the transcriptional activator cAMP-CRP. It is subject of CRP-mediated catabolite repression, being inhibited in the presence of glucose and induced in the presence of the C₄-dicarboxylates succinate, aspartate, fumarate, malate or maleate and by the tricarboxylate citrate, but not by the monocarboxylates lactate or pyruvate. This induction by C₄-dicarboxylates occurs in a DcuS-DcuR-dependent manner. The repression by glucose is not surpassed by adding succinate, suggesting that the CRP-mediated expression is stronger than expression activated by the substrate. In anaerobiosis, *dctA* expression is repressed by ArcA. Furthermore, DctA regulates its own expression repressing its own synthesis in the absence of the substrate (Davies *et al.*, 1999).

5.1.2.2 DauA

DauA is an aerobic succinate transporter belonging to the Sulfate Permease (SulP) Family (TCDB # 2.A.53) with 10 predicted transmembrane domains.

Growth in succinate at pH 5.0 is inhibited in the absence of *dauA*, while at pH 7.0 one can observe a growth inhibition both in a Δ *dauA* as well as in a Δ *dctA* and in a double mutant Δ *dauA* Δ *dctA* (Karinou *et al.*, 2013). The DauA protein is expressed both in cells grown in succinate at pH 5.0 as well as pH 7.0 while DctA is only present at pH 7.0 being DauA the main transporter at pH 5.0 with an apparent K_m of 0.56 ± 0.15 mM, weaker affinity and lower apparent transport rate than DctA (Janausch *et al.*, 2001; Karinou *et al.*, 2013). DauA is able to transport both the mono and di-carboxylate forms of succinate explaining the activity at both pHs while DctA only transports the dicarboxylate form (Karinou *et al.*, 2013). This transporter is strongly inhibited by aspartate or fumarate but also by oxaloacetate and butyrate at a lesser extent (Janausch *et al.*, 2001; Karinou *et al.*, 2013). Aspartate and fumarate were confirmed as real substrates of DauA by performing radiolabeled uptake assays with both compounds (Karinou *et al.*, 2013).

DauA expression, unlike DctA, is not dependent on the DcuSR system in response to carboxylic acids. This protein besides being a transporter seems to be involved in the regulation of the expression of DctA since in the absence of DauA, DctA shows diminished activity and expression, probably through its STAS domain that functions as sensors or transcription factors in other proteins (Karinou *et al.*, 2013).

5.1.2.3 DcuA and DcuB

DcuA and DcuB function as anaerobic antiporters of aspartate, malate, fumarate and succinate. These proteins share 36 % sequence identity and 65 % similarity and are grouped in the C₄-Dicarboxylate Uptake (Dcu) Family (TCDB # 2.A.13) with 12 putative transmembrane segments (Six *et al.*, 1994; Janausch *et al.*, 2002).

Whole cells of *E. coli* grown anaerobically accumulate fumarate and succinate and C₄-dicarboxylates fumarate, succinate, malate, maleinate, aspartate and oxaloacetate cause rapid extrusion of internal fumarate. Export of one of the substrates drives the accumulation of the other pointing to an antiport system when cells are in anaerobic conditions functioning in fumarate respiration (Engel *et al.*, 1992). This system is inactivated in the presence of oxidizing agents and reactivated by reducing agents (Engel

et al., 1992). In terms of substrate charge there is not a clear preference between substrate species and depending on the pH both mono (at pH 6.0) and divalent (pH between 6.0 and 9.0) fumarate is accepted by the system (Engel *et al.*, 1994). This antiport system is electroneutral and is not responsive to the dissipation of the membrane potential (Engel *et al.*, 1994). Both DcuA and DcuB are capable of exchange and uptake of C₄-dicarboxylates with a preference for the exchange mode (Engel *et al.*, 1994; Zientz *et al.*, 1996). The Dcu system is involved in the uptake of fumarate in glucose anaerobically grown cells, depending on the proton motive force, and can catalyse the reverse reaction and efflux fumarate without exchange by other C₄-dicarboxylate (Engel *et al.*, 1992; Engel *et al.*, 1994). Both activities are repressed in the presence of oxygen and nitrate and are activated in the presence of the anaerobic transcriptional regulator FNR (Engel *et al.*, 1994).

Studies with wild type cells and single *dcuA* and *dcuB* mutants showed that these two transport systems have similar activities being the loss of one compensated by increased activity of the other (Six *et al.*, 1994). They have similar substrate specificity accepting aspartate, malate, fumarate, succinate and maleate (Six *et al.*, 1994). However DcuA shows reduced malate transport (Six *et al.*, 1994). Inactivating both *dcuA* and *dcuB* has no effect on the aerobic uptake of dicarboxylates through *dctA* (Six *et al.*, 1994). The DcuAB system is essential in fumarate:succinate exchange supporting growth by fumarate respiration with DcuB showing the highest rate of antiport activity (Six *et al.*, 1994; Zientz *et al.*, 1996).

The gene *dcuA* is located downstream of the aspartase gene *aspA* while *dcuB* is upstream of the anaerobic fumarase gene *fumB* with both *aspA* and *fumB* possessing promoter binding sites for FNR (transcriptional regulator essential in anaerobiosis) and CRP (cyclic AMP receptor protein that mediates catabolite repression) (Six *et al.*, 1994). The gene *dcuA* is expressed constitutively both in aerobic and anaerobic conditions, with lower expression in aerobiosis, while *dcuB* is expressed anaerobically, dependent on FNR, and is repressed in the presence of nitrate by the nitrate/nitrite response regulator protein NarL (Golby *et al.*, 1999). Furthermore, *dcuB* is subject to moderate catabolite repression through CRP and induced by the presence of the C₄-dicarboxylates fumarate, malate, aspartate, succinate and maleate (Golby *et al.*, 1999).

The expression of *dcuB* requires transcriptional activation by the dicarboxylate sensor and regulator DcuS-DcuR while *dcuA* is independent of this sensor. Inactivating DcuB causes constitutive expression DcuS-DcuR dependent genes in the absence of C₄-

dicarboxylates, meaning that DcuB also plays a regulatory role, independent of the transport role, possessing residues that play a specific role in this regulation, namely Thr394 and Asp398 (Kleefeld *et al.*, 2009).

The DcuA is organized into 10 predicted transmembrane domains arranged as two groups of five helices connected by a large cytoplasmic loop with N- and C-terminus located in the periplasm (Golby *et al.*, 1998; Bauer *et al.*, 2011). DcuB on the other hand is organized in 12 transmembrane domains with N- and C-terminal periplasmic termini revealed by cysteine scanning and AMS accessibility (Bauer *et al.*, 2011).

Several residues were identified both by random and site-directed mutagenesis in DcuB as essential for the regulatory and transport function. Residues K353, T394 and D398 are involved in the regulation of DcuS-DcuR, with specific mutations leading to fumarate independent expression but no loss of anaerobic growth in fumarate or transport activity. Residues E79, R83 and R127 are crucial for succinate uptake and strongly decrease growth in glycerol plus fumarate, meaning that the fumarate respiration system is not functioning. These residues are conserved in the DcuA and DcuB proteins while the residues important for regulation are only conserved in DcuB proteins and are located at the large cytoplasmic loop that is specific to DcuB. Mutations in residues D119 and D405 lead to low amounts of DcuB in the membrane affecting both the regulatory and transport functions of this protein. The residues identified as being crucial for regulation are mostly at the C-terminus of DcuB while the residues critical for transport are concentrated at the N-terminus (Kleefeld *et al.*, 2009).

5.1.2.4 DcuC

The DcuC protein is the sole characterized member of the C₄-dicarboxylate Uptake C (DcuC) Family (TCDB # 2.A.61).

A strain with inactivated *dcuA* and *dcuB* is capable of anaerobic growth in glycerol plus fumarate being able to grow on fumarate respiration using DcuC. A triple mutant with inactivated *dcuA*, *dcuB* and *dcuC* is unable to grow by fumarate respiration. The DcuC carrier like the other Dcu proteins catalyses the electroneutral exchange of C₄-dicarboxylates as well the uptake of dicarboxylates using the proton gradient with lower transport activities (Zientz *et al.*, 1996; Zientz *et al.*, 1999).

The *dcuC* carrier gene is expressed with high activities in anaerobiosis dependent on the transcriptional regulator FNR but repressed in the presence of oxygen. Glucose does not influence the expression of this carrier. Fumarate and other C₄-dicarboxylates increase

DcuC expression, independent of the fumarate respiration regulator DcuR, and electron acceptors such as nitrate slightly repress it (Zientz *et al.*, 1999).

Fumarate uptake by DcuAB is increased when DcuC is inactivated suggesting a role of DcuC in succinate efflux. DcuC is also able to compensate for DcuAB activities when overexpressed suggesting that the Dcu carriers have overlapping functions to enable a more efficient fumarate respiration (Zientz *et al.*, 1999).

5.1.2.5 TtdT

The L-tartrate:succinate exchanger TtdT belongs to the Divalent Anion:Na⁺ Symporter (DASS) Family (TCDB # 2.A.47), also denominated the SLC13 family. This family is divided into two groups: the Na⁺-sulfate (NaS) cotransporters and the Na⁺-carboxylate (NaC) cotransporters. TtdT belongs to the NaC cotransporters which have a substrate preference for Krebs cycle intermediates (di- or tricarboxylates).

The deletion of *ttdT* impairs L-tartrate fermentation and is essential for anaerobic growth in L-tartrate however it doesn't affect anaerobic growth on fumarate plus glycerol. In a strain lacking the known dicarboxylate transporters (Dcu, Dct, CitT) and TtdT, uptake of tartrate is not impaired but succinate uptake is significantly lower, probably due to alternative carriers for tartrate. TtdT is induced by tartrate and repressed by glucose, being this effect more pronounced in succinate rather than tartrate uptake. The high tartrate uptake background activity after deletion of *ttdT* suggests that there is another carrier fulfilling this function but it is not an antiporter. The activity of this antiporter in L-tartrate grown cells is maximum at neutral pH (pH 7.0 to 8.0) and follows a Michaelis-Menten kinetics with a K_m of 700 μM tartrate and 400 μM succinate and a V_{\max} of 110 $\mu\text{mol}\cdot\text{min}^{-1}\cdot\text{g}^{-1}$ dry weight for tartrate and 16 $\mu\text{mol}\cdot\text{min}^{-1}\cdot\text{g}^{-1}$ dry weight for succinate. This transporter is rather specific for L-tartrate uptake and succinate efflux being the reverse reaction (L-tartrate efflux and succinate uptake) 13 fold less efficient (Kim and Unden, 2007).

The *ttdT* gene is located downstream of the *ttdA* and *ttdB* genes which encode for the L-tartrate dehydratase that converts L-tartrate to oxaloacetate which is further converted into succinate through fumarate respiration (Kim *et al.*, 2009). The operon *ttdABT* is regulated by the LysR-type regulator TtdR which is subject also to positive autoregulation (Kim *et al.*, 2009). Expression of this operon is induced in the presence of L- and meso-tartrate and repressed by O₂ and nitrate (Kim *et al.*, 2009). The enzymes fumarase B and fumarate reductase required for L-tartrate fermentation as well as fumarate respiration are

regulated by DcuS-DcuR. The DcuS-DcuR system also confers positive regulation to TtdR in response to C₄-dicarboxylates. Both TtdR and DcuS seem to control both the uptake and metabolism of L- and *meso*-tartrate and the two different regulators independently regulate the pathways for L-tartrate fermentation and for a more general C₄-dicarboxylate metabolism. The L-tartrate metabolism is therefore physiologically separated from general C₄-dicarboxylate metabolism although L-tartrate also ends up in fumarate respiration (Kim *et al.*, 2009).

D-tartrate which is a minor form of tartrate in nature, enters cells through DcuB being this transporter essential for anaerobic growth on D-tartrate in the presence of an electron donor such as glycerol (Kim *et al.*, 2007). Both DcuB and TtdT have stereoisomer specificity for D- and L-tartrate, with DcuB only accepting the hydroxyl groups at C2 and C3 of the D-tartrate form (*S*-configuration) while TtdT only accepts L-tartrate (*R*-configuration) (Kim *et al.*, 2007).

5.1.2.6 CitT

The citrate:succinate antiporter CitT is also a member of the Divalent Anion:Na⁺ Symporter (DASS) Family (TCDB # 2.A.47) and shares 40 % sequence identity with L-tartrate:succinate exchanger TtdT. This protein consists of 497 amino acids arranged in 12 putative transmembrane helices (Pos *et al.*, 1998).

In aerobic growth conditions, *E. coli* strains are unable to use citrate due to the lack of a citrate transport system. However, in anaerobic conditions this bacterium can use citrate as long as an oxidizable substrate is present to provide the reducing power for the conversion of citrate to succinate and acetate (Lütgens and Gottschalk, 1980). Pos and colleagues (1998) described CitT as a sodium independent antiporter with broad specificity for C₄-dicarboxylates and tricarboxylates. CitT expressing cells uptake [1,5-¹⁴C]citrate with an initial rate of 1.4 nmol min⁻¹ mg protein⁻¹ independent of sodium. Addition of succinate or citrate leads to the efflux of the radiolabeled citrate accumulated inside the cell with an initial rate of 3.7 nmol min⁻¹ mg protein⁻¹. Addition of fumarate also leads to efflux of citrate although at a lower rate. Uptake of tartrate was also measured in cells expressing CitT with addition of citrate leading to complete efflux of tartrate, being efflux faster than uptake of tartrate. The higher rates of efflux compared to uptake observed suggest that CitT works as an exchanger (Pos *et al.*, 1998).

The transporter CitT is encoded in an operon *CitABCDEFXGT*. This operon includes the subunits of citrate lyase, *citDEF*, the citrate lyase synthetase, *citC*, a synthase that

catalyzes the synthesis of the citrate lyase prosthetic group, *citG*, and a transferase, *citX*, which leads to the conversion of the acyl carrier protein of citrate lyase into its active form (Pos *et al.*, 1998; Schneider *et al.*, 2000). It is also composed of a sensor kinase, *citA*, and a response regulator, *citB* which are responsible to regulate the genes involved in anaerobic citrate fermentation. In the presence of citrate, *citAB* induce the transcription of the genes *citCDEFXGT* in the absence of oxygen and nitrate. CitA/CitB expression is modulated by the system DcuS/DcuR (Yamamoto *et al.*, 2009; Scheu *et al.*, 2012).

5.2 A gram-positive bacterium: *Corynebacterium glutamicum*

C. glutamicum is a Gram-positive, non-motile, aerobic, rod-shaped bacterium. Because it is a soil organism it can grow on several substrates including sugars, alcohols, amino acids and carboxylates (Jolkver *et al.*, 2009). Growth of carboxylates such as acetate, lactate, pyruvate and succinate suggest the presence of transport systems for these substrates (Ebbighausen *et al.*, 1991; Wendisch *et al.*, 2000; Inui *et al.*, 2004). Bioinformatic approaches predict that *C. glutamicum* possesses 14 transporters (Figure 18) with predicted substrate specificity for carboxylates (Winnen *et al.*, 2005).

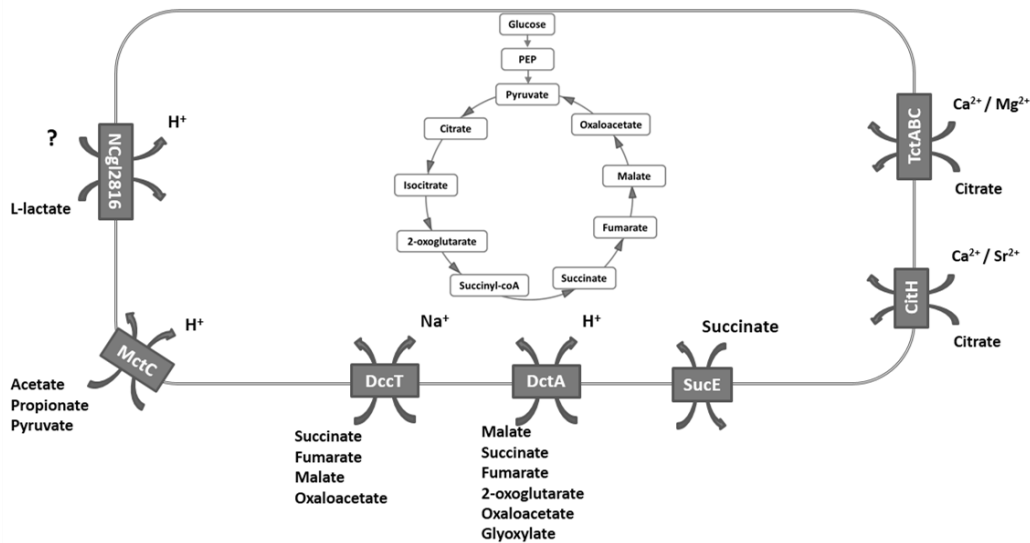


Figure 18 – Carboxylate transporters in *C. glutamicum*. From the 14 transporters from *C. glutamicum* with predicted specificity for carboxylates, only 7 have their specificity physiologically demonstrated.

5.2.1 Monocarboxylate uptake

C. glutamicum is able to grow in the monocarboxylates acetate, pyruvate and lactate. A mutant library of *C. glutamicum* was used to identify the putative monocarboxylate

transporter by growth on pyruvate (low membrane permeability). This experiment led to the identification of *mctC* which when lacking in cells leads to severely impaired growth on pyruvate and no pyruvate uptake measurable at pH 6.0 (Jolkver *et al.*, 2009). This mutant was also affected in acetate and propionate uptake with the measurable activity being attributed to diffusion across the membrane (Jolkver *et al.*, 2009). MctC is a transporter composed of 551 amino acids arranged into 12 to 13 transmembrane span domains, depending on the prediction algorithm, that belongs to the Solute:Sodium Symporter (SSS) Family (TCDB # 2.A.21).

Pyruvate-grown cells at pH 6.0 show a saturable kinetics for pyruvate uptake with a maximum activity of 5.6 ± 0.6 nmol pyruvate min^{-1} mg dry weight $^{-1}$, a $K_{0.5}$ of 250 ± 55 μM pyruvate and a Hill coefficient of 2.13 ± 0.6 . The pyruvate uptake activity is strongly dependent on external pH being maximum at pH 7.0 and with higher pH having lower uptake values being only 15 % at pH 9.0. Acetate or acetate and propionate-grown cells show saturable uptake of labelled acetate and propionate at pH 8.0 (Jolkver *et al.*, 2009). At this pH the diffusion component is clearly distinguishable from the uptake component (Ebbighausen *et al.*, 1991). A Hill coefficient of 1.30 ± 0.15 and 3.65 ± 1.07 were found for acetate and propionate, respectively, with V_{max} values of 143 ± 4 and 14 ± 0.8 nmol min^{-1} mg dry weight $^{-1}$ and $K_{0.5}$ values of 31 ± 2.1 μM acetate and 9 ± 0.7 μM propionate (Jolkver *et al.*, 2009). At alkaline conditions MctC is essential for this uptake activity. MctC is therefore an acetate and propionate proton symporter presenting as an additional substrate pyruvate.

The *mctC* gene is cotranscribed with *cg0952*, a small membrane protein of unknown function which might represent a subunit of the transporter. The promoter region of this operon contains binding sites for RamA and RamB, transcriptional regulators. RamA acts as an activator of expression and RamB exerts a weak negative control of expression in the presence of glucose, acetate and pyruvate. *mctC* expression is induced in the presence of the substrates being regulated by the carbon source in the media (Jolkver *et al.*, 2009). This transporter is an advantage in natural conditions where the substrate is limiting since it allows the fast utilization of acetate, propionate and pyruvate uptake, permitting cell growth.

Despite recognizing other monocarboxylates the MctC transporter is not responsible for L-lactate uptake and *C. glutamicum* is also able to grow on L-lactate as sole carbon and energy source (Stansen *et al.*, 2005). A candidate to accomplish this function is the protein NCgl2816 which codes for a putative permease of the Major Facilitator Superfamily co-

transcribed with the L-lactate dehydrogenase *lldD* (Stansen *et al.*, 2005; Georgi *et al.*, 2008). This operon is induced by L-lactate and regulated by the FadR-type regulator LldR (Stansen *et al.*, 2005; Georgi *et al.*, 2008). Upon introduction of *lldD*, a strain inactivated in *NCgl2816* regains the ability to grow on lactate suggesting that other L-lactate transporters exist in *C. glutamicum* (Stansen *et al.*, 2005). In fact, transcriptome analysis of L-lactate-grown cells showed high levels of the putative permeases NCgl2713 and NCgl2965 (Stansen *et al.*, 2005).

5.2.2 Dicarboxylate uptake and export

Two different transporters for C₄-dicarboxylates were identified in *C. glutamicum*: DccT and DctA which are required at high levels of expression for growth in succinate, fumarate and L-malate (Youn *et al.*, 2008; Youn *et al.*, 2009). Mutants able to grow on succinate depend primarily on *dccT* while appearance of mutants able to grow on L-malate depend either on *dccT* or *dctA* (Youn *et al.*, 2009).

5.2.2.1 DccT (DcsT)

Isolation of mutants able to grow on fumarate and succinate as sole carbon and energy source lead to the identification of DccT, the dicarboxylic acid corynebacterial transporter also named DcsT, that belongs to the Divalent Anion:Na⁺ Symporter (DASS) Family (TCDB # 2.A.47).

Disruption of *dccT* leads to impaired aerobic growth on succinate, fumarate and malate as sole carbon and energy sources while its overexpression enhances the utilization of these dicarboxylates (Teramoto *et al.*, 2008). Uptake of fumarate and succinate in the wild type *C. glutamicum* strain is very low while in the DccT-overexpressing strain, after subtracting the values obtained for the wild type, a saturation kinetics was observed with a $K_{0.5}$ of $30 \pm 4 \mu\text{M}$ for succinate and of $79 \pm 7 \mu\text{M}$ for fumarate. Cooperative binding of the substrate was suggested since a Hill coefficient greater than 1.5 was determined for both substrates (2.2 ± 0.7 for succinate and 2.4 ± 0.5 for fumarate). In the case of malate the affinity for the substrate was around 10 times lower with a $K_{0.5}$ of $361 \pm 87 \mu\text{M}$ L-malate and a Hill coefficient of 1.3 ± 0.2 . The maximum rate of transport was between 30 and 35 $\text{nmol min}^{-1} \text{mg dry weight}^{-1}$ for all cases (Youn *et al.*, 2008). Inhibition assays have shown that this protein also transports oxaloacetate with low affinity (Youn *et al.*,

2008). DccT uptake is dependent on the presence of Na⁺ ions and on the membrane potential having an optimum pH around 8.5 (Ebbighausen *et al.*, 1991; Youn *et al.*, 2008). Expression of the *dccT* gene is dependent on the growth phase being induced in the early exponential growth phase and repressed from the mid-exponential phase. This expression has little enhancement in the presence of succinate and is repressed by glucose (Teramoto *et al.*, 2008).

5.2.2.2 DctA

Isolation of *C. glutamicum* mutants able to grow on L-malate as sole carbon source lead to the identification of the transporter DctA which belongs to the Dicarboxylate/Amino Acid:Cation (Na⁺ or H⁺) Symporter (DAACS) Family (TCDB # 2.A.23).

DctA mediates malate uptake with a V_{\max} of 41 ± 1.6 nmol min⁻¹ mg dry weight⁻¹ and a K_m of 561 ± 46 μ M when overexpressed while in the wild type *C. glutamicum* a V_{\max} of 91 ± 3 nmol min⁻¹ mg dry weight⁻¹ and a K_m of 736 ± 40 μ M L-malate is observed. The uptake of L-malate was affected by pH but not upon the addition of the ionophore valinomycin suggesting that the driving force of DctA is the proton potential (Youn *et al.*, 2009). Overexpression of DctA also increased fumarate and succinate activities with K_m values of 218 ± 69 μ M for succinate and 232 ± 28 μ M for fumarate. Inhibition assays showed that besides fumarate, malate and succinate, DctA also accepts 2-oxoglutarate and oxaloacetate (intermediates of the TCA cycle) and glyoxylate (Youn *et al.*, 2009). Given that DctA has lower affinity for succinate, fumarate and malate than DccT, and that the presence of DccT is sufficient to elicit utilization of these substrates when added to complex media, the physiological role of DctA is not clearly understood. Knowledge on the expression profile of this transporter is also scarce since the conditions that elicit expression of its homologue proteins don't promote *C. glutamicum* DctA expression (Youn *et al.*, 2009).

5.2.2.3 SucE – Succinate export

The SucE protein consists of 539 amino acid residues arranged in 10-12 putative transmembrane domains with a large central cytoplasmic loop. It belongs to the Aspartate:Alanine Exchanger (AAEx) Family (TCDB # 2.A.81).

In cells lacking SucE there is increased concentration of internal succinate and a lower excretion of succinate (Huhn *et al.*, 2011). Other systems for succinate export must exist

in *C. glutamicum* since the inactivation of *sucE* did not inhibit succinate production entirely and there is an adjustment of succinate steady levels in this species (Huhn *et al.*, 2011). This gene is induced under microaerobic conditions and its overexpression increases succinate production under anaerobic conditions (Fukui *et al.*, 2011). Furthermore, deletion of *sucE* leads to an intracellular accumulation of succinate and other glycolytic metabolites due to the failed capacity to export succinate (Fukui *et al.*, 2011).

Purification of this protein and reconstitution into proteoliposomes demonstrated counterflow and self-exchange activities for succinate with an exchange rate of 2.4 nmol min⁻¹ mg protein⁻¹ (Fukui *et al.*, 2011).

5.2.3 Citrate uptake – CitH and TctABC

Transcriptome analysis of *C. glutamicum* citrate-grown cells and on citrate plus glucose revealed enhanced levels of expression of the transporter genes *citH* and *tctABC* (Polen *et al.*, 2007). Expression of both genes in an *E. coli* strain unable to grow on citrate lead to cells ability to aerobically grow on citrate, suggesting that both CitH and TctABC are functional citrate transporters in *C. glutamicum* (Brocker *et al.*, 2009).

CitH is a protein of 526 amino acids that belongs to the Citrate-Mg²⁺:H⁺ (CitM) Citrate-Ca²⁺:H⁺ (CitH) Symporter (CitMHS) Family (TCDB # 2.A.11) and is homologous to the *Bacillus subtilis* CitM and CitH. TctABC is composed of 3 subunits: TctA (12 TM), TctB (4 TM) and TctC (1 TM) homologous to the ones found in *Salmonella enterica* serovar Typhimurium and belongs to the Tripartite Tricarboxylate Transporter (TTT) Family (TCDB # 2.A.80). Both permeases transport citrate in a Ca²⁺ dependent manner and, in fact, *C. glutamicum* growth on citrate only occurs in media supplemented with calcium. Furthermore, CitH can also transport citrate in complex with Sr²⁺ and TctABC in complex with Mg²⁺ (Brocker *et al.*, 2009).

Expression of *citH* and *tctABC* is induced by citrate and is not subject to glucose repression. Induction of expression is dependent on the transcriptional regulator CitAB with CitA probably functioning as the citrate sensor and CitB as the transcriptional activator (Brocker *et al.*, 2009).

5.3 An aerobic bacterium: *Bacillus subtilis*

B. subtilis is a Gram-positive bacterium, commonly found in soil. It forms endospores under nutrient exhaustion conditions. Although considered as a strict aerobe, now it is known that it can grow in anaerobic conditions making it a facultative anaerobe (Nakano and Zuber, 1998). It can grow on a wide variety of substrates when glucose is absent from the medium (Hueck and Hillen, 1995). The main by-products of glucose fermentation are acetic, lactic and formic acids and acetoin (Saier *et al.*, 2002). The transporters involved in the uptake of carboxylates that have been identified so far are represented in Figure 19.

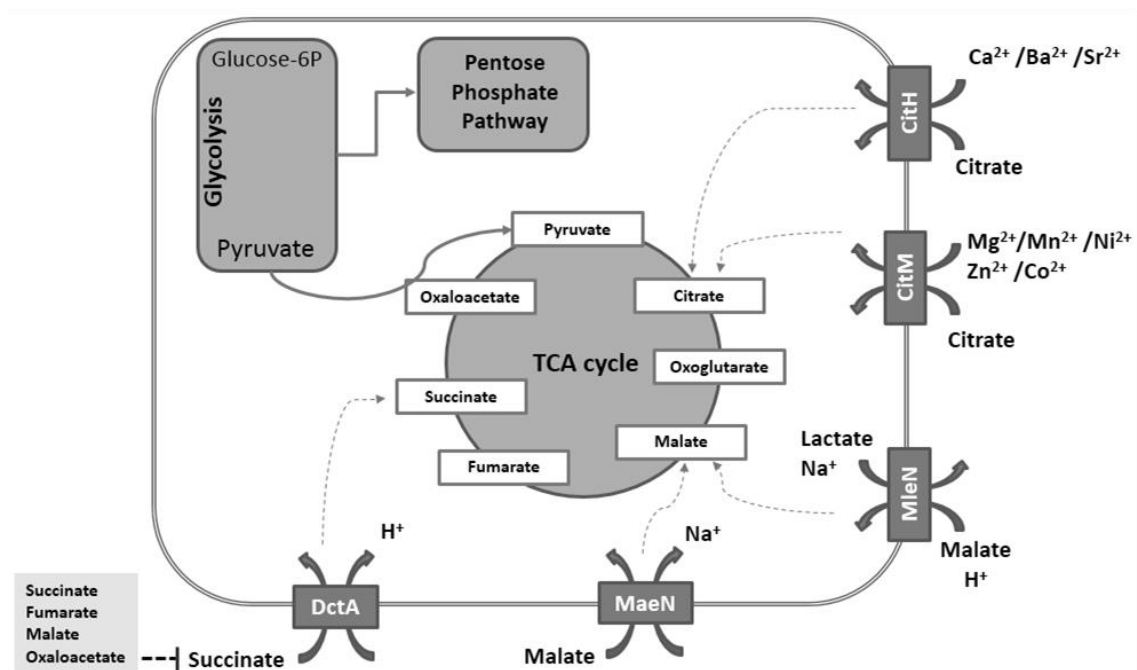


Figure 19 – Carboxylate transporters in *Bacillus subtilis*. A simplified scheme of carbon metabolism in *B. subtilis* and a representation of the characterized carboxylate transporters is shown.

5.3.1 Monocarboxylate uptake

Little is known about the transport of monocarboxylates in *B. subtilis*. In this bacterium the glyoxylate shunt is absent and acetate is a poor carbon source requiring the addition of TCA intermediates like glutamate (Grundy *et al.*, 1993). Acetate is excreted during glucose exponential growth of *B. subtilis* and can be metabolized when other carbon sources are depleted (Hanson *et al.*, 1963; Speck and Freese, 1973). Selection of mutants of *Bacillus stearothermophilus* resistant to fluoroacetate lead to the identification of a mutant defective in acetate transport with a functional TCA cycle and unable to utilize acetate as sole carbon source (Mallinder and Moir, 1991). In wild type cells acetate uptake

was saturable with a V_{\max} of 60 nmol min⁻¹ mg protein⁻¹ and a K_m of 300-350 μ M acetate, sensitive to the uncoupler CCCP and induced by acetate (Mallinder and Moir, 1991). The low K_m observed for this system suggests that it might play a role on excretion of the acetate formed during glucose fermentation (Mallinder and Moir, 1991).

Matin and Konings (1973) have demonstrated that lactate accumulates inside *B. subtilis* vesicles in a non-stereospecific manner in the presence of the electron donor NADH. This system is repressed in glucose grown cells and uptakes D-lactate with an affinity constant of 22 μ M and L-lactate with a K_m of 60 μ M (Matin and Konings, 1973). In anaerobic fermentation *B. subtilis* cells excrete lactate, acetate, and 2,3-butanediol as the major fermentation by-products. It was shown that lactate formation is dependent on the *lctEP* locus. LctE encodes a lactate dehydrogenase and its disruption leads to almost no lactate accumulation (Cruz Ramos *et al.*, 2000). LctP encodes a putative lactate permease but its disruption leads to no discernable phenotype in L-lactate minimal medium (Chai *et al.*, 2009). The major L-lactate permease is believed to be encoded by *lutP* since this protein is required for growth on L-lactate (Chai *et al.*, 2009).

5.3.2 Dicarboxylate uptake

Bacillus subtilis can grow aerobically on a variety of dicarboxylates like malate, fumarate or succinate having a complete TCA cycle (Fournier and Pardee, 1974). To use these carboxylic acids as carbon sources *B. subtilis* has three characterized transporters that accomplish this function, DctA, YufR and YqkI.

5.3.2.1 DctA – The dicarboxylate transporter protein

The *B. subtilis* DctA (or DctP) protein is a member of the DAACS (dicarboxylate/amino acid:cation Symporter) family (TCDB # 2.A.23) with 56 % sequence identity with *E. coli* DctA.

A strain with this gene inactivated is unable to use succinate or fumarate but not malate. The absence of a defect on malate utilization distinguishes this protein from the remaining bacterial homologues characterized. Its expression is dependent on the sensor kinase–regulator pair, YdbF (or DctS – sensor kinase) and YdbG (or DctR – response regulator) (Asai *et al.*, 2000). Expression of DctA in membrane vesicles showed [¹⁴C]-succinate uptake with a V_{\max} of 1.4 nmol succinate s⁻¹ mg protein⁻¹ and a K_m of 2.6 ± 1.4 μ M

succinate, at pH 7.0, which was inhibited by the addition of succinate, fumarate, malate and oxaloacetate. Succinate transport was not only dependent on the variation of external pH but also electrogenic. *B. subtilis* DctA has a narrower specificity than its *E. coli* homologue being insensitive to orotate, glyoxylate and α -ketoglutarate (Groeneveld *et al.*, 2010).

5.3.2.2 The malate transporters – YufR and YqkI

The *B. subtilis* YufR (or MaeN) protein is a member of the 2-Hydroxycarboxylate Transporter (2-HCT) Family (TCDB # 2.A.24). Members of 2-HCT family catalyse citrate or malate uptake with either Na^+ or H^+ as the co-transported cation. When expressed in vesicles in *E. coli* YufR is responsible for malate uptake in the presence of sodium (Wei *et al.*, 2000). It was also shown to support growth on malate but not succinate, citrate or fumarate. This transporter is induced by the regulator YufM while the sensor YufL is important for signal detection and signalling specificity (Tanaka, 2003).

The YqkI (or MleN) belongs to the NhaC $\text{Na}^+:\text{H}^+$ Antiporter (NhaC) Family (TCDB # 2.A.35) with 12 putative transmembrane segments (TMS). Expressing *mleN* in *E. coli* vesicles showed electroneutral malate exchange with lactate coupled to proton uptake and sodium efflux ($\text{malic}^{-2}-2\text{H}^+/\text{Na}^+-\text{lactate}^{-1}$). This transporter is important to support high density growth on malate at low protonmotive force. This gene is organized in an operon with *mleA* which encodes the malolactate enzyme that converts malate to lactate (Wei *et al.*, 2000).

5.3.3 Citrate transporters

Citrate is abundant in nature, forming stable complexes with divalent metal ions. Citrate transporters in *B. subtilis* have evolved to recognize citrate in complex with divalent metal ions since it is available in this form in their habitat.

5.3.3.1 The CitMHS Family – CitM and CitH

Two of the citrate carriers found in *B. subtilis*, CitM and CitH, form the Citrate- $\text{Mg}^{2+}:\text{H}^+$ (CitM) Citrate- $\text{Ca}^{2+}:\text{H}^+$ (CitH) Symporter (CitMHS) Family (TCDB # 2.A.11). CitM and

CitH share 60 % sequence identity and secondary structure prediction suggests organization of CitM and CitH in 12 TMDs.

CitM and CitH are citrate-metal transporters with complementary metal ion specificities (Boorsma *et al.*, 1996; Krom *et al.*, 2000). Transport occurs in symport with protons with a stoichiometry of one proton per one complex of citrate-divalent metal ion (Boorsma *et al.*, 1996; Li and Pajor, 2002). Expression of CitM and CitH in *E. coli* revealed that their main difference lies on the metal specificity with CitM transporting citrate in complex with Mg^{2+} , Mn^{2+} , Ni^{2+} , Zn^{2+} and Co^{2+} ions, in this order of preference, while CitH transports citrate²⁻ in complex with Ca^{2+} , Ba^{2+} and Sr^{2+} (Krom *et al.*, 2000). The affinity constant (K_m) for both transporters and for all complexes is very similar with values ranging from 35 to 63 μM citrate for CitM and between 33 and 50 μM citrate for CitH. Greater differences were found for their maximal rates with CitM ranging from 214 to 600 $pmol\ min^{-1}\ mg\ protein^{-1}$ and CitH from 51 to 155 $pmol\ min^{-1}\ mg\ protein^{-1}$ (Krom *et al.*, 2000). Since the affinities for the several citrate-metal complexes are similar the recognition site in CitM and CitH should be similar being the main differences in the translocation of the substrate since there are most notable differences in the maximum velocity of translocation (Krom *et al.*, 2000). Growth of *B. subtilis* on citrate and D-isocitrate is supported by CitM in the presence of metal ions (namely Mg^{2+}) and this transporter is responsible for isocitrate uptake in complex with the same metal specificity than for citrate (Warner and Lolkema, 2002).

Transcription of CitM is stimulated by the presence of citrate and isocitrate and is inhibited by glucose being under the control of carbon catabolite repression (Krom *et al.*, 2000; Warner *et al.*, 2000; Warner and Lolkema, 2002). The presence of citrate in the growth media is sensed by the CitS-CitT two-component system which acts as a positive regulator of expression of CitM (Yamamoto *et al.*, 2000).

5.3.3.2 CimH – the L-malate/citrate:H⁺ symporter

CimH is a 2-Hydroxycarboxylate Transporter (2-HCT) Family member (TCDB # 2.A.24) is a citrate and malate proton symporter (Krom *et al.*, 2001).

The transport is electroneutral being driven by the ΔpH across the membrane. Uptake assays with CimH in *E. coli* vesicles revealed an affinity of 10 μM citrate (free anion form) and 1.5 mM malate and a maximal rate of transport of 167 and 37 $nmol\ min^{-1}\ mg\ protein^{-1}$ for L-malate and citrate respectively. This transporter is therefore a high-affinity,

low-capacity citrate transporter and a low-affinity, high-capacity L-malate proton symporter. It also binds but does not transport L-citramalate (Krom *et al.*, 2001).

CimH is a protein with 11 putative TMDs. To identify the CimH interaction site with the carboxylate group of the substrate, residues that are positively charged and conserved within the 2-HCT family were mutated. The positively charged residues (R143, R420, Q428) that were putatively capable of forming hydrogen bonds did not play a role in the activity of CimH since mutations did not affect the kinetic properties of the transporter. Another arginine residue at position 432, similar to *Leuconostoc mesenteroides* CitP, is involved in the interaction with one of the carboxylate groups of the substrate since its substitution by a cysteine or lysine lowered the affinity for citrate (Krom and Lolkema, 2003). Accessibility of residues R420 and Q428 was accessed with membrane impermeable agents revealing that both are accessible in membranes unless citrate is present suggesting that the cytoplasmic loop between TMD X and XI is possibly a re-entrant loop optimizing the translocation pathway for small, negatively charged substrates (Krom and Lolkema, 2003).

5.4 Nonsulfur purple photosynthetic bacteria – *Rhodobacter capsulatus*

Rhodobacter capsulatus is a well-studied nonsulfur purple photosynthetic bacterium in terms of carboxylate transporters. This bacterium is able to grow anaerobically under light or aerobically in the dark using several organic acids as carbon sources, such as intermediates of the TCA cycle, as well as acetate and pyruvate. Citrate can be used only by a few species of nonsulfur purple photosynthetic bacteria.

5.4.1 Acetate and other monocarboxylates

Acetate when assimilated by *R. capsulatus* is converted to malate via the glyoxylate cycle (Willison, 1988). Acetate enters *R. capsulatus* cells via ActP, a member of the SSS family (TCDB # 2.A.21), with an apparent K_m of 1.89 mM and a V_{max} of 17.74 nmol min⁻¹ mg protein⁻¹ in cells grown in aerobic and photosynthetic conditions (Borghese *et al.*, 2008). The uptake is abolished in the presence of the protonophore FCCP (a protonophore and uncoupler of oxidative phosphorylation in mitochondria), KCN (an electron transport

inhibitor) and NEM (which blocks vesicular transport) (Borghese *et al.*, 2008). Acetate uptake through ActP is inhibited by tellurite, pyruvate and lactate suggesting that they are substrates of this transporter. In fact, tellurite is transported through this protein with an apparent K_m of 163.0 μM , and is inhibited by acetate (Borghese *et al.*, 2008; Borghese and Zannoni, 2010). ActP expression in this organism is dependent on the carbon source, with increased activity in the presence of malate, succinate, pyruvate and acetate (Borghese *et al.*, 2011).

The monocarboxylates pyruvate and 2-oxobutyrate enter the cells through RRC01191, a member of the Tripartite ATP-independent Periplasmic Transporter (TRAP-T) Family (TCDB # 2.A.56) (Thomas *et al.*, 2006). Tryptophan fluorescence of purified RRC01191 revealed a dissociation constant (K_d) of 3.4 μM pyruvate and 0.32 μM 2-oxobutyrate with a binding mechanism similar to DctP (Thomas *et al.*, 2006). RRC01191 only binds monocarboxylate 2-oxoacids with an aliphatic backbone being the 2-oxo and 1-carboxyl groups essential and with the ligand-binding affinity increasing with chain length of the aliphatic backbone (Thomas *et al.*, 2006).

5.4.2 Dicarboxylate uptake

Dicarboxylic acids promote fast growth of purple bacteria both in photo- and chemoheterotrophic conditions. In *R. capsulatus* high affinity dicarboxylate uptake is mediated by DctPQM system which is the prototype of the Tripartite ATP-independent Periplasmic Transporter (TRAP-T) Family (TCDB # 2.A.56). Inactivation of this system renders cells unable to grow in dark aerobic conditions on malate, succinate or fumarate as sole carbon sources although these mutants could still grow slowly on malate and succinate in photoheterotrophic conditions (Hamblin *et al.*, 1990).

The *dctPQM* operon originates 3 proteins, all essential for dicarboxylates transport activity (Forward *et al.*, 1997). DctP is a periplasmic solute-binding receptor, DctM is a 12 TMD protein predicted to catalyse the substrate translocation while DctQ is a small protein with 4 TMD which is essential for dicarboxylate transport although its function has not been clarified (Wyborn *et al.*, 2001). Binding assays in purified DctP yielded a dissociation constant (K_d) of 8.4 ± 1.49 μM malate which is competitively inhibited by succinate (K_i of 8 μM) and fumarate (K_i of 2 μM) (Shaw *et al.*, 1991). D-malate also inhibited the system albeit with a much lower affinity (Shaw *et al.*, 1991; Walmsley *et al.*, 1992). This system is regulated by ΔpH with a high internal pH corresponding to an

activation of the transport system, and uses the proton-motive potential as its driving force (Shaw and Kelly, 1991; Forward *et al.*, 1997). Binding occurs in 3 steps with isomerization between non-binding and binding forms followed by the rapid binding phase and isomerization (Walmsley *et al.*, 1992).

5.5 Lactic acid and Acetic acid bacteria

Lactic acid and acetic acid bacteria play an important role in the production of fermented foods being applied in fermentation processes worldwide. Lactic acid bacteria ferment carbohydrates mainly to lactate or to a mixture of lactate, ethanol or acetate and carbon dioxide. Acetic acid bacteria also have a very particular metabolism in which oxidation of sugars and ethanol are coupled with the citric acid cycle and the respiratory chain generating as the major product of fermentation acetic acid.

5.5.1 Acetic acid bacteria

Acetic acid bacteria oxidize sugars, sugar alcohols and ethanol, producing acetate as the major metabolic end product. The production of high titters of acetic acid shows that these microorganisms are resistant both to high acetic acid concentrations and to low pH values (Steiner and Sauer, 2001). Study of cells induced in acetic acid revealed the presence of proteins associated to several mechanisms underlying acetate resistance including membrane functions such as acetate transport and respiration (Steiner and Sauer, 2001). Acetic acid bacteria have, at least, two known acetate transport mechanisms: a proton dependent assimilation mechanism of acetic acid and AatA, an ABC efflux protein. Both proteins reduce intracellular acetic acid concentration contributing to acetic acid resistance in these bacteria (Nakano and Fukaya, 2008). Analysis of intact cells as well as inside-out membrane vesicles revealed acetate accumulation at low external pH which was stimulated in the presence of respiratory substrates and inhibited by the addition of CCCP (Matsushita *et al.*, 2005). These results point to the presence of efflux pump(s) dependent on the proton motive force which can be specific for acetic acid but can also export high concentrations of propionic and butyric acids (Matsushita *et al.*, 2005).

The acetic acid transporter AatA from *Acetobacter aceti* is a protein belonging to the ATP-binding Cassete Superfamily (TCDB # 3.A.1) since it contains Walker A and B motifs, as well as ABC signatures I and II (Nakano *et al.*, 2006). This transporter is a member of the (Putative) Drug Resistance ATPase-1 (Drug RA1) Family (TCDB # 3.A.1.120). It is strongly induced by acetic acid and inactivation of *aatA* decreases *A. aceti* cells resistance to acetic, formic, propionic and lactic acids, being this phenotype reversed when *aatA* is reintroduced in the mutant strain (Nakano *et al.*, 2006). Furthermore, overexpression of this protein leads to enhanced growth in high acetic acid concentrations in the parental strain, suggesting its role as an efflux protein for acetic acid (Nakano *et al.*, 2006).

5.5.2 Lactic acid bacteria

Lactic acid bacteria, as the name indicates, produce lactic acid as the main metabolic end-product of carbohydrate fermentation, making this group of bacteria important in the food industry. These bacteria use two major pathways of sugar metabolism: the glycolytic pathway with lactic acid as the main end-product (homolactic fermentation) or the phosphoketolase pathway yielding also other end-products as acetic and propionic acids, carbon dioxide and ethanol, as well as lactic acid (heterolactic fermentation) (Papagianni, 2012b). *Lactococcus lactis*, a model organism within lactic acid bacteria, is a homolactic fermentative bacteria but in sugar limiting conditions can also shift to a mixed acid fermentation, producing also formate, acetate and ethanol (Andersen *et al.*, 2001).

In *L. lactis* malolactic fermentation occurs upon decarboxylation of the L-malate that enters cells by the malolactic enzyme to yield L-lactate and carbon dioxide (Poolman *et al.*, 1991). The malate permease MleP (or MaeP) catalyzes the exchange of the malate that enters the cells with the lactate that is exiting (precursor/product exchange), generating a membrane potential (Poolman *et al.*, 1991). Studies of whole cells defective in the malolactic enzyme or in membrane vesicles demonstrated that transport can occur as malate:H⁺/lactic acid exchange or malate:H⁺ uniport accompanied by efflux of lactic acid. The pH gradient stimulates the electrogenic exchange while the membrane potential inhibits it, resulting in higher growth yields at low pH values (Poolman *et al.*, 1991; Bandell *et al.*, 1997).

Citrolactic fermentation occurs in three steps: citrate transport, conversion of citrate into oxaloacetate by citrate lyase and conversion of oxaloacetate into pyruvate and carbon

dioxide. Pyruvate can yield several end-products such as lactate, formate, acetate, ethanol as well as aroma compounds (acetoin and butanediol). Lactic acid bacteria at the end of fermentation accumulate high concentrations of lactate into the medium which can inhibit growth. The citrate permease (CitP or CitN) by catalysing the electrogenic exchange of divalent citrate with monovalent lactate can circumvent the inhibitory effects of lactate accumulation (precursor/product exchange) originating a membrane potential (Bandell *et al.*, 1998; Magni *et al.*, 1999). CitP is encoded the plasmid pCIT264 and is transcribed as part of the *citQRP* operon (*citQ* is the leader peptide, *citR* the regulatory protein and *citP* the permease) induced by acidification of the media during cell growth but not by the presence of citrate in the medium (García-Quintáns *et al.*, 1998; Magni *et al.*, 1999). CitP shows a broad substrate specificity to physiological and nonphysiological 2-hydroxycarboxylates and besides the exchange with lactate can also use the intermediates of citrate metabolism α -acetolactate, pyruvate and acetate (Pudlik and Lolkema, 2011). In the absence of metabolic intermediates or final products CitP operates in a slow citrate- H^+ symport mode accumulating the intermediate metabolic products. These are then used in a fast exchange mode with citrate leading to the consumption of citrate. The exchange product utilized by CitP depends on substrate availability and concentration (Pudlik and Lolkema, 2011).

Both CitP and MleP transporters share as substrates the 2-hydroxycarboxylate motif $HO-CR_2-COO^-$. The R group can be substituted by groups varying in size and polarity nevertheless smaller substrates are preferred by MleP while larger substrates by CitP. In what concerns the hydroxyl group both transporters have a clear preference for 2-hydroxycarboxylates but can also transport 2-oxocarboxylates. The carboxylate group on the other hand is irreplaceable showing its relevance in defining the motif transported by MleP and CitP (Bandell *et al.*, 1997). Analysis of the kinetics of CitP and MleP was performed by heterologous exchange measuring efflux of radiolabelled substrate from membrane vesicles by adding nonlabelled compounds to the assay mixture originating affinity constants of the substrates (K_m) or by counterflow experiments measuring the uptake of a labelled compound into vesicles loaded with nonlabelled substrates giving the inhibition constant (K_i) of the substrate. Measurement of the exchange rates revealed a K_m for *S*-malate of 0.1 mM in the case of CitP and of 0.46 mM for MleP. Citrate affinity in the case of CitP was of 56 μ M while for MleP was 9 mM but in MleP citrate can bind the transporter but is not translocated. Lactate affinity on the other hand was lower with a K_m of 26 ± 8 mM for CitP and 4.6 ± 0.9 mM for MleP. For all these substrates a lower

affinity was observed for the respective *R*-enantiomers. The higher affinities for malate and citrate when compared to lactate prevents the inhibition of the malolactic and citrolactic pathways by the accumulation of lactate in the medium (Bandell and Lolkema, 1999). Chimeric protein analysis and site-directed mutagenesis allowed the identification of the putative binding site of CitP in which both the carboxylate and hydroxyl groups of the 2-hydroxycarboxylate motif interacts with specific sites of the protein allowing the orientation of the substrate in the binding pocket. This analysis revealed that the conserved residue R425 is responsible for the binding with the second carboxylate of the substrate (Bandell and Lolkema, 2000). With this proposed model it was possible to further explore the binding site of CitP identifying as substrates of this protein secondary metabolites of the amino acid metabolism (Pudlik and Lolkema, 2012).

Outline of the present thesis

Carboxylic acids are important compounds in cell functionality, being both potential carbon and energy sources as well as by-products of metabolism. A current demand on clean alternatives for industrial applications has brought a new focus to this important group of compounds and more physiological as well as structural knowledge on the transporters that allow both uptake and extrusion of these acids will increase the available tools for biotechnology use of carboxylic acids. The aim of this thesis was to increase the current knowledge on yeast monocarboxylate permeases and its homologues in bacteria (*E. coli*) and fungi (*A. nidulans*).

In the introduction a bibliographic revision on carboxylate transporters is presented. Over several years, several carboxylate transporter systems have been physiologically characterized. The mechanisms of transport across the membrane are deciphered, the features of Ady2 and Jen1 yeast carboxylate transporters are described, and a general characterization of the structure of the MFS superfamily permease is given. A bibliographic revision on carboxylate transporters in bacteria is also presented focusing on model systems representative of several groups of bacteria namely *E. coli*, *C. glutamicum*, *B. subtilis*, *R. capsulatus* and on lactic and acetic acid bacteria.

In chapter II the work concerning the structural-functional analysis of Jen1 from *S. cerevisiae* is presented. This study resulted in the identification of amino acid residues involved in activity and substrate specificity. Furthermore, a structural homology model was generated and a potential substrate translocation trajectory was defined (Soares-Silva *et al.*, 2010) which is supported by the experimental data presented herein as well as by previous work from our group (Soares-Silva *et al.*, 2007).

Carboxylic acids such as lactic acid are commonly used in food, cosmetic and pharmaceutical industries. They can be produced by microbial fermentation and yeast, due to its resistance to low pH, is potentially a good microbial factory for the production of carboxylic acids. Aiming at improving lactic acid yield in *S. cerevisiae* through metabolic engineering, the role of the monocarboxylate transporters Jen1 and Ady2 as modulators for lactic acid export by the cell was evaluated.

Chapter four describes the results obtained for the characterization of the bacterial (*E. coli*) homologue of Ady2, the acetate-succinate permease SatP (YaaH). A full characterization of the specificity and kinetics of this permease was performed and the physiological role of the two acetate permeases from *E. coli* was evaluated.

The filamentous fungus *A. nidulans* AcpA permease is analysed in chapter five. The specificity profile of this acetate transporter was analysed and a potential role on ammonia export is discussed.

The main outcomes of the work performed in the scope of this thesis are presented in chapter six, as well as some perspectives for future work to be undertaken.

References

- Abramson J., Kaback H.R., and Iwata S. (2004) Structural comparison of lactose permease and the glycerol-3-phosphate antiporter: members of the major facilitator superfamily. *Curr Opin Struct Biol* **14**: 413–9
- Aguilera L., Campos E., Giménez R., Badía J., Aguilar J., and Baldoma L. (2008) Dual role of LldR in regulation of the *lldPRD* operon, involved in L-lactate metabolism in *Escherichia coli*. *J Bacteriol* **190**: 2997–3005
- Akita O., Nishimori C., Shimamoto T., Fujii T., and Iefuji H. (2000) Transport of pyruvate in *Saccharomyces cerevisiae* and cloning of the gene encoded pyruvate permease. *Biosci Biotechnol Biochem* **64**: 980–4
- Andersen H.W., Pedersen M.B., Hammer K., and Jensen P.R. (2001) Lactate dehydrogenase has no control on lactate production but has a strong negative control on formate production in *Lactococcus lactis*. *Eur J Biochem* **268**: 6379–89
- Andrade R.P. and Casal M. (2001) Expression of the lactate permease gene *JEN1* from the yeast *Saccharomyces cerevisiae*. *Fungal Genet Biol* **32**: 105–11
- Andrade R.P., Kötter P., Entian K.-D., and Casal M. (2005) Multiple transcripts regulate glucose-triggered mRNA decay of the lactate transporter *JEN1* from *Saccharomyces cerevisiae*. *Biochem Biophys Res Commun* **332**: 254–62
- Asai K., Baik S.H., Kasahara Y., Moriya S., and Ogasawara N. (2000) Regulation of the transport system for C4-dicarboxylic acids in *Bacillus subtilis*. *Microbiology* **146** (Pt 2): 263–71
- Augstein A., Barth K., Gentsch M., Kohlwein S.D., and Barth G. (2003) Characterization, localization and functional analysis of Gpr1p, a protein affecting sensitivity to acetic acid in the yeast *Yarrowia lipolytica*. *Microbiology* **149**: 589–600
- Baker K.E., Ditullio K.P., Neuhard J., and Kelln R.A. (1996) Utilization of orotate as a pyrimidine source by *Salmonella typhimurium* and *Escherichia coli* requires the dicarboxylate transport protein encoded by *dctA*. *J Bacteriol* **178**: 7099–105
- Bandell M., Ansanay V., Rachidi N., Dequin S., and Lolkema J.S. (1997) Membrane potential-generating malate (MleP) and citrate (CitP) transporters of lactic acid bacteria are homologous proteins. Substrate specificity of the 2-hydroxycarboxylate transporter family. *J Biol Chem* **272**: 18140–6
- Bandell M., Lhotte M.E., Marty-Teyssset C., Veyrat A., Prévost H., Dartois V. *et al.* (1998) Mechanism of the citrate transporters in carbohydrate and citrate cometabolism in *Lactococcus* and *Leuconostoc* species. *Appl Environ Microbiol* **64**: 1594–600
- Bandell M. and Lolkema J.S. (1999) Stereoselectivity of the membrane potential-generating citrate and malate transporters of lactic acid bacteria. *Biochemistry* **38**: 10352–60

- Bandell M. and Lolkema J.S. (2000) Arg-425 of the citrate transporter CitP is responsible for high affinity binding of di- and tricarboxylates. *J Biol Chem* **275**: 39130–6
- Baranowski K. and Radler F. (1984) The glucose-dependent transport of L-malate in *Zygosaccharomyces bailii*. *Antonie Van Leeuwenhoek* **50**: 329–40
- Barnett J. a and Kornberg H.L. (1960) The utilization by yeasts of acids of the tricarboxylic acid cycle. *J Gen Microbiol* **23**: 65–82
- Bauer J., Fritsch M.J., Palmer T., and Uden G. (2011) Topology and accessibility of the transmembrane helices and the sensory site in the bifunctional transporter DcuB of *Escherichia coli*. *Biochemistry* **50**: 5925–38
- Beatty C.M., Browning D.F., Busby S.J.W., and Wolfe A.J. (2003) Cyclic AMP receptor protein-dependent activation of the *Escherichia coli acsP2* promoter by a synergistic class III mechanism. *J Bacteriol* **185**: 5148–57
- Becuwe M., Vieira N., Lara D., Gomes-Rezende J., Soares-Cunha C., Casal M. *et al.* (2012) A molecular switch on an arrestin-like protein relays glucose signaling to transporter endocytosis. *J Cell Biol* **196**: 247–59
- Beyer L., Doberenz C., Falke D., Hunger D., Suppmann B., and Sawers R.G. (2013) Coordination of FocA and pyruvate formate-lyase synthesis in *Escherichia coli* demonstrates preferential translocation of formate over other mixed-acid fermentation products. *J Bacteriol* **195**: 1428–35
- Boorsma a, Rest M.E. van der, Lolkema J.S., and Konings W.N. (1996) Secondary transporters for citrate and the Mg⁽²⁺⁾-citrate complex in *Bacillus subtilis* are homologous proteins. *J Bacteriol* **178**: 6216–22
- Borghese R., Cicerano S., and Zannoni D. (2011) Fructose increases the resistance of *Rhodobacter capsulatus* to the toxic oxyanion tellurite through repression of acetate permease (ActP). *Antonie Van Leeuwenhoek* **100**: 655–8
- Borghese R., Marchetti D., and Zannoni D. (2008) The highly toxic oxyanion tellurite (TeO (3-)) enters the phototrophic bacterium *Rhodobacter capsulatus* via an as yet uncharacterized monocarboxylate transport system. *Arch Microbiol* **189**: 93–100
- Borghese R. and Zannoni D. (2010) Acetate permease (ActP) is responsible for tellurite (TeO₃²⁻) uptake and resistance in cells of the facultative phototroph *Rhodobacter capsulatus*. *Appl Environ Microbiol* **76**: 942–4
- Brockner M., Schaffer S., Mack C., and Bott M. (2009) Citrate utilization by *Corynebacterium glutamicum* is controlled by the CitAB two-component system through positive regulation of the citrate transport genes *citH* and *tctCBA*. *J Bacteriol* **191**: 3869–80
- Busch W. and Saier M.H. (2004) The IUBMB-endorsed transporter classification system. *Mol Biotechnol* **27**: 253–62

- Casal M., Cardoso H., and Leão C. (1996) Mechanisms regulating the transport of acetic acid in *Saccharomyces cerevisiae*. *Microbiology* **142** (Pt 6): 1385–90
- Casal M., Paiva S., Andrade R.P., Gancedo C., and Leão C. (1999) The lactate-proton symport of *Saccharomyces cerevisiae* is encoded by JEN1. *J Bacteriol* **181**: 2620–3
- Casal M., Paiva S., Queirós O., and Soares-Silva I. (2008) Transport of carboxylic acids in yeasts. *FEMS Microbiol Rev* **32**: 974–94
- Cássio F. and Leão C. (1993) A comparative study on the transport of L(-)malic acid and other short-chain carboxylic acids in the yeast *Candida utilis*: evidence for a general organic acid permease. *Yeast* **9**: 743–52
- Cássio F., Leão C., and Uden N. van (1987) Transport of lactate and other short-chain monocarboxylates in the yeast *Saccharomyces cerevisiae*. *Appl Environ Microbiol* **53**: 509–13
- Chai Y., Kolter R., and Losick R. (2009) A widely conserved gene cluster required for lactate utilization in *Bacillus subtilis* and its involvement in biofilm formation. *J Bacteriol* **191**: 2423–30
- Conde A., Diallinas G., Chaumont F., Chaves M., and Gerós H. (2010) Transporters, channels, or simple diffusion? Dogmas, atypical roles and complexity in transport systems. *Int J Biochem Cell Biol* **42**: 857–68
- Cruz Ramos H., Hoffmann T., Marino M., Nedjari H., Presecan-Siedel E., Dreesen O. *et al.* (2000) Fermentative metabolism of *Bacillus subtilis*: physiology and regulation of gene expression. *J Bacteriol* **182**: 3072–80
- Dang S., Sun L., Huang Y., Lu F., Liu Y., Gong H. *et al.* (2010) Structure of a fucose transporter in an outward-open conformation. *Nature* **467**: 734–8
- Davies S.J., Golby P., Omrani D., Broad S. a, Harrington V.L., Guest J.R. *et al.* (1999) Inactivation and regulation of the aerobic C(4)-dicarboxylate transport (*dctA*) gene of *Escherichia coli*. *J Bacteriol* **181**: 5624–35
- Dong J.M., Taylor J.S., Latour D.J., Iuchi S., and Lin E.C. (1993) Three overlapping *lct* genes involved in L-lactate utilization by *Escherichia coli*. *J Bacteriol* **175**: 6671–8
- Ebbighausen H., Weil B., and Krämer R. (1991) Carrier-mediated acetate uptake in *Corynebacterium glutamicum*. *Arch Microbiol* **155**: 505–510
- Engel P., Krämer R., and Uden G. (1992) Anaerobic fumarate transport in *Escherichia coli* by an *fnr*-dependent dicarboxylate uptake system which is different from the aerobic dicarboxylate uptake system. *J Bacteriol* **174**: 5533–9
- Engel P., Krämer R., and Uden G. (1994) Transport of C4-dicarboxylates by anaerobically grown *Escherichia coli*. Energetics and mechanism of exchange, uptake and efflux. *Eur J Biochem* **222**: 605–14

- Faham S., Watanabe A., Besserer G.M., Cascio D., Specht A., Hirayama B.A. *et al.* (2008) The crystal structure of a sodium galactose transporter reveals mechanistic insights into Na⁺/sugar symport. *Science* **321**: 810–4
- Feng Z., Hou T., and Li Y. (2012) Concerted movement in pH-dependent gating of FocA from molecular dynamics simulations. *J Chem Inf Model* **52**: 2119–31
- Flippi M., Robellet X., Dequier E., Leschelle X., Felenbok B., and Vélot C. (2006) Functional analysis of *alcS*, a gene of the *alc* cluster in *Aspergillus nidulans*. *Fungal Genet Biol* **43**: 247–60
- Forward J. a, Behrendt M.C., Wyborn N.R., Cross R., and Kelly D.J. (1997) TRAP transporters: a new family of periplasmic solute transport systems encoded by the *dctPQM* genes of *Rhodobacter capsulatus* and by homologs in diverse gram-negative bacteria. *J Bacteriol* **179**: 5482–93
- Fournier R.E. and Pardee A.B. (1974) Evidence for inducible, L-malate binding proteins in the membrane of *Bacillus subtilis*. Identification of presumptive components of the C4-dicarboxylate transport systems. *J Biol Chem* **249**: 5948–54
- Fukui K., Koseki C., Yamamoto Y., Nakamura J., Sasahara A., Yuji R. *et al.* (2011) Identification of succinate exporter in *Corynebacterium glutamicum* and its physiological roles under anaerobic conditions. *J Biotechnol* **154**: 25–34
- Gancedo J.M. (1998) Yeast carbon catabolite repression. *Microbiol Mol Biol Rev* **62**: 334–61
- García-Quintáns N., Magni C., Mendoza D. de, and López P. (1998) The citrate transport system of *Lactococcus lactis* subsp. *lactis* biovar diacetylactis is induced by acid stress. *Appl Environ Microbiol* **64**: 850–7
- Gentsch M., Kuschel M., Schlegel S., and Barth G. (2007) Mutations at different sites in members of the Gpr1/Fun34/YaaH protein family cause hypersensitivity to acetic acid in *Saccharomyces cerevisiae* as well as in *Yarrowia lipolytica*. *FEMS Yeast Res* **7**: 380–90
- Georgi T., Engels V., and Wendisch V.F. (2008) Regulation of L-lactate utilization by the FadR-type regulator LldR of *Corynebacterium glutamicum*. *J Bacteriol* **190**: 963–71
- Gimenez R., Nuñez M.F., Badia J., Aguilar J., and Baldoma L. (2003) The gene *yjcG*, cotranscribed with the gene *acs*, encodes an acetate permease in *Escherichia coli*. *J Bacteriol* **185**: 6448–55
- Golby P., Davies S., Kelly D.J., Guest J.R., and Andrews S.C. (1999) Identification and characterization of a two-component sensor-kinase and response-regulator system (DcuS-DcuR) controlling gene expression in response to C4-dicarboxylates in *Escherichia coli*. *J Bacteriol* **181**: 1238–48
- Golby P., Kelly D.J., Guest J.R., and Andrews S.C. (1998) Topological analysis of DcuA, an anaerobic C4-dicarboxylate transporter of *Escherichia coli*. *J Bacteriol* **180**: 4821–7

- Groeneveld M., Weme R.G.J.D.O., Duurkens R.H., and Slotboom D.J. (2010) Biochemical characterization of the C4-dicarboxylate transporter DctA from *Bacillus subtilis*. *J Bacteriol* **192**: 2900–7
- Grundy F.J., Waters D. a, Takova T.Y., and Henkin T.M. (1993) Identification of genes involved in utilization of acetate and acetoin in *Bacillus subtilis*. *Mol Microbiol* **10**: 259–71
- Guaragnella N. and Butow R.A. (2003) *ATO3* encoding a putative outward ammonium transporter is an RTG-independent retrograde responsive gene regulated by GCN4 and the Ssy1-Ptr3-Ssy5 amino acid sensor system. *J Biol Chem* **278**: 45882–7
- Hamblin M.J., Shaw J.G., Curson J.P., and Kelly D.J. (1990) Mutagenesis, cloning and complementation analysis of C4-dicarboxylate transport genes from *Rhodobacter capsulatus*. *Mol Microbiol* **4**: 1567–74
- Hanson R.S., Srinivasan V.R., and Halvorson H.O. (1963) Biochemistry of sporulation. I. Metabolism of acetate by vegetative and sporulating cells. *J Bacteriol* **85**: 451–60
- Henderson P.J.F. (2012) Membrane Proteins for Secondary Active Transport and their Molecular Mechanisms. In *Comprehensive Biophysics, Vol 8, Bioenergetics*. Ferguson, S. (ed.). Academic Press, Oxford. pp. 265–288.
- Hueck C.J. and Hillen W. (1995) Catabolite repression in *Bacillus subtilis*: a global regulatory mechanism for the gram-positive bacteria? *Mol Microbiol* **15**: 395–401
- Huhn S., Jolkver E., Krämer R., and Marin K. (2011) Identification of the membrane protein SucE and its role in succinate transport in *Corynebacterium glutamicum*. *Appl Microbiol Biotechnol* **89**: 327–35
- Inui M., Murakami S., Okino S., Kawaguchi H., Vertès A. a, and Yukawa H. (2004) Metabolic analysis of *Corynebacterium glutamicum* during lactate and succinate productions under oxygen deprivation conditions. *J Mol Microbiol Biotechnol* **7**: 182–96
- Janausch I., Kim O., and Uden G. (2001) DctA- and Dcu-independent transport of succinate in *Escherichia coli* : contribution of diffusion and of alternative carriers. *Arch Microbiol* **176**: 224–230
- Janausch I.G., Garcia-Moreno I., and Uden G. (2002) Function of DcuS from *Escherichia coli* as a fumarate-stimulated histidine protein kinase in vitro. *J Biol Chem* **277**: 39809–14
- Jin K., Zhang Y., Fang W., Luo Z., Zhou Y., and Pei Y. (2010) Carboxylate transporter gene *JEN1* from the entomopathogenic fungus *Beauveria bassiana* is involved in conidiation and virulence. *Appl Environ Microbiol* **76**: 254–63
- Jolkver E., Emer D., Ballan S., Krämer R., Eikmanns B.J., and Marin K. (2009) Identification and characterization of a bacterial transport system for the uptake of pyruvate, propionate, and acetate in *Corynebacterium glutamicum*. *J Bacteriol* **191**: 940–8
- Kaback H.R., Sahin-Tóth M., and Weinglass a B. (2001) The kamikaze approach to membrane transport. *Nat Rev Mol Cell Biol* **2**: 610–20

- Kang S.Y. (1978) Mechanism of autoenergized transport and nature of energy coupling for D-lactate in *Escherichia coli*. *J Bacteriol* **136**: 867–73
- Karinou E., Compton E.L.R., Morel M., and Javelle A. (2013) The *Escherichia coli* SLC26 homologue YchM (DauA) is a C(4)-dicarboxylic acid transporter. *Mol Microbiol* **87**: 623–40
- Kay W.W. (1972) Genetic control of the metabolism of propionate by *Escherichia coli* K12. *Biochim Biophys Acta* **264**: 508–21
- Kay W.W. and Kornberg H.L. (1969) Genetic control of the uptake of c4-dicarboxylic by *Escherichia coli*. *FEBS Lett* **3**: 93–96.
- Kay W.W. and Kornberg H.L. (1971) The uptake of C4-dicarboxylic acids by *Escherichia coli*. *Eur J Biochem* **18**: 274–81
- Kim O. Bin, Lux S., and Uden G. (2007) Anaerobic growth of *Escherichia coli* on D-tartrate depends on the fumarate carrier DcuB and fumarase, rather than the L-tartrate carrier TdtT and L-tartrate dehydratase. *Arch Microbiol* **188**: 583–9
- Kim O. Bin, Reimann J., Lukas H., Schumacher U., Grimpo J., Dünwald P., and Uden G. (2009) Regulation of tartrate metabolism by TdtR and relation to the DcuS-DcuR-regulated C4-dicarboxylate metabolism of *Escherichia coli*. *Microbiology* **155**: 3632–40
- Kim O. Bin and Uden G. (2007) The L-tartrate/succinate antiporter TdtT (YgjE) of L-tartrate fermentation in *Escherichia coli*. *J Bacteriol* **189**: 1597–603
- Kleefeld A., Ackermann B., Bauer J., Krämer J., and Uden G. (2009) The fumarate/succinate antiporter DcuB of *Escherichia coli* is a bifunctional protein with sites for regulation of DcuS-dependent gene expression. *J Biol Chem* **284**: 265–75
- Koch a L. (2005) Bacterial choices for the consumption of multiple resources for current and future needs. *Microb Ecol* **49**: 183–97
- Kok S., Nijkamp J.F., Oud B., Roque F.C., Ridder D., Daran J.-M. *et al.* (2012) Laboratory evolution of new lactate transporter genes in a *jen1Δ* mutant of *Saccharomyces cerevisiae* and their identification as *ADY2* alleles by whole-genome resequencing and transcriptome analysis. *FEMS Yeast Res* **12**: 359–374
- Kreth J., Lengeler J.W., and Jahreis K. (2013) Characterization of Pyruvate Uptake in *Escherichia coli* K-12. *PLoS One* **8**: e67125
- Krishnamurthy H., Piscitelli C.L., and Gouaux E. (2009) Unlocking the molecular secrets of sodium-coupled transporters. *Nature* **459**: 347–55
- Krom B.P., Aardema R., and Lolkema J.S. (2001) *Bacillus subtilis* YxkJ is a secondary transporter of the 2-hydroxycarboxylate transporter family that transports L-malate and citrate. *J Bacteriol* **183**: 5862–9

- Krom B.P. and Lolkema J.S. (2003) Conserved residues R420 and Q428 in a cytoplasmic loop of the citrate/malate transporter CimH of *Bacillus subtilis* are accessible from the external face of the membrane. *Biochemistry* **42**: 467–74
- Krom B.P., Warner J.B., Konings W.N., and Lolkema J.S. (2000) Complementary metal ion specificity of the metal-citrate transporters CitM and CitH of *Bacillus subtilis*. *J Bacteriol* **182**: 6374–81
- Kumari S., Beatty C.M., Browning D.F., Busby S.J., Simel E.J., Hovel-Miner G., and Wolfe a J. (2000) Regulation of acetyl coenzyme A synthetase in *Escherichia coli*. *J Bacteriol* **182**: 4173–9
- Lang V.J., Leystra-Lantz C., and Cook R. a (1987) Characterization of the specific pyruvate transport system in *Escherichia coli* K-12. *J Bacteriol* **169**: 380–5
- Law C.J., Maloney P.C., and Wang D. (2008) Ins and outs of major facilitator superfamily antiporters. *Annu Rev Microbiol* **62**: 289–305
- Li H. and Pajor a M. (2002) Functional characterization of CitM, the Mg²⁺-citrate transporter. *J Membr Biol* **185**: 9–16
- Lo T.C., Rayman M.K., and Sanwal B.D. (1972) Transport of succinate in *Escherichia coli*. I. Biochemical and genetic studies of transport in whole cells. *J Biol Chem* **247**: 6323–31
- Lodi T., Diffels J., Goffeau A., and Baret P. V (2007) Evolution of the carboxylate Jen transporters in fungi. *FEMS Yeast Res* **7**: 646–56
- Lodi T., Fontanesi F., Ferrero I., and Donnini C. (2004) Carboxylic acids permeases in yeast: two genes in *Kluyveromyces lactis*. *Gene* **339**: 111–9
- Lü W., Du J., Schwarzer N.J., Gerbig-Smentek E., Einsle O., and Andrade S.L.A. (2012) The formate channel FocA exports the products of mixed-acid fermentation. *Proc Natl Acad Sci U S A* **109**: 13254–9
- Lü W., Du J., Wacker T., Gerbig-Smentek E., Andrade S.L. a, and Einsle O. (2011) pH-dependent gating in a FocA formate channel. *Science* **332**: 352–4
- Lütgens M. and Gottschalk G. (1980) Why a co-substrate is required for anaerobic growth of *Escherichia coli* on citrate. *J Gen Microbiol* **119**: 63–70
- Magni C., Mendoza D. de, Konings W.N., and Lolkema J.S. (1999) Mechanism of citrate metabolism in *Lactococcus lactis*: resistance against lactate toxicity at low pH. *J Bacteriol* **181**: 1451–7
- Magnuson J. and Lasure L. (2004) Organic acid production by filamentous fungi. In *Advances in Fungal Biotechnology for Industry, Agriculture, and Medicine - Book III*. Tkacz, J.S., and Lange, L. (eds). Springer US, pp. 307–340
- Mallinder P.R. and Moir A. (1991) Mutants of *Bacillus stearothermophilus* defective in the uptake and metabolism of acetate. *J Gen Microbiol* **137**: 779–785

- Matin a and Konings W.N. (1973) Transport of lactate and succinate by membrane vesicles of *Escherichia coli*, *Bacillus subtilis* and a pseudomonas species. *Eur J Biochem* **34**: 58–67
- Matsushita K., Inoue T., Adachi O., and Toyama H. (2005) *Acetobacter aceti* possesses a proton motive force-dependent efflux system for acetic acid. *J Bacteriol* **187**: 4346–52
- Mazier S., Quick M., and Shi L. (2011) Conserved tyrosine in the first transmembrane segment of solute:sodium symporters is involved in Na⁺-coupled substrate co-transport. *J Biol Chem* **286**: 29347–55
- McDermott J.R., Rosen B.P., and Liu Z. (2010) Jen1p: a high affinity selenite transporter in yeast. *Mol Biol Cell* **21**: 3934–41
- Nakano M.M. and Zuber P. (1998) Anaerobic growth of a “strict aerobe” (*Bacillus subtilis*). *Annu Rev Microbiol* **52**: 165–90
- Nakano S. and Fukaya M. (2008) Analysis of proteins responsive to acetic acid in *Acetobacter*: molecular mechanisms conferring acetic acid resistance in acetic acid bacteria. *Int J Food Microbiol* **125**: 54–9
- Nakano S., Fukaya M., and Horinouchi S. (2006) Putative ABC transporter responsible for acetic acid resistance in *Acetobacter aceti*. *Appl Environ Microbiol* **72**: 497–505
- Núñez M.F., Kwon O., Wilson T.H., Aguilar J., Baldoma L., and Lin E.C.C. (2002) Transport of L-Lactate, D-Lactate, and glycolate by the LldP and GlcA membrane carriers of *Escherichia coli*. *Biochem Biophys Res Commun* **290**: 824–9
- Núñez M.F., Pellicer M.T., Badía J., Aguilar J., and Baldomà L. (2001) The gene *yghK* linked to the *glc* operon of *Escherichia coli* encodes a permease for glycolate that is structurally and functionally similar to L-lactate permease. *Microbiology* **147**: 1069–77
- Osothsilp C. and Subden R.E. (1986) Malate transport in *Schizosaccharomyces pombe*. *J Bacteriol* **168**: 1439–43
- Paiva S., Devaux F., Barbosa S., Jacq C., and Casal M. (2004) Ady2p is essential for the acetate permease activity in the yeast *Saccharomyces cerevisiae*. *Yeast* **21**: 201–10
- Paiva S., Kruckeberg A.L., and Casal M. (2002) Utilization of green fluorescent protein as a marker for studying the expression and turnover of the monocarboxylate permease Jen1p of *Saccharomyces cerevisiae*. *Biochem J* **363**: 737–44
- Paiva S., Vieira N., Nondier I., Haguenaer-Tsapis R., Casal M., and Urban-Grimal D. (2009) Glucose-induced ubiquitylation and endocytosis of the yeast Jen1 transporter: role of lysine 63-linked ubiquitin chains. *J Biol Chem* **284**: 19228–36
- Palková Z., Devaux F., Icíková M., Mináriková L., Crom S. Le, and Jacq C. (2002) Ammonia pulses and metabolic oscillations guide yeast colony development. *Mol Biol Cell* **13**: 3901–14
- Papagianni M. (2012a) Recent advances in engineering the central carbon metabolism of industrially important bacteria. *Microb Cell Fact* **11**: 50

- Papagianni M. (2012b) Metabolic engineering of lactic acid bacteria for the production of industrially important compounds. *Comput Struct Biotechnol J* **3**: 1–8
- Pellicer M.T., Fernandez C., Badía J., Aguilar J., Lin E.C., and Baldom L. (1999) Cross-induction of *glc* and *ace* operons of *Escherichia coli* attributable to pathway intersection. Characterization of the *glc* promoter. *J Biol Chem* **274**: 1745–52
- Peng J., Schwartz D., Elias J.E., Thoreen C.C., Cheng D., Marsischky G. *et al.* (2003) A proteomics approach to understanding protein ubiquitination. *Nat Biotechnol* **21**: 921–6
- Piper P., Calderon C.O., Hatzixanthis K., and Mollapour M. (2001) Weak acid adaptation: the stress response that confers yeasts with resistance to organic acid food preservatives. *Microbiology* **147**: 2635–42
- Polen T., Schluesener D., Poetsch A., Bott M., and Wendisch V.F. (2007) Characterization of citrate utilization in *Corynebacterium glutamicum* by transcriptome and proteome analysis. *FEMS Microbiol Lett* **273**: 109–19
- Poolman B., Molenaar D., Smid E.J., Ubbink T., Abee T., Renault P.P., and Konings W.N. (1991) Malolactic fermentation: electrogenic malate uptake and malate/lactate antiport generate metabolic energy. *J Bacteriol* **173**: 6030–7
- Pos K.M., Dimroth P., and Bott M. (1998) The *Escherichia coli* citrate carrier CitT: a member of a novel eubacterial transporter family related to the 2-oxoglutarate/malate translocator from spinach chloroplasts. *J Bacteriol* **180**: 4160–5
- Pudlik A.M. and Lolkema J.S. (2011) Citrate uptake in exchange with intermediates in the citrate metabolic pathway in *Lactococcus lactis* IL1403. *J Bacteriol* **193**: 706–14
- Pudlik A.M. and Lolkema J.S. (2012) Substrate specificity of the citrate transporter CitP of *Lactococcus lactis*. *J Bacteriol* **194**: 3627–35
- Queirós O., Pereira L., Paiva S., Moradas-Ferreira P., and Casal M. (2007) Functional analysis of *Kluyveromyces lactis* carboxylic acids permeases: heterologous expression of *KIJEN1* and *KIJEN2* genes. *Curr Genet* **51**: 161–9
- Radestock S. and Forrest L.R. (2011) The alternating-access mechanism of MFS transporters arises from inverted-topology repeats. *J Mol Biol* **407**: 698–715
- Ren Q. and Paulsen I.T. (2005) Comparative analyses of fundamental differences in membrane transport capabilities in prokaryotes and eukaryotes. *PLoS Comput Biol* **1**: e27
- Reyes-Ramírez F. and Sawers R.G. (2006) Aerobic activation of transcription of the anaerobically inducible *Escherichia coli* *focA-pfl* operon by fumarate nitrate regulator. *FEMS Microbiol Lett* **255**: 262–7
- Rიცოვ M., Kucerov H., Vchov L., and Palkov Z. (2007) Association of putative ammonium exporters Ato with detergent-resistant compartments of plasma membrane during yeast colony development: pH affects Ato1p localisation in patches. *Biochim Biophys Acta* **1768**: 1170–8

- Robellet X., Flippi M., Pégot S., Maccabe A.P., and Vélot C. (2008) AcpA, a member of the GPR1/FUN34/YaaH membrane protein family, is essential for acetate permease activity in the hyphal fungus *Aspergillus nidulans*. *Biochem J* **412**: 485–93
- Rodriguez S.B. and Thornton R.J. (1990) Factors influencing the utilisation of L-malate by yeasts. *FEMS Microbiol Lett* **60**: 17–22
- Rohlin L. and Gunsalus R.P. (2010) Carbon-dependent control of electron transfer and central carbon pathway genes for methane biosynthesis in the Archaeon, *Methanosarcina acetivorans* strain C2A. *BMC Microbiol* **10**: 62
- Royce L. a, Liu P., Stebbins M.J., Hanson B.C., and Jarboe L.R. (2013) The damaging effects of short chain fatty acids on *Escherichia coli* membranes. *Appl Microbiol Biotechnol* **97**: 8317–27
- Russell J.B. (1992) Another explanation for the toxicity of fermentation acids at low pH: anion accumulation versus uncoupling. *J Appl Bacteriol* **73**: 363–370
- Saier M.H. (2000) A functional-phylogenetic classification system for transmembrane solute transporters. *Microbiol Mol Biol Rev* **64**: 354–411
- Saier M.H., Goldman S.R., Maile R.R., Moreno M.S., Weyler W., Yang N., and Paulsen I.T. (2002) Transport capabilities encoded within the *Bacillus subtilis* genome. *J Mol Microbiol Biotechnol* **4**: 37–67
- Saier M.H., Tran C. V, and Barabote R.D. (2006) TCDB: the Transporter Classification Database for membrane transport protein analyses and information. *Nucleic Acids Res* **34**: D181–6
- Saier M.H., Yen M.R., Noto K., Tamang D.G., and Elkan C. (2009) The Transporter Classification Database: recent advances. *Nucleic Acids Res* **37**: D274–8
- Salmond C. V, Kroll R.G., and Booth I.R. (1984) The effect of food preservatives on pH homeostasis in *Escherichia coli*. *J Gen Microbiol* **130**: 2845–50
- Sá-Pessoa J., Paiva S., Ribas D., Silva I.J., Viegas S.C., Arraiano C.M., and Casal M. (2013) SatP (YaaH), a succinate-acetate transporter protein in *Escherichia coli*. *Biochem J* **454**: 585–95
- Sauer M., Porro D., Mattanovich D., and Branduardi P. (2008) Microbial production of organic acids: expanding the markets. *Trends Biotechnol* **26**: 100–8
- Sawers R.G. (2005) Evidence for novel processing of the anaerobically inducible dicistronic *focA-pfl* mRNA transcript in *Escherichia coli*. *Mol Microbiol* **58**: 1441–53
- Scheu P.D., Witan J., Rauschmeier M., Graf S., Liao Y.-F., Ebert-Jung a *et al.* (2012) CitA/CitB two-component system regulating citrate fermentation in *Escherichia coli* and its relation to the DcuS/DcuR system in vivo. *J Bacteriol* **194**: 636–45
- Schneider K., Dimroth P., and Bott M. (2000) Biosynthesis of the prosthetic group of citrate lyase. *Biochemistry* **39**: 9438–50

- Shaw J.G., Hamblin M.J., and Kelly D.J. (1991) Purification, characterization and nucleotide sequence of the periplasmic C4-dicarboxylate-binding protein (DctP) from *Rhodobacter capsulatus*. *Mol Microbiol* **5**: 3055–62
- Shaw J.G. and Kelly D.J. (1991) Binding protein dependent transport of C4-dicarboxylates in *Rhodobacter capsulatus*. *Arch Microbiol* **155**: 466–472
- Six S., Andrews S.C., Uden G., and Guest J.R. (1994) *Escherichia coli* possesses two homologous anaerobic C4-dicarboxylate membrane transporters (DcuA and DcuB) distinct from the aerobic dicarboxylate transport system (Dct). *J Bacteriol* **176**: 6470–8
- Soares-Silva I., Paiva S., Diallinas G., and Casal M. (2007) The conserved sequence NXX[S/T]HX[S/T]QDXXXT of the lactate/pyruvate:H(+) symporter subfamily defines the function of the substrate translocation pathway. *Mol Membr Biol* **24**: 464–74
- Soares-Silva I., Paiva S., Kötter P., Entian K.-D., and Casal M. (2004) The disruption of *JEN1* from *Candida albicans* impairs the transport of lactate. *Mol Membr Biol* **21**: 403–11
- Soares-Silva I., Sá-Pessoa J., Myriantopoulos V., Mikros E., Casal M., and Diallinas G. (2011) A substrate translocation trajectory in a cytoplasm-facing topological model of the monocarboxylate/H⁺ symporter Jen1p. *Mol Microbiol* **81**: 805–17
- Soares-Silva I., Schuller D., Andrade R.P., Baltazar F., Cássio F., and Casal M. (2003) Functional expression of the lactate permease Jen1p of *Saccharomyces cerevisiae* in *Pichia pastoris*. *Biochem J* **376**: 781–7
- Speck E.L. and Freese E. (1973) Control of metabolite secretion in *Bacillus subtilis*. *J Gen Microbiol* **78**: 261–75
- Stansen C., Uy D., Delaunay S., Eggeling L., Goergen J., and Wendisch V.F. (2005) Characterization of a *Corynebacterium glutamicum* lactate utilization operon induced during temperature-triggered glutamate production. *Appl Environ Microbiol* **71**: 5920–8
- Steiner P. and Sauer U. (2001) Proteins induced during adaptation of *Acetobacter aceti* to high acetate concentrations. *Appl Environ Microbiol* **67**: 5474–81
- Strachotová D., Holoubek A., Kučerová H., Benda A., Humpolíčková J., Váchová L., and Palková Z. (2012) Ato protein interactions in yeast plasma membrane revealed by fluorescence lifetime imaging (FLIM). *Biochim Biophys Acta* **1818**: 2126–34
- Suppmann B. and Sawers G. (1994) Isolation and characterization of hypophosphite--resistant mutants of *Escherichia coli*: identification of the FocA protein, encoded by the *pfl* operon, as a putative formate transporter. *Mol Microbiol* **11**: 965–82
- Tanaka K. (2003) The *Bacillus subtilis* YufLM two-component system regulates the expression of the malate transporters MaeN (YufR) and YflS, and is essential for utilization of malate in minimal medium. *Microbiology* **149**: 2317–2329

- Teramoto H., Shirai T., Inui M., and Yukawa H. (2008) Identification of a gene encoding a transporter essential for utilization of C4 dicarboxylates in *Corynebacterium glutamicum*. *Appl Environ Microbiol* **74**: 5290–6
- Thomas G.H., Southworth T., León-Kempis M.R., Leech A., and Kelly D.J. (2006) Novel ligands for the extracellular solute receptors of two bacterial TRAP transporters. *Microbiology* **152**: 187–98
- Valgepea K., Adamberg K., Nahku R., Lahtvee P., Arike L., and Vilu R. (2010) Systems biology approach reveals that overflow metabolism of acetate in *Escherichia coli* is triggered by carbon catabolite repression of acetyl-CoA synthetase. *BMC Syst Biol* **4**: 166
- Veit A., Polen T., and Wendisch V.F. (2007) Global gene expression analysis of glucose overflow metabolism in *Escherichia coli* and reduction of aerobic acetate formation. *Appl Microbiol Biotechnol* **74**: 406–21
- Vieira N., Casal M., Johansson B., MacCallum D.M., Brown A.J.P., and Paiva S. (2010) Functional specialization and differential regulation of short-chain carboxylic acid transporters in the pathogen *Candida albicans*. *Mol Microbiol* **75**: 1337–54
- Waight A.B., Love J., and Wang D.-N. (2010) Structure and mechanism of a pentameric formate channel. *Nat Struct Mol Biol* **17**: 31–7
- Walmsley a R., Shaw J.G., and Kelly D.J. (1992) The mechanism of ligand binding to the periplasmic C4-dicarboxylate binding protein (DctP) from *Rhodobacter capsulatus*. *J Biol Chem* **267**: 8064–72
- Wang Y., Huang Y., Wang J., Cheng C., Huang W., Lu P. *et al.* (2009) Structure of the formate transporter FocA reveals a pentameric aquaporin-like channel. *Nature* **462**: 467–72
- Warner J.B., Krom B.P., Magni C., Konings W.N., and Lolkema J.S. (2000) Catabolite repression and induction of the Mg(2+)-citrate transporter CitM of *Bacillus subtilis*. *J Bacteriol* **182**: 6099–105
- Warner J.B. and Lolkema J.S. (2002) Growth of *Bacillus subtilis* on citrate and isocitrate is supported by the Mg²⁺-citrate transporter CitM. *Microbiology* **148**: 3405–12
- Watanabe A., Choe S., Chaptal V., Rosenberg J.M., Wright E.M., Grabe M., and Abramson J. (2010) The mechanism of sodium and substrate release from the binding pocket of vSGLT. *Nature* **468**: 988–91
- Wei Y., Guffanti a a, Ito M., and Krulwich T. a (2000) *Bacillus subtilis* YqkI is a novel malic/Na⁺-lactate antiporter that enhances growth on malate at low protonmotive force. *J Biol Chem* **275**: 30287–92
- Wendisch V.F., Graaf a a de, Sahm H., and Eikmanns B.J. (2000) Quantitative determination of metabolic fluxes during coutilization of two carbon sources: comparative analyses with *Corynebacterium glutamicum* during growth on acetate and/or glucose. *J Bacteriol* **182**: 3088–96

- Willison J.C. (1988) Pyruvate and Acetate Metabolism in the Photosynthetic Bacterium *Rhodobacter capsulatus*. *Microbiology* **134**: 2429–2439
- Winnen B., Felce J., and Saier M.H. (2005) Genomic analyses of transporter proteins in *Corynebacterium glutamicum* and *Corynebacterium efficiens*. 149–186
- Wolfe A.J. (2005) The acetate switch. *Microbiol Mol Biol Rev* **69**: 12–50
- Wyborn N.R., Alderson J., Andrews S.C., and Kelly D.J. (2001) Topological analysis of DctQ, the small integral membrane protein of the C4-dicarboxylate TRAP transporter of *Rhodobacter capsulatus*. *FEMS Microbiol Lett* **194**: 13–7
- Yamamoto H., Murata M., and Sekiguchi J. (2000) The CitST two-component system regulates the expression of the Mg-citrate transporter in *Bacillus subtilis*. *Mol Microbiol* **37**: 898–912
- Yamamoto K., Matsumoto F., Minagawa S., Oshima T., Fujita N., Ogasawara N., and Ishihama A. (2009) Characterization of CitA-CitB Signal Transduction Activating Genes Involved in Anaerobic Citrate Catabolism in *Escherichia coli*. *Biosci Biotechnol Biochem* **73**: 346–350
- Yan N. (2013) Structural advances for the major facilitator superfamily (MFS) transporters. *Trends Biochem Sci* **38**: 151–9
- Youn J.-W., Jolkver E., Krämer R., Marin K., and Wendisch V.F. (2008) Identification and characterization of the dicarboxylate uptake system DccT in *Corynebacterium glutamicum*. *J Bacteriol* **190**: 6458–66
- Youn J.-W., Jolkver E., Krämer R., Marin K., and Wendisch V.F. (2009) Characterization of the dicarboxylate transporter DctA in *Corynebacterium glutamicum*. *J Bacteriol* **191**: 5480–8
- Zientz E., Janusch I.G., Six S., and Uden G. (1999) Functioning of DcuC as the C4-dicarboxylate carrier during glucose fermentation by *Escherichia coli*. *J Bacteriol* **181**: 3716–20
- Zientz E., Six S., and Uden G. (1996) Identification of a third secondary carrier (DcuC) for anaerobic C4-dicarboxylate transport in *Escherichia coli*: roles of the three Dcu carriers in uptake and exchange. *J Bacteriol* **178**: 7241–7
- Zmijewski M.J. and MacQuillan a M. (1975) Dual effects of glucose on dicarboxylic acid transport in *Kluyveromyces lactis*. *Can J Microbiol* **21**: 473–80

Chapter II

A substrate translocation trajectory in a cytoplasm-facing topological model of the monocarboxylate/H⁺ symporter Jen1p

CHAPTER II

A SUBSTRATE TRANSLOCATION TRAJECTORY IN A CYTOPLASM-FACING TOPOLOGICAL MODEL OF THE MONOCARBOXYLATE/H⁺ SYMPORTER JEN1P.

Adapted from:

Soares-Silva, I.*, Sá-Pessoa, J.*, Myriantopoulos, V., Mikros, E., Casal, M., and Diallinas, G. (2011) A substrate translocation trajectory in a cytoplasm-facing topological model of the monocarboxylate/H⁺ symporter Jen1p. *Mol Microbiol* **81**: 805–17.

*Both authors contributed equally for this work

Abstract

Previous mutational analysis of Jen1p, a *Saccharomyces cerevisiae* monocarboxylate/H⁺ symporter of the Major Facilitator Superfamily, has suggested that the consensus sequence ³⁷⁹NXX[S/T]HX[S/T]QD³⁸⁷ in transmembrane segment VII (TMS-VII) is part of the substrate translocation pathway. Here, we rationally design, analyse and show that several novel mutations in TMS-V and TMS-XI directly modify Jen1p function. Among the residues studied, F270 (TMS-V) and Q498 (TMS-XI) are critical specificity determinants for the distinction of mono- from di-carboxylates, and N501 (TMS-XI) is a critical residue for function. Using a model created on the basis of Jen1p similarity with the GlpT permease, we show that all polar residues critical for function within TMS-VII and TMS-XI (N379, H383, D387, Q498, N501) are perfectly aligned in an imaginary axis that lies parallel to a protein pore. This model and subsequent mutational analysis further reveal that an additional polar residue facing the pore, R188 (TMS-II), is irreplaceable for function. Our model also justifies the role of F270 and Q498 in substrate specificity. Finally, docking approaches reveal a ‘trajectory-like’ substrate displacement within the Jen1p pore, where R188 plays a major dynamic role mediating the orderly relocation of the substrate by subsequent H-bond interactions involving itself and residues H383, N501 and Q498.

Introduction

The transport of monocarboxylates, such as lactate, pyruvate and acetate, is essential for the metabolism and homeostasis of most cells. A family of monocarboxylate transporters (MCTs) has been reported that includes mainly mammalian members, which seem to be implicated in leukocyte-mediated immunity, hypoxia induced cellular responses, tissue partitioning of energy supply and tumour suppression (Ganapathy *et al.*, 2008; Merezhinskaya *et al.*, 2009). In fungi, activities for monocarboxylate-proton symporters have been found and shown to belong to two evolutionary distinct families. In *Saccharomyces cerevisiae*, one is encoded by the *JEN1* gene (Casal *et al.*, 1999) and another by the *ADY2* gene (Paiva *et al.*, 2004). These permeases exhibit differences in their mechanisms of regulation and specificity. Jen1p is a lactate-pyruvate-acetate-propionate transporter induced in lactic or pyruvic acid-grown cells, whereas Ady2p, which recognizes acetate, propionate or formate, is present in cells grown in non-fermentable carbon sources (Casal *et al.*, 2008). Interestingly, Jen1p also transports selenite in a proton-dependent manner, which resembles the transport mechanism for lactate or pyruvate (McDermott *et al.*, 2010).

Jen1p, which is the only *S. cerevisiae* member of the Sialate:H⁺ Symporter (SHS) Family (2.A.1.12) belonging to the Major Facilitator Superfamily (see below), has been extensively studied. It was the first permease of *S. cerevisiae* characterized by heterologous expression in *Pichia pastoris* at both the cell and the membrane vesicle levels (Soares-Silva *et al.*, 2003). The addition of glucose to lactic acid-grown cells very rapidly triggers loss of Jen1p activity and repression of *JEN1* gene expression (Andrade *et al.*, 2005). Jen1p activity is rapidly lost due to vacuolar degradation by endocytic internalization and sorting of newly synthesized polypeptides from the *trans*-Golgi to the MVB pathway. For both down-regulation pathways, Jen1p needs to be modified by ubiquitination with ubiquitin-Lys⁶³ linked chain(s), through the action of the HECT-ubiquitin ligase Rsp5. Casein kinase 1-dependent phosphorylation is also required for Jen1p endocytosis (Paiva *et al.*, 2009). An evolutionary analysis has shown that several Jen1p homologues exist in all kinds of fungi (Lodi *et al.*, 2007). In yeasts like *Kluyveromyces lactis* and *Candida albicans*, the existence of two phylogenetically related Sc*JEN1*-like transporters with different specificities, namely for monocarboxylate (Jen1p subfamily) and dicarboxylate (Jen2p subfamily), was clearly demonstrated (Casal *et al.*, 2008; Lodi *et al.*, 2004; Soares-Silva *et al.*, 2004; Vieira *et al.*, 2010).

The MFS, where Jen1 belongs, constitutes the largest known family of secondary transporter proteins (Law *et al.*, 2008). They are responsible for the ion-coupled transport of a wide range of substrates, from monoamines to sugars to peptides. X-ray crystallography studies solving the structures of a handful of MFS revealed that the 12 TMS are arranged into two domains of 6 TMS each, which are related by a 2-fold pseudo-symmetry with an axis that runs normal to the membrane and between the two halves. Lactose permease (LacY), a proton/sugar co-transporter, is the prototype of the MFS proteins, not only because it is among the first crystallized, but mainly because there is a plethora of genetic, biochemical and molecular data, which have been accumulated within the last 30 years, mostly through the excellent work of the group of R. Kaback. These data have validated the structural model and have shed light on how this molecule works through an alternating-access transport mechanism (Kaback *et al.*, 2011).

Structure-function relationships in Jen1p have been approached by using a rational mutational analysis of conserved amino acid residues (Soares-Silva *et al.*, 2007). In particular, functional studies of mutants concerning the conserved sequence ³⁷⁹NXX[S/T]HX[S/T]QDXXXT³⁹¹, located towards the periplasmic side of putative transmembrane segment seven (TMS-VII), led to the observation that residues N379, H383 or D387 are necessary for function and specificity, while Q386 is important for the kinetics of Jen1p-mediated transport. Furthermore, 3D *in silico* modelling by homology threading using the structure of LacY (Guan *et al.*, 2006), further suggested that the conserved motif analyzed could be part of the substrate translocation pathway of Jen1p (Soares-Silva *et al.*, 2007). In this work we identified novel residues critical for the function and specificity of Jen1p. Subsequently, using a novel refined model created on the basis of Jen1p similarity with GlpT permease, an antiporter of glycerol-3-phosphate/inorganic phosphate (P_i) (Huang *et al.*, 2003), and independent substrate docking studies, we reveal a substrate translocation trajectory in the inward-facing conformation of Jen1p, consisting mostly of the polar residues genetically identified as important for function.

Experimental Procedures

Yeast strains and growth conditions

The *S. cerevisiae* strain W303-1A *jen1*Δ *ady2*Δ, lacking monocarboxylate uptake capacity, was used to express *JEN1* mutants from a low copy plasmid (pDS-1, see below). Cultures were maintained on slants of yeast extract (1%, w/v), peptone (1%, w/v), glucose (2%, w/v) and agar (2%, w/v) or minimal media with required supplements for growth. Yeast cells were grown in yeast nitrogen base (Difco), 0.67%, w/v (YNB medium), supplemented as required, or in yeast extract (1%, w/v), peptone (1%, w/v) (YP medium). Carbon sources were glucose (2%, w/v), lactic acid (0.5%, v/v, pH 5.0), pyruvic acid (0.5%, w/v, pH 5.0), succinic acid (1%, w/v, pH 5.0), malic acid (1% w/v, pH 5.0). Growth was carried out at 30 °C. Cultures were always harvested during the exponential phase of growth. For derepression conditions glucose-grown cells were centrifuged, washed twice in ice-cold deionised water and cultivated into fresh YNB medium supplemented with lactic acid for 4 hours. For drop tests, cells were grown on YNB Glu-Ura media, until a OD_{640nm} of 0.1 was reached. A set of three 1:10 serial dilutions was performed and 3 µl of each suspension was inoculated in the desired medium, using YNB Glu-Ura as a control. Cells were incubated at 18°C for 10 days or alternatively at 30°C for 3 days. At 18 °C carboxylic acid uptake by diffusion is drastically reduced so that growth on lactic acid as sole carbon source is directly dependent on a functional Jen1p transporter. For selenite sensitivity tests, strains were grown on YNB-glucose medium supplemented with 200 µM sodium selenite.

Construction of *JEN1* mutations

Plasmid isolation from *E. coli* strains and DNA manipulations were performed by standard protocols. *JEN1* mutations were constructed in centromeric plasmids, under the control of the GPD promoter, pDS1 (WT-Jen1) or pDS1-GFP, the latter carrying a gfp-tagged version of *JEN1*, with oligonucleotide-directed mutagenesis as previously described (Soares-Silva *et al.*, 2007). The oligonucleotides used are listed in Table 1. Mutations were confirmed by sequencing. The mutant alleles were introduced in a *S. cerevisiae* W303-1A *jen1*Δ *ady2*Δ strain, and transformants were selected on complementation of uracil auxotrophy. As a control the strain was also transformed with the original vector p416GPD.

Table 1 – Sequence of the forward primers used in the *Jen1* mutagenesis.

Mutation	Wt codon	Mutant codon	Primers
R188K	cgt	aaa	5' GGATTGGTGTATTTGTTAAATCAGCAGGTGCTGTC 3'
R188A	cgt	gct	5' GGATTGGTGTATTTGTTGCTTCAGCAGGTGCTGTC 3'
S266T	tca	aca	5' GCACGTTTCGTTCCCTAACAGGTCTATTTTTTTCTG 3'
S266A	tca	gca	5' GCACGTTTCGTTCCCTAGCAGGTCTATTTTTTTCTG 3'
F270G	ttt	ggt	5' CTATCAGGTCTATTTGGTTCTGCTTACGCTATGG 3'
F270L	ttt	ctt	5' CTATCAGGTCTATTTCTTTCTGCTTACGCTATGG 3'
F270P	ttt	cct	5' CTATCAGGTCTATTTCTTCTGCTTACGCTATGG 3'
F270Y	ttt	tat	5' CTATCAGGTCTATTTTATTCTGCTTACGCTATGG 3'
F270Q	ttt	caa	5' CTATCAGGTCTATTTCAATCTGCTTACGCTATGG 3'
F270A	ttt	gct	5' CTATCAGGTCTATTTGCTTCTGCTTACGCTATGG 3'
S271Q	tct	caa	5' CTATCAGGTCTATTTTTTTCAAGCTTACGCTATGGGG 3'
S271E	tct	gaa	5' CTATCAGGTCTATTTTTTTGAAGCTTACGCTATGGGG 3'
F270QS271Q	ttttct	caacaa	5' CTATCAGGTCTATTTCAACAAGCTTACGCTATGGGG 3'
F270QS271E	ttttct	caagaa	5' CTATCAGGTCTATTTCAAGAAGCTTACGCTATGGGG 3'
A272G	gct	ggt	5' GGTCTATTTTTTTCTGGTTACGCTATGGGGTTC 3'
Y273A	tac	gct	5' CTATTTTTTTCTGCTGCTGCTATGGGGTTCATATTTG 3'
Y284Q	tac	caa	5' CATATTTGCTATCATTTTTCAAAGAGCCTTTGGCTAC 3'
Y284T	tac	act	5' CATATTTGCTATCATTTTTACTAGAGCCTTTGGCTAC 3'
Y284A	tac	gct	5' CATATTTGCTATCATTTTTGCTAGAGCCTTTGGCTAC 3'
Q498N	cag	aat	5' GCCGGTTTATCTTACAATCTAGGTAATCTAGCTTC 3'
Q498E	cag	gaa	5' GCCGGTTTATCTTACGAACTAGGTAATCTAGCTTC 3'
Q498A	cag	gct	5' GCCGGTTTATCTTACGCTCTAGGTAATCTAGCTTC 3'
N501Q	aat	caa	5' GTTTATCTTACCAGCTAGGTCAACTAGCTTCTGCAGCG 3'
N501D	aat	gat	5' GTTTATCTTACCAGCTAGGTGATCTAGCTTCTGCAGCG 3'
N501A	aat	gct	5' GTTTATCTTACCAGCTAGGTGCTCTAGCTTCTGCAGCG 3'

Epifluorescent microscopy

Samples for fluorescence microscopy were grown, at 30 °C until midexponential growth phase and then shifted under derepressed conditions for *Jen1p* expression (YNB lactate 0.5% (v/v), pH 5.0) for 4 h (Soares-Silva *et al.*, 2007). Samples were at this point immobilized on coverslips using one volume of low-melting agarose and then directly observed on a Leica DM5000B epifluorescent microscope with appropriate filters. The resulting images were acquired with a Leica DFC 350FX R2 digital camera using the LAS AF V1.4.1 software. Images were then processed in the Adobe Photoshop CS2 V9.0.2 software.

Transport assays

Measurement of transport activity and competition assays were performed as previously described (Soares-Silva *et al.*, 2007) using radiolabelled D,L-[U-¹⁴C] lactic acid (Amersham Biosciences).

Model construction, validation and molecular simulations

Sequence similarity was determined by a HMM-HMM comparison with HHpred software (<http://toolkit.tuebingen.mpg.de/hhpred>). The HMM profile query afforded four distinct structural templates from bacteria, the glycerol-3-phosphate transporter GlpT (pdb entry: 1PW4) (Huang *et al.*, 2003), the lactose permease LacY (pdb entry: 1PV7) (Abramson *et al.*, 2003), the fucose permease FucP (pdb entry:3O7Q) (Dang *et al.*, 2010) and the oligopeptide permease PepT (pdb entry:2XUT) (Newstead *et al.*, 2011). Alignments were created for all four templates and relevant models were built using MODELLER software (Sali *et al.*, 1995). A stepwise validation approach was followed, consisting of MD model optimization, comparison with existing experimental data and, finally, visual inspection. First, theoretical models were subjected to 2.5ns of Stochastic Dynamics simulation and found relatively stable, with a measured RMS deviation of alpha carbons from starting coordinates not exceeding 3Å. After SD optimization, the two best models, those built on GlpT and LacY, were tested for structural consistency by considering all available experimental data. Both were in good accordance with the proposed substrate translocation pathway as it was outlined by observations based on mutagenesis and kinetics studies presented previously and in the present study. The constructed models were not of identical structural quality. Visual inspection has revealed a number of secondary structure inconsistencies on the homology-derived model built on LacY. A second issue regarding this particular model was the width of the protein pore. The LacY transporter facilitates the translocation of disaccharides, molecules that are far bulkier than the corresponding substrates of GlpT transporter. As a result, the pore of the two templates differs in width significantly. Given that the homology modeling protocol utilized herein does not allow for major conformational changes of the modeled proteins and induced fit, the pore width would be solely dependent on the template used. It was reasoned that the pronounced similarity of the physicochemical profile and steric volume between glycerol-3-phosphate and lactate advocates in favor of the assumption that Jen1p protein pore would be of greater geometric similarity to the less wide channel of GlpT as

compared to the one of LacY. On the basis of this hypothesis and the higher accordance of the GlpT-based model with mutagenesis data, all subsequent docking calculations were performed on the GlpT-based model. The conformational space of the protein-ligand complex was extensively explored by the use of a mixed sampling protocol implementing stochastic Monte Carlo and low frequency mode conformational searches (Kolossvary *et al.*, 1996). The method has proven highly efficient in sampling molecular systems and although inferior to MD simulations from the physical point of view concerning intermediate search steps, it is considered as a robust technique. Simulations performed on the basis of the aforementioned extensive sampling protocol afforded a fair amount of structural as well as dynamic insight regarding factors that govern or influence the translocation of the various substrates across the pore of the transporter. All molecular simulations were performed using the AMBER* forcefield and the GB/SA implicit water model as they are implemented in MacroModel v.9 software (Mohamadi *et al.*, 1990).

Results

Rationale of mutation design

A rational, rather than a systematic, mutagenesis approach for Jen1p was based on two criteria. First, identify Jen1p amino acids that correspond to residues shown by crystallographic and functional studies to be involved in substrate recognition in LacY and GlpT, the two MFS permeases which exhibit the highest similarity score with Jen1p in homology threading approaches (described in the Experimental procedures). Second, identify by primary amino acid sequence alignments, Jen1p residues conserved in monocarboxylate transporters, but replaced by another conserved residue in dicarboxylate transporters of the Jen2p subfamily. While in both LacY and GlpT, a number of residues from several TMS contribute to substrate and H⁺ binding, two residues in each case have been proposed to play primary roles in direct interactions with substrates. These are R144 (TMS-V) and K358 (TMS-XI) in LacY (Guan *et al.*, 2006), and R45 (TMS-I) and R269 (TMS-VII) in GlpT (Huang *et al.*, 2003). In Jen1p, these residues correspond to F270, N501, F156 and H383, respectively. We have previously analyzed mutations concerning H383 and have shown that this residue is absolutely essential for function (Soares-Silva *et al.*, 2007).

In the present work, we undertook the analysis of F270, N501 and several of their neighboring residues. Our choice was further strengthened by the following observations. F270 is a well conserved hydrophobic residue in monocarboxylate transporters (Phe or Leu), but is replaced by a conserved Gln in dicarboxylate transporters (Figure 1). An evolutionary relationship of mono and di-carboxylate transporters was previously reported (Casal *et al.*, 2008). Based on α -helical wheel projection of TMS-V, we also noticed that on the same side of F270 lies an absolutely conserved Ser residue (S266) and three well conserved bulky aromatic amino acids (Y273, F277, Y284). Among the latter, Y284 is replaced by Gln in dicarboxylic acid transporters and Ala or Asn in other Jen1p homologues of unknown specificity. Furthermore, we noticed that on the opposite side of the TMS-V helix of Jen1p, A272 is conserved in monocarboxylic acid transporters, but is replaced by Gly in dicarboxylic acid-specific homologues (see Figure 1). Finally, N501 and its neighboring Q498 are two absolutely conserved polar residues, present in the middle of TMS-XI of all Jen1p homologues, including mono- and di-carboxylate permeases (Figure 1).

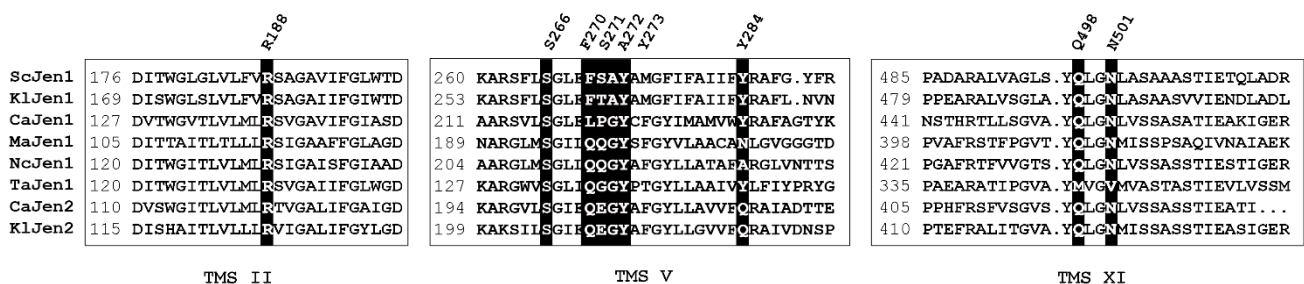


Figure 1 – Multiple sequence alignment of TMS-II, TMS-V and TMS-XI of Jen1 homologues. Residues mutated in this work are highlighted in black boxes. The alignment was built using the ClustalW2 bioinformatics tool. (<http://www.ebi.ac.uk/Tools/clustalw2/>). Sc, Kl and Ca denote *S. cerevisiae*, *K. lactis* and *C. albicans* permeases of known specificity for mono- (Jen1) or dicarboxylates (Jen2). MaJen1, NcJen1 and TaJen1 denote Jen1 homologues of unknown function from *Metarhizium anisopliae*, *Neurospora crassa* and *Thermoplasma acidophilum*. Accession numbers, in order of appearance, NP_012705, CAG99769, XP_716108, AAM77971, XP_962841, CAC11721, XP_717031, CAG98245. An evolutionary relationship of mono and di-carboxylate transporters can be found in Casal *et al.*, 2008.

Based on the above observations we made the following 23 *JEN1* mutations: F270Q, F270L, F270A, F270P, F270G, F270Y, S271Q, S271E, F270Q/S271Q, F270Q/S271E, Y273A, Y284T, Y284A, Y284Q, S266T, S266A, A272G, Q498A, Q498N, Q498E, N501A, N501Q, N501D. All mutations were constructed on plasmid pDS-1, which

contains the *JEN1* sequence under the control of the *GPD* promoter, and introduced through genetic transformation into a *S. cerevisiae jen1Δ ady2Δ* strain, based on *ura3* complementation (Soares-Silva *et al.*, 2007). The recipient strain lacks carrier-mediated monocarboxylate transport activity and thus allows the direct assessment of plasmid-borne *JEN1* mutations.

Jen1p function and specificity is differentially affected in several mutants

Figure 2 shows a relative comparison of Jen1p-mediated [¹⁴C]-lactic acid transport in control strains and mutants. Mutants could be classified into two basic types:

- those reducing or abolishing ($\leq 30\%$) Jen1p-mediated transport (S266T, F270L, F270P, F270Q, F270Q/S271E, Y273A, Q498E, N501Q, N501D and N501A),
- those affecting moderately ($\sim 60\text{-}210\%$) Jen1p-mediated transport (S266A, F270G, F270Y, F270A, S271Q, S271E, F270Q/S271Q, A272G, Y284Q, Y284T, Y284A, Q498N, Q498A).

Our results showed that several specific substitutions of S266, F270, Y273 and Q498, and all substitutions of N501, behave as loss-of-function mutations.

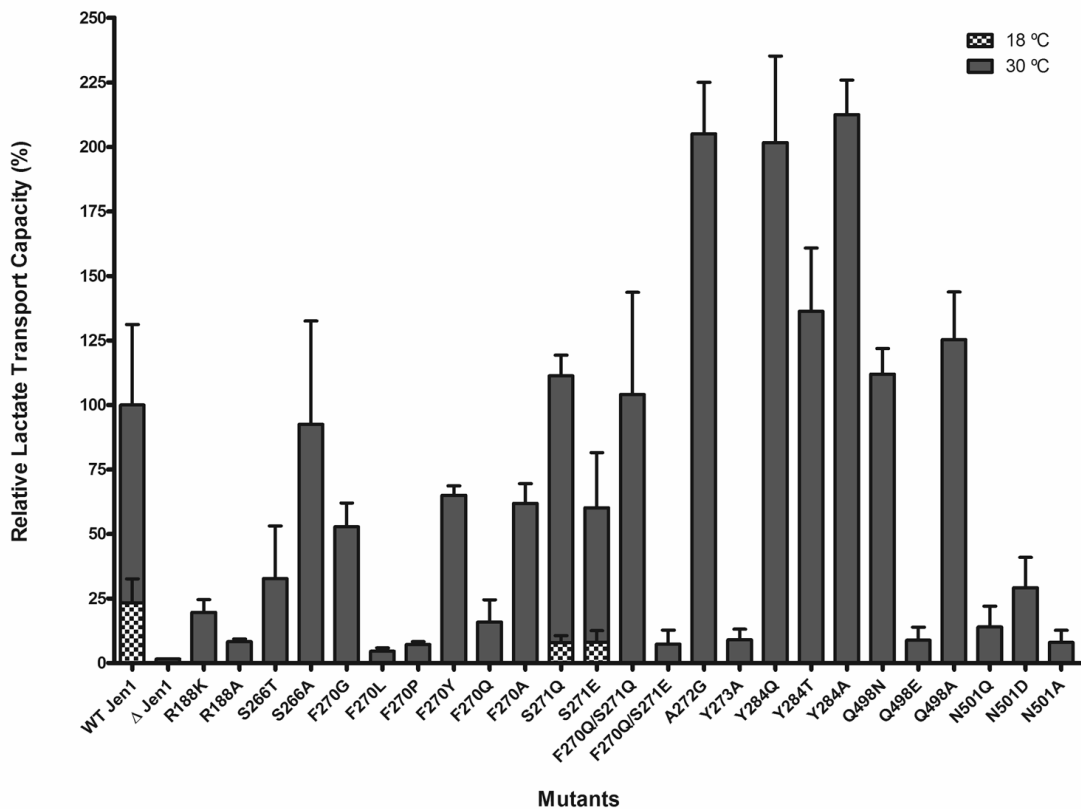


Figure 2 – Relative % of Jen1p-mediated [¹⁴C]-lactic acid transport in mutants at 30 °C. The % uptake rate of the wild-type Jen1p (WT Jen1 – *S. cerevisiae Δjen1Δady2* carrying the plasmid pDS1) is considered

100%. For wild-type and the cryosensitive mutants S271Q or S271E similar uptake measurements were also performed at 18 °C (see text). The data shown are mean values of at least 3 independent experiments and the error bars represent standard deviation.

In order to test whether mutations affecting the apparent Jen1p activity do so due to a direct effect on transport, rather than an effect on Jen1p expression in the plasma membrane, we re-constructed several of these mutations in a fully functional GFP-tagged version of Jen1p (see Experimental Procedures), giving particular priority to those negatively affecting Jen1p-mediated transport. Figure 3 shows that none of the mutations tested affects the expression of Jen1p in the plasma membrane of *S. cerevisiae*, strongly indicating that these mutations affect Jen1p transport function *per se*.

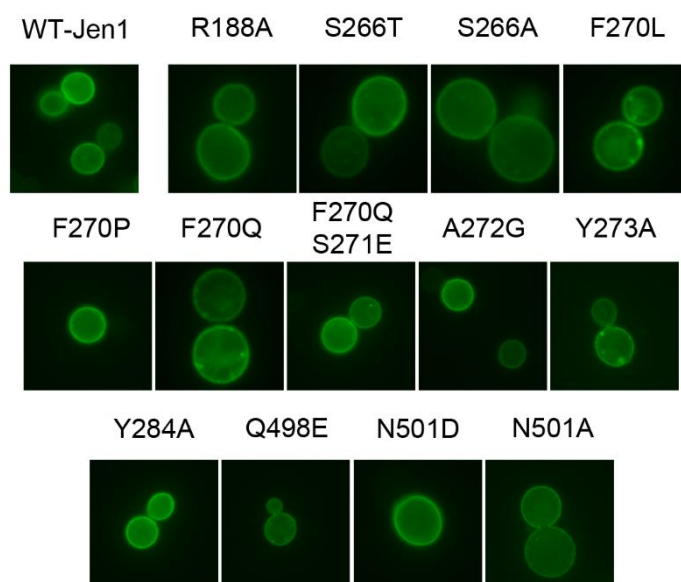


Figure 3 – Epifluorescent microscopy of GFP-tagged version of Jen1p in a control strain and mutants (for details see Experimental procedures). In all cases, Jen1-GFP molecules label the plasma membrane.

We tested the growth of control strains and mutants on monocarboxylates and dicarboxylates (succinic or malic acid) as sole carbon sources. In the conditions used (see Experimental Procedures), *S. cerevisiae* does not possess detectable dicarboxylate transporter activities, so any mutation conferring to Jen1p the ability to take up dicarboxylates could be revealed by these growth tests. Figure 4A shows that all Jen1p mutants carrying alleles reducing Jen1p activity (< 33 %) led to practically no growth on lactic acid. Two exceptions concerned mutants S271Q and S271E, which do not grow on lactic acid media, although they are active (>60 %) for [¹⁴C]-lactic acid transport. As

growth tests were performed at 18 °C and uptakes at 30 °C, for technical reasons, we thought that this apparent discrepancy might be due to cryosensitivity of these mutants in respect to Jen1p function. We confirmed that this was indeed the case by performing uptake assays at lower temperatures (18 °C), which showed that both S271Q and S271E had very low Jen1p activity at this temperature (see Figure 2).

Most interestingly, specific mutants (F270G, F270A, F270Q/S271Q, Q498A) showed significant Jen1p-dependent growth on succinic acid. No mutant showed significant Jen1p-mediated growth on malic acid, but this might have been expected as *S. cerevisiae* has a low effectiveness of malate metabolism (Boles *et al.*, 1998). These results confirmed that N501 is a critical residue for function, whereas residues F270 and Q498 are critical for function, but mostly act as determinants of Jen1p specificity.

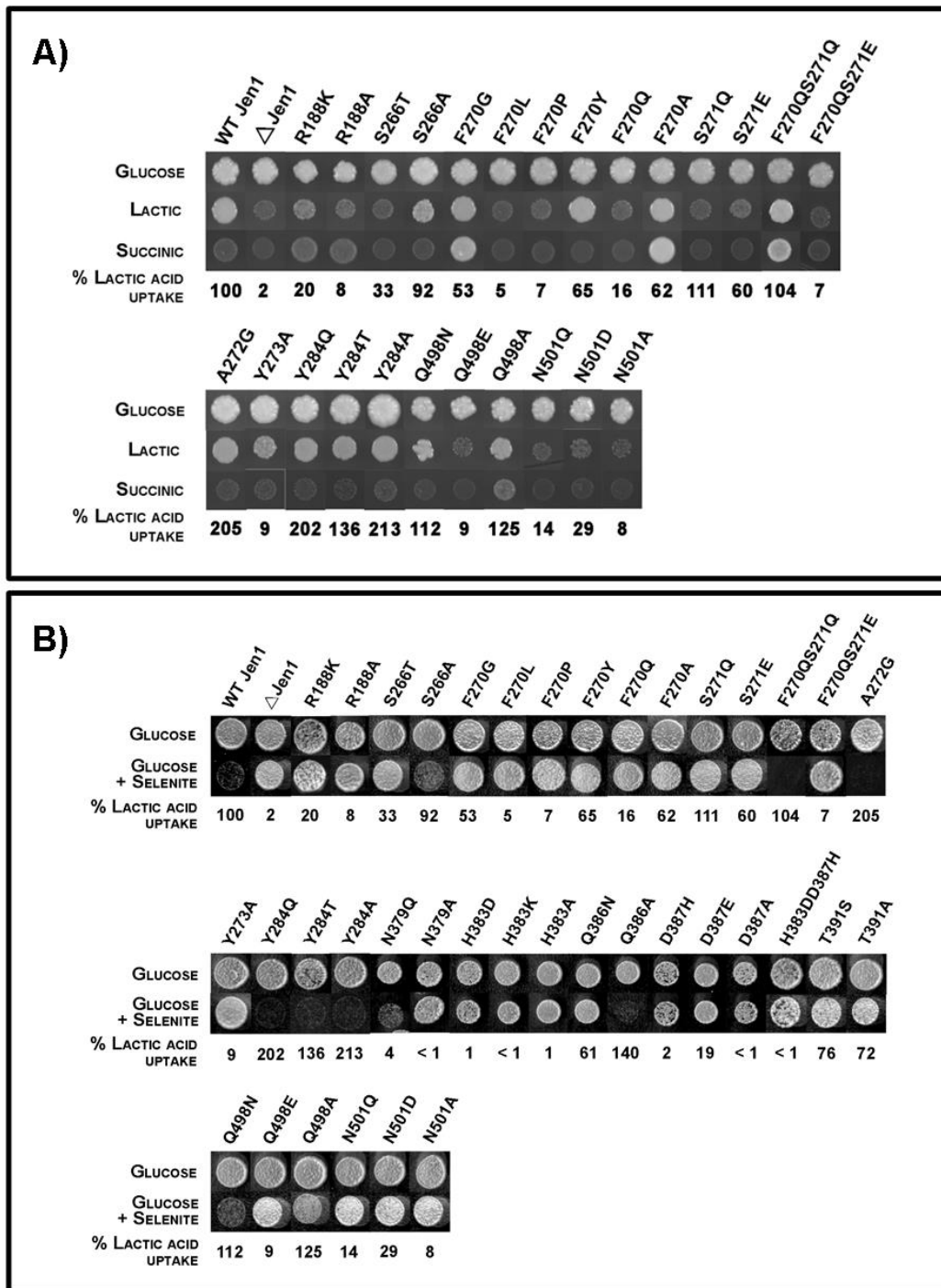


Figure 4 – Growth test of control and mutant strains. A) Growth test of control strains and mutants on glucose (2%), lactic acid (0.5%) or succinic acid (1%). All strains are isogenic (*S. cerevisiae* W303-1A Δ jen1 Δ ady2) expressing from a low copy plasmid either wild-type Jen1 (WT-Jen1) or the relevant Jen1 alleles. The negative control is a strain carrying an empty vector (Δ Jen1). B) Relative resistance/sensitivity of control strains and mutants on 200 μ M Selenite. The relative % of Jen1 [14 C]-lactic acid uptake is indicated in both A and B.

We finally tested the growth behaviour of all mutants described previously (Soares-Silva *et al.*, 2007) and herein in respect to their resistance/sensitivity to selenite (McDermott *et*

al., 2010). Figure 4B shows that, as expected, most loss-of-function mutants (transport activities < 65%) are relatively resistant to selenite, whereas fully active mutants (transport activities > 104%) are fully sensitive. However, there are three exceptions concerning mutants S271Q, Q498A and N379Q, in which lactate transport and selenite sensitivity were uncoupled. This observation is in line with a fine role of a relevant residue in determining Jen1p specificity (see later).

Specificity and kinetic profile of functional mutants

We estimated inhibition values for the uptake of radiolabelled lactate in the presence of non-radiolabelled lactic, pyruvic, succinic and malic acids (Table 2). The inhibitors were supplied at concentrations close to previously established $K_{m/i}$ values for lactic (0.3 mM) and pyruvic (0.7 mM) acid, or at 60 mM for the non-physiological substrates, succinic and malic acid. In these conditions, the control strain expressing wild-type Jen1p conserves 30-40% [^{14}C]-lactic acid transport activity in the presence of unlabelled lactic or pyruvic acids and 100% activity in the presence of either succinic or malic acids.

Table 2 – Relative capacity (%) of ^{14}C -lactic acid uptake in the presence of non-labelled carboxylic acids, at the indicated concentration, acting as competitors for the transport of lactate in mutants having a measurable transport capacity (>25%). The data shown are mean values, in percentage, of at least 3 independent experiments, with three replicas, and the respective standard deviation preceded by \pm .

Mutant	% ^{14}C -Lactic acid uptake							
	Lactic 0.3mM		Pyruvic 0.7mM		Succinic 60mM		Malic 60mM	
WT Jen1	29.9	\pm 0.0	39.4	\pm 0.0	100.0	\pm 0.0	100.0	\pm 0.0
S266A	30.8	\pm 4.1	13.2	\pm 1.1	66.1	\pm 0.7	61.5	\pm 5.1
F270G	29.9	\pm 0.1	19.3	\pm 0.0	24.3	\pm 10.7	37.4	\pm 4.3
F270Y	39.0	\pm 0.4	63.4	\pm 8.6	63.6	\pm 3.1	68.3	\pm 4.1
F270A	71.2	\pm 15.6	20.5	\pm 5.6	34.9	\pm 10.1	48.9	\pm 13.4
S271Q	74.5	\pm 31.2	42.2	\pm 15.8	107.9	\pm 17.6	112.6	\pm 2.4
S271E	54.9	\pm 21.9	34.1	\pm 16.7	99.3	\pm 13.6	91.9	\pm 14.4
F270QS271Q	32.0	\pm 0.8	26.7	\pm 0.0	50.6	\pm 1.2	44.8	\pm 2.6
A272G	18.9	\pm 0.5	9.9	\pm 0.2	61.5	\pm 2.6	55.8	\pm 4.2
Y284Q	27.3	\pm 1.3	18.8	\pm 0.2	86.7	\pm 5.8	83.7	\pm 5.9
Y284T	31.8	\pm 6.0	24.1	\pm 2.4	104.8	\pm 17.7	95.1	\pm 5.0
Q498N	49.9	\pm 17.7	28.9	\pm 10.9	99.8	\pm 14.7	110.5	\pm 8.5
Q498A	32.5	\pm 0.2	14.7	\pm 1.3	60.1	\pm 8.5	67.6	\pm 0.2
N501D	110.4	\pm 0.1	78.1	\pm 19.7	117.7	\pm 11.3	127.3	\pm 10.7

Most functional mutants ($\geq 20\%$ Jen1p transport activity) conserve a wild-type specificity profile with a practically unchanged capacity for lactate or pyruvate binding, and an inability to bind succinate or malate. However, five mutants showed a significantly different profile. In A272G, Jen1p seems to be more efficiently inhibited by unlabelled lactic and pyruvic acid. In contrast, in N501D, Jen1p activity is much less efficiently inhibited by unlabelled lactic or pyruvic acid. These results suggested (and subsequently shown) that A272G and N501D have increased and reduced affinity for lactate, respectively. Three other mutants, F270G, F270A and F270Q/S271Q, showed an increase in their binding affinity for succinic or malic acids. In these mutants, the remaining activity for radiolabelled lactic acid transport in the presence of succinic or malic acids ranged from 24-50%, compared to 62-104% in the wild-type and other mutants. In mutant Q498A, which could only grow weakly on succinic acid (see Figure 4A), we did not detect any measurable competitive effect of dicarboxylic acids on [^{14}C]-lactic acid transport.

K_m and V_m values for lactate transporter were determined in selected mutants, namely S266A, F270G, F270Q/S271Q, A272G, Q498A and N501D (Table 3).

Table 3 – Kinetic parameters of ^{14}C -lactic acid transport (maximum velocity, V_{\max} , and affinity constant, K_m) for some mutants, compared to the wild-type protein. The transport kinetics best fitting the experimental initial uptake rates and the kinetic parameters were determined by a computer-assisted nonlinear regression analysis (GraphPAD Software, San Diego, CA, USA). The data shown are mean values of at least 3 independent experiments, with three replicas, and the respective standard deviation preceded by \pm .

Lactic acid transport kinetic parameters		
Mutant	V_{\max} (nmol.s ⁻¹ .mg dry wt ⁻¹)	K_m (mM)
WT Jen1	0.16 \pm 0.02	0.68 \pm 0.30
S266A	0.08 \pm 0.01	0.40 \pm 0.13
F270G	0.15 \pm 0.01	0.97 \pm 0.16
F270QS271Q	0.22 \pm 0.01	0.21 \pm 0.05
A272G	0.24 \pm 0.02	0.21 \pm 0.07
Q498A	0.18 \pm 0.03	1.61 \pm 0.58
N501D	0.14 \pm 0.01	1.42 \pm 0.33

As expected, mutations Q498A and N501D led to reduced affinity for lactate (~2.5-fold increase in K_m values compared to wild-type), whereas F270Q/S271Q and A272G led to increased affinity for lactate (3.5-fold reduction in K_m values). V_{max} values were little affected (~0.5-fold increased or reduced) in all mutants analyzed. K_i values for succinic and malic acids were also estimated in F270G, F270Q/S271Q and Q498A (Table 4).

Table 4 – Inhibition constant (K_i) of ^{14}C -lactic acid uptake for succinic and malic acids of the mutants able to grow in dicarboxylates. The kinetic parameters were determined by a computer-assisted nonlinear regression analysis (GraphPAD Software, San Diego, CA, USA). The data shown are mean values of at least 3 independent experiments, with three replicas.

Mutant	Inhibitor	K_i (mM)	
		Succinic	Malic
F270G		1.92	3.38
F270QS271Q		1.85	28.07
Q498A		29.83	33.46

The first two mutants had acquired relatively high affinities for succinic acid binding (<2 mM), whereas Q498 showed measurable but low affinity (30 mM) for this acid. Finally, although all three mutants had measurable affinities for malic acid, only F270G had relatively high affinity for this substrate. These results showed that Jen1p mutants F270G, F270A and F270Q/S271Q and Q498A recognize and transport dicarboxylates.

A structural model for Jen1p and prediction of a major functional role of R188

Molecular simulations were undertaken in order to build a Jen1p model on the basis of its sequence similarity with four different MFS proteins of known crystallographic structure, namely GlpT (Glycerol transporter of *E. coli* (Huang *et al.*, 2003), LacY (Lactose permease of *E. coli* (Guan *et al.*, 2006), FucP (Fucose Transporter of *E. coli* (Dang *et al.*, 2010)) and PepT (Oligopeptide of *Shewanella oneidensis* (Newstead *et al.*, 2011)). LacY, FucP and PepT are bacterial proton symporters, whereas GlpT functions as an inorganic phosphate antiporter. Among them, the first three correspond to an inward-facing conformation, occluded from the periplasmic side of the membrane, whereas the FucP is the only MFS member captured in an outward-facing conformation.

The best model was obtained on the GlpT structure (for details see Experimental procedures). The overall topology of the modeled Jen1p (Figure 5) was in good agreement with all the structures of other MFS members.

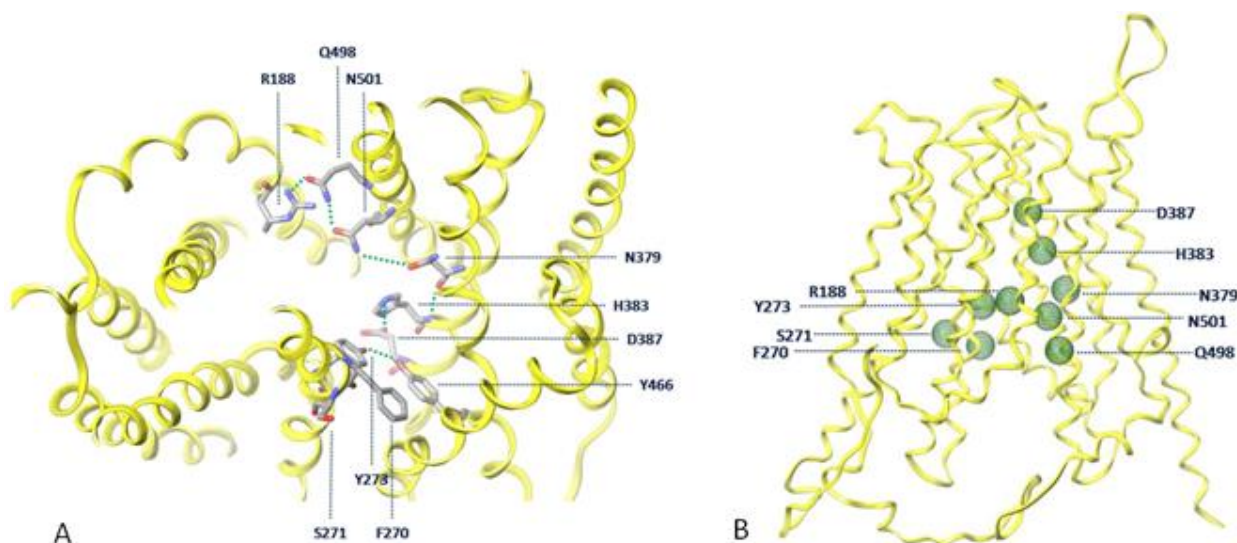


Figure 5 – Overall structure of the Jen-1 model. A) A section of the transporter as viewed from the periplasmic side. Visible is the spiral rim-like network of hydrogen bonds that is formed. B) Side view of the protein. Residues that define the translocation pathway are illustrated as green spheres.

In the modeled Jen1 structure (Figure 5), the occurrence of polar residues within the core helical domains was, as might be expected, markedly low, with the exception of residues annotated as critical for function (N379, H383, Q386, D387, Q498 and N501), plus a fully conserved Arg residue (R188) located within TMS-II (Figure 1). We mutated R188 (R188A and R188K) and found that substitution of R188 does not affect the plasma membrane expression of Jen1 (see Figure 3), but abolishes Jen1p transport activity (see Figures 2 and 4). Thus, R188 proved to be a novel residue absolutely essential for Jen1p function. The importance of this residue is further discussed later. Almost all acidic and basic residues were located mostly at the two termini and in interhelical or interdomain flexible regions of the protein, where they appeared as engaged in salt-bridging pairs. Notably, the occurrence of polar residues in transmembrane domains was mostly limited to helices VII and XI, with the exception of R188 belonging to TMS-II. Most interestingly, the side-chains of all polar residues faced the protein pore and formed an extended network of hydrogen bonds along the entire open pore cavity (Figure 5). This network was located approximately at the central part of the pore, demonstrating a very characteristic, spiral rim-like arrangement. Furthermore, functionally essential polar

residues (N379, H383, Q386, D387, Q498 and N501) were aligned in a row along an imaginary axis that lies parallel to the protein pore.

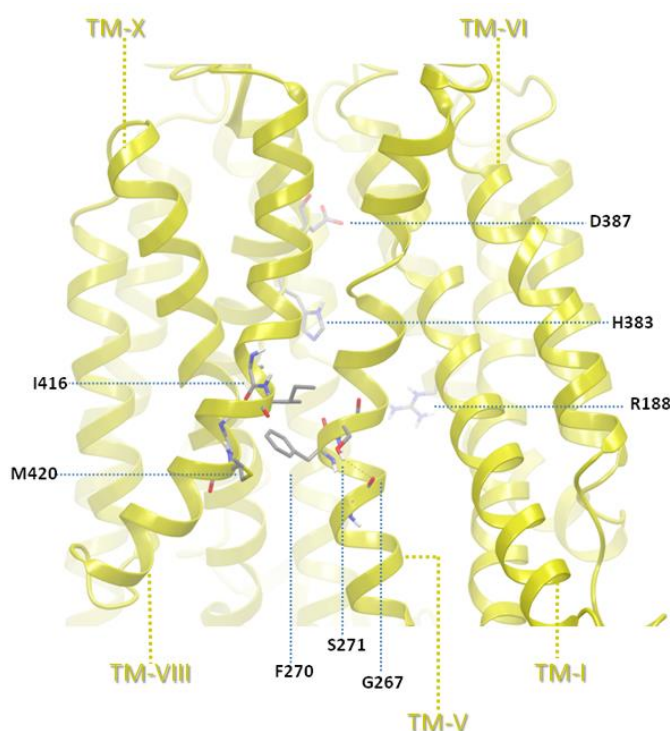


Figure 6 – Illustration of the F270-S271 residue pair location within helix V and their surrounding environment with respect to the overall Jen1 topology. F270 forms a close contact with helix VIII, at the position where a kink appears at half-length of the latter. The phenyl group of F270 demonstrates extensive packing interactions with the hydrophobic sidechains of I416 and M420, both belonging to TMS VIII. On the other side of TMS V, the polar S271 is engaged in an intrahelical hydrogen bond with the backbone carbonyl of G267. The position as well as the interaction pattern of F270 with surrounding tertiary structure elements could support the hypothesis that this specific residue holds an important role in facilitating helix packing, stabilizing tertiary structure and, ultimately, influencing the dynamics of the inward-to-outward transition of the protein, thus accounting for its functionality as a substrate specificity determinant.

The phenyl side-chain of F270 (TMS-V) was in close proximity to helices VIII and X, forming extensive edge-to-face π - π stacking interactions with F470 and W473 (TMS-X), and was in close contact with surrounding aromatic residues (W149, Y246, F269 and F270), forming a wide network of local hydrophobic interactions. Notably, the phenyl ring of F270 showed an additional close contact with TMS-VIII and more particularly at the middle of the helix where a characteristic kink appears. On the other side, its adjacent residue S271 interacted in an intra-helical fashion with the backbone of G267 and also formed an interhelical interaction with the side-chain of Y146 (TMS-I) (Figure 6). While

the location of the pair F270-S271 along the pore axis could account for their role as substrate specificity determinants, the aromatic ring of F270 could also facilitate helix packing and consequently enhance tertiary structure stabilization.

Molecular simulations of substrate-transporter recognition

Jen1p-substrate recognition was addressed by docking calculations. The simulation of the complex of Jen1p and lactate resulted in an unambiguous "trajectory-like" displacement of the monocarboxylate within the pore (Figures 7 and 8).

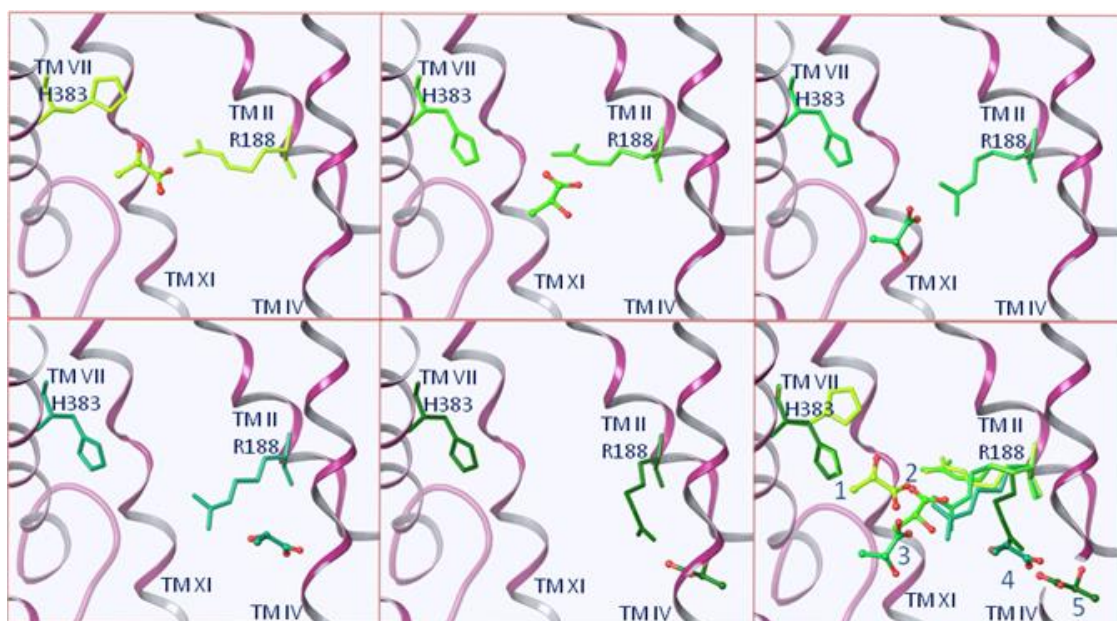


Figure 7 – The stepwise translocation pathway of lactate across the Jen1p pore, as proposed by simulations performed on the lactate-transporter complex. A flexible pattern of interactions formed mainly between the substrate and the side-chain of R188 mediates the sliding movement of the former towards the cytoplasmic side of the transporter for a total length exceeding 10Å. This movement is accompanied by the reorientation of the R188 side-chain which, to this respect and according to simulations, could hold the role of a mobile anchoring point that drives the substrate translocation process through sequential attractive interactions originating by pairing the aforementioned arginine with H383, N501 or Q498.

The starting point of this trajectory was in close proximity to the periplasmic side while the ending point was in the depth of the pore, towards its cytoplasmic opening. The substrate translocation course was almost parallel to the transporter axis and sequentially engaged a number of attractive hydrogen bonding interactions originating from residues H383, R188, N501 and Q498. The translocation of the substrate was accompanied by a

conjugated reorientation of the side-chains of the aforementioned residues. In such a mode, the collective conformational change observed through calculations suggested an orderly relocation of the substrate over a hypothetical track defined by subsequent interactions formed between it and the side-chains of those four critical residues. Among them, the side-chain of R188 seemed to undergo the more pronounced rotameric transition. A 4.4Å shift of the guanidinium group was observed as accompanying the repositioning of lactate from the vicinity of H383 towards N501 and Q498 at the inward-facing exit of the pore (Figure 5 and 7). Interestingly, when non-interacting with the substrate, the R188 guanidinium was stably anchored to those two specific side-chain amides by three hydrogen bonds (Figure 7). In the majority, however, of docked poses the lactate molecule was fully hydrogen bonded to the corresponding residue pairs (R188-H383, R188-N501 and R188-Q498) along the course of the translocation. Due to its inherent flexibility, the side-chain of R188 could be considered as a key residue in a mechanistic interpretation of the translocation process. Additionally the loss of R188 side-chain flexibility in the Q498E mutant due to the expected formation of a salt bridge between R188 guanidinium and E498 carboxylate could explain the observed loss of function of this mutant, further illustrating R188 critical role.

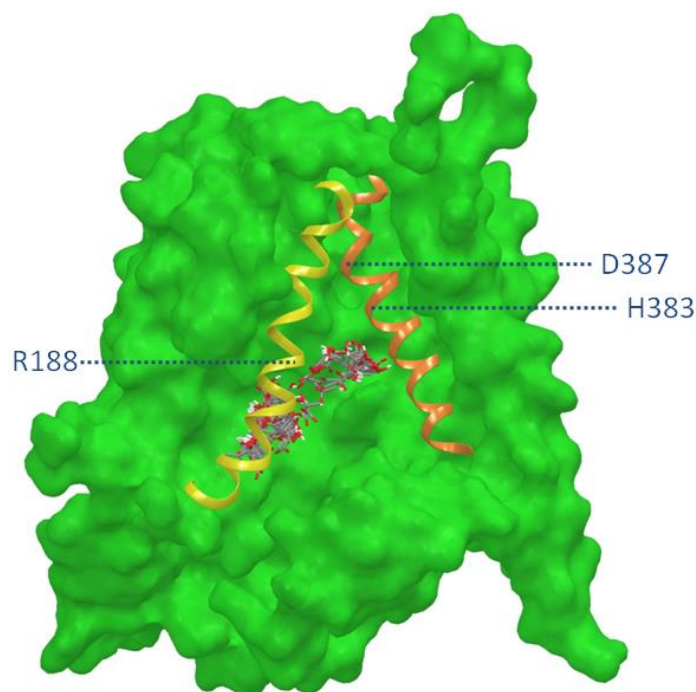


Figure 8 – The translocation pathway followed by the substrate along the pore of Jen1p transporter, as revealed by molecular simulations. The transporter is represented by its molecular surface and lactate is depicted in a stick representation. Transmembrane helices IV and XI are partially not shown for clarity. Helices II (yellow) and VII (orange) are presented as ribbons. Extended stochastic sampling of the

substrate-protein complex conformational space resulted in an ensemble of low-energy conformations, thus defining a (hypothetical/potential) track along which the transport could be carried out. This simulated translocation course of the substrate within the pore was fully consistent with the topology of the residues identified and characterized as critical by kinetics and mutagenesis experiments. The positioning of those among the critical residues that are specifically located on helices II and VII are indicated by dashed lines.

In contrast to results derived from docking calculations of the Jen1p-lactate complex, simulating the recognition of a dicarboxylic species (succinate) by the transporter afforded no acceptable docked poses, with this outcome being in agreement with experimental data. On the other hand, the simulation of F270G or the doubly mutated F270Q/S271Q Jen1p versions in association with succinate, did afford several docked poses resembling the wild-type transporter-lactate recognition and translocation track. This was in line with the fact that these mutants exhibited relatively high affinities for this dicarboxylic acid (Table 3). Finally, simulation of the Q498A mutant, which had very low affinity for succinic acid (Table 3), did not show any docked pose for this substrate.

Discussion

We have mutated several residues in TMS-V and TMS-XI of Jen1p, based on the rationale that their location might be analogous to that of residues known to be involved in substrate binding in MFS permeases or the observation that they are differentially conserved in mono- and dicarboxylate transporters. Functional analysis of the mutants showed that N501 is critical for physiological function (all relevant substitutions led to < 30% activity), whereas F270 and Q498 are critical for transport kinetics and for restricting Jen1p specificity to monocarboxylates. Several other residues (S266, S271, A272, Y273) in the vicinity of F270 were also shown to be relatively important for the transport characteristics of Jen1p. In a previous mutational analysis, we have shown that residues N379, H383 and D387, in TMS-VII, are irreplaceable for function, whereas Q386 affects the kinetics of Jen1p-mediated transport.

Using a novel refined model created on the basis of Jen1p similarity with GlpT permease, we subsequently located the relative position of all functional residues, as identified by mutational analysis, within the 3D structure of Jen1p. All critical polar residues were thus shown to be perfectly aligned in a row (in the order D387, H383, N379, N501, Q498)

along an imaginary axis that lies parallel to a protein pore, which is occluded towards the periplasmic side and open towards the cytoplasm. Most importantly, the model predicted a major functional role of another polar residue facing the pore, namely R188. Mutational analysis of this residue confirmed this prediction and further validates the model. The 3D model built also predicts that the location of F270 and Q498 could justify their role in substrate specificity. More specifically, the proximity of the phenyl ring to the kink of TMS-VIII might seriously influence the dynamic behavior of the transporter during the transition between the inward and outward conformations. This is consistent with mutational analysis showing that replacement of phenylalanine by residues of the same bulk that lack aromaticity (F270P, F270L, F270Q) impaired Jen1p function, whereas substitutions with more flexible or polar residues (F270A, F270G or F270Q/S271Q) facilitated the recognition and accommodation of dicarboxylates. What is also noticeable is that F270 and Q498 are positioned at the same level towards the opening of the inward-facing pore, and thus could act as gating element or filters which restrict the translocation of substrates other than monocarboxylates. Similar inward-facing selectivity elements have been recently described in the UapA transporter of *Aspergillus nidulans* (Kosti *et al.*, 2010).

Independent substrate docking approaches revealed a putative ‘trajectory-like’ displacement of the substrate within the Jen1p pore. The major residues involved in this trajectory were H383, N501, Q498 and R188. In this trajectory, the Arg residue seems to play a dynamic role by mediating the orderly translocation of the substrate through subsequent H-bond interactions involving itself and residues H383, N501 and Q498. This idea is in line with the observation that R188 mutations impair Jen1p. In GlpT, two conserved arginine residues, R45 from TM-I and R269 from TM-VII, are located at the inner end of the substrate-translocation pore of the GlpT structure, strategically placed to interact directly with substrate as central components of the binding site (Huang *et al.*, 2003). Noticeably, R269 of GlpT corresponds to H383 in Jen1p, in line with the observation that basic residues are often essential for function in MFS transporters (Huang *et al.*, 2003). Two other residues that have been reported as critical for GlpT function, H165 and D274 (Huang *et al.*, 2003), correspond to functionally important residues in Jen1p: Y273 and D387, respectively.

Residues D387 and N379, which are elements of the “signature” motif located across the half-length of the pore, and which have been shown to be functionally irreplaceable (Soares-Silva *et al.*, 2007), did not form any direct interactions with the substrate. At least

for D387, this should be expected since in the inward-facing modeled conformation of the transporter, this residue lays almost totally buried within the contracted periplasmic lobe of the protein. As the Jen1p model was built based on the inward-facing conformation of GltT, the substrate trajectory defined does not mean to describe the entire trajectory that lactate follows in order to be translocated along the membrane axis. In agreement with the model proposed by Kaback and co-workers (Guan *et al.*, 2006; Mirza *et al.*, 2006), we speculate that upon binding of the substrate-proton pair at the end of a putative outward-facing trajectory, a major conformational change might be elicited to create the inward-facing trajectory. In this mechanism, substrate translocation might involve sliding between critical nodal points within the outward- and inward-facing alternating pores. This notion is supported by recent molecular dynamic approaches which showed that in a modeled outward-facing conformation of LacY, based on the outward-open conformation of FucP (Dang *et al.*, 2010), the substrate remains in the pocket but slides and binds with several different residues compared to the view obtained from the inward-facing structure (Newstead *et al.*, 2011). Interestingly, sequential binding sites and substrate sliding from one (external) to the other (internal) have been recently proposed in the AdiC transporter (Kowalczyk *et al.*, 2011) and the GLUT MFS subfamily of hexose transporters (Cunningham *et al.*, 2006; Manolescu *et al.*, 2007; Naula *et al.*, 2010).

References

- Abramson J., Smirnova I., Kasho V., Verner G., Kaback R.H., and Iwata S. (2003) Structure and Mechanism of the Lactose Permease of *Escherichia coli*. *Science* **301**:610-615.
- Andrade R.P., Kötter P., Entian K.D., and Casal M. (2005) Multiple transcripts regulate glucose-triggered mRNA decay of the lactate transporter JEN1 from *Saccharomyces cerevisiae*. *Biochem Biophys Res Commun.* **332**:254-262.
- Boles E., de Jong-Gubbels P., and Pronk J.T. (1998) Identification and characterization of MAE1, the *Saccharomyces cerevisiae* structural gene encoding mitochondrial malic enzyme. *J Bacteriol.* **180**:2875-82.
- Casal M., Paiva S., Andrade R.P., Gancedo C., and Leão C. (1999) The lactate-proton symport of *Saccharomyces cerevisiae* is encoded by *JEN1*. *J Bacteriol* **181**:2620-2623.

- Casal M., Paiva S., Queirós O., and Soares-Silva I. (2008) Transport of carboxylic acids in yeasts. *FEMS Microbiology Reviews*. **32**: 974–994
- Cunningham P., Afzal-Ahmed I., and Naftalin R. (2006) Docking studies show that D-glucose and quercetin slide through the transporter GLUT1. *J.Biol.Chem.* **281**:5797-5803.
- Dang S., Sun L., Huang Y., Lu F., Liu Y., Gong H., Wang J., and Yan N. (2010) Structure of a fucose transporter in an outward-open conformation. *Nature* **467**:734-738.
- Ganapathy V., Thangaraju M., Gopal E., Martin P.M., Itagaki S., Miyauchi S., and Prasad P.D. (2008) Sodium-coupled monocarboxylate transporters in normal tissues and in cancer. *AAPS J.* **10**:193-9.
- Guan L. and Kaback H.R. (2006) Lessons from lactose permease. *Annu Rev Biophys Biomol Struct.* **35**:67-91.
- Huang Y., Lemieux M.J., Song J., Auer M., and Wang D.N. (2003) Structure and mechanism of the glycerol-3-phosphate transporter from *Escherichia coli*. *Science* **301**:616-620.
- Kaback H.R., Smirnova I., Kasho V., Nie Y., and Zhou Y. (2011) The alternating access transport mechanism in LacY. *J Membr Biol.* **239**:85-93.
- Kolossváry I., and Guida C.W. (1996) Low Mode Search. An Efficient, Automated Computational Method for Conformational Analysis: Application to Cyclic and Acyclic Alkanes and Cyclic Peptides. *J.Am.Chem.Soc.* **118**:5011-5019.
- Kosti V., Papageorgiou I., and Diallinas G. (2010) Dynamic elements at both cytoplasmically and extracellularly facing sides of the UapA transporter selectively control the accessibility of substrates to their translocation pathway. *J Mol Biol.* **397**:1132-43.
- Kowalczyk L., Ratera M., Paladino A., Bartoccioni P., Errasti-Murugarren E., Valencia E., Portella G., Bial S., Zorzano A., Fita I., Orozco M., Carpena X., Vázquez-Ibar J.L., and Palacín M. (2011) Molecular basis of substrate-induced permeation by an amino acid antiporter. *Proc Natl Acad Sci U S A.* **108**:3935-40.
- Law C.J., Maloney P.C., Wang D.N. (2008) Ins and outs of major facilitator superfamily antiporters. *Annu Rev Microbiol.* **62**:289-305.
- Lodi T., Diffels J., Goffeau A., and Baret P.V. (2007) Evolution of the carboxylate Jen transporters in fungi. *FEMS Yeast Res.* **7**:646-656.
- Lodi T., Fontanesi F., Ferrero I., and Donnini C. (2004) Carboxylic acids permeases in yeast: two genes in *Kluyveromyces lactis*. *Gene* **339**: 111-119.
- Manolescu A.R., Augustin R., Moley K., and Cheeseman C. (2007) A highly conserved hydrophobic motif in the exofacial vestibule of fructose transporting SLC2A proteins acts as a critical determinant of their substrate selectivity. *Mol Membr Biol.* **24**:455-463.
- McDermott J.R., Rosen B.P., and Liu Z. (2010) Jen1p: A High Affinity Selenite Transporter in Yeast. *Mol. Biol. Cell* **21**:3934-41.

- Merezhinskaya N., and Fishbein W.N. (2009) Monocarboxylate transporters: past, present, and future. *Histol Histopathol.* **24**:243-64.
- Mirza O., Guan L., Verner G., Iwata S., and Kaback H.R. (2006) Structural evidence for induced fit and a mechanism for sugar/H⁺ symport in LacY. *EMBO J.* **25**:1177-1183.
- Mohamadi F., Richard N.G.J., Guida W.C., Liskamp R., Lipton M., Caufield C., Chang G., Hendrickson T., and Still W.C. (1990) MacroModel-an Integrated Software System for Modeling Organic and Bioorganic Molecules Using Molecular Mechanics. *J.Comput.Chem.* **11**:440-467.
- Naula C., Logan M.F., Wong E.P., Barrett P.M., and Burchmore R.J. (2010) A glucose transporter can mediate ribose uptake. Definition of residues that confer substrate specificity in a sugar transporter. *J.Biol.Chem.* **285**:29721-29728.
- Newstead S., Drew D., Cameron A.D., Postis V.L., Xia X., Fowler P.W., Ingram J.C., Carpenter E.P., Sansom M.S., McPherson M.J., Baldwin S.A., and Iwata S. (2011) Crystal structure of a prokaryotic homologue of the mammalian oligopeptide-proton symporters, PepT1 and PepT2. *EMBO J.* **30**:417-26.
- Paiva S., Devaux F., Barbosa S., Jacq C., and Casal M. (2004) Ady2p is essential for the acetate permease activity in the yeast *Saccharomyces cerevisiae*. *Yeast* **21**:201-210.
- Paiva S., Vieira N., Nondier I., Haguenaer-Tsapis R., Casal M., and Urban-Grimal D. (2009) Glucose-induced ubiquitylation and endocytosis of the yeast Jen1 transporter: role of lysine 63-linked ubiquitin chains. *J Biol Chem.* **284**:19228-19236.
- Sali A., Potterton L., Yuan F., van Vlijmen H., and Karplus M. (1995) Evaluation of comparative protein modelling by MODELLER. *Proteins* **23**:318-326.
- Soares-Silva I., Paiva S., Diallinas G., and Casal M. (2007) The conserved sequence NXX[S/T]HX[S/T]QDXXXT of the lactate/pyruvate:H⁺ symporter subfamily defines the function of the substrate translocation pathway. *Mol Membr Biol.* **24**:464-474.
- Soares-Silva I., Paiva S., Kötter P., Entian K.D., and Casal M. (2004) The disruption of JEN1 from *Candida albicans* impairs the transport of lactate. *Mol Membr Biol.* **21**:403-411.
- Soares-Silva I., Schuller D., Andrade R.P., Baltazar F., Cássio F., and Casal M. (2003) Functional expression of the lactate permease Jen1p of *Saccharomyces cerevisiae* in *Pichia pastoris*. *Biochem J* **376**:781-787.
- Vieira N., Casal M., Johansson B., MacCallum D.M., Brown A.J., and Paiva S. (2010) Functional specialization and differential regulation of short-chain carboxylic acid transporters in the pathogen *Candida albicans*. *Mol Microbiol.* **75**:1337-1354.

Chapter III

The monocarboxylate transporters Jen1 and Ady2 as modulators of lactic acid production in *Saccharomyces cerevisiae*

CHAPTER III

THE MONOCARBOXYLATE TRANSPORTERS JEN1 AND ADY2 AS MODULATORS OF LACTIC ACID PRODUCTION IN *SACCHAROMYCES CEREVISIAE*.

Adapted from:

Pacheco A., Talaia G., Sá-Pessoa J., Bessa D., Gonçalves M.J., Moreira R., Paiva S., Casal M. and Queirós O. (2012) Lactic acid production in *Saccharomyces cerevisiae* is modulated by expression of the monocarboxylate transporters Jen1 and Ady2. *FEMS Yeast Res.* **12**: 375–81.

Personal contribution for this work: Ady2 transport characterization

Abstract

We aimed to manipulate the metabolism of *Saccharomyces cerevisiae* to produce lactic acid and search for the potential influence of acid transport across the plasma membrane in this process. *S. cerevisiae* W303-1A is able to use L-lactic acid but its production in our laboratory has not previously been detected. When the *l-LDH* gene from *Lactobacillus casei* was expressed in *S. cerevisiae* W303-1A and in the isogenic mutants *jen1Δ*, *ady2Δ* and *jen1Δ ady2Δ*, all strains were able to produce lactic acid, but higher titres were achieved in the mutant strains. In strains constitutively expressing both *LDH* and *JEN1* or *ADY2*, a higher external lactic acid concentration was found when glucose was present in the medium, but when glucose was exhausted, its consumption was more pronounced. These results demonstrate that expression of monocarboxylate permeases influences lactic acid production. Ady2 has been previously characterized as an acetate permease but our results demonstrated its additional role in lactate uptake. Overall, we demonstrate that monocarboxylate transporters Jen1 and Ady2 are modulators of lactic acid production and may well be used to manipulate lactic acid export in yeast cells.

Introduction

Lactic acid is commonly used in food, cosmetic and pharmaceutical industries, however new uses for this compound are emerging. That is the case of the production of polylactic acid, a biodegradable and biocompatible polymer, with biomedical and environmental applications which represents an annual industrial investment of several million dollars (van Maris *et al.*, 2004; Sauer *et al.*, 2010). Lactic acid can be produced by sugar fermentation, namely by lactic acid bacteria. However, these microorganisms present sensitivity to low pH, and lactic acid production at industrial level requires the addition of high amounts of neutralizing agents, such as CaCO₃, NaOH and NH₄OH (Benninga, 1990). This will limit lactic acid bioproduction in large quantities, because it compromises the regeneration of the precipitated lactate salts, and higher costs are involved. Yeast cells are very promising organisms for the production of carboxylic acids since they have simple nutritional requirements and are easily manipulated being widely used as cell factories. Additionally, they are able to grow at lower pH than bacteria, therefore tolerating the production of acids to higher levels. In the attempt to produce lactic acid, several yeast species have already been metabolically manipulated through the heterologous expression of lactate dehydrogenases (Ldh; EC 1.1.1.27), namely *Saccharomyces cerevisiae* (Dequin & Barre, 1994; Porro *et al.*, 1995), *Kluyveromyces lactis* (Porro *et al.*, 1999a; Bianchi *et al.*, 2001), *Pichia spitiensis* (Ilmén *et al.*, 2007), *Zygosaccharomyces bailii* (Branduardi *et al.*, 2004), *Torulopsis delbrueckii* (Porro *et al.*, 1999b), *Candida utilis* (Ikushima *et al.*, 2009) or *Candida boidinii* (Osawa *et al.*, 2009). *S. cerevisiae* was the first and most widely engineered yeast species used to produce lactic acid namely by the heterologous expression of *LDH* genes, creating novel metabolic pathways for lactic acid production (Dequin & Barre, 1994; Porro *et al.*, 1995). Several approaches arose to improve lactic acid yield by suppressing the activity of enzymes involved in ethanol formation, e.g. pyruvate decarboxylase (Pdc) and alcohol dehydrogenase (Adh), channeling the pyruvate produced in glycolysis to the synthesis of lactate (van Maris *et al.*, 2004; Ishida *et al.*, 2006; Tokuhiro *et al.*, 2009). Although inhibition of alcoholic fermentation has been achieved, the accumulation of the lactic acid produced inside the cell promotes intracellular acidification and Ldh inhibition, leading to a decrease in lactic acid yield (Branduardi *et al.*, 2006; Sauer *et al.*, 2010). The efflux of the acid is, in this way, one possible target to improve lactic acid titers. Understanding in detail the metabolism and transport of short-chain monocarboxylic acids across plasma

membrane has become more important than ever. In *S. cerevisiae*, two monocarboxylate permeases were identified, Jen1 (Casal *et al.*, 1999) and Ady2 (Paiva *et al.*, 2004): Jen1 mediates the transport of lactate, pyruvate, acetate and propionate whereas Ady2 mediates the transport of acetate, propionate and formate, being both induced by non-fermentable carbon sources, and repressed in the presence of glucose. An additional role of Jen1 in the export of lactate has been demonstrated when the acid is accumulated inside the cell (Porro *et al.*, 1999b; Branduardi *et al.*, 2006). In fact, it has been reported that overexpression of *JEN1* improved lactate yield (Porro *et al.*, 1999b; Branduardi *et al.*, 2006). In this work we engineered yeast strains and demonstrated the role of the monocarboxylate transporters Jen1 and Ady2 as modulators for lactic acid export by the cell.

Experimental Procedures

Yeast strains and growth conditions

All the yeast in this work were derived from W303-1A and are listed in table 1. Growth of the strains was performed at 30°C in a synthetic minimal media with 0.67% w/v Yeast Nitrogen Base, 2% w/v glucose and supplemented with aminoacids to meet auxotrophic requirements. Yeast strains were maintained in YPD media and bacteria strains in solid LB medium supplemented with ampicillin (100 mg/L).

Table 1 – *Saccharomyces cerevisiae* strains used in this study.

Strain	Genotype	Reference
W303-1A	MATa <i>ade2 can1 ura3 leu2 his3 trp1</i>	Thomas and Rothstein, 1989
<i>jen1</i> Δ	W303-1A <i>jen1::KanMX4</i>	M.Casal collection
<i>ady2</i> Δ	W303-1A <i>ady2::KanMX4</i>	Paiva <i>et al.</i> , 2004
<i>jen1</i> Δ <i>ady2</i> Δ	W303-1A <i>jen1::HphMx4 ady2::KanMX4</i>	Soares-Silva <i>et al</i> , 2007
W303-1A-LDH	W303-1A transformed with p426-LDH	This work
<i>jen1</i> Δ -LDH	<i>jen1</i> Δ transformed with p426-LDH	This work
<i>ady2</i> Δ -LDH	<i>ady2</i> Δ transformed with p426-LDH	This work
<i>jen1</i> Δ <i>ady2</i> Δ -LDH	<i>jen1</i> Δ <i>ady2</i> Δ transformed with p426-LDH	This work
<i>jen1</i> Δ -JEN1-LDH	<i>jen1</i> Δ transformed with p426-LDH and p415-JEN1	This work
<i>ady2</i> Δ -ADY2 -LDH	<i>jen1</i> Δ transformed with p426-LDH and p415-ADY2	This work
<i>jen1</i> Δ <i>ady2</i> Δ-p416-GPD	<i>jen1</i> Δ transformed with p416-GPD	This work
<i>jen1</i> Δ <i>ady2</i> Δ-ADY2	<i>jen1</i> Δ transformed with p416-ADY2	This work

Expression of *LDH*, *JEN1* and *ADY2* in *S. cerevisiae*

Lactobacillus casei *LDH* was cloned into the plasmid p426-GPD (Mumberg *et al.*, 1995) by the gap-repair method (Orr-Weaver & Szostak, 1983). The *LDH* gene was amplified with the primers LDH-p426fwd (TCTAGA AACTAGTGGATCCCC GGGCTGCAGAATGGCAAGTATTACGGATAAGG, the sequence homologous to the *LDH* gene is underlined) and LDH-p426rev (CGACGGTATCGATAAGCTT GATATCGAATTCTGACGGGTTTCGATG, the sequence homologous to the *LDH* gene is underlined). The plasmid p426-GPD was digested with *Eco*RI, dephosphorylated with alkaline phosphatase and co-transformed with the PCR product. Correct clones were verified by colony PCR and sequencing.

S. cerevisiae *JEN1* and *ADY2* were transferred from the plasmid p416-GPD, where they were former cloned, to p415-GPD, in order to co-express in *S. cerevisiae* *LDH* and *JEN1* or *ADY2*. Both genes were isolated from the plasmids where they were inserted by digestion with *Bam*HI and *Xho*I, and ligated to p415-GPD digested with the same enzymes. The ligation product was used directly to transform the appropriate yeast strains. The LiAc/PEG/ss-DNA protocol was used in all assays of yeast transformations (Gietz & Woods, 2002). The vectors were rescued from the transformed strains using glass beads and commercial minipreps and transformed to *E. coli* and correct integration of the genes was verified.

Transport assays

S. cerevisiae *jen1* Δ *ady2* Δ -*ADY2* glucose-grown cells were harvested at mid-exponential phase, washed twice with ice-cold water and transferred to YNB acetic acid medium (0.5 % acetic acid, pH 6.0). After 6 hours of incubation, the derepressed cells were harvested by centrifugation, washed twice with ice-cold water and resuspended in ice-cold water to a final biomass concentration of 30-40 mg dry wt. ml⁻¹. Uptake rates of labeled lactic acid were determined as described by Casal & Leão (1995). Briefly, 10 μ l of this cell suspension were mixed with 30 μ l of 0.1 M KH₂PO₄ (pH 5.0) in a 10 ml conical tube. The reaction mixture was incubated for 2 minutes in a bath at 26 ° C. The reaction was started by adding 10 μ l of the radiolabeled substrate (D,L-[U-¹⁴C] lactic acid, sodium salt (CFB97) or [1-¹⁴C] acetic acid, sodium salt (CFA13), both purchased from Amersham Biosciences) at the desired concentration and pH, and stopped after 5 seconds by dilution, adding 5 ml of ice-cold water. The sample was immediately filtered under vacuum

through a Whatman GF / C membrane and washed on the filter with 10 ml of ice-cold water. The membrane filter was transferred to a vial containing 5 ml of scintillation liquid (Opti-phase HiSafe II, LKB FSA Laboratory Supplies, Loughborough, UK) and the radioactivity incorporated by the cells measured in a Packard Tri-Carb 2200 CA liquid scintillation counter. The non-specific adsorption of the acid to the cells or to the filters was measured adding 5 ml of ice-cold water to the reaction mixture, before the addition of the radioactive acid. The transport kinetics best fitting the experimental values of initial uptake rates, as well as the kinetic parameters, were determined using a computer-assisted nonlinear regression analysis (GraphPad Software, San Diego, CA, USA). Inhibition studies were assayed adding simultaneously nonlabeled lactic acid at the desired concentration and the labeled acetic acid.

Measurement of lactate, glucose and ethanol

During growth of the cultures of the strains listed in table 1, samples of the media were collected along the time and analyzed for different metabolites. Lactate, glucose and ethanol were measured using diagnostic enzymatic kits (Lactate assay kit, Spinreact; Glucose GOD-POD assay kit, Spinreact, and Ethanol assay kit, Megazyme K-EtOH, respectively), according to manufacturer's instructions and using the appropriate dilutions. Cell growth was also evaluated measuring optical densities at 600 nm along the time.

Results and Discussion

Heterologous expression of *Lactobacillus casei* LDH in the isogenic yeast mutants *jen1Δ*, *ady2Δ* and *jen1Δ ady2Δ*

S. cerevisiae W303-1A is able to consume lactic acid, but its production is very ineffective and not detected in our conditions (not shown). Through the heterologous expression of *LDH* gene from the lactic acid bacteria *Lactobacillus casei* we have created this metabolic pathway in yeast cells. As expected, the *LDH* transformant strain was able to produce lactic acid, but after glucose exhaustion the titers of lactic acid significantly decreased, probably due to its metabolism (not shown). Having this behavior in consideration we wondered whether *JEN1* and *ADY2* genes, coding for monocarboxylate

permeases, would influence lactic acid production and consumption profiles. To check this hypothesis the *LDH* gene from *L. casei* was also expressed in the isogenic *jen1Δ*, *ady2Δ* and *jen1Δady2Δ* mutants. These strains were grown on glucose and samples were collected over time to evaluate cell density, lactic acid, glucose and ethanol concentration (Figure 1). The growth profile and glucose consumption were very similar in the four strains (Figure 1A and 1B), as well as the ability to convert glucose both to lactic acid (Figure 1C) and ethanol (Figure 1D). *JEN1* and *ADY2* disruption did not lead to significant differences in lactic acid production in the first hours of growth, when glucose was still present in the medium. However, after glucose exhaustion, lactic acid concentration in the media was considerably higher in *jen1Δ* and *ady2Δ* mutants leading to a reduction in the acid consumption (Figure 1C), an observation even more pronounced in the double mutant. The first step of the acid metabolism is its entrance into the cell and these results highlight the important role of Jen1 and Ady2 transporters for an efficient use of lactic acid.

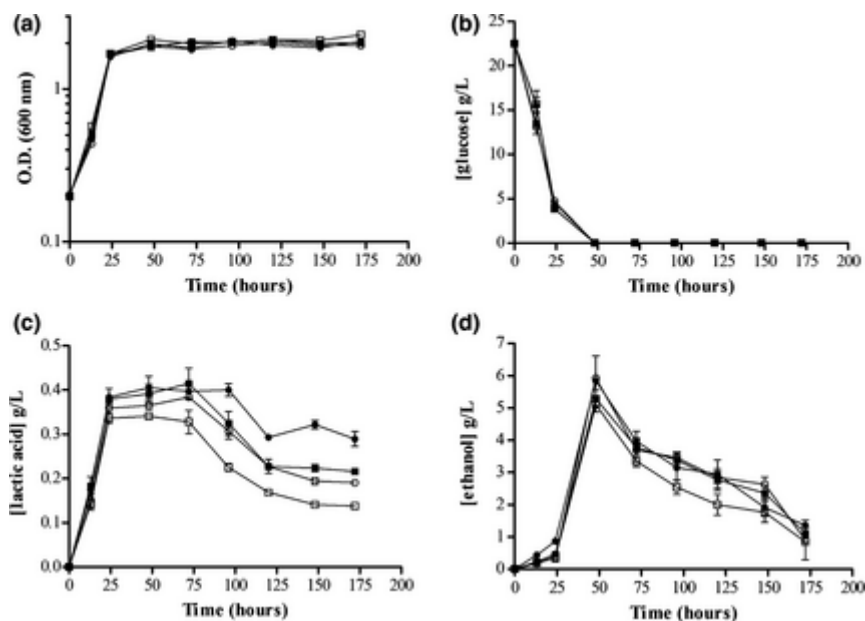


Figure 1 – Growth profile (A), glucose (B), lactic acid (C) and ethanol (D) concentration in the medium, for the strains *S. cerevisiae* W303-1A-LDH (□), *jen1Δ*-LDH (■), *ady2Δ*-LDH (○) and *jen1Δ ady2Δ*-LDH (●), over time.

Characterization of Ady2 as a lactate transporter

Ady2 has previously been described as an acetate, propionate and formate transporter (Paiva *et al.*, 2004, Casal *et al.*, 1996), however its ability to transport lactic acid has never

been reported. In order to clarify this aspect, we constructed a strain lacking activity for Jen1 and constitutively expressing Ady2. The *S. cerevisiae* *jen1* Δ *ady2* Δ -*ADY2*, harboring the plasmid p416-*GPD-ADY2*, containing the *ADY2* coding sequence, under the control of the *GPD* promoter, was used to perform transport assays with labeled monocarboxylic acids. The cells were grown on glucose, harvested during mid-exponential phase of growth and transferred to fresh media supplemented with acetic acid for 6 hours, as mentioned in the Experimental Procedures. A Michaelis-Menten kinetics was found for the initial uptake rates of labeled lactic acid, at pH 5.0, with a K_m of 2.11 ± 0.27 mM of total lactic acid and a V_{max} of 0.38 ± 0.02 nmol of total lactic acid s^{-1} mg dry weight $^{-1}$ (Figure 2).

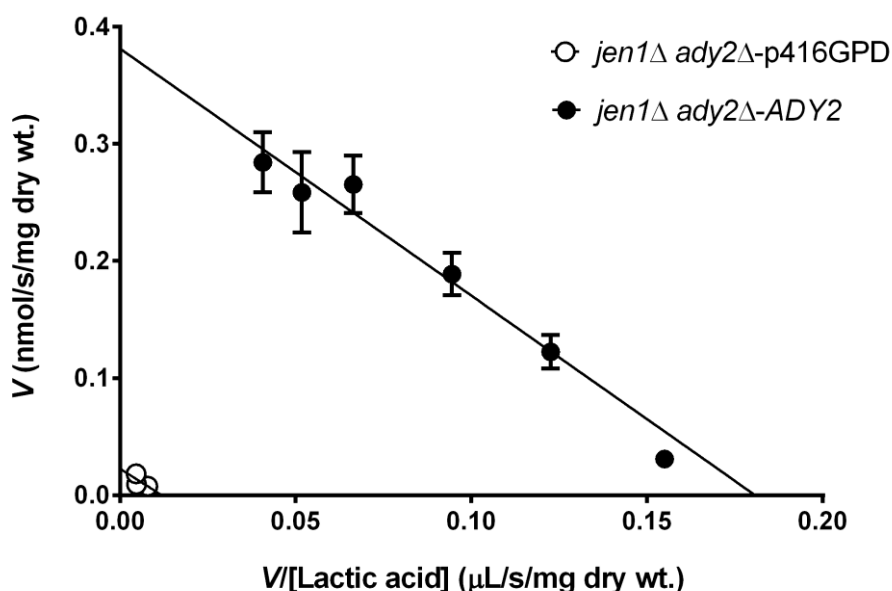


Figure 2 – Eadie-Hofstee plots of the initial uptake rates of labeled lactic acid as a function of the acid concentration, at pH 5.0, in *S. cerevisiae* *jen1* Δ *ady2* Δ -p416-GPD (○) and *jen1* Δ *ady2* Δ -*ADY2* (●).

In the same culture conditions, cells of the double mutant transformed with the empty vector p416-GPD exhibited no saturable kinetics and the values for the uptake were negligible. Additionally, it was observed that initial uptake rates of labeled acetic acid were competitively inhibited by lactic acid, demonstrating that both acids share the same permease (Figure 3). The kinetic parameters for acetic acid at pH 6.0 were: K_m of 0.21 ± 0.03 mM of total acetic acid and a V_{max} of 0.53 ± 0.02 nmol of total acetic acid s^{-1} per mg dry weight of cells. The inhibition constant (K_i) for lactic acid was 1.8 mM, ranging from 1.4 to 2.5 mM (inset of Figure 3), an expected value of the same order of magnitude of

the K_m . Altogether these results indicate that Ady2 is a lactate transporter, however with a 7-fold lower affinity for lactate, when compared with Jen1 with a K_m of 0.3 mM (Casal, 1999).

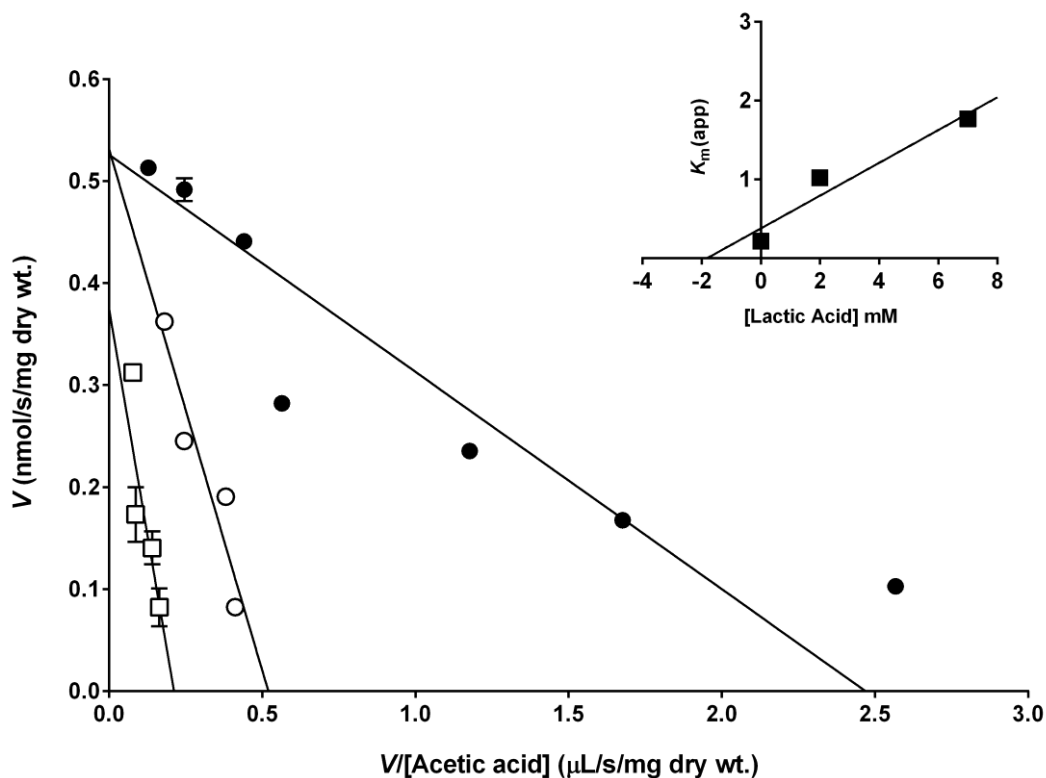


Figure 3 – Eadie-Hofstee plots of the initial uptake rates of labeled acetic acid, pH 6.0, as a function of its concentration, in *S. cerevisiae jen1Δ ady2Δ-ADY2* cells. (●) Absence of other non-labeled substrate; (○), (□), presence of 2 mM and 7 mM cold lactic acid, respectively. Inset: A K_i of 1.8 mM for total lactic acid was determined, plotting the apparent K_m of labeled acetic acid kinetics against lactic acid concentration.

Constitutive expression of *Lactobacillus casei* LDH and JEN1 or ADY2 in *Saccharomyces cerevisiae*

JEN1 and *ADY2* genes were also constitutively expressed in *S. cerevisiae jen1Δ-LDH* and *ady2Δ-LDH*, respectively, using the p415-GPD vector. Lactic acid and glucose were measured over time in glucose grown cells (Figure 4). The constitutive expression of either *JEN1* or *ADY2* leads to higher outer lactic acid concentrations when glucose is present. Concerning *JEN1* expression, these results are in agreement with the ones already published (Porro *et al.*, 1999b; Branduardi *et al.*, 2006). Jen1 is involved in lactic acid uptake, but when the acid accumulates into the cell, it can also mediate its efflux. The

expression of *ADY2* gave similar results to the ones obtained with the constitutive expression of *JEN1*. When glucose is absent, lactic acid is totally consumed in both strains expressing *JEN1* or *ADY2*, probably due to the activity of both transporters. In summary, the constitutive expression of *JEN1* and *ADY2*, leads to higher outer lactic acid concentration when glucose is present due to their role in the efflux of the acid, but when glucose is exhausted are also involved in lactic acid uptake and consumption.

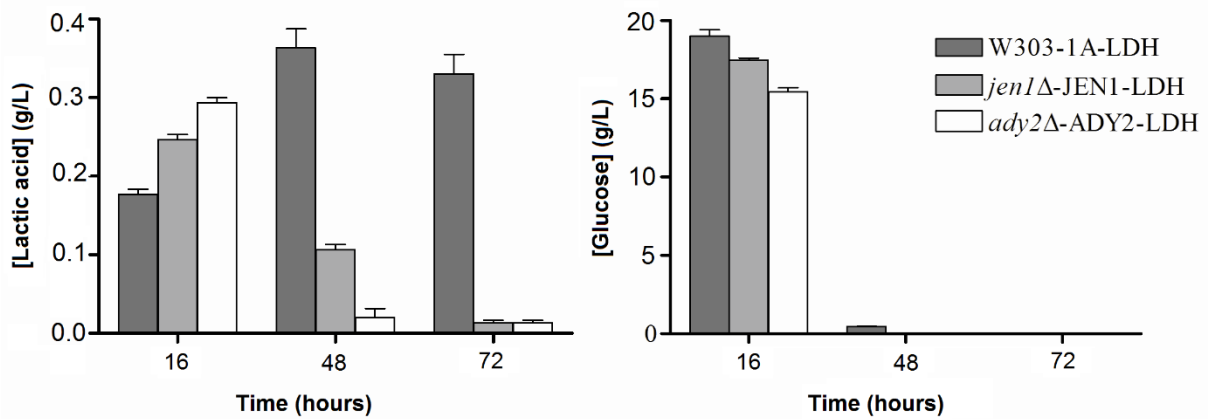


Figure 4 – Effect of Jen1 and Ady2 constitutive expression on lactic acid production (A) and on glucose (B) consumption over time in *S. cerevisiae* strains expressing constitutively *LDH*: W303-1A-*LDH*, W303-1A *jen1*Δ-*JEN1*-*LDH* and W303-1A *ady2*Δ-*ADY2*-*LDH*.

Glucose is a preferential substrate for yeast cells and its presence represses non-fermentable carbon sources metabolism, as is the case of lactic acid. In *LDH* transformed cells, the fermented glucose is converted either in ethanol or lactic acid, and the acid produced (most probably the anionic form considering the physiological pH of the cytoplasm) is exported via Jen1 and Ady2. However, after glucose utilization, lactic acid metabolism becomes operational and the expression of *JEN1/ADY2* also leads to a higher consumption of the acid.

It is not yet clear whether Jen1 and Ady2 are the sole transporters carrying out the efflux of the acid or if another lactic acid exporter (not yet identified) is also involved. The existence of other lactic acid exporter besides Jen1 has been previously proposed (Branduardi *et al.*, 2006). Our results support the hypothesis that Jen1 acts as a lactic acid exporter and suggest a similar role for Ady2. However, the existence of other exporter cannot be ruled out since in the strain *jen1*Δ *ady2*Δ p426-*LDH*, lactic acid efflux is still operational. A transcriptome analysis of *S. cerevisiae* cells constitutively expressing *JEN1* and *ADY2* could give valuable clues regarding this question.

Branduardi and collaborators (2006) demonstrated that the yield of lactic acid production changed significantly depending on the strain and *LDH* gene used. The lactic acid titers achieved in this work were much lower than the ones reported in other modified yeast strains (reviewed in Sauer *et al.*, 2010), but higher than the described for this strain (*S. cerevisiae* W303-1A) transformed with a heterologous *LDH* (Branduardi *et al.*, 2006). It is reported that *S. cerevisiae* W303-1A expressing a *Bacillus taurus LDH* has a titer of lactic acid of 20 mg L⁻¹ after 30 hours of growth in YNB glucose 2% medium (Branduardi *et al.*, 2006). In our work we have used the *LDH* gene of *L. casei* and we obtained an amount of lactic acid 15-fold higher, in the same time frame. This work clearly shows the influence of monocarboxylate permeases expression in lactic acid titers. Additional metabolic manipulations, such as Pdc and Adh inactivation should be done in other *S. cerevisiae* strains in order to have comparative yields of lactic acid produced by the engineered strains.

References

- Barnett J.A., Payne R.W. and Yarrow D. (2000). Yeast, characteristics and identification. Third Edition. Cambridge University Press.
- Benninga H.A. (1990) A history of lactic acid making. Kluwer Academic Publishers, Dordrecht, The Netherlands.
- Bianchi M.M., Brambilla L., Protani F., Liu C.L., Lievens J. and Porro D. (2001) Efficient homolactic fermentation by *Kluyveromyces lactis* strains defective in pyruvate utilization and transformed with the heterologous LDH gene. *Appl Environ Microbiol* **67**: 5621–5625.
- Branduardi P., Valli M., Brambilla L., Sauer M., Alberghina L. and Porro D. (2004) The yeast *Zygosaccharomyces bailii*: a new host for heterologous protein production, secretion and for metabolic engineering applications. *FEMS Yeast Res* **4**: 493–504
- Branduardi P., Sauer M., de Gioia L., Zampella G., Valli M., Mattanovich D. and Porro D. (2006) Lactate production yield from engineered yeasts is dependent from the host background, the lactate dehydrogenase source and the lactate export. *Microb Cell Fact* **5**: 4
- Casal M. and Leão C. (1995) Utilization of short-chain monocarboxylic acids by the yeast *Torulasporea delbruekii*: specificity of the transport systems and their regulation. *Biochim Biophys Acta* **1267**: 122-130
- Casal M., Cardoso H. and Leão C. (1996) Mechanisms regulating the transport of acetic acid in *Saccharomyces cerevisiae*. *Microbiology* **142**, 1385-1390.

- Casal M., Paiva S., Andrade R.P. and Leão C. (1999) The lactate-proton symport of *Saccharomyces cerevisiae* is encoded by *JEN1*. *J. Bacteriol.* **181**: 2620-2623
- Casal M., Paiva S., Queirós O. and Soares-Silva I. (2008) Transport of carboxylic acids in yeasts. *FEMS Microbiol Rev.* **32**: 974-994
- Dequin S. and Barre P. (1994) Mixed lactic acid-alcoholic fermentation by *Saccharomyces cerevisiae* expressing the *Lactobacillus casei* L(+)-LDH. *Biotechnology (NY)* **12**: 173-177.
- Gancedo J.M. (1998) Yeast carbon catabolite repression. *Microbiology and Molecular Biology Reviews.* **62**: 334-361.
- Guiard B. (1985) Structure, expression and regulation of a nuclear gene encoding a mitochondrial protein: the yeast L(+)-lactate cytochrome c oxidoreductase (cytochrome b2). *EMBO J.* **4**: 3265-3272
- Ikushima S., Fujii T., Kobayashi O., Yoshida S. and Yoshida A. (2009) Genetic engineering of *Candida utilis* yeast for efficient production of L-lactic acid. *Biosci Biotechnol Biochem.* **73**: 1818-1824
- Ilmen M., Koivuranta K., Ruohonen L., Suominen P. and Penttilä M. (2007) Efficient production of L-lactic acid from xylose by *Pichia stipitis*. *Appl Environ Microbiol* **73**: 117–123.
- Ishida N., Saitoh S., Onishi K., Tokuhiko T., Nagamori E., Kitamoto K. and Takahashi H. (2006) The effect of pyruvate decarboxylase gene knockout in *Saccharomyces cerevisiae* on L-lactic acid production. *Biosci. Biotechnol. Biochem.* **70**: 1148-1153.
- Osawa F., Fujii T., Nishida T., Tada N., Ohnishi T., Kobayashi O., Komeda T. and Yoshida S. (2009) Efficient production of L-lactic acid by Crabtree-negative yeast *Candida boidinii*. *Yeast* **26**: 485-496
- Paiva S., Devaux F., Barbosa S., Jacq C. and Casal M. (2004) Ady2p is essential for the acetate permease activity in the yeast *Saccharomyces cerevisiae*. *Yeast.* **21**: 201-210.
- Porro D, Brambilla L, Ranzi BM, Martegani E & Alberghina L (1995) Development of metabolically engineered *Saccharomyces cerevisiae* cells for the production of lactic acid. *Biotechnol Prog* **11**: 294-298.
- Porro D, Bianchi MM, Brambilla L, Menghini R, Bolzani D, Carrera V, Lievens J, Liu CL, Ranzi BM, Frontali L & Alberghina L (1999a) Replacement of a metabolic pathway for large-scale production of lactic acid from engineered yeasts. *Appl Environ Microbiol.* **65**: 4211-4215
- Porro D, Bianchi MM, Ranzi BM, Frontali L, Vai M, Winkler AA & Alberghina L (1999b) Yeast strains for the production of lactic acid. *International patent application* WO 99/14335.
- Sauer M, Porro D, Mattanovich D & Branduardi P (2010) 16 years research on lactic acid production with yeast – ready for the market? *Biotechnol and Genetic Engineer Rev.* **27**: 229-256
- Tokuhiko K, Ishida N, Nagamori E, Saitoh S, Onishi T, Kondo A & Takahashi H (2009) Double mutation of the *PDC1* and *ADH1* genes improves lactate production in the yeast

Saccharomces cerevisiae expressing the bovine lactate dehydrogenase gene. *Appl Microbiol Biotechnol.* **82**: 883-890.

van Maris AJA, Winkler AA, Porro D, van Dijken JP & Pronk JT (2004) Homofermentative lactate production cannot sustain anaerobic growth of engineered *Saccharomyces cerevisiae*: possible consequence of energy-dependent lactate export. *Appl. Environ. Microbiol.* **70**: 2898–2905.

Additional data not published

Ady2 specificity profile characterization

Aiming at further characterizing the Ady2 transporter we tested the specificity of the acetate transporter Ady2 for a broad range of carboxylic acids, mono-, di- or tricarboxylates.

Experimental procedures

The *S. cerevisiae* strain W303-1A *jen1* Δ *ady2* Δ , lacking monocarboxylate uptake capacity, harboring the plasmid p416-*GPD-ADY2* (pAdy2), was used to perform transport assays with labeled monocarboxylic acids. The cells were grown on glucose, harvested during mid-exponential phase of growth and transferred to fresh media supplemented with acetic acid for 6 hours (derepression). The derepressed cells were harvested by centrifugation, washed twice with ice-cold water and resuspended in ice-cold water to a final biomass concentration of 30-40 mg dry wt. ml⁻¹. The uptake assays were performed following a technique used for the characterization of Jen1 mutants (Soares-Silva et al, 2007). Briefly, 30 μ L of yeast cell suspension was mixed in microtubes with 60 μ L of 0.1 M potassium phosphate buffer, pH 6.0. After 2 min of incubation at 30 °C, the reaction was started by the addition of 10 μ L of an aqueous solution of [1-¹⁴C] acetate (s.a. 10000 dpm/nmol), sodium salt (Amersham Biosciences) at 0.3 mM concentration and pH 6.0, and stopped by the addition of cold 100 mM non-labelled acid, pH 6.0, after 2 min. The inhibition effect of non-labelled substrates on the initial uptake velocities of labelled acid was assayed by adding simultaneously the labelled and non-labelled substrate 1000-fold concentrated. The reaction mixtures were centrifuged for 5 min at 13200 rpm, the pellet was resuspended by vortex in 1 mL of deionized cold water and centrifuged again for 5 min at 13200 rpm. The pellet was finally resuspended in 1 mL of scintillation liquid (Opti-Phase HiSafe II; LKB FSA Laboratory Supplies, Loughborough, UK). Radioactivity was measured in a Packard TriCarb 2200 CA liquid scintillation spectrophotometer with disintegrations per minute correction.

Results and Discussion

Both mono- and dicarboxylates were tested for their capacity to inhibit Ady2-mediated uptake of labelled acetate (Figure 5).

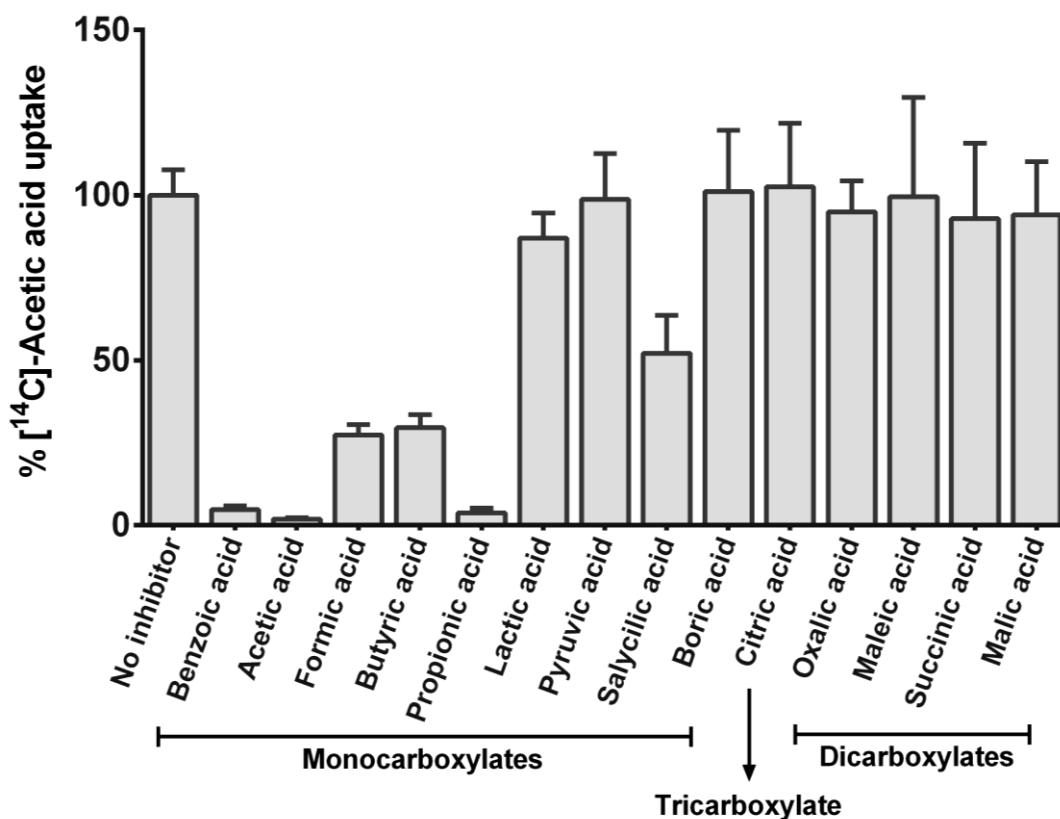


Figure 5 – Specificity profile of Ady2. Relative transport percentage of labelled acetate (30 μ M) in the presence of unlabelled inhibitors 1000-fold concentrated (30 mM) in *S. cerevisiae* *Ajen1* Δ *ady2* transformed with pAdy2. Cells were grown on minimal media with glucose until mid-exponential phase and derepressed for 6 hours in minimal media with acetate (0.5 %, v/v). The graphic represents the percentage of acetic acid uptake of pAdy2 considering that the uptake in the absence of an inhibitor was 100%.

The monocarboxylates benzoic, formic, butyric and propionic acids inhibited the uptake of acetate by > 60 % (Figure 5). The results obtained for formic, propionic and acetic acids are in line with the ones obtained previously showing that the acetate permease could also transport formate and propionate (Casal *et al.*, 1996). On the other hand, the monocarboxylate salicylate inhibited by 50 % Ady2-mediated acetate uptake. . The aromatic carboxylic acids benzoic and salicylic acids have also shown to be inhibitors of the lactate transporter Jen1 (Soares-Silva *et al.*, 2007). Lactate, the monocarboxylate studied previously as a substrate of Ady2, inhibits Ady2 mediated acetic acid uptake albeit at a low rate in the conditions used. The monocarboxylate pyruvate as well as the dicarboxylates maleic, succinic, malic and oxalic acids had no inhibitory effect on acetate uptake. Overall, these results point to a clear preference of AcpA for the binding of short-chain monocarboxylic acids.

Chapter IV

SatP (YaaH), a succinate-acetate
transporter protein in *Escherichia coli*

CHAPTER IV

SATP (YAAH), A SUCCINATE-ACETATE TRANSPORTER PROTEIN IN *ESCHERICHIA COLI*.

Adapted from:

Sá-Pessoa J., Paiva S., Ribas D., Silva I.J., Viegas S.C., Arraiano C.M., and Casal M. (2013) SatP (YaaH), a succinate-acetate transporter protein in *Escherichia coli*. *Biochem J* **454**: 585–95

Abstract

In this work we describe a new carboxylic acid transporter in *Escherichia coli* encoded by the gene *yaaH*. In contrast to what had been described for other YaaH family members, the *E. coli* transporter is highly specific for acetic acid (a monocarboxylate) and for succinic acid (a dicarboxylate), presenting the following affinity constants at pH 6.0, 1.24 ± 0.13 mM acetic acid and 1.18 ± 0.10 mM succinic acid. In glucose grown-cells the $\Delta yaaH$ mutant is compromised for the uptake of both labelled acetic and succinic acids. YaaH, together with ActP, previously described as an acetate transporter, affect the use of acetic acid as sole carbon and energy source. Both genes have to be deleted simultaneously to abolish acetate transport. The uptake of acetate and succinate was restored when *yaaH* was expressed in *trans* in $\Delta yaaH \Delta actP$ cells. We also demonstrate the critical role of YaaH amino acid residues Leu131 and Ala164 on the enhanced ability to transport lactate. Due to its functional role in acetate and succinate uptake we propose its assignment as SatP: the Succinate-Acetate Transporter Protein.

Introduction

The acetate switch in *E. coli* has been defined as a dynamic alteration of the cell physiology that occurs when acetate dissimilation equals its assimilation. This happens when cells are transiting from a rapid growth phase, associated to the production and excretion of acetate, to a slower growth phase, supported by the import and utilization of acetate (Wolfe, 2005). Acetic acid is a weak carboxylic acid that can dissociate in aqueous solution, and the amount of both anionic and lipophilic form is dependent on the pH of the medium. As the pK_a of acetic acid is 4.76, at neutral pH the acetate ion accounts for more than 99% of the acid form. Thus, acetic acid producing cells must possess plasma membrane transporters to efficiently export acetate in its anion form out of the cell. Although the metabolic pathways associated with acetate dissimilation and assimilation in *E. coli* have been extensively studied (for a review see Wolfe, 2005), the identification of the plasma membrane transporters responsible for the export and/or import of acetate have not been yet fully elucidated. An acetate permease (*actP*), cotranscribed with acetyl-CoA synthetase (*acs*) is involved in scavenging micromolar concentrations of acetate from the extracellular medium in *E. coli* (Gimenez *et al.*, 2003). The ActP transporter belongs to the Sodium:Solute Symporter Family (<http://www.tcdb.org/>) and is highly specific for short-chain aliphatic monocarboxylates, namely acetate, glycolate and propionate. However, Gimenez *et al.* (2003) also claimed that besides ActP, another transporter must exist in *E. coli* since the *actP* deficient mutant strain displays low but not null rates of acetate transport. The identification of such transporter remains to be done and our working hypothesis is based on the assumption that this function should be accomplished by the YaaH protein.

The AceTr (former YaaH) family members are polytopic proteins with a predicted topology arranged in six transmembrane segments, containing a conserved motif (N-P-[AV]-P-[LF]-G-L-x-[GSA]-F) located at the first putative transmembrane region of the N-terminus of the protein (<http://www.tcdb.org/>). Members of the AceTr family are found in archaea, eukaryotes and bacteria, with some members experimentally demonstrated as acetate transporters such as *Ady2* in the yeast *Saccharomyces cerevisiae* (Paiva *et al.*, 2004) and *AcpA* in the filamentous fungus *Aspergillus nidulans* (Robellet *et al.*, 2008). An *acpA* deletion in *A. nidulans* leads to reduced growth on acetate as a sole carbon source, at low concentration and in a high pH medium, which is fully restored upon reintroduction of the *acpA* gene. This gene is also required for the induction of the acetate

assimilation pathways and direct measurement of acetate incorporation into germinating conidia confirmed that AcpA is fundamental for acetate uptake, especially at low substrate concentrations (Robellet *et al.*, 2008). The *acpA* transcript level increases as the demand for acetate uptake increases and its expression is induced in the presence of several weak monocarboxylic acids such as glyoxylate, propionate, lactate, pyruvate and formate (Robellet *et al.*, 2008).

Acetic acid-grown cells of the yeast *S. cerevisiae* display activity for a monocarboxylate/proton symporter, shared by acetate, propionate and formate, dependent on the Δ pH across the plasma membrane (Casal *et al.*, 1996), found to be associated to Ady2 expression. *S. cerevisiae* ADY2 is subjected to glucose repression and its expression occurs upon a shift from glucose medium to a non-fermentable carbon source, such as acetic acid (Paiva *et al.*, 2004). The deletion of ADY2 results in the loss of mediated acetate uptake measured at pH 6.0, implying that this gene is essential for the acetate permease activity in *S. cerevisiae* (Paiva *et al.*, 2004). The same protein was also hypothesized to be an ammonium exporter (Palková *et al.*, 2002; Váchová *et al.*, 2009) since the null mutant displays a reduction in ammonia production when cells are growing in colonies (Palková *et al.*, 2002), and the appearance of Ady2 at the plasma membrane correlated with ammonia release (Váchová *et al.*, 2009). However, more recently, two independent teams have found that Ady2 is also implicated in lactic acid uptake (Pacheco *et al.*, 2012; Kok *et al.*, 2012). It was demonstrated that the double mutant strain for Ady2 and for the lactate permease Jen1 (*ady2 Δ jen1 Δ*), but with ADY2 gene expressed in a centromeric plasmid under the control of a strong constitutive promoter, displays a Michaelis–Menten kinetics for initial uptake rates of labelled lactic acid at pH 5.0 (Pacheco *et al.*, 2012). By using a laboratory evolution strategy of a *S. cerevisiae* *jen1 Δ* strain, Kok *et al.* (2012) found two genomic mutants in *Ady2*, Leu219Val and Ala252Gly, with enhanced ability to grow on lactic acid. All these evidence supports a role for Ady2 as a monocarboxylate transporter located at the plasma membrane of yeast cells.

Although not directly shown to be functionally implicated in acetate uptake, other YaaH family members have been linked to acetic acid adaptation, such as Gpr1 in the yeast *Yarrowia lipolytica* and MA4008 in the archaea species *Methanosarcina acetivorans*. In *Y. lipolytica* GPR1 mRNA expression is enhanced by acetic acid and although its deletion did not impair growth on acetic acid as a carbon source (Augstein *et al.*, 2003), mutations in the C-terminal part of Gpr1 were found to be detrimental for acetic acid sensitivity (Gentsch *et al.*, 2007). In the methanogen archaeobacteria *M. acetivorans* by quantitative

transcription analysis, the gene *MA4008* was found to be highly expressed in acetic acid-grown cells versus methanol-grown cells. The expression of this gene was similar to acetate kinase (*ack*) and acetyl-CoA phosphotransferase (*pta*), two of the enzymes required for acetate utilization, suggesting a role of *MA4008* in acetate uptake (Rohlin and Gunsalus, 2010).

The YaaH protein of *E. coli*, responsible for naming the family to which it belongs to, has its annotation exclusively based on homology assumptions. In this work we present for the first time experimental evidence for the functional role of YaaH as an acetate-succinate transporter proposing a new nomenclature for this protein.

Experimental Procedures

Bacterial strains, plasmids and growth conditions

All the bacterial strains and plasmids used in this study are listed in Table 1 and 2, respectively. All strains used are isogenic with the wild type *E. coli* K12 derivative strain MG1693. The cultures were maintained on slants of Luria-Bertani (LB). All strains were grown in Minimal Media (MM) (Boronat and Aguilar, 1979) [34 mM NaH₂PO₄, 64 mM K₂HPO₄, 20 mM (NH₄)₂SO₄, 1 μM FeSO₄, 0.1 mM MgSO₄, and 10 μM CaCl₂] in shake flasks, ratio 1:10, at 37 °C and 200 r.p.m. throughout this study, unless stated otherwise. Carbon sources were glucose (1%, w/v) or acetic acid (1.67, 8.3, 16.6, 33.3, 50, 66.7 and 83.3 mM, pH 6.0) as given in figure legends. Growth medium was supplemented with thymine (50 μg/mL) and the following antibiotics when appropriate: ampicillin (100 μg/mL), chloramphenicol (50 μg/mL) and kanamycin (50 μg/mL).

For the growth experiments in acetic acid, *E. coli* strains were cultured overnight in minimal media supplemented with glucose 1 % (w/v), collected by centrifugation at 5000 g for 1 min, washed twice in minimal media (carbon source free) and diluted to an optical density at 600 nm of 0.05 in 150 μL of minimal media, pH 6, supplemented with 1.7, 8, 16, 33.3, 50.0, 66.7 or 83.3 mM acetic acid, into a 96-well microplate. Growth was monitored for 36 h using a Spectramax plus 384 absorbance microplate reader (Molecular Devices).

Table 1 – List of strains used in this work.

Strain	Relevant markers/Genotype	Reference
MG1693	<i>thyA715</i>	(Arraiano <i>et al.</i> , 1988)
BBC232	MG1693 <i>yaaH</i> ($\Delta yaaH::Cm^R$)	This work
BBC233	MG1693 <i>actP</i> ($\Delta actP::Kan^R$)	This work
BBC234	MG1693 <i>yaaH actP</i> ($\Delta yaaH::Cm^R/\Delta actP::Kan^R$)	This work
BBC235	BBC234 transformed with pUC18	This work
BBC236	BBC234 transformed with pSVA9	This work
BBC237	BBC234 transformed with pWSK29	This work
BBC238	BBC234 transformed with pSVA10	This work
BBC239	BBC234 transformed with pL131V	This work
BBC240	BBC234 transformed with pA164G	This work
BBC241	BBC233 transformed with pUC18	This work

Table 2 – List of plasmids used in this work.

Plasmid	Comments	Origin/Marker	Reference
pKD3	Template for mutants construction; carries chloramphenicol-resistance cassette	oriR γ /Amp ^R	(Datsenko and Wanner, 2000)
pKD4	Template for mutants construction; carries kanamycin-resistance cassette	oriR γ /Amp ^R	(Datsenko and Wanner, 2000)
pKD46	Temperature-sensitive λ -red recombinase expression plasmid	oriR101/Amp ^R	(Datsenko and Wanner, 2000)
pUC18	High copy plasmid, constitutive expression	pMB1/Amp ^R	Fermentas
pWSK29	Low-copy plasmid, constitutive expression	pSC101/Amp ^R	(Wang and Kushner 1991)
pSVA9	pUC18 derivative; constitutive expression of <i>yaaH</i>	pUC18/Amp ^R	This work
pSVA10	pWSK29 derivative; constitutive expression of <i>yaaH</i>	pWSK29/Amp ^R	This work
pL131V	pSVA9 with the substitution L131V in <i>yaaH</i>	pMB1/Amp ^R	This work
pA164G	pSVA9 with the substitution A164G in <i>yaaH</i>	pMB1/Amp ^R	This work

Construction of *E. coli* mutants

The *yaaH* (BBC232) and *actP* (BBC233) null mutants were constructed using the primer pairs dyaaH1/dyaaH2 and dactP1/dactP2, respectively, and following the λ -*red* recombinase method (Datsenko and Wanner, 2000) with few modifications, as previously described (Viegas *et al.*, 2007). The chloramphenicol-resistance cassette of plasmid pKD3 replaces nucleotides +5 to +535 of the *yaaH* gene and the kanamycin-resistance cassette of plasmid pKD4 replaces nucleotides +69 to +1596 of *actP*. The gene deletions were verified by colony PCR using the primer pair P1yaaH/P2yaaH for *yaaH* and kt/P3actP and emb282/P1actP for *actP*. All chromosomal mutations were subsequently transferred to a fresh genetic background (MG1693 strain) by P1 transduction. The same method was used for the construction of the double mutant *yaaH/actP* (BBC234), from the respective single mutants.

For construction of pSVA9 plasmid expressing *yaaH*, a PCR fragment containing the entire *yaaH* coding sequence was amplified from MG1693 chromosome using the primer pair P3yaaH and P5yaaH. The resultant PCR fragment was cleaved with *Xba*I and *Hind*III and ligated into the high copy pUC18 plasmid (GenBank/EMBL accession number L09136) digested with the same enzymes. Plasmid pWSK29 (GenBank accession number AF016889-1), expressing *yaaH* gene under its own putative promoter signals (pSVA10), was constructed using the same strategy but with the primer pair P4yaaH/P5yaaH. Correct clones were verified by colony PCR and sequencing. All primers were obtained from StabVida (Portugal) and are listed in Table 3.

Table 3 – List of oligos used in this work.

Oligo	Sequence 5' to 3' *
dyaaH1	<u>CGAGCGGGGGGATCTCAAAACAATTAGTGGGATTCACCAATCGGC</u> <u>AGAACGTGTAGGCTGGAGCTGCTTC</u>
dyaaH2	<u>TCAGGGAAATTATTTACACCATTCATTCGATGATGATTTTTGAGGAA</u> <u>TTATGGGGTCCATATGAATATCCTCCTTAG</u>
P1yaaH	ATGCCGCGCCCTGAAAACACTAC
P2yaaH	AGTGCAAGACGCGACGTTAGCGAAT
P3yaaH	GTTTTTTCTAGACCATTCATTCGATGATGATTTTTGAG
P4yaaH	GTTTTTTCTAGACAGGTCTGATACCGGAAAC
P5yaaH	GTTTTTTTAAGCTTGCAAGACGCGACGTTAGC

dactP1	<u>GATTAATGCGCGCGGCCTTGCTCAACGCCAAAGCCGGTCTGGGAG</u> <u>CGGATAAACTGGTGTAGGCTGGAGCTGCTTC</u>
dactP2	<u>CGGCGCTTGCCGCCACACTCCCTTTTCGCAGCTAACGCCGCGGATGC</u> <u>TATTAGGGTCCATATGAATATCCTCCTTAG</u>
P1actP	TCTACATCTGGCGGGCGAAC
P3ActP	AGGCATATTCTCTGCATTATC
kt	CGGCCACAGTCGATGAATCC
Emb282	ACGCTTGATCCGGCTACCTGCCC
P6yaaHmut (L131V)	CAATTCGTTTTCTTTTAGC GTG ACCGTGCTGTTTGCC
P7yaaHmut (A164G)	GATCTGCGGTGCCAGC GGC ATCTATCTGGCGATG
RT_16s fwd	AAGTCGAACGGTAACAGGAAG
RT_16s rev	AGGCAGTTTCCCAGACATTAC
RT2_yaaH fwd	TTTTGCTGGTCTGCTGGAGT
RT2_yaaH rev	AGACCCAGTTTCGGCATCAG
RT2_actP fwd	TCTTTCGGCCTGTGGTTCTC
RT2_actP rev	AGCACCACCGCAATGTGATA

*the restriction sequences in the primers for cloning procedures are shown in bold. The sequence of homology to the gene in the primers used for the generation of deletion mutants is underlined. The codon mutated is shown in bold underlined.

HPLC measurements

Samples at specific time points of growth were analysed for their concentration in organic acids namely succinic and acetic acids and in carbohydrates namely glucose. Cellular density was measured at 600 nm on a Genesys 20 spectrophotometer (Thermo Spectronic) and 1.5 mL samples were collected and centrifuged for 5 min at 16100 g. The supernatants were filtered through 0.22 µm syringe filters and were monitored using a Rezex™ 8 µm ROA-organic acid H+ (8 %) HPLC column (Phenomenex). 2.5 mM H₂SO₄ was used for the mobile phase, the column was maintained at 60 °C and detection was by refractive index measurement with an Elite LaChrom L-2490 RI detector (VWR Hitachi) at 40 °C. An Elite LaChrom (VWR Hitachi) chromatography system was used with the EZChrom Elite 3.3.2 SP2 software for data collection and analysis.

Transport assays

Cells were incubated in minimal media supplemented with the respective carbon source and harvested by centrifugation at specific time points (as given in figure legends). Cells

were then washed in minimal media and resuspended in a 0.1 M potassium phosphate buffer (pH 6.0) containing 0.25 mM MgCl₂ to a final concentration of about 5-15 mg dry weight ml⁻¹. 90 μL of bacterial cell suspension was placed in microtubes and after 2 min of incubation at 37 °C, the reaction was started by the addition of 10 μL of an aqueous solution of [1-¹⁴C] acetate (s.a. 10000 dpm/nmol), sodium salt (Amersham Biosciences) at 0.5 mM concentration and pH 6.0 (unless otherwise stated), and stopped by the addition of cold 100 mM non-labelled acid, pH 6.0, after 2 min. A time course assay was carried out for acetic acid uptake and the initial uptake rate of this carboxylate was linear for 3 min (data not shown) so we chose an incubation time of 2 min for the transport kinetics determination. The reaction mixtures were centrifuged for 5 min at 16100 g, the pellet was resuspended by vortex in 1 mL of minimal media and centrifuged again for 5 min at 16100 g. The pellet was finally resuspended in 1 mL of scintillation liquid (Opti-Phase HiSafe II; LKB FSA Laboratory Supplies, Loughborough, UK). Radioactivity was measured in a Packard Tri-Carb 2200CA liquid scintillation spectrophotometer with disintegrations per minute correction. The inhibition effect of non-labelled substrates on the initial uptake velocities of labelled acid was assayed by adding simultaneously the labelled and non-labelled substrate. Non-specific ¹⁴C adsorption to the cells, as well as the diffusion component, was determined by adding a mixture of labelled acid and unlabelled acid 1000-fold concentrated. The values estimated represent less than 5-10 % of the total incorporated radioactivity. Uptake measurements were also performed using [1,4-¹⁴C]-succinic acid (s.a. 4000 dpm/nmol), purchased from Moravek Biochemicals, and with D,L-[U-¹⁴C]-lactic acid (s.a. 4000 dpm/nmol), purchased from Amersham Biosciences, at the desired concentration as described for acetic acid. The transport kinetics best fitting the experimental initial uptake rates and the kinetic parameters were determined by a computer-assisted non-linear regression analysis (using GraphPad Prism version 5.01 for Windows, GraphPad Software, San Diego California USA, www.graphpad.com). The data shown are mean values of at least three independent experiments, with three replicas of each.

Gene expression analysis by RT-PCR

Cells were incubated in minimal media supplemented with 1% glucose (w/v) or 1.67 mM (0.1 %, v/v) to 83.3 mM (0.5 %, v/v) acetic acid and 1x10⁹ cultured bacterial cells were harvested by centrifugation at specific time points (as given in figure legends). For total

RNA isolation and purification the kit GRS Total RNA Kit – Blood & Cultured Cells from GRISP Research Solutions© was used according to the manufacturer instructions. Purity and concentration of total RNA was evaluated by measuring the optical density at 260 and 280 nm using a NanoDrop1000 spectrophotometer. Transcription of isolated RNA to cDNA was performed with the iScript™ cDNA Synthesis Kit (Bio-Rad). Relative quantitative RT-PCR of the cDNA samples was carried out in a CFX96 Touch™ Real-Time PCR Detection System from Bio-Rad using KAPA SYBR® FAST qPCR Master Mix with SYBR® Green I as the detection agent. The primers used to amplify the selected genes using qPCR were designed using Primer Blast (Rozen and Skaletsky, 2000; Ye *et al.*, 2012) and are listed in Table 3. Reactions were set up in a total volume of 20 µl using 2 µl of cDNA (diluted to 10⁻¹), 10 µl KAPA SYBR® FAST qPCR master mix (Kapa Biosystems), nuclease-free water and 200 nM of each gene-specific primer (Table 3) and performed in the CFX96 Touch™ machine (Bio-Rad). Amplification conditions were as follows: 95 °C for 3 min, 40 cycles at 95 °C for 3 s and 57.6 °C for 30 s. Specificity of the PCR products was confirmed by analysis of the dissociation curve. The melting curve program consisted of temperatures between 65 °C and 95 °C with a heating rate of 0.5 °C/5 s and a continuous fluorescence measurement. Additionally, the amplicons' expected size and the absence of nonspecific products were confirmed by analysis of the real-time PCR products in 1 % agarose gels (w/v) in 1 × TAE, stained with Midori Green and visualized under UV light. A negative control without template was conducted for each gene in each PCR run, and a control of DNA contamination was implemented by using the purified RNA samples as template. A positive control with the target cloned in an expression plasmid was conducted for each gene in each PCR run. qPCR reactions were performed in triplicate for each cDNA sample tested. Threshold cycle (C_T) values were calculated by using Bio-Rad CFX Manager software, and fold changes were calculated as $2^{-\Delta\Delta C_T}$ with inner normalization to the 16S rRNA housekeeping gene (Livak and Schmittgen, 2001). All samples were then compared to the expression levels of the mid-exponential (3 hour) samples of growth in glucose and expressed as relative fold expression. Standard deviations of ΔC_T values for three biological triplicates were propagated to obtain standard errors for each fold change value (Schmittgen and Livak, 2008).

Construction of *yaaH* mutations by site-directed mutagenesis

yaaH mutations were constructed in the plasmid pSVA9, with the oligonucleotide-directed mutagenesis technique (Ansaldi *et al.*, 1996). The mutagenesis was performed using the DNA Polymerase KAPA HiFi™ (Kapa Biosystems) with proofreading activity as follows: 10 ng of the template plasmid pSVA9 were combined with 10 pmol of the forward oligonucleotides P6yaaHmut or P7yaaHmut and the respective complementary reverse oligonucleotides (Table 3) containing the desired substitution (L131V or A164G) and used in the following PCR reaction: 5 min at 95 °C followed by 25 cycles of 20 s at 98 °C, 15 s at 65 °C, 5 min at 72 °C, and a final extension step of 5 min at 72 °C. In order to destroy the parental strands, the PCR reaction was incubated with the restriction enzyme *DpnI* (Fermentas) for 2 h at 37 °C. This mixture was then used to transform *E. coli* XL1-Blue and plasmid extraction was performed on several clones with the Gene Elute™ Plasmid miniprep Kit (Sigma) to obtain plasmids pL131V and pA164G. Mutations were confirmed by sequencing using appropriate oligonucleotides for both DNA strands. The genes containing the desired mutations were introduced in *E. coli* $\Delta yaaH \Delta actP$ cells made competent by the rubidium chloride method (Hanahan, 1983).

Results

Distinct physiological roles for *yaaH* and *actP* on acetate uptake

Single and double mutants for the genes *yaaH* and *actP* were constructed in the strain *E. coli* MG1693, as described in the Experimental Procedures. The uptake of [¹⁴C]-acetic acid 0.5 mM pH 6.0, was assessed in all above mentioned strains aerobically grown on mineral media containing glucose, as sole carbon and energy source, collected in mid-exponential phase (Figure 1). A strong decrease in the transport activity of labelled acetic acid was found in the double mutant $\Delta yaaH \Delta actP$, whereas for the respective single mutants only a partial reduction in activity was detected compared with the wild type strain (100% of activity). These observations were indicative of separate roles for YaaH and ActP in acetate transport.

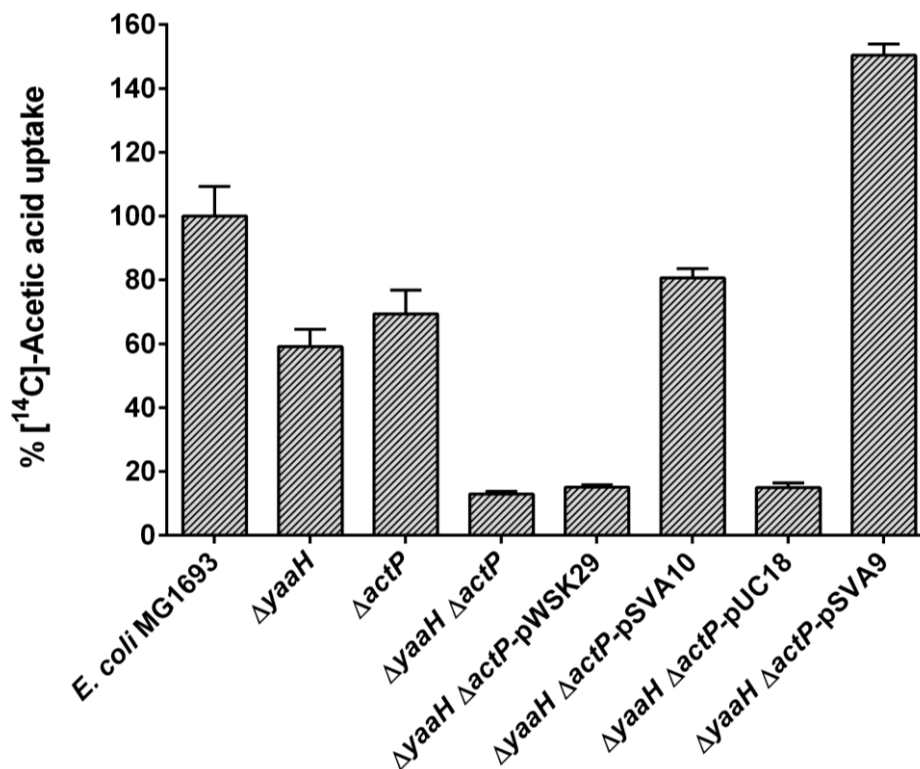


Figure 1 – The functional role of *yaaH* and *actP* genes as acetate transporters in *E. coli*. The graphic represents the percentage of 0.5 mM [¹⁴C]-acetic acid uptake, at pH 6.0, considering 100% the velocity of transport found for the wild type *E. coli* MG1693 strain. The cells were collected at the mid-exponential growth phase in minimal medium with glucose 1 % (w/v), containing the required supplements for growth as indicated in materials and methods. The strain Δ*yaaH* Δ*actP* was transformed with the plasmids pSVA9 and pSVA10, expressing *yaaH* from a high or low copy number plasmid, respectively (Table 2). Each data point represents the mean ± SD of 3 independent experiments (n=9).

The uptake of acetate was restored when *yaaH* was expressed in *trans* in Δ*yaaH* Δ*actP* cells either from a low or a high copy number plasmid (Figure 1). The level of activity produced from the low copy number plasmid was very similar to the one found for the single Δ*actP* mutant, while for the high copy number plasmid the uptake values exceeded, in about 50 %, the activity of the wild type strain.

Energetics and kinetics of the YaaH transporter

The effect of pH on the acetate transport activity associated with YaaH expression was measured in *E. coli* Δ*yaaH* Δ*actP* cells transformed with the high copy plasmid, not expressing (pUC18) or expressing *yaaH* (pSVA9). Data was taken from cells growing exponentially in mineral media with glucose as sole carbon and energy source (Figure 2 A). Under the pH range analysed, the uptake was maximum at pH 6.0 in cells harbouring

pSVA9, with a decrease of activity in more acidic or more alkaline pH values while, in cells transformed with pUC18, this pH effect was not found.

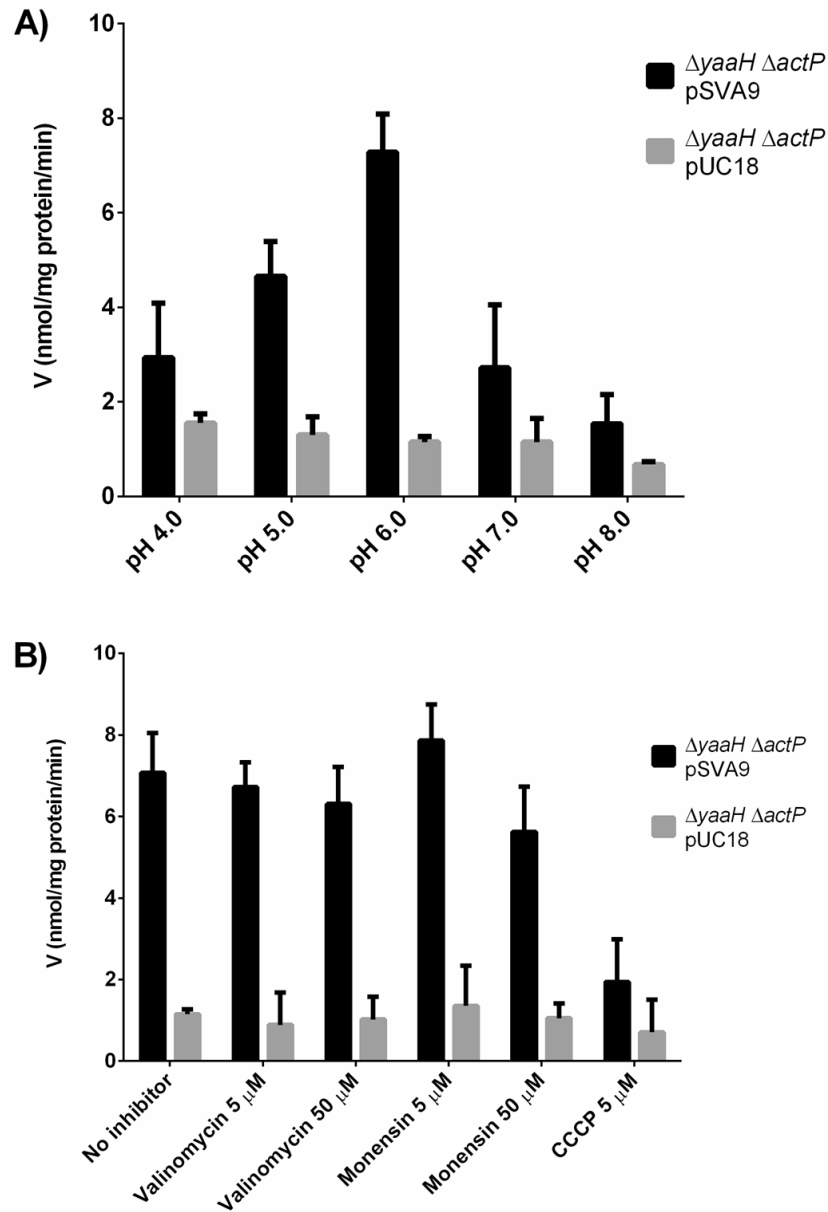


Figure 2 – Energetics of the YaaH transporter. Effect of pH and of CCCP, valinomycin and monensin on the uptake of [1-¹⁴C]-acetic acid 0.5 mM, in cells of *E. coli* MG1693 $\Delta yaaH \Delta actP$ transformed with pSVA9 or pUC18 plasmids, grown as indicated in Figure 1 legend. A) Transport activity was determined in cells buffered in potassium phosphate at the pH values indicated. B) Cells were pre-incubated with the compounds mentioned, at the concentration indicated, pH 6.0, for 1 min before adding the radiolabeled substrate. Each data point represents the mean \pm SD of 3 independent experiments (n=6).

The protonophore CCCP that collapses the proton motive force, lowered transport to almost negligible values at pH 6.0 in cells expressing *yaaH* (Figure 2 B). The potassium ionophore valinomycin and the sodium ionophore monensin, that disrupt the membrane electrical potential $\Delta\psi$, had no significant effect on acetate uptake. In *E. coli* $\Delta yaaH \Delta actP$ cells transformed with pUC18 no visible inhibitory effect was observed with the protonophores and ionophores tested.

The dependence of the transporter activity on ΔpH , together with the effect of the protonophore CCCP, suggest that YaaH behaves as a secondary active acetate/proton symporter, energetically dependent on the proton motive force.

The initial uptake rates of [¹⁴C]-acetic acid as a function of acetic acid concentration in *E. coli* $\Delta yaaH \Delta actP$ cells transformed with the empty pUC18 plasmid were residual for acetic acid uptake (Figure 3). Cells of the $\Delta actP$ mutant were used to assess the kinetic parameters associated with YaaH activity revealing an apparent K_m of 1.24 ± 0.13 mM acetic acid and an apparent V_{max} of 8.72 ± 0.37 nmol acetic acid mg protein⁻¹ min⁻¹ (Figure 3). As expected when overexpressing *yaaH* in $\Delta yaaH \Delta actP$ cells, a higher acetate transport activity (apparent V_{max} of 14.49 ± 0.63 nmol acetic acid mg protein⁻¹ min⁻¹) was found. All these findings support the involvement of YaaH protein as an acetate transporter in *E. coli*.

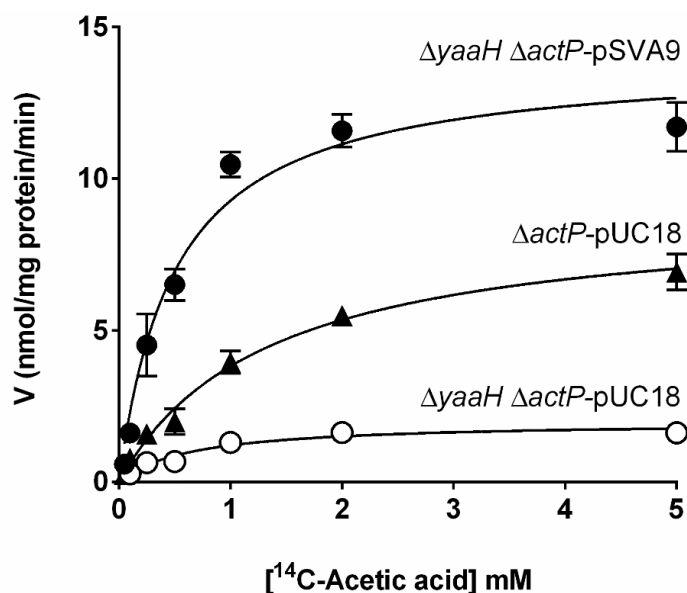


Figure 3 – Acetic acid kinetics of the YaaH transporter. Eadie-Hofstee plots of initial uptake rates of [¹⁻¹⁴C]-acetic acid, pH 6.0, in glucose-grown cells, as indicated in Figure 1 legend. *E. coli* strains used: ●, $\Delta yaaH \Delta actP$ transformed with pSVA9 plasmid, expressing the *yaaH* transporter; ▲, $\Delta actP$ transformed with pUC18 multicopy plasmid; ○, $\Delta yaaH \Delta actP$ transformed with pUC18 multicopy plasmid. Inset:

Kinetics of [1-¹⁴C]-acetic acid uptake at pH 6.0, as a function of the acid concentration. Each data point represents the mean ± SD of 3 independent experiments (n=9).

The physiological role of YaaH and ActP on acetate assimilation

Wild type cells display ability to growth on acetic acid (pH 6.0) in a range of concentrations varying from 1.67 mM (0.01 %, v/v) to 83.3 mM (0.5 %, v/v) (Figure 4), with concomitant acetic acid consumption as well as measurable acetic acid uptake.

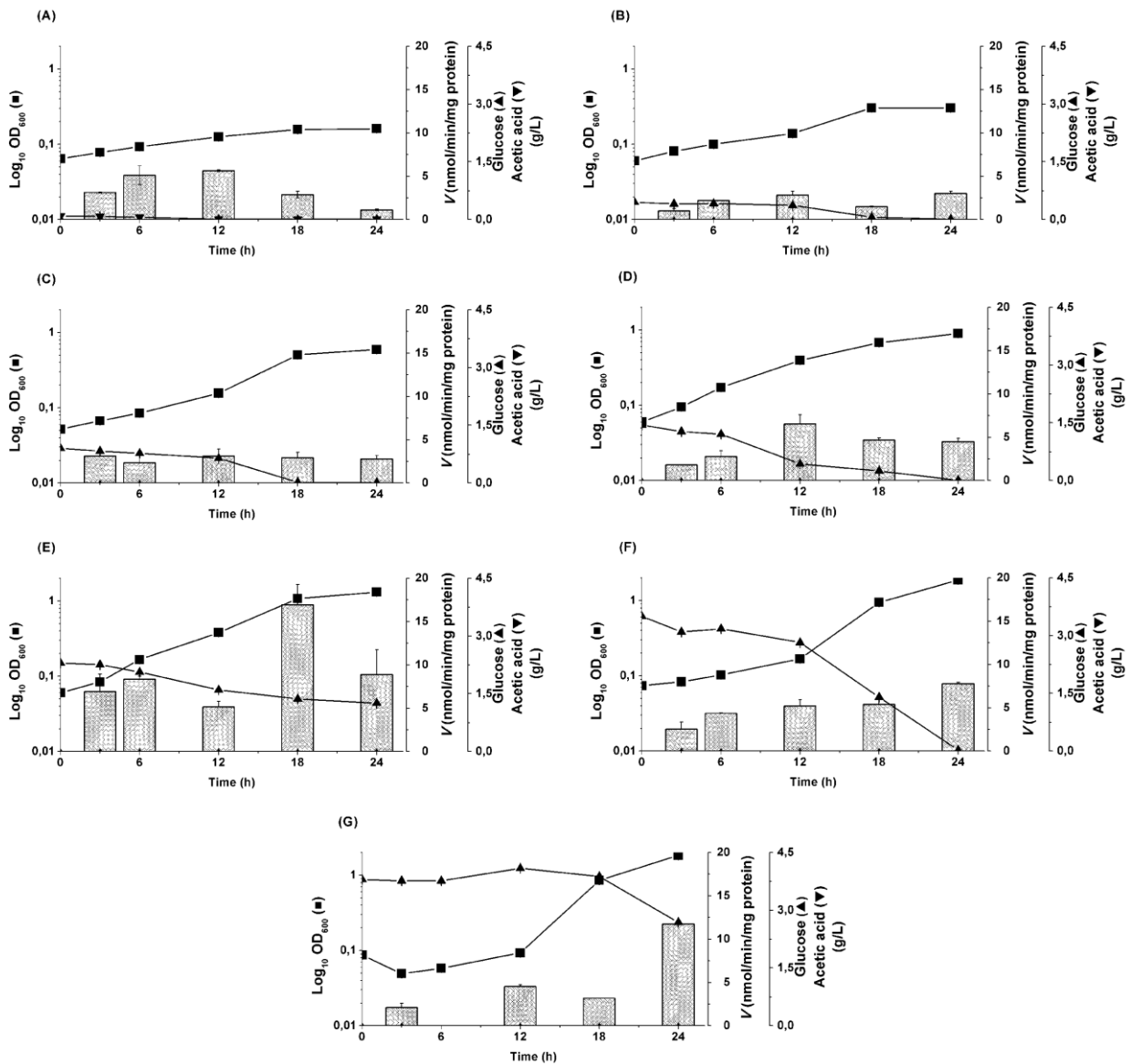


Figure 4 – Acetate uptake profiles of cells grown on acetic acid. Growth profiles of *E. coli* MG1693 grown on minimal medium with acetic acid 1.67 mM (A), 8.3 mM (B), 16.6 mM (C), 33.3 mM (D), 50 mM (E), 66.7 mM (F) and 83.3 mM (G), pH 6.0. Symbols: ■, OD₆₀₀; ▲, acetic acid (g/L); bars, transport activity measured with [¹⁴C]-acetic acid, 0.5 mM, pH 6.0.

Based on this evidence we wondered about the role of acetate transporters in cells' ability to grown on acetic acid. We have found that single and double mutants revealed a significant alteration in the ability to grow in acetic acid as sole carbon and energy source at 66.7 mM (0.4 %, v/v). This phenotype was even more pronounced at 83.3 mM (0.5 %, v/v), where the double and the $\Delta actP$ mutants display a longer lag phase (Figure 5). The mRNA expression of *yaaH* and *actP* accessed at three time points (6, 12 and 24 h) has a similar profile (Figure 5 H), with *yaaH* presenting a lower relative fold expression when compared to *actP*. In general, the expression of both genes increased over time independent of the acetic acid concentration used for growth with a maximum level detected at 24 h, in cultures with 66.7 mM acetic acid. Overall, these results highlight the relevance of acetate transporters on acetic acid utilization.

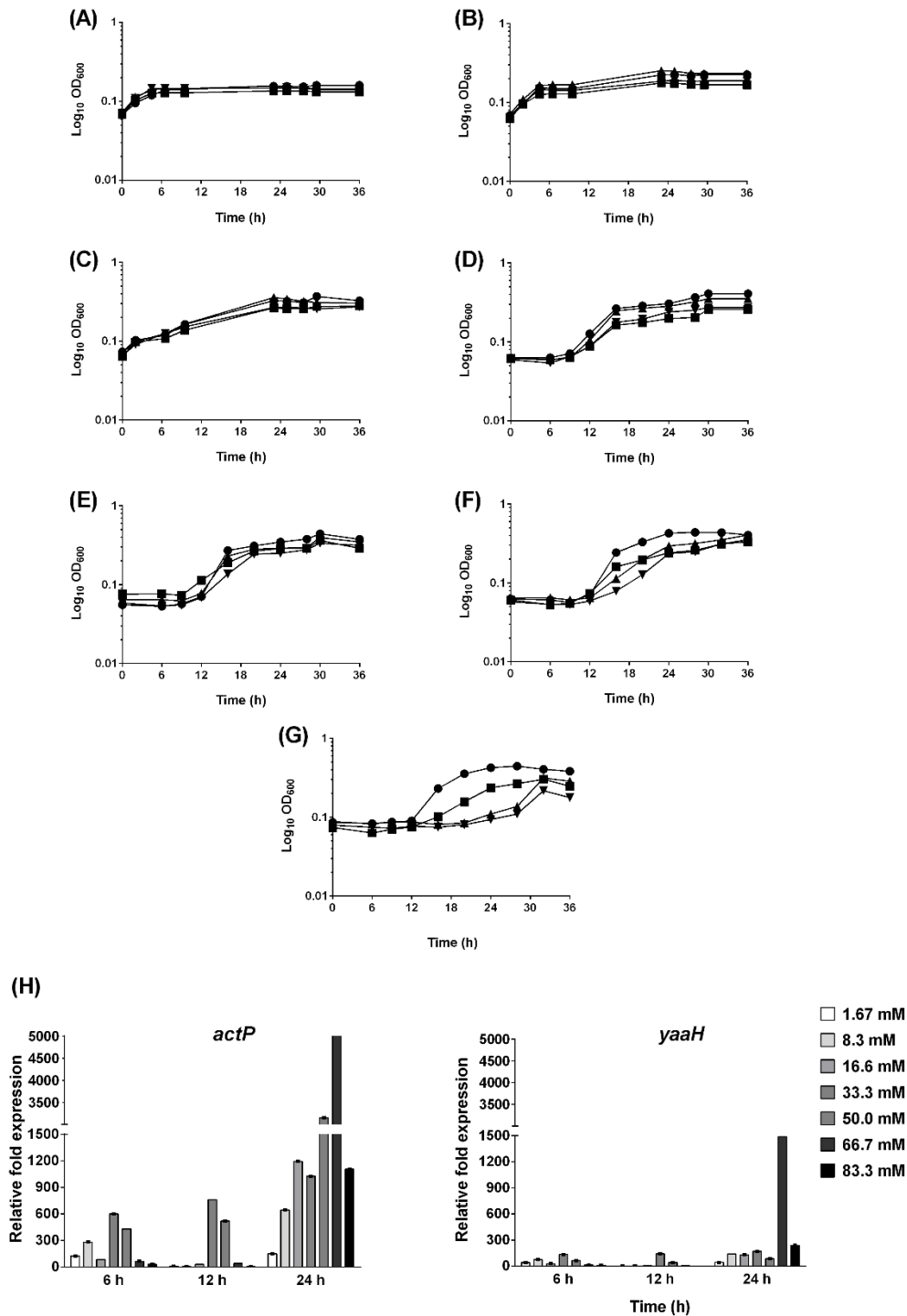


Figure 5 – The physiological role of YaaH and ActP on acetate assimilation. Growth profiles of *E. coli* MG1693 (●) and isogenic $\Delta actP$ (△), $\Delta yaaH$ (□) and $\Delta yaaH \Delta actP$ (▽) mutants in minimal medium with acetic acid 1.67 mM (A), 8.3 mM (B), 16.6 mM (C), 33.3 mM (D), 50.0 mM (E), 66.7 mM (F) and 83.3 mM (G), pH 6.0. H) Relative fold expression of *yaaH* and *actP* genes evaluated by RT-PCR in wild type cells collected at 6, 12 and 24 hours of growth, normalized to *16S* with standard deviations of ΔC_T values propagated for each fold change value, as described in the experimental procedures. Each data point represents the mean \pm SD of 3 independent experiments (n=6).

Distinct physiological roles for distinct acetate transporters

The observation that both YaaH and ActP act independently in the transport of acetate raised the question about what their respective distinctive physiological role might be during aerobic growth on glucose. We evaluated the expression of both *yaaH* and *actP* in cells grown on 0.2, 0.4 and 1.0 % w/v glucose in the wild type strain as well as the relative acetic acid uptake over time. At low (0.2 %) and intermediary (0.4 %) glucose concentration *yaaH* expression was almost negligible (Figure 6) while *actP* had a peak following entry into stationary phase. Taking the expression pattern into account we can infer that at these concentrations of glucose the relative activity for acetate uptake is probably more associated with *actP*.

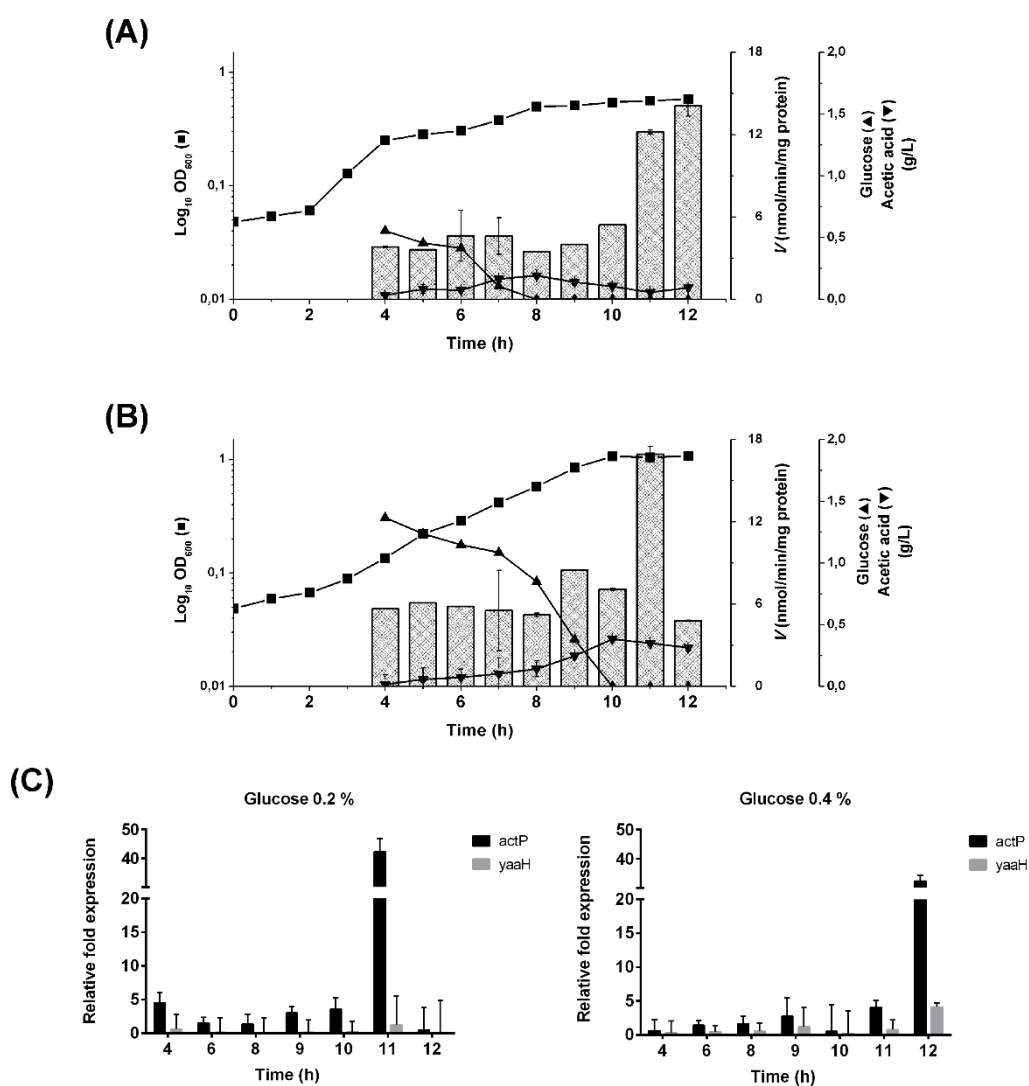


Figure 6 – Acetate uptake profiles of cells grown on glucose. Growth profiles of *E. coli* MG1693 grown on minimal medium with glucose 0.2 %, w/v (A) and 0.4 %, w/v (B). Symbols: ■, OD₆₀₀; ▲, glucose (g/L); ▼, acetic acid (g/L); bars, transport activity measured with [¹⁴C]-acetic acid, 0.5 mM, pH 6.0. C)

Relative fold expression of *yaaH* and *actP* genes evaluated by RT-PCR in wild type cells collected at 6, 12 and 24 hours of growth, normalized to *16S* with standard deviations of ΔC_T values propagated for each fold change value, as described in the experimental procedures. Each data point represents the mean \pm SD of 3 independent experiments (n=6).

A distinct behaviour was found for cells grown on high (1 %) glucose concentration where both *yaaH* and *actP* are expressed. To access the distinct physiological role of each transporter we compared the behaviour of the single and double mutant strains with the wild type. In the experiment described in Figure 7, the glucose consumption profiles over time (\blacktriangle) were very similar in all strains, which displayed the following specific growth rates (hr^{-1}): wild type 0.15; $\Delta actP$ 0.14; $\Delta yaaH$ 0.14; $\Delta yaaH \Delta actP$ 0.12. Regarding acetate accumulation in the extracellular medium (\blacktriangledown) the levels detected were identical in all four strains.

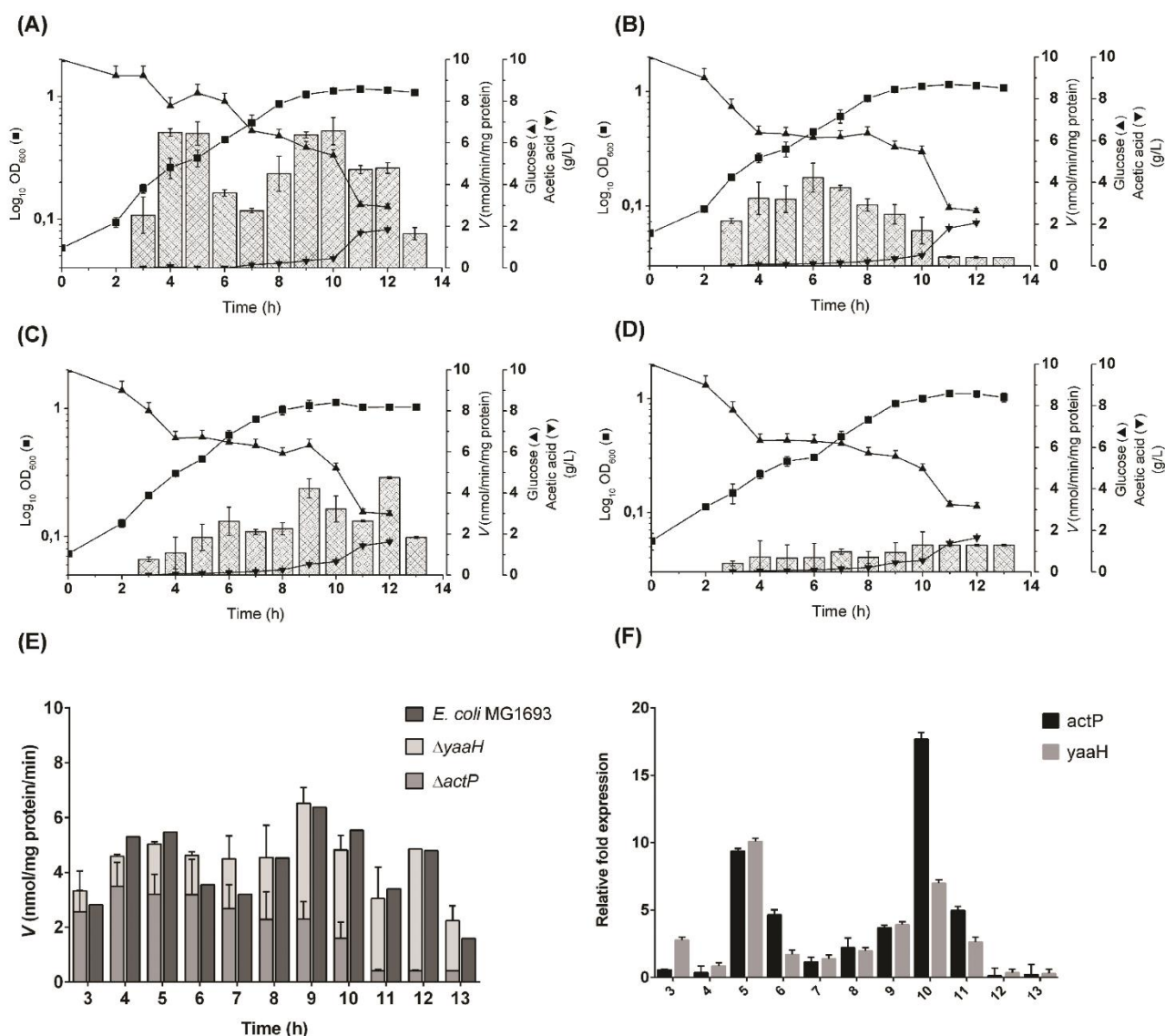


Figure 7 – Distinct physiological roles of the two *E. coli* acetate transporters. Growth profiles of *E. coli* MG1693 (A), and isogenic *ΔactP* (B), *ΔyaaH* (C) and *ΔyaaH ΔactP* (D) mutants in minimal medium with glucose 1% (w/v) and the required supplements, as indicated in materials and methods. Symbols: ■, OD₆₀₀; ▲, glucose (g/L); ▼, acetic acid (g/L); bars, transport activity measured with [¹⁴C]-acetic acid, 0.5 mM, pH 6.0. E) Time course analysis for acetate uptake of the wild type strain (dark bars, data from A) compared to the sum of the activities of the strains *ΔactP* (light grey bars, data from B) and *ΔyaaH* (dark grey bars, data from C). F) Relative fold expression of *yaaH* and *actP* genes evaluated by RT-PCR normalized to *16S* with standard deviations of ΔC_T values propagated for each fold change value, as described in the experimental procedures. Each data point represents the mean \pm SD of 3 independent experiments (n=6).

The four strains achieved the same final OD₆₀₀ after 13 h of growth (Figure 7 A-D, ■), however regarding the acetate transport activity a distinct profile was observed for each strain (Figure 7 A-D, bars). In the wild type strain, two peaks of activity were detected

(Figure 7 A), which in fact can be correlated with the behaviour of the single mutants. The first peak, between 4-6 hours of growth, is mostly associated with YaaH activity (Figure 7 B), whereas the second peak, between 8-12 hours, correlates with the ActP permease (Figure 7 C). The double mutant displays only a residual acetate uptake activity all over the growth curve (Figure 7 D). It is worth mentioning that acetate uptake activity profile detected in wild type correlates well with the sum of the values found for each single mutant (Figure 7 E).

In the wild type strain the mRNA expression profile was similar for both genes (Figure 7 F), where two main peaks are detected, one at 5 h (middle exponential growth phase) and another at 10 h (stationary growth phase). These peaks of expression correlate with the mutants' acetate uptake profiles. This behaviour suggests the existence of an unknown regulatory system at the transcriptional and/ or translational level connecting the expression of these two genes.

Overall, the differences found among the four strains lead us to postulate distinct physiological roles played by the two transporters when cells are grown in high glucose concentrations, with YaaH being more active at the exponential growth phase, while ActP is most active in the entry to stationary growth phase, as previously postulated by Gimenez *et al.* (2003).

YaaH as a succinate transporter

The range of YaaH transporter substrates was determined in the strain *E. coli* $\Delta yaaH \Delta actP$ transformed with pSVA9 plasmid, by adding non-labelled substrates (30 mM) to the reaction mixture containing labelled acetic acid, 0.3 mM, pH 6.0. Boric, oxalic, pyruvic, lactic, malic and citric acid had no inhibitory effect on the uptake of acetate (not shown). However, an inhibitory effect, higher than 80 %, was found for formic, propionic, benzoic, salicylic and butyric acid (all monocarboxylic acids), as well as the dicarboxylate succinic acid. As can be seen in Figure 8 all these monocarboxylic acids behaved as non-competitive inhibitors of acetic acid uptake, possibly by affecting the binding site for acetic acid. A different result was found for succinic acid which behaved as a competitive inhibitor for acetate uptake by the YaaH transporter (Figure 8), where an alteration of the slope (K_m) of the plots is observed instead of an alteration on the V_{max} .

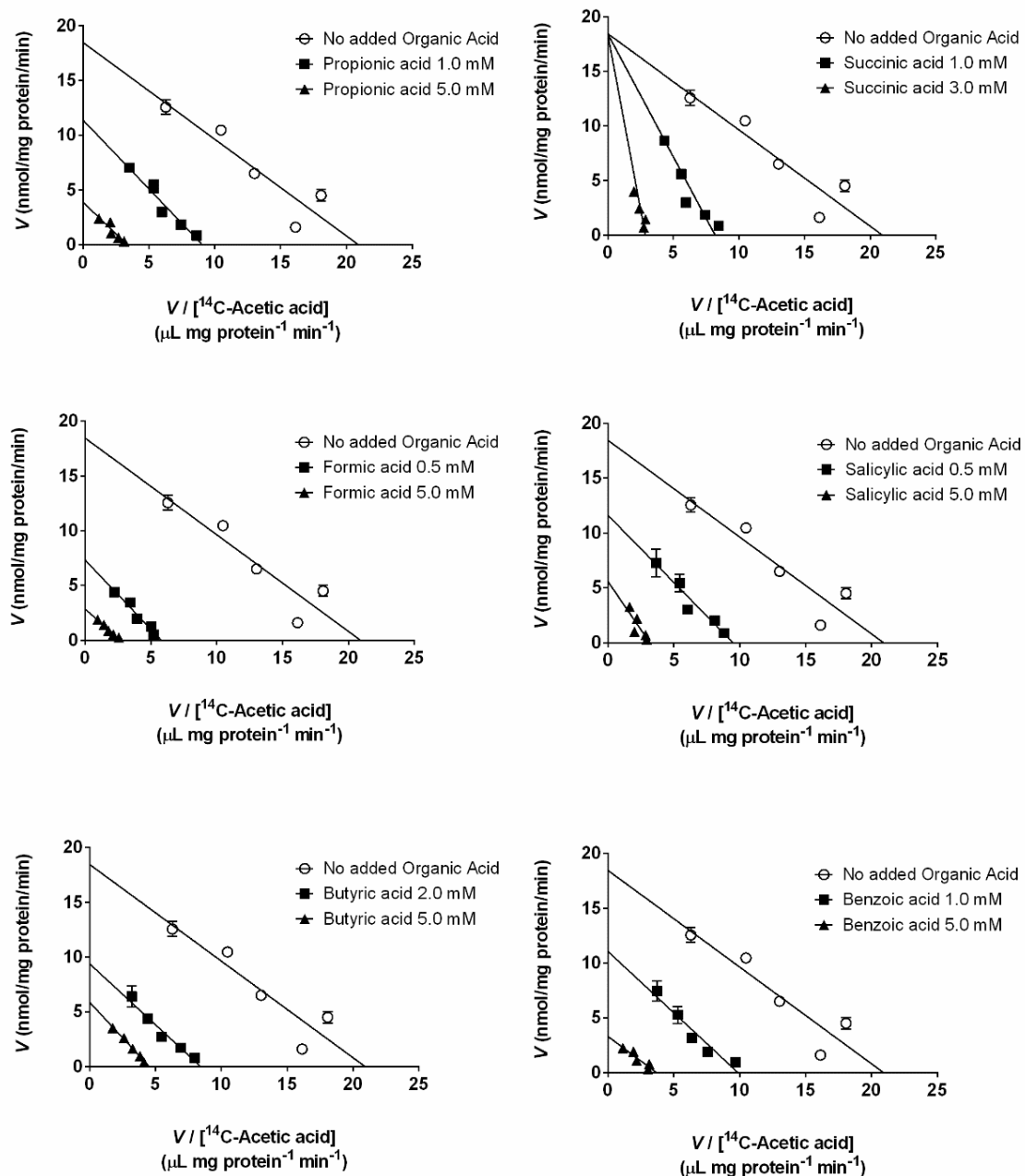


Figure 8 – Substrate specificity of the YaaH transporter. Eadie-Hofstee plots of initial uptake rates of [1-¹⁴C]-acetic acid, pH 6.0 in the absence (o) and in the presence (■, ▲) of non-labelled acids, at the concentration indicated in each plot. The cells were grown and collected as described in Figure 1 legend. Each data point represents the mean ± SD (n=6).

To confirm this observation the kinetic parameters for the initial uptake rates of [1,4-¹⁴C]-succinic acid were determined in cells of the double mutant transformed with pSVA9 plasmid (Figure 9), using as control the same strain transformed with pUC18 plasmid. In both strains labelled succinic acid exhibited a Michaelis-Menten kinetics with the following kinetic parameters: apparent K_m of 1.18 ± 0.10 mM succinic acid and apparent

V_{\max} values of 10.05 ± 0.34 nmol succinic acid mg protein⁻¹ min⁻¹ for pSVA9 transformants; apparent K_m of 2.19 ± 0.33 mM succinic acid and apparent V_{\max} of 5.50 ± 0.43 nmol succinic acid mg protein⁻¹ min⁻¹ for pUC18 transformants. This data suggests that YaaH plays a role as a succinic acid transporter.

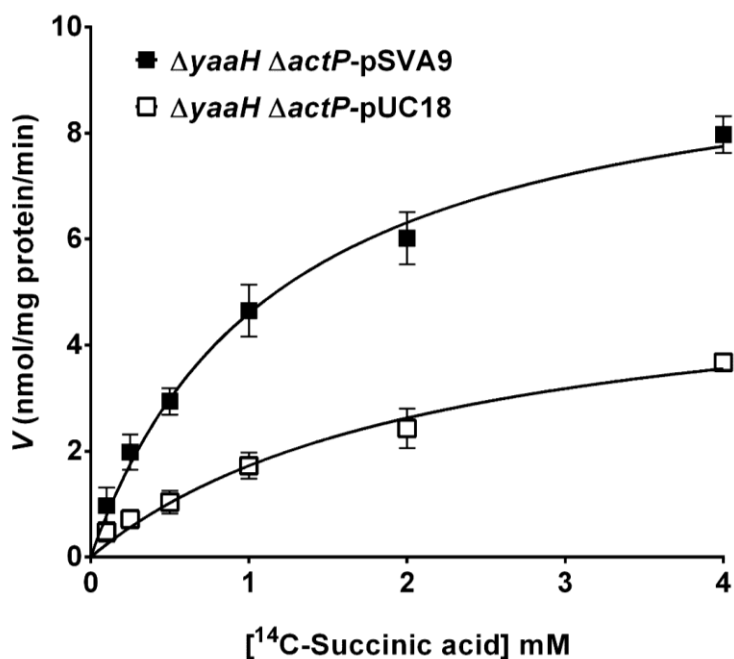


Figure 9 – Succinic acid kinetics of the YaaH transporter. Initial uptake rates of [1,4-¹⁴C]-succinic acid, pH 6.0 as a function of the acid concentration in *E. coli* $\Delta yaaH \Delta actP$ cells transformed with the plasmid pSVA9 (■). As control the same strain was transformed with the pUC18 plasmid (□). The cells were grown and collected as described in Figure 1 legend. Each data point represents the mean \pm SD (n=6).

To further elucidate the functional role of YaaH in succinate uptake, the concentration of succinic acid was measured in the extracellular media from experiments described in Figure 7. In all strains succinic acid appeared as a minor sub-product during growth in glucose, but two distinct profiles were observed among the four strains studied (not shown). A sole peak of 10 ± 0.5 mg/L of succinic acid was detected in the samples collected at 10 h of growth both in the wild type and $\Delta actP$ strains. However, in the strains $\Delta yaaH$ and $\Delta yaaH \Delta actP$ 14 ± 0.7 and 16 ± 0.8 mg/L of succinic acid were found at 9 h and 10 h of growth, respectively. The highest levels of succinic acid found for the $\Delta yaaH$ deleted strains, both single and double mutant, are consistent with a decrease of succinate import due to the absence of the YaaH protein.

Two single residue mutations change the specificity in YaaH

Two single-nucleotide mutations (C755G/Leu219Val and C655G/Ala252Gly) in the yeast *Ady2* promote a change in substrate specificity of this transporter allowing an efficient utilization of lactic acid (Kok *et al.*, 2012) so we asked whether these residues could behave as in its bacteria homologue. The equivalent residues were identified based on the alignment between YaaH and *Ady2* using ClustalW2 (Goujon *et al.*, 2010) (Figure 10 A) and the two mutants (Leu131Val and Ala164Gly) were obtained by site-directed mutagenesis in the pSVA9 plasmid.

The YaaH alleles were tested for the uptake of labelled D,L-[U-¹⁴C]-lactic acid, pH 5.0 (Figure 10 B) and as expected, both substitutions improved the affinity and capacity of the acid uptake. The kinetic parameters estimated from the plots shown in Figure 10 B revealed an apparent K_m of 4.15 ± 0.59 mM lactic acid for the wild type, 2.88 ± 0.45 mM lactic acid for Ala164Gly and the highest affinity detected for the Leu131Val mutant with an apparent K_m of 1.97 ± 0.25 mM lactic acid. The transport capacity in both mutants was also increased, with the following apparent V_{max} (nmol lactic acid.min⁻¹.mg protein⁻¹): 10.15 ± 0.76 for pSVA9, 11.17 ± 0.82 for Ala164Gly, 14.25 ± 0.79 for Leu131Val. In both mutants lactic acid uptake was competitively inhibited by acetic and succinic acid, showing that these acids are still accepted by the YaaH transporter (Figure 10 C).

All these assays were performed on glucose grown cells, conditions where the *E. coli* lactate transporters (*lldP* and *glcA*) are down regulated, thus the level of lactic acid transport detected in cells transformed with the empty pUC18 plasmid (○, Figure 8 B) is only basal.

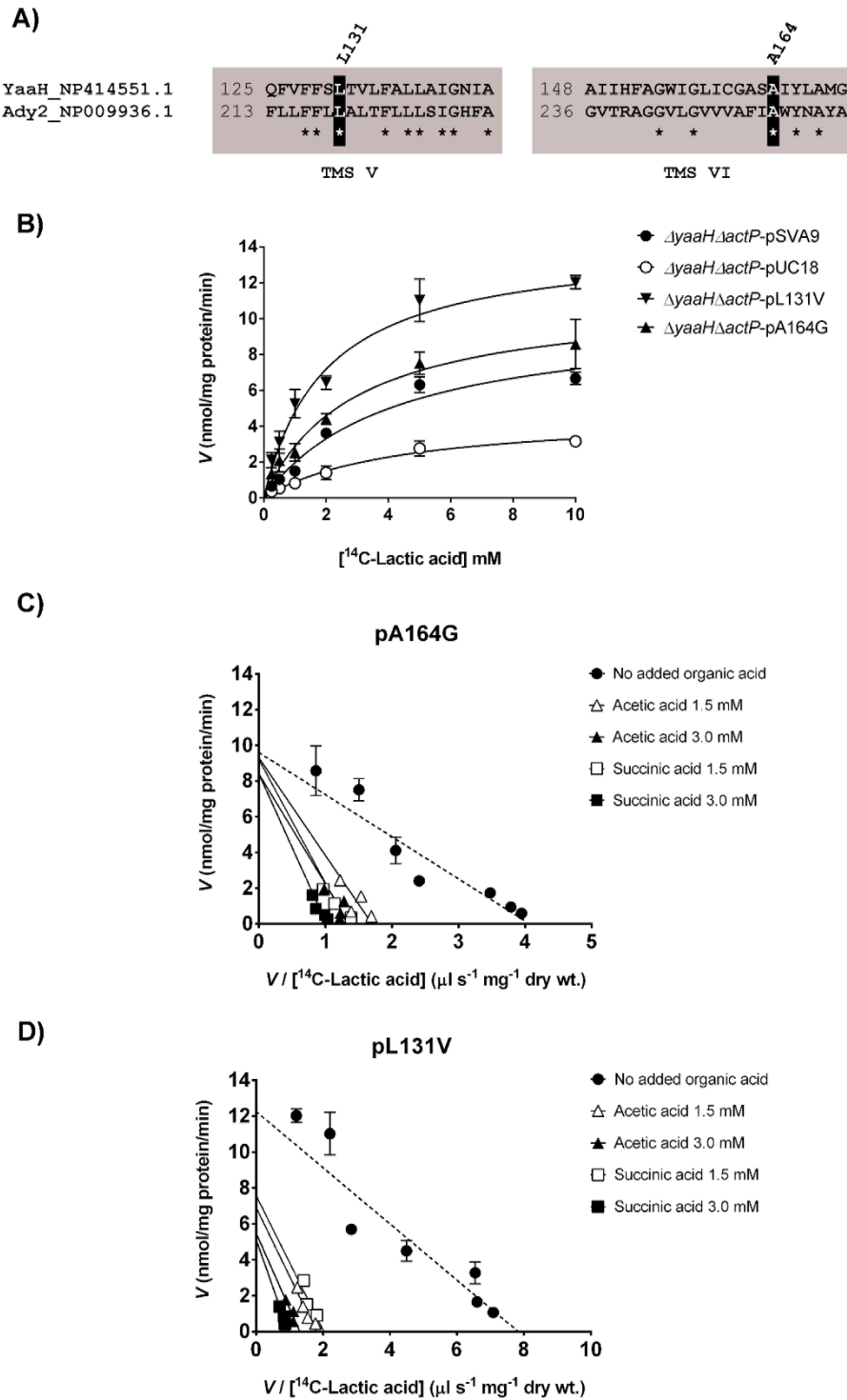


Figure 10 – Site-directed mutagenesis of the *yaaH* gene. (A) Predicted transmembrane segments V and VI of YaaH (<http://www.cbs.dtu.dk/services/TMHMM/>) aligned with Ady2 using ClustalW2. The conserved residues are marked with a star (*) and the residues mutated in this work are highlighted in black boxes. (B) Initial uptake rates of D,L-[U-¹⁴C]-lactic acid, pH 5.0 as a function of the acid concentration. Strains of *E. coli* $\Delta yaaH \Delta actP$ transformed with plasmids pSVA9 (●), pA164G (▲) or pL131V (▼). As a control, the same strain transformed with the pUC18 plasmid was used (○). (C) Eadie-Hofstee plot of the initial uptake rates of D,L-[U-¹⁴C]-lactic acid, pH 5.0 in the absence (●) and in the presence (■, □, ▲, △) of non-labelled acetic and succinic acid, at the concentration indicated in each plot in cells transformed

with pA164G (D) Eadie-Hofstee plot of initial uptake rates of [¹⁴C]-lactic acid, pH 5.0 in the absence (●) and in the presence (■, □, ▲, △) of non-labelled acetic and succinic acid, at the concentration indicated in each plot in cells transformed with pL131V. Cells were grown and collected as described in Figure 1 legend. Each data point represents the mean ± SD of 3 independent experiments (n=6).

Discussion

YaaH is an acetate/proton symporter

In this work we demonstrate that acetate transport in *E. coli* occurs via, at least, two distinct proteins: ActP, a member of the Solute:Sodium Symporter (SSS) Family (TCDB # 2.A.21, www.tcdb.org) and YaaH, a member of the AceTr Family (TCDB # 2.A.96), here characterized. Our data fully agrees with the previous work of Wagner *et al.* (1972) reporting the presence of two separate processes for acetate transport that to our knowledge are, most probably, associated with the ActP and YaaH proteins.

The single mutants on the genes *yaaH* and *actP* revealed a partial reduction in acetate uptake when compared with the wild type strain while the double mutant displays a significant reduction, indicative of separate roles for YaaH and ActP in acetate transport activity. Additionally, the level of acetate uptake activity in $\Delta yaaH \Delta actP$ cells, expressing *yaaH* gene in *trans*, fully agrees with its role as a transporter. When *yaaH* is expressed in a low copy number plasmid, a lower apparent V_{max} was found when compared to the one observed for the wild type since the *actP* gene is missing. However, as expected, when using the high copy number plasmid there was an increase in the acetate uptake, associated with the overexpression of the YaaH protein. A 50 % increase in activity is quite significant since overexpressed membrane proteins have to be accommodated at the plasma membrane, limiting the level of maximum activity.

The basal level of acetate uptake found in the double mutant $\Delta yaaH \Delta actP$ (Figure 1) can be attributed either to the existence of other transporters or to the simple diffusion of the undissociated form of the acid across the plasma membrane. It is commonly accepted that the undissociated form of the acid enters bacteria mostly by diffusion (Baronofsky *et al.*, 1984) while the dissociated form needs assistance from acetate carrier systems (Warnecke and Gill, 2005). As our assays were carried out at pH 6.0, and taking into account the pK_a of acetic acid (4.74), only 5.44 % of the acid is in its lipid-soluble (uncharged) form. Since the acid is mostly in the dissociated form, passive diffusion is limited by its solubility and

permeability (Walter and Gutknecht, 1984; Salmond *et al.*, 1984; Baronofsky *et al.*, 1984). Acetate uptake in glucose-grown cells of the double mutant $\Delta yaaH \Delta actP$ follows a saturable kinetics in a pH ranging from 5.0 to 7.0 (not shown) with similar kinetic parameters found for $\Delta yaaH \Delta actP$ transformed with pUC18 (Figure 3). Overall, our data suggests that the existence of other yet unidentified acetate transporter(s) in *E. coli* cannot be ruled out.

The YaaH acetate uptake activity was optimal at pH 6.0 with decreasing activity both at more acidic and alkaline pH values. This observation further strengthens our hypothesis about the minor role that passive diffusion plays on acetate influx in the conditions analysed. If the undissociated acid was permeating the membrane mostly by simple diffusion, decreasing the pH would increase the acid influx due to an increase in the relative amount of the undissociated acid, but this increase in uptake was not observed. Furthermore, the inhibition of acetate transport by the uncoupler CCCP in the $\Delta yaaH \Delta actP$ transformed with pSVA9, indicates that the driving force used by YaaH is the transmembrane electrochemical potential. The fact that this uncoupler had no effect on $\Delta yaaH \Delta actP$ cells carrying pUC18 demonstrates that CCCP, in the conditions and incubation times tested, had no other pleiotropic effects (Possot *et al.*, 1997; Wang *et al.*, 2010).

In summary, our results suggest that YaaH behaves as a secondary active acetate/proton symporter with an apparent K_m of 1.24 ± 0.13 mM acetic acid and an apparent V_{max} of 8.72 ± 0.37 nmol acetic acid mg protein⁻¹ min⁻¹, at pH 6.0, energetically dependent on the proton motive force, as many carboxylate transporters found in microorganisms (Núñez *et al.*, 2002; Hosie *et al.*, 2002; Gimenez *et al.*, 2003; Casal *et al.*, 2008; Jolkver *et al.*, 2009).

YaaH is a succinic acid transporter

In contrast to what had been described for other family members (Casal *et al.*, 1996; Robellet *et al.*, 2008), the YaaH transporter in *E. coli* seems to be highly specific for acetic acid (a monocarboxylic acid) and for succinic acid (a dicarboxylic acid). It had been reported that *E. coli* cells lacking the known aerobic and anaerobic C4-dicarboxylate carriers (DctA, DcuA, DcuB, DcuC, and DcuD or CitT) still display ability to aerobically grow on succinate at pH 6.0, by expressing a different succinic acid carrier (Janausch *et al.*, 2001). The authors mentioned that such carrier was not specific for C4-

dicarboxylates, displaying also low affinity for monocarboxylates, such as propionate, butyrate and acetate. A recent study in *E. coli* reported that in succinic acid aerobically grown cells, two succinate transporters DctA and DauA co-exist, with DauA as the lower affinity and lower capacity transporter. The authors demonstrated that DauA is essential for the expression and activity of DctA, with DctA as the main transporter at pH 7.0 and DauA at pH 5.0 (Karinou *et al.*, 2013). The mutants $\Delta dauA$ at pH 5.0 and $\Delta dctA$ at pH 7.0, grown in succinate, display residual succinic acid transport activity pointing to the presence of a very low affinity uncharacterized transporter (Karinou *et al.*, 2013). Our finding that YaaH is able to transport succinic acid with a lower apparent K_m (1.18 ± 0.10 mM succinic acid, at pH 6.0) compared to the ones found for the above mentioned transporters, can contribute to fill this gap. Furthermore, YaaH only recognizes succinate, and does not accept other C4-dicarboxylates, a feature that is in good agreement with the literature (Janausch *et al.*, 2001).

Taking into account the role of the YaaH protein in acetic and succinic acid uptake, we propose a new nomenclature for this permease, SatP, a Succinate-Acetate Transporter Protein.

L131V and A164G change the specificity of YaaH

The yeast homologue of YaaH is Ady2, a monocarboxylate/proton symporter, shared by acetate, propionate, lactate and formate, whose expression is repressed by glucose (Casal *et al.*, 1996; Paiva *et al.*, 2004; Pacheco *et al.*, 2012). By direct evolution for growth in lactic acid two mutant alleles Leu219Val and Ala252Gly were identified in Ady2 (Kok *et al.*, 2012). We wondered if the corresponding mutations in YaaH, Leu131Val and Ala164Gly (Figure 10 A), would lead to a gain of function for lactic acid uptake. It is known that the uptake of lactate in *E. coli* is mediated by two distinct proton symporters: the L-lactate permease (*lldP*) and the glycolate permease (*glcA*) (Núñez *et al.*, 2002). These transporters are repressed in glucose (Matin and Konings, 1973) thus only a basal level of lactic acid uptake was detected in the conditions used in the present work for the control strain ($\Delta yaaH \Delta actP$ transformed with pUC18). Glucose grown cells of $\Delta yaaH \Delta actP$ expressing the *yaaH* mutant alleles L131V and A164G display an enhanced affinity and capacity for lactic acid revealing an acquired ability to transport this substrate compared with the wild type allele. Despite the distinct range of substrates of YaaH and Ady2 they share common molecular traits regarding the substrate binding site since

mutations in conserved amino acid residues lead to similar physiological behaviour, as we have shown for the gain of function for lactic acid uptake.

YaaH and the acetate switch

In the present work we addressed the physiological relevance of the existence of two acetate carriers ActP and YaaH by following their activity along aerobic growth in glucose minimal media. When *E. coli* is grown aerobically in glucose as the carbon source a rapid growth phase is observed, with the consumption of the sugar and the excretion of acetate. This is followed by a slower growth phase with a switch to the use of the excreted acetate as a source of carbon and energy (Wolfe, 2005). The formation of acetate depends primarily on the PTA-ACKA pathway with PTA (acetyl-CoA transferase) reversibly converting acetyl-CoA and inorganic phosphate to acetyl~P and coenzyme A while ACKA (acetate kinase) reversibly converts acetyl~P and ADP to acetate and ATP (for a review see Wolfe, 2005). YaaH functions primarily during the exponential phase of growth prior to the acetate switch.

When the carbon flux exceeds the capacity of the central metabolic pathways, acetate is assimilated by acetyl-CoA synthetase (*acs*), which activates acetate to acetyl-CoA with the concomitant conversion of ATP to AMP and pyrophosphate (Brown *et al.*, 1977; Kumari *et al.*, 2000). Acetyl-CoA can be used in the tricarboxylic acid cycle via the glyoxylate bypass (Cozzzone, 1998). ActP seems to be involved in this step being responsible for the reutilization of acetate, scavenging micromolar concentrations of this compound (Gimenez *et al.*, 2003). This idea was reinforced in this work by showing a more active role of this permease at the stationary phase after the acetate switch. Furthermore, previous work has shown that transcription of the *acs-yjcH-actP* operon is low in the presence of glucose excess due to low cAMP levels that regulate this operon (Beatty *et al.*, 2003) and that *acs* transcription increases with extracellular acetate formation (Kumari *et al.*, 2000). This is in accordance to what was observed for *actP* expression that increased at the entry into stationary phase.

YaaH in acetate assimilation

We have shown that cells' ability to assimilate acetic acid is not strictly dependent on either YaaH or ActP activity. As shown in Figure 5, wild type and deleted mutant strains were able to grow over a range of concentrations varying from 1.67 to 83.3 mM acetic

acid, as sole carbon and energy source at pH 6.0. Both YaaH and ActP display a functional role at the highest concentrations, followed by an increased level of expression, with a peak for both genes at 66.7 mM acetic acid. These are evidences for the role of these transporters in acetate assimilation allowing cells to better control the uptake of the acid, in particular at very high concentrations.

Acetate-metabolizing cultures of *E. coli* are particularly relevant for the biotechnology industry since the accumulation of acetate in the extracellular medium poses an obstacle to high cell density cultivation and protein production (Eiteman and Altman, 2006; Collins *et al.*, 2013). Acetate toxicity and growth inhibition can be attributed to an acidification of the cytoplasm. It has been assumed that acetate excretion into the environment is a problem due to the lipophilic nature of the undissociated form that can permeate membranes, uncoupling the transmembrane pH gradient and becoming highly toxic (Salmond *et al.*, 1984; Baronofsky *et al.*, 1984; Luli and Strohl, 1990; Shin *et al.*, 2009). However, acetate seems to have only a small effect on the decrease of the intracellular pH and therefore the growth inhibition is possibly not only correlated to the acidification of the intracellular medium (Salmond *et al.*, 1984) but rather to a complex result of the anion balance of the cell (Roe *et al.*, 1998). Although not crucial for cells to grow on glucose or acetic acid, YaaH and ActP contribute to the acetate-succinate intracellular balance. Acetate transporters might be future targets for improving existing protein expression systems as *E. coli* is one of the most important microorganisms for biotechnological applications where acetate represents a major unwanted by-product.

References

- Ansaldi M., Lepelletier M., and Méjean V. (1996) Site-specific mutagenesis by using an accurate recombinant polymerase chain reaction method. *Anal Biochem* **234**: 110–1
- Arraiano C.M., Yancey S.D., and Kushner S.R. (1988) Stabilization of discrete mRNA breakdown products in *ams pnp rnb* multiple mutants of *Escherichia coli* K-12. *J Bacteriol* **170**: 4625–33
- Augstein A., Barth K., Gentsch M., Kohlwein S.D., and Barth G. (2003) Characterization, localization and functional analysis of Gpr1p, a protein affecting sensitivity to acetic acid in the yeast *Yarrowia lipolytica*. *Microbiology* **149**: 589–600

- Baronofsky J.J., Schreurs W.J., and Kashket E.R. (1984) Uncoupling by Acetic Acid Limits Growth of and Acetogenesis by *Clostridium thermoaceticum*. *Appl Environ Microbiol* **48**: 1134–9
- Beatty C.M., Browning D.F., Busby S.J.W., and Wolfe A.J. (2003) Cyclic AMP receptor protein-dependent activation of the *Escherichia coli* *acsP2* promoter by a synergistic class III mechanism. *J Bacteriol* **185**: 5148–57
- Boronat a and Aguilar J. (1979) Rhamnose-induced propanediol oxidoreductase in *Escherichia coli*: purification, properties, and comparison with the fucose-induced enzyme. *J Bacteriol* **140**: 320–6
- Brown T.D., Jones-Mortimer M.C., and Kornberg H.L. (1977) The enzymic interconversion of acetate and acetyl-coenzyme A in *Escherichia coli*. *J Gen Microbiol* **102**: 327–36
- Casal M., Cardoso H., and Leão C. (1996) Mechanisms regulating the transport of acetic acid in *Saccharomyces cerevisiae*. *Microbiology* **142** (Pt 6: 1385–90
- Casal M., Paiva S., Queirós O., and Soares-Silva I. (2008) Transport of carboxylic acids in yeasts. *FEMS Microbiol Rev* **32**: 974–94
- Collins T., Azevedo-Silva J., Costa A. da, Branca F., Machado R., and Casal M. (2013) Batch production of a silk-elastin-like protein in *E. coli* BL21(DE3): key parameters for optimisation. *Microb Cell Fact* **12**: 21
- Cozzone a J. (1998) Regulation of acetate metabolism by protein phosphorylation in enteric bacteria. *Annu Rev Microbiol* **52**: 127–64
- Datsenko K. a and Wanner B.L. (2000) One-step inactivation of chromosomal genes in *Escherichia coli* K-12 using PCR products. *Proc Natl Acad Sci U S A* **97**: 6640–5
- Eiteman M. a and Altman E. (2006) Overcoming acetate in *Escherichia coli* recombinant protein fermentations. *Trends Biotechnol* **24**: 530–6
- Gentsch M., Kuschel M., Schlegel S., and Barth G. (2007) Mutations at different sites in members of the Gpr1/Fun34/YaaH protein family cause hypersensitivity to acetic acid in *Saccharomyces cerevisiae* as well as in *Yarrowia lipolytica*. *FEMS Yeast Res* **7**: 380–90
- Gimenez R., Nuñez M.F., Badia J., Aguilar J., and Baldoma L. (2003) The gene *yjcG*, cotranscribed with the gene *acs*, encodes an acetate permease in *Escherichia coli*. *J Bacteriol* **185**: 6448–55
- Goujon M., McWilliam H., Li W., Valentin F., Squizzato S., Paern J., and Lopez R. (2010) A new bioinformatics analysis tools framework at EMBL-EBI. *Nucleic Acids Res* **38**: W695–9
- Hanahan D. (1983) Studies on transformation of *Escherichia coli* with plasmids. *J Mol Biol* **166**: 557–80

- Hosie A.H.F., Allaway D., and Poole P.S. (2002) A Monocarboxylate Permease of *Rhizobium leguminosarum* Is the First Member of a New Subfamily of Transporters. *J Bacteriol* **184**: 5436–5448
- Janausch I., Kim O., and Uden G. (2001) DctA- and Dcu-independent transport of succinate in *Escherichia coli*: contribution of diffusion and of alternative carriers. *Arch Microbiol* **176**: 224–230
- Jolkver E., Emer D., Ballan S., Krämer R., Eikmanns B.J., and Marin K. (2009) Identification and characterization of a bacterial transport system for the uptake of pyruvate, propionate, and acetate in *Corynebacterium glutamicum*. *J Bacteriol* **191**: 940–8
- Karinou E., Compton E.L.R., Morel M., and Javelle A. (2013) The *Escherichia coli* SLC26 homologue YchM (DauA) is a C(4)-dicarboxylic acid transporter. *Mol Microbiol* **87**: 623–40
- Kok S., Nijkamp J.F., Oud B., Roque F.C., Ridder D., Daran J.-M. *et al.* (2012) Laboratory evolution of new lactate transporter genes in a *jen1Δ* mutant of *Saccharomyces cerevisiae* and their identification as *ADY2* alleles by whole-genome resequencing and transcriptome analysis. *FEMS Yeast Res* **12**: 359–374
- Kumari S., Beatty C.M., Browning D.F., Busby S.J.W., Simel E.J., Hovel-Miner G., and Wolfe A.J. (2000) Regulation of Acetyl Coenzyme A Synthetase in *Escherichia coli*. *J Bacteriol* **182**: 4173–4179
- Livak K.J. and Schmittgen T.D. (2001) Analysis of relative gene expression data using real-time quantitative PCR and the $2^{-\Delta\Delta C_T}$ Method. *Methods* **25**: 402–8
- Luli G.W. and Strohl W.R. (1990) Comparison of growth, acetate production, and acetate inhibition of *Escherichia coli* strains in batch and fed-batch fermentations. *Appl Environ Microbiol* **56**: 1004–11
- Matin a and Konings W.N. (1973) Transport of lactate and succinate by membrane vesicles of *Escherichia coli*, *Bacillus subtilis* and a *Pseudomonas* species. *Eur J Biochem* **34**: 58–67
- Núñez M.F., Kwon O., Wilson T.H., Aguilar J., Baldoma L., and Lin E.C.C. (2002) Transport of L-Lactate, D-Lactate, and glycolate by the LldP and GlcA membrane carriers of *Escherichia coli*. *Biochem Biophys Res Commun* **290**: 824–9
- Pacheco A., Talaia G., Sá-Pessoa J., Bessa D., Gonçalves M.J., Moreira R. *et al.* (2012) Lactic acid production in *Saccharomyces cerevisiae* is modulated by expression of the monocarboxylate transporters Jen1 and Ady2. *FEMS Yeast Res* **12**: 375–81
- Paiva S., Devaux F., Barbosa S., Jacq C., and Casal M. (2004) Ady2p is essential for the acetate permease activity in the yeast *Saccharomyces cerevisiae*. *Yeast* **21**: 201–10
- Palková Z., Devaux F., Icíková M., Mináriková L., Crom S. Le, and Jacq C. (2002) Ammonia pulses and metabolic oscillations guide yeast colony development. *Mol Biol Cell* **13**: 3901–14

- Possot O.M., Letellier L., and Pugsley a P. (1997) Energy requirement for pullulanase secretion by the main terminal branch of the general secretory pathway. *Mol Microbiol* **24**: 457–64
- Robellet X., Flippi M., Pégot S., Maccabe A.P., and Vélot C. (2008) AcpA, a member of the GPR1/FUN34/YaaH membrane protein family, is essential for acetate permease activity in the hyphal fungus *Aspergillus nidulans*. *Biochem J* **412**: 485–93
- Roe A.J., McLaggan D., Davidson I., O’Byrne C., and Booth I.R. (1998) Perturbation of anion balance during inhibition of growth of *Escherichia coli* by weak acids. *J Bacteriol* **180**: 767–72
- Rohlin L. and Gunsalus R.P. (2010) Carbon-dependent control of electron transfer and central carbon pathway genes for methane biosynthesis in the Archaeon, *Methanosarcina acetivorans* strain C2A. *BMC Microbiol* **10**: 62
- Rozen S. and Skaletsky H. (2000) Primer3 on the WWW for general users and for biologist programmers. *Methods Mol Biol* **132**: 365–86
- Salmond C. V, Kroll R.G., and Booth I.R. (1984) The effect of food preservatives on pH homeostasis in *Escherichia coli*. *J Gen Microbiol* **130**: 2845–50
- Schmittgen T.D. and Livak K.J. (2008) Analyzing real-time PCR data by the comparative CT method. *Nat Protoc* **3**: 1101–1108 .
- Shin S., Chang D., and Pan J.G. (2009) Acetate consumption activity directly determines the level of acetate accumulation during *Escherichia coli* W3110 growth. *J Microbiol Biotechnol* **19**: 1127–34
- Váchová L., Chernyavskiy O., Strachotová D., Bianchini P., Burdíková Z., Fercíková I. *et al.* (2009) Architecture of developing multicellular yeast colony: spatio-temporal expression of Ato1p ammonium exporter. *Environ Microbiol* **11**: 1866–77
- Viegas S.C., Pfeiffer V., Sittka A., Silva I.J., Vogel J., and Arraiano C.M. (2007) Characterization of the role of ribonucleases in *Salmonella* small RNA decay. *Nucleic Acids Res* **35**: 7651–64
- Wagner C., Odom R., and Briggs W. (1972) The uptake of acetate by *Escherichia coli* w. *Biochem Biophys Res ...* **47**: 1036–1043
- Walter a and Gutknecht J. (1984) Monocarboxylic acid permeation through lipid bilayer membranes. *J Membr Biol* **77**: 255–64
- Wang P., Kuhn A., and Dalbey R.E. (2010) Global change of gene expression and cell physiology in YidC-depleted *Escherichia coli*. *J Bacteriol* **192**: 2193–209
- Wang R.F. and Kushner S.R. (1991) Construction of versatile low-copy-number vectors for cloning, sequencing and gene expression in *Escherichia coli*. *Gene* **100**: 195–9
- Warnecke T. and Gill R.T. (2005) Organic acid toxicity, tolerance, and production in *Escherichia coli* biorefining applications. *Microb Cell Fact* **4**: 25
- Wolfe A.J. (2005) The acetate switch. *Microbiol Mol Biol Rev* **69**: 12–50

Ye J., Coulouris G., Zaretskaya I., Cutcutache I., Rozen S., and Madden T.L. (2012) Primer-BLAST: a tool to design target-specific primers for polymerase chain reaction. *BMC Bioinformatics* **13**: 134.

Chapter V

The fungal Ady2 homologue:
AcpA from *Aspergillus nidulans*

CHAPTER V

THE FUNGAL ADY2 HOMOLOGUE.

ACPA FROM *ASPERGILLUS NIDULANS*

Manuscript in preparation

Abstract

In *Aspergillus nidulans* AcpA is an acetate permease induced by ethanol and ethyl acetate necessary for the use of acetate as sole carbon source at low concentration in a high pH medium (Robellet *et al.*, 2008). In this work, we provide direct biochemical evidence that AcpA expression is activated in response to conidiospore germination, reaching the highest expression level at the time of germ tube emergence, and decreasing to low basal levels in germlings and young mycelium. AcpA expression is neither carbon or nitrogen catabolite repressed, nor the permease is inactivated at a post-transcriptional level. The substrate specificity of AcpA was further explored by standard transport competition assays and growth tests on toxic concentrations of carboxylic acids. Our results showed that AcpA can also mediate the uptake of propionate, as well as, of other short-chain monocarboxylic acids (benzoate, formate and butyrate), albeit with different transport capacities. Transport kinetic measurements and growth tests further showed that although ammonia increases moderately AcpA-mediated acetate uptake, AcpA is not involved in ammonia export, in contrast to what was hypothesised for its *S. cerevisiae* homologue.

Introduction

The genus *Aspergillus* is a diverse group of fungi that includes species classified as human and animal pathogens (e.g. *Aspergillus fumigatus*), as toxin-producing food contaminants (e.g. *Aspergillus flavus*), as producers of useful extracellular enzymes and organic acids (e.g. *Aspergillus niger*) or biotechnologically important secondary metabolites (e.g. *Aspergillus oryzae*) and as models for cellular processes (e.g. *Aspergillus nidulans*).

A. nidulans has been an important model system for the study of diverse biological questions. This species is easily maintained in laboratory conditions, reverse genetic approaches are easily used and several molecular tools are available (Scazzocchio, 2009). These assets have led to a better understanding of several metabolic and cellular processes through the analysis of growth phenotypes, genetic screens and metabolite uptake studies. In terms of life cycle (depicted in Figure 1), *A. nidulans* is homothallic but it may fuse to form a heterokaryon. The asexual cycle is maintained through differentiation of vegetative hyphae to produce spores (conidia) in conidiophores. It can also differentiate to produce sexual spores (ascospores) in sexual fruiting bodies (cleistothecia). Furthermore, *A. nidulans* also holds a parasexual cycle which occurs when haploid nuclei fuse in the heterokaryon (reviewed in Casselton and Zolan, 2002).

23 *Aspergillus* spp. (including *A. nidulans*, the prominent pathogens *A. fumigatus*, *A. flavus*, and the biotechnologically important *A. niger*; see <http://genome.jgi.doe.gov/programs/fungi/index.jsf> and <http://www.aspgd.org/>) have their genome sequenced and publically available allowing the comparison of carbon metabolism versatility between these filamentous fungi (Flipphi *et al.*, 2009). This comparison evidenced that primary metabolism in the *Aspergilli* has evolved by gene duplications, horizontal gene transfer or gene clustering, with some gene products having acquired new physiological functions, revealing an intrinsic complexity in fungal carbon metabolism (Flipphi *et al.*, 2009).

In comparison with bacteria or yeast, information on carboxylate transporters in filamentous fungi is scarce. A proper knowledge on carbon uptake and metabolism will allow to track changes in metabolism that accompany fungal infections and to improve the production of biotechnological interesting secondary metabolites (Hynes *et al.*, 2011). *A. nidulans* is not very selective in what concerns the abiotic growth conditions, being able to use a diversity of organic compounds as carbon sources including acetic acid and

ethanol (Armitt *et al.*, 1976). Ethanol is converted into acetate via the actions of alcohol dehydrogenase I (*alcA*) and aldehyde dehydrogenase (*aldA*). Acetate is then converted to acetyl-coA by the acetyl-coA synthetase (*facA*) which is further metabolized via the tricarboxylic acid cycle or the glyoxylate cycle (Figure 2) whereby acetyl-coA is converted to oxaloacetate which is used in gluconeogenesis (Todd *et al.*, 1998). Regulation occurs by the positive regulators of ethanol (*alcR*) and acetate (*facB*) utilization (Hynes *et al.*, 2006) and repression by the general carbon repression molecule *creA* together with metabolic changes (Georgakopoulos *et al.*, 2012).

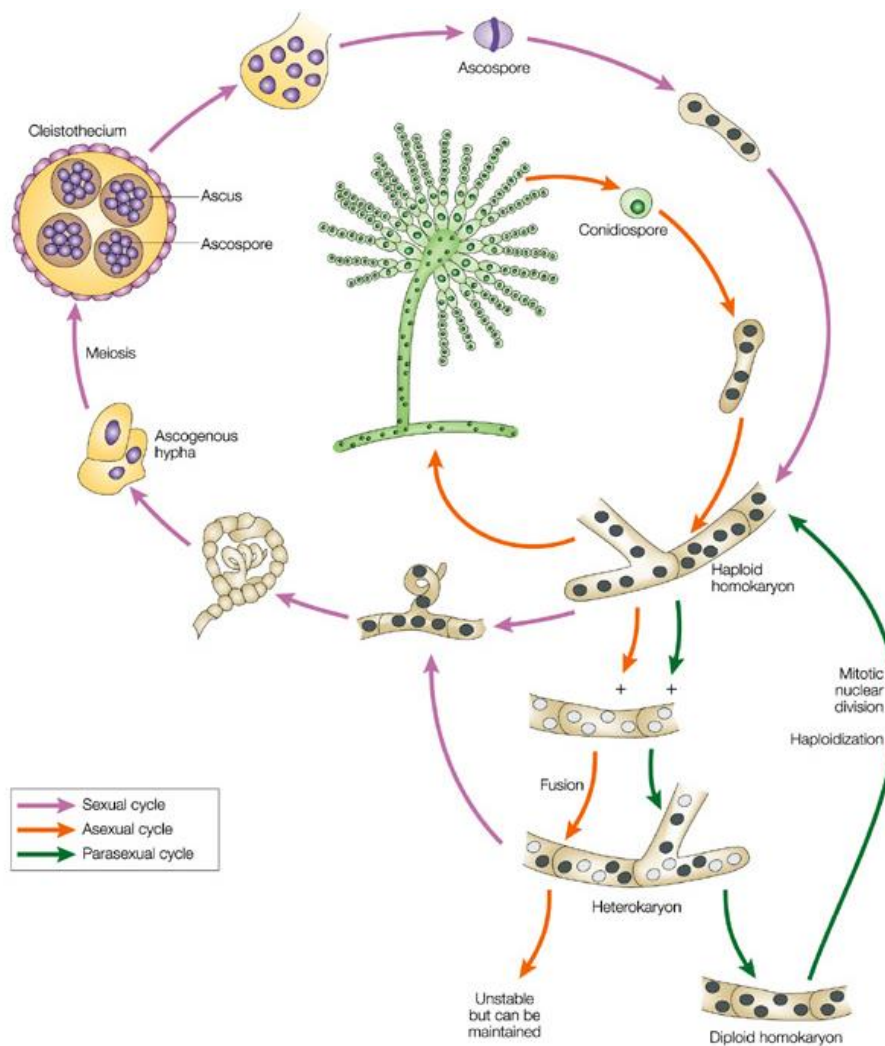


Figure 1 – *A. nidulans* life cycle. *A. nidulans* can undergo three life cycles: an asexual cycle where it produces conidia that germinate to form hyphae; a sexual cycle involving self- or out-crossing to generate cleistothecia containing ascospores that germinate to form hyphae or a parasexual cycle whereby hyphae fuse to form a heterokaryon followed by nuclear fusion to generate diploid homokaryons. (Adapted from Casselton and Zolan, 2002)

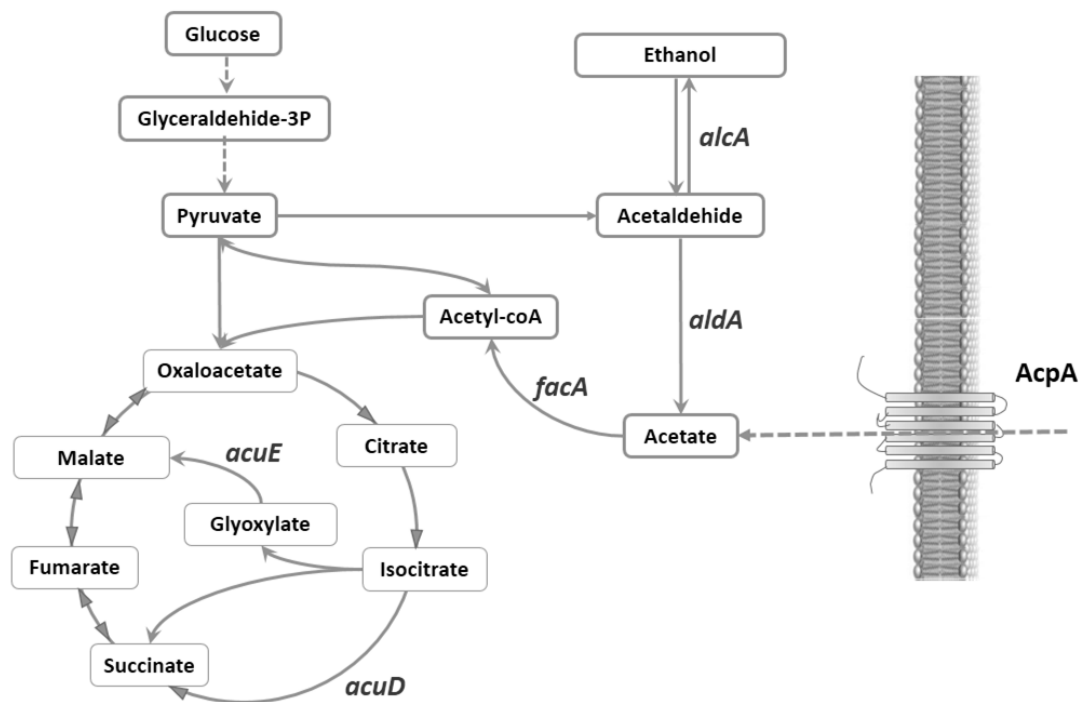


Figure 2 – Central carbon metabolism of *A. nidulans*. Only representative steps of glycolysis, tricarboxylic acid cycle, glyoxylate shunt and ethanol catabolism are represented. Dashed lines indicate more than one step involved in the conversion. *facA* (or *acuA*), acetyl-CoA synthase; *acuD*, isocitrate lyase; *acuE*, malate synthase; *alcA*, alcohol dehydrogenase; *aldA*, aldehyde dehydrogenase; *acpA*, acetate permease A.

Little is known on carboxylic acid transporters in *A. nidulans*. An anion selective channel (AnBEST1) permeable to citrate and, eventually, to a range of other organic ions including propionate and benzoate was identified in this filamentous fungus (Roberts *et al.*, 2011). AmcA, a member of the Monocarboxylate Transporter (MCT) family, was found to be induced at the transcriptional level by the monocarboxylates acetate, lactate and pyruvate playing a potential role in monocarboxylate transport and drug efflux (Semighini *et al.*, 2004). The AlcS protein from the Acetate Uptake Transporter (AceTr) Family was demonstrated to be located at the plasma membrane and highly induced by ethanol and repressed by glucose (Fillinger and Felenbok, 1996) although not involved in the transport of this molecule or of acetate and acetaldehyde (Flippini *et al.*, 2006). Another member of this family, AcpA, is the only characterized acetate transporter to date (Robellet *et al.*, 2008).

The acetate permease AcpA is essential for *A. nidulans* growth in media with low acetate concentrations and high pH values, conditions under which the protonated form of the acid is limited. Induction of the *acpA* gene by limiting concentrations of acetate and

propionate is under the control of the acetate catabolic pathway activator FacB although this is not the case at high acid concentrations. Expression of *acpA* is induced in the presence of several weak monocarboxylic acids such as glyoxylate, propionate, lactate, pyruvate and formate. Comparison of the acetate transport in gene-deleted strains and wild type *A. nidulans*, revealed its role as an acetate permease (Robellet et al, 2008).

The orthologue of AcpA in the yeast *Saccharomyces cerevisiae* is Ady2, which has been associated with the uptake of acetate, propionate, formate and lactate (Casal *et al.*, 1996; Paiva *et al.*, 2004; Pacheco *et al.*, 2012). This protein is also putatively involved in ammonia export (Palková *et al.*, 2002, Váchová *et al.*, 2009) since the null mutant has a reduced ammonia production when cells are growing in colonies (Palková *et al.*, 2002). Also, an Ady2-GFP fluorescence signal is observed at the plasma membrane upon ammonia release (Váchová *et al.*, 2009).

The present chapter focus on the characterization of AcpA in what concerns to its specificity, development and putative role in ammonia export. Furthermore a strategy for structure characterization is devised in the fungal and bacterial characterized members of the Acetate Uptake Transporter (AceTr) Family.

Experimental Procedures

Media, Strains, Growth Conditions, and Transformation Genetics

Standard complete (CM) and minimal media (MM) for *A. nidulans* were based on those described by Cove (1966). Nitrogen sources were used at the final concentrations of 5 mM urea or 10 mM ammonium tartrate. Carbon sources were used at the final concentrations of 1 % (w/v) glucose or other carbon sources in the concentrations specified in figure legends. CM was used for strain maintenance and MM for growth tests and uptake assays. The pH of all media was adjusted to 6.8 before autoclaving. Strains were cultured at 37 °C unless otherwise stated. To characterize *acpA*, two strains obtained from Christian Vélot (Robellet *et al.*, 2008) were used: ***acpA*Δ** (*pabaA1*, *panB100*, *riboB2*; *Tr. ΔacpA::panB*) and ***acpA*⁺** (*pabaA1*, *panB100*, *riboB2*; *Tr. panB*).

Transport assays

[1-¹⁴C]-acetic acid uptake in *A. nidulans* was assayed in germinating conidiospores. Briefly spores scratched from a quarter of a plate are transferred to an Erlenmeyer with MM (pH 6.8; ratio 1:4) and incubated at 37 °C, 140 r.p.m., for 3-4 hours (polarity maintenance stage). Germinating conidiospores are then concentrated by centrifugation at 10⁷ conidiospores per 100 μL (Amillis *et al.*, 2004). 90 μL of the conidiospore suspension is transferred to microtubes and after 5 min of incubation at 37 °C, the reaction is started by the addition of radiolabelled substrate. Acetate uptake in response to time (30, 60, 90, 120, 180 seconds) was performed with 30 μM [1-¹⁴C]-acetate. Initial velocities were measured at 1 min of incubation with 30 μM of radiolabeled substrate. Acetate uptake in response to concentration was performed for 1 min at 0.025, 0.05, 0.1, 0.2, 0.5, 1.0, 2.0 mM concentrations of [1-¹⁴C]-acetate. The effect of inhibitors was assayed through the addition of non-labelled compounds to the radiolabeled mixture. Reactions were terminated with the addition of equal volumes of minimal medium containing 1000-fold excess of non-radiolabelled substrate. The reaction mixtures were centrifuged for 5 min at 16100 g, the pellet was resuspended by vortex in 1 mL of minimal media and centrifuged again for 5 min at 16100 g. The pellet was finally resuspended in 1 mL of scintillation liquid. Radioactivity was measured in a Packard Tri-Carb 2200CA liquid scintillation spectrophotometer with disintegrations per minute correction.

Background uptake values were corrected by subtracting values obtained in the simultaneous presence of 1000-fold excess of non-radiolabelled substrate. The H⁺-

uncoupler carbonylcyanide chlorophenylhydrazone (CCCP) was added at a final concentration of 30 μM for 10 min before initiating the uptake assay. All transport assays were carried out in at least three independent experiments, with three replicates for each concentration or time point. Standard deviation was $< 20\%$. Radiolabelled [^{14}C] acetate, sodium salt (59 mCi mmol^{-1}) was purchased from Amersham Biosciences, USA. The transport kinetics best fitting the experimental initial uptake rates and the kinetic parameters were determined by a computer-assisted non-linear regression analysis (using GraphPad Prism version 5.01 for Windows, GraphPad Software, San Diego California USA, www.graphpad.com).

In experiments investigating the effect of internally accumulated ammonium on [^{14}C]-acetate uptake (30 μM), cells were preloaded with non-radiolabelled ammonium for 5 min, 37 $^{\circ}\text{C}$, washed three times in ice-cold MM followed by radiolabelled acetate uptake measurements (Diallinas, 2013). Incubation with non-radiolabelled acetate was used as a control in this experiment. To investigate the efflux of methyl-ammonium, [^{14}C]-methylamine hydrochloride (20 μM), was allowed to accumulate for 5 min at 37 $^{\circ}\text{C}$, cells were washed three times with ice-cold MM and then loaded with 10 mM of non-labelled acetate and incubated for 5 min at 37 $^{\circ}\text{C}$, stopped on ice and washed again (Diallinas, 2013). Cells with not loaded with acetate were used as a control of efflux measurements. Radioactivity accumulated in the cells and in the supernatant was measured (Diallinas, 2013). Radiolabelled [^{14}C]-Methylamine hydrochloride (57 mCi/mmol) was obtained from Amersham Pharmacia Biotech.

Results and Discussion

Optimization of the conditions for AcpA activity characterization

A time assay was carried out for AcpA-mediated acetate uptake using isogenic *A. nidulans* *acpA* Δ and *acpA*⁺ strains. As can be seen in Figure 3, the initial uptake rate of labelled monocarboxylates was linear for at least 100 seconds for the wild type strain whereas no measurable uptake was found for the isogenic mutant *acpA* Δ . The time 60 s was the incubation time chosen for the transport assays performed in this work.

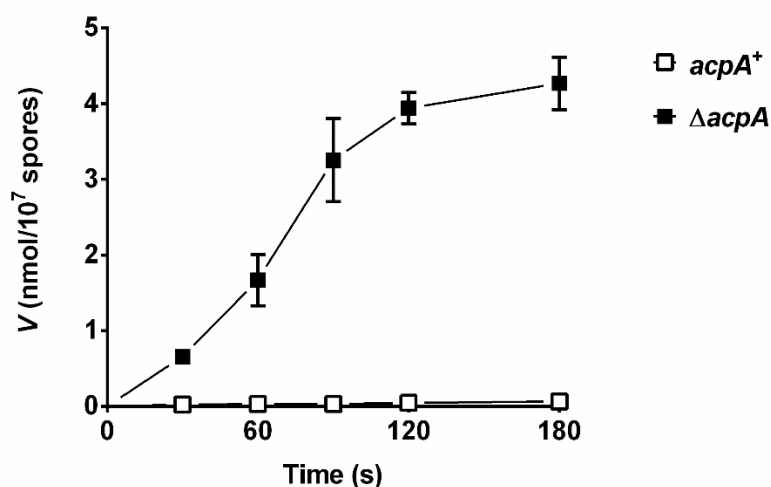


Figure 3 – Evaluation of the uptake of labelled acetate (30 μ M final concentration) in *A. nidulans* *acpA*⁺ and *acpA* Δ strains. Spores were cultivated in glucose for 4 hours and concentrated for the uptake assay as described in the experimental procedures.

Growth conditions were also optimized. Cells were grown in carbon repressing (glucose) and derepressing (fructose) conditions, and in nitrogen repressing (ammonium) and derepressing (urea) conditions. No significant difference was observed between glucose and fructose or between ammonium and urea (Figure 4 A). Furthermore, we also verified whether sodium acetate (0.1 %, w/v) induces AcpA expression or activation by growing cells in this carbon source. A significant decrease in labelled acetate uptake to approximately 40 % was observed (Figure 4 A), which might be due to the potential toxic effects of acetate as a carbon source. To verify the toxicity of acetic acid as a carbon source, acetic acid uptake measurements and cell viability were performed at two different time points (Figure 4 B). No significant differences were observed in cell viability between the different conditions (results not shown) therefore the differences

observed are in apparent uptake rates, and not due to a toxic effect of acetate at this concentration.

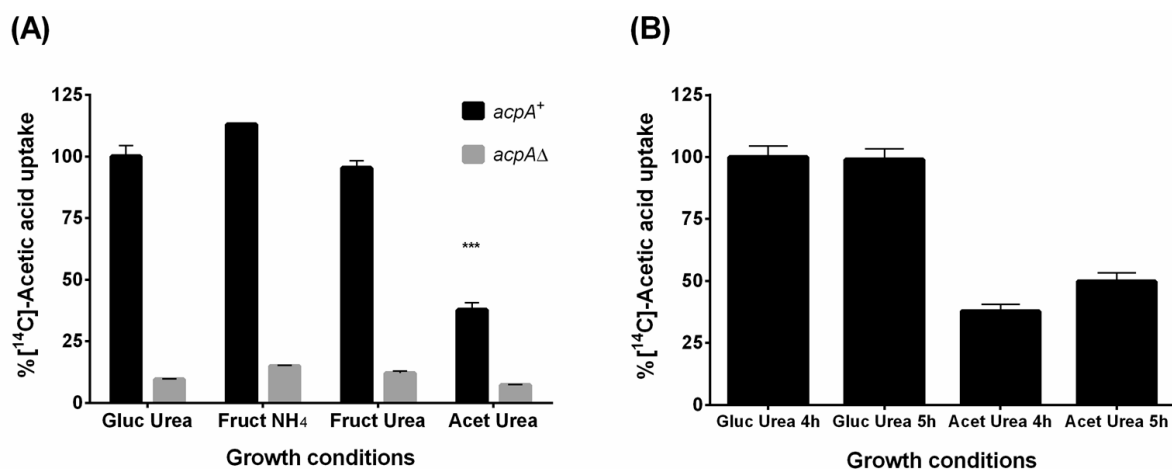


Figure 4 – Relative percentage uptake of labelled acetate in *A. nidulans* spores grown in different conditions. The graphics represent the percentage of the initial uptake in the several conditions considering that the initial uptake of cells grown on glucose and urea was 100 %. Each data point represents the mean \pm SD (n=6). Gluc – glucose; Fruct – fructose; NH₄ – ammonium; Acet – Sodium acetate 0.1 % (w/v).

We proceeded by further testing the nature of the acetate effect on AcpA, by adding acetate to glucose cultures. Cells were grown on glucose for 4 hours after which sodium acetate (0.1 %, w/v) was added to the cultures and uptake activity was monitored at 0, 1, 2 and 3 hours after this pulse of acetate (Figure 5). A clear induction effect was observed upon addition of acetate being the transport activity 10-fold higher after 2 hours of induction (Figure 5). No induction was found in *acpA*Δ cells suggesting that induction of AcpA acetate uptake activity is probably due to increasing transcriptional expression of the *acpA* gene, as described by Robellet and co-workers (2008) when acetate is added up to a concentration of 28 mM. Using acetate as the sole carbon source in cultures, on the other hand, has a negative effect (Figure 4). This can be caused by either a direct effect on permease activity or on protein levels (post-translational control) by a reduction in the number of AcpA molecules present in the membrane (degradation) or by a reduction in *de novo* made AcpA (direct sorting from the secretory compartments). Some yeast plasma membrane transporters are removed from the membrane in response to excess substrate such as Gap1 and Fur4 (reviewed in Haguenaer-Tsapis and André, 2004). UapA, an *A. nidulans* purine permease, was also shown to undergo substrate induced endocytosis

(Gournas *et al.*, 2010). This degradation elicited by the substrate is believed to avoid excess uptake of potentially toxic metabolites (Hicke and Dunn, 2003).

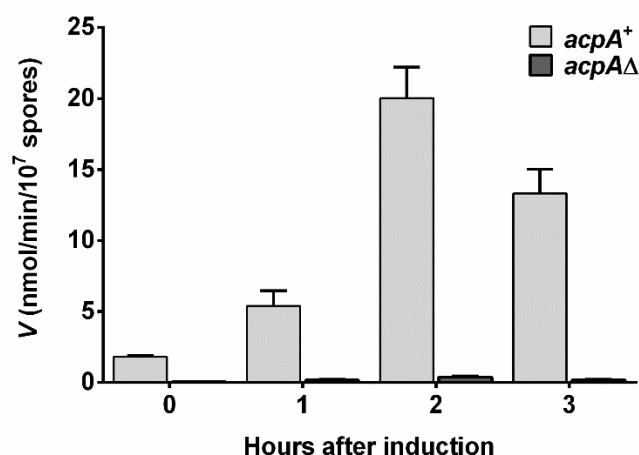


Figure 5 – Evaluation of the uptake of labelled acetate (30 μ M final concentration) in *A. nidulans* *acpA*⁺ and *acpA*Δ upon addition of acetate. Cells were cultivated in glucose for 4 hours, induced by the addition of 0.1 % (w/v) sodium acetate and collected at 0, 1, 2 and 3 hours after the pulse of acetate for the uptake assay. Each data point represents the mean \pm SD (n=6).

Based on these results, as the working conditions to measure the transport of acetic acid we chose to germinate spores in MM containing glucose as the carbon source and urea as the nitrogen source.

Kinetic characterization of AcpA

To determine acetate uptake kinetics, initial velocities were measured at 1 min of incubation with a range of concentrations from 0.025 to 2.0 mM of [1-¹⁴C]-acetic acid, pH 6.0, at the polarity maintenance stage (3 – 4 h, 130 r.p.m.). As can be observed in Figure 6, the initial uptake rates of [¹⁴C]-acetic acid, as a function of acetic acid concentration, in *acpA*⁺ revealed a Michaelis–Menten saturation kinetics with an apparent V_{\max} of 0.92 ± 0.02 nmol min⁻¹ 10⁷ spores⁻¹ and an apparent K_m of 0.15 ± 0.01 mM acetate. In *acpA*Δ cells acetate uptake was residual (Figure 6). The affinity constant value was in agreement with the one obtained previously by Robellet and colleagues (2008).

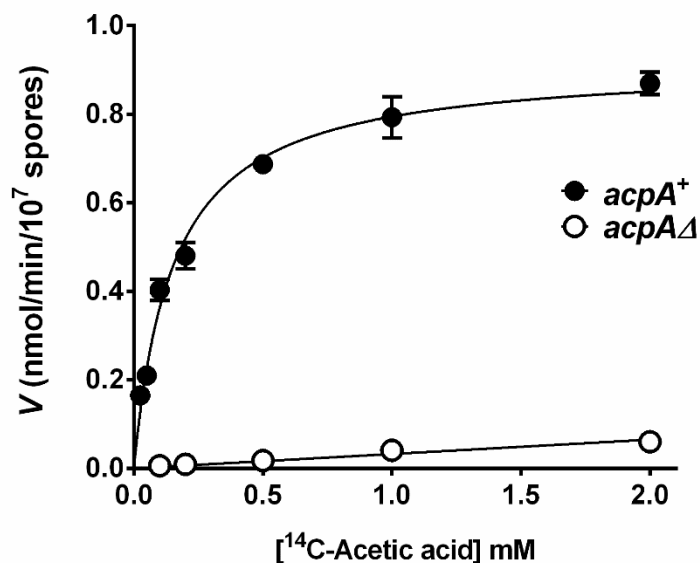


Figure 6 – Initial uptake rates of [¹⁴C]-acetic acid as a function of the acid concentration in *A. nidulans* *acpA*⁺ and *acpA*Δ cells. Cells were grown in glucose urea and collected at the polarity maintenance stage (3-4h). Each data point represents the mean ± SD (n=6).

Regarding the mechanism underlying the transport of acetate, a co-transport with protons appears to be involved since an inhibition of 95.2 % was observed when the uptake of labelled acetic acid was measured at pH 6.0, after incubation of *acpA*⁺ cells for 10 min with 30 μM of carbonyl cyanide m-chlorophenyl hydrazone (CCCP) which causes an uncoupling of the proton gradient (not shown). The effect of pH on the acetate transport activity associated with AcpA was measured in *A. nidulans* *acpA*⁺ and *acpA*Δ after growth in the standard working conditions (glucose, urea), in a pH range from 4.5 to 8.0. In the *acpA*Δ strain no difference was verified with the change in pH. In *acpA*⁺ the uptake was only affected in conidiospores grown at pH 4.5 which is below the p*K*_a of acetic acid (Figure 7), suggesting that the chemical species transported by AcpA is the dissociated form of the acid.

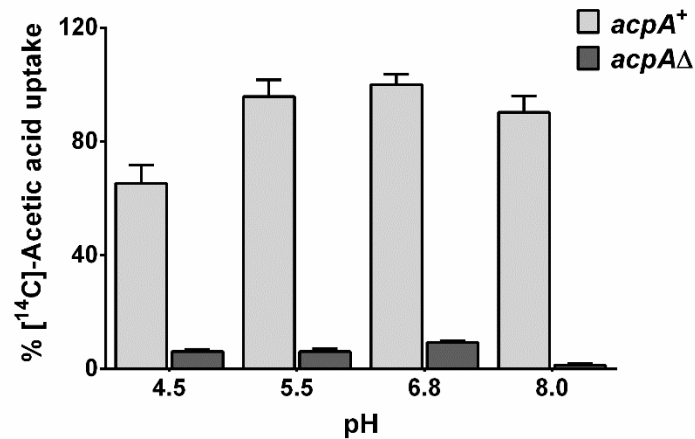


Figure 7 - Evaluation of the uptake of labelled acetate (30 μ M final concentration) in *A. nidulans* *acpA*⁺ and *acpA*Δ grown at the pH values indicated. Each data point represents the mean \pm SD (n=6).

Monitoring AcpA transport activity in response to germination and mycelium development

We studied the activity of the AcpA permease in germinating conidiospores, until young mycelia development. Germination was carried out in minimal media (MM), supplemented with urea as the sole nitrogen source and glucose (1 %, w/v) as the sole carbon source, at 37 °C, and acetate uptake was followed from 0 to 8 hours of germination. Low AcpA-mediated acetate uptake was present in resting conidiospores, in contrast to what has been reported for the majority of *A. nidulans* transporters specific for amino acids, purines or pyrimidines that show null levels of uptake in dormant conidia (Tazebay *et al.*, 1997; Amillis *et al.*, 2004). A significant increase in AcpA activity was recorded at the end of the isotropic growth phase (2 h of germination), and continued to increase until the onset of germ tube appearance (5 h). Immediately after that, AcpA activity diminished rapidly and dramatically in germlings and young mycelia (Figure 8). The activation of AcpA activity during the isotropic growth phase is in accordance with what was observed for other solute transporters in *A. nidulans*, which are also activated during germination. It has been shown that transporter activation during germination is developmentally controlled and serves a sensing mechanism for adapting uptake and metabolic systems the growth medium (Amillis *et al.*, 2004).

Interestingly, at 8 hours of germination acetate uptake activity increased also in the *acpA*Δ strain, suggesting that in young mycelia another acetate transporter is actively expressed. In the yeast *S. cerevisiae*, two transporters exist for acetate, Ady2, specific for acetate, propionate and formate, and Jen1, specific for lactate, propionate and acetate. We proceeded by testing whether a lactate-specific transporter, probably homologous to Jen1,

is also responsible for acetate uptake in *A. nidulans* mycelia. A blast search for Jen1 homologues in *A. nidulans* revealed two proteins (AN6703 and AN6095), with 39 and 30 % identities respectively, that are possible homologues of Jen1. AN6703 is annotated as a sugar transport and AN6095 as a carboxylic acid transporter, both from the MFS superfamily. Analysis of their sequences revealed the presence of the conserved sequence ³⁷⁹NXX[S/T]HX[S/T]QDXXXT³⁹¹ (Soares-Silva *et al.*, 2007) as well as the presence of other residues critical for function (Soares-Silva *et al.*, 2011). To analyse whether these two homologues of Jen1 are responsible for the acetate transport present in *acpAΔ*, we measured lactate transport activity in both *acpA*⁺ and *acpAΔ* strains after 4 or 8 h of germination. Our results showed that both strains had similar lactate transport rates (results not shown), suggesting that the lactate transporter(s) is not responsible for the low acetate transport activity in the mycelia of the *acpAΔ* strain.

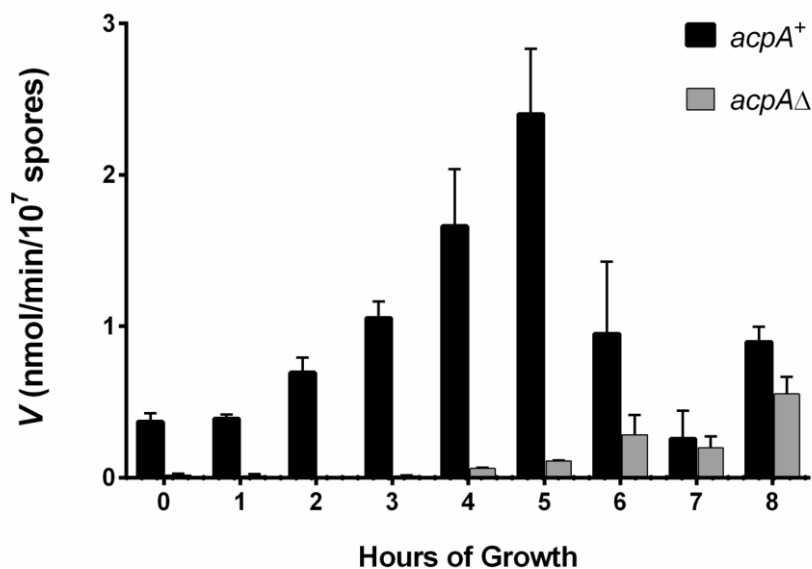


Figure 8 – Evaluation of the uptake of labelled acetate (30 μ M final concentration), in both *A. nidulans* *acpA*⁺ and *acpAΔ* strains. Cells were cultivated in glucose and urea and 10 mL of culture was removed at each time point for the uptake assay (described in the experimental procedures).

Specificity of the AcpA permease

In an attempt to elucidate the biological role of AcpA in *A. nidulans*, the corresponding gene deletion mutant and the wild type strain were grown on acetate and different carbon sources to verify the potential substrates of this permease. Previous studies showed that an *acpAΔ* mutant manifests a growth defect at a low acetate concentration (Robellet *et al.*, 2008). We confirmed this phenotype and further demonstrated that AcpA is essential

for acetate utilization at 37 °C, when acetate is the sole carbon source supplied (Figure 9). Additionally, we showed that AcpA contributes to acetate toxicity when spores are germinated in the presence of a rich carbon source, such as glucose at 25 °C. These two growth tests provided rigorous evidence that AcpA mediates acetate transport *in vivo*.

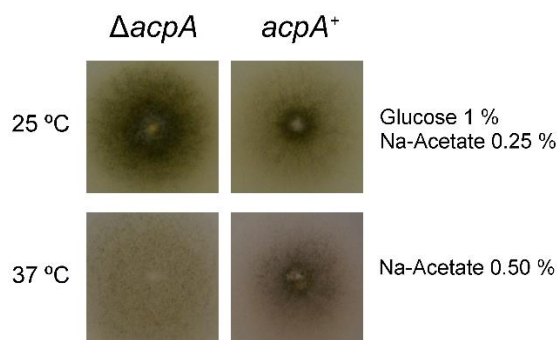


Figure 9 – The effect of acetate as a carbon source. Growth test of *A. nidulans acpA*⁺ and *acpA*Δ on minimal media supplemented with urea as the nitrogen source. Cells were grown on sodium acetate (Na-Acetate), 0.5 % (w/v), at 37 °C, for 4 days and on glucose 1 % (w/v) plus sodium acetate 0.25 % (w/v), at 25 °C, for 10 days.

The growth of *A. nidulans acpA*⁺ and *acpA*Δ cells was also analysed on minimal medium (MM) containing mono- and dicarboxylic acids as sole carbon sources grown at 37 and 25 °C. As shown in Figure 10, at 25 °C, which is the physiological temperature of *A. nidulans*, acetate is the only carbon source among those tested that supports relatively significant AcpA-dependent growth. A functional AcpA seems also to mediate stronger growth on malic and succinic acid, when compared to the *acpA*Δ mutant. In contrast, a functional AcpA led to increased toxicity of propionic, benzoic, lactic and butyric acid, in comparison with the *acpA*Δ mutant. Some of these acids (e.g. butyric, benzoic, acetic and propionic acid) are indeed known for their toxic effects in fungi, and therefore used as food preservatives (Brock and Buckel, 2004). At 37 °C, the growth differences between *acpA*⁺ and *acpA*Δ were much less prominent, but again AcpA seemed to confer stronger growth on acetic acid and succinic acid, and increased sensitivity in butyric acid. No growth was observed on boric and salicylic acids (results not shown), probably due to their toxicity at the conditions tested (10 mM, pH 5.0). The above picture suggests that, besides acetic acid, AcpA can also mediate the uptake of malic, succinic, butyric and propionic acids.

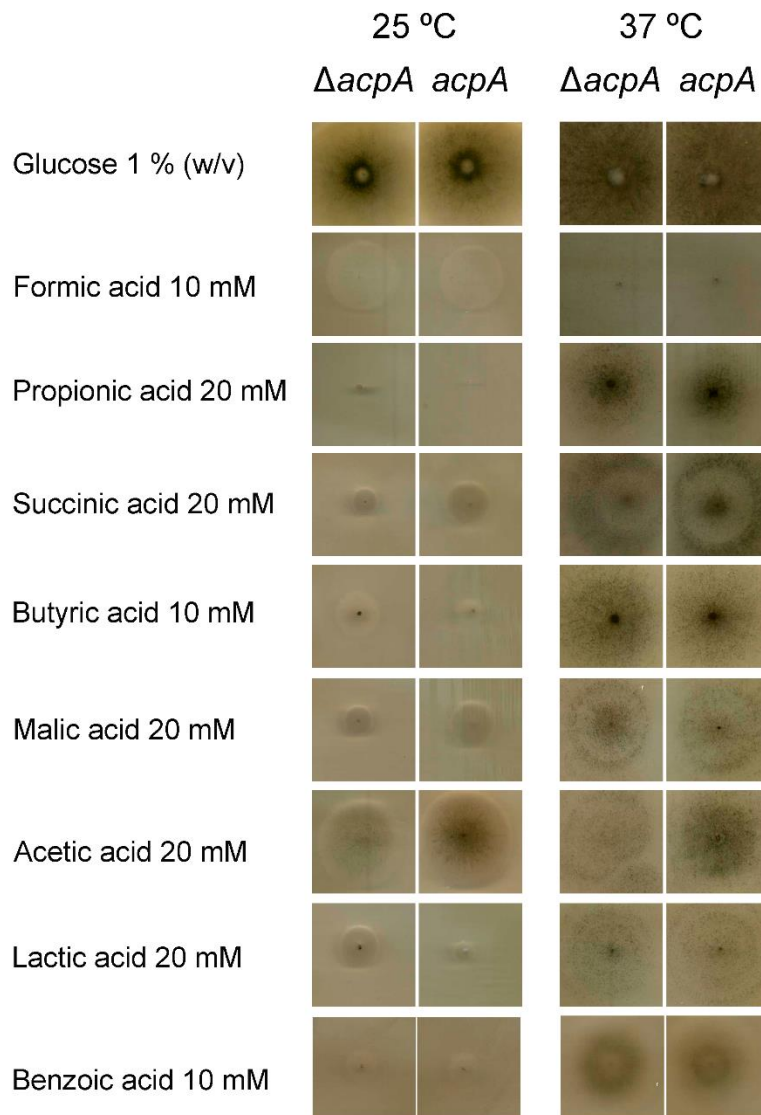


Figure 10 – Growth test of *acpA*⁺ and *acpA*Δ in minimal media supplemented with urea as the nitrogen source and several mono- and dicarboxylic acids as carbon sources (buffered at pH 5.0 except acetic acid which was buffered at pH 6.0, concentrations indicated in the figure). Growth on glucose (1 %, w/v) was used as a control in this experiment. Strains were grown for 3 days at 37 °C and for 7 days at 25 °C.

To characterize further the specificity of AcpA, both mono- and dicarboxylates, at 1000-fold excess, were tested for their capacity to inhibit AcpA-mediated uptake of labelled acetate. The monocarboxylates benzoic, formic, butyric and propionic acids inhibited the uptake of acetate by > 70% (Figure 11). On the other hand, the monocarboxylates salicylate, lactate and pyruvate as well as the dicarboxylates maleic, succinic, malic and oxalic acids, had no inhibitory effect on acetate uptake. Overall, these results point to a clear preference of AcpA for the binding of short-chain monocarboxylic acids. This result

is partially in agreement with growth test results at 37 °C (the temperature of the completion assays). A somehow paradoxical moderate up-effect (~130 % of the value obtained with no inhibitor) on acetate transport was observed in the simultaneous presence of excess malic, succinic and maleic acid. A similar observation was found previously with the UapA uric acid-xanthine transporter of *A. nidulans*, where the simultaneous presence of allopurinol led to an increased xanthine uptake. In that case, it was shown that allopurinol, was indeed a substrate of UapA, but follows a different mechanism and translocation trajectory compared to xanthine (Diallinas, 2013). A similar case might occur with AcpA in what concerns transport of some monocarboxylates, especially if we take into account the possible contribution of AcpA for a better growth on succinic and malic acid, in comparison with *acpAΔ* (Figure 10).

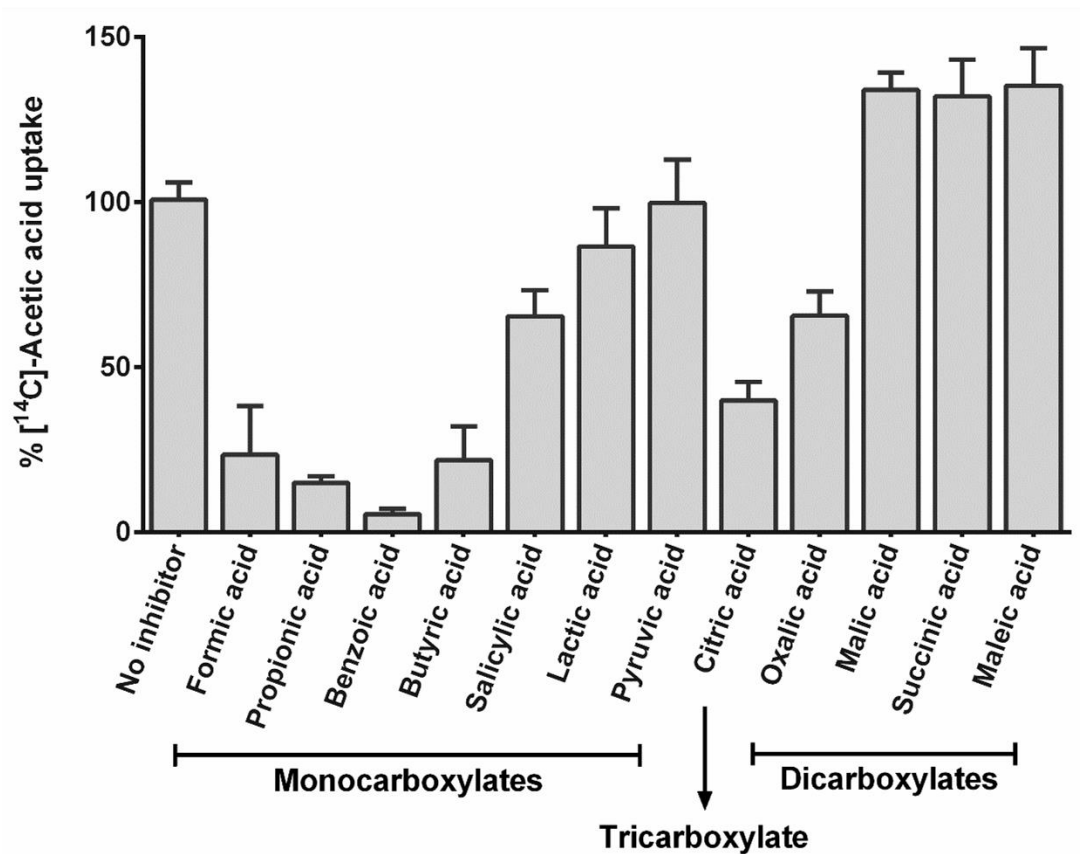


Figure 11 - Relative transport percentage of labelled acetate (30μM) in the presence of unlabelled inhibitors 1000-fold concentrated (30 mM) in *A. nidulans acpA⁺* grown on glucose urea and collected at the polarity maintenance stage. The graphic represents the percentage of acetic acid uptake of *acpA⁺* considering that the uptake in the absence of an inhibitor was 100%.

To further characterize AcpA, we estimated the K_i values for the monocarboxylates that inhibited acetate uptake (Table 1). Our results showed that AcpA binds all tested monocarboxylates, at concentration ranging from 1.44 to 16.89 mM, with the following affinity order: acetate > propionate > butyrate > formate > benzoate.

Table 1 – K_i values (mM) of AcpA for benzoate, butyrate, formate and propionate.

Inhibitor	K_i (mM)
Benzoic	16.89 ± 2.12
Butyric	9.25 ± 1.01
Formic	12.06 ± 3.29
Propionic	1.44 ± 0.13

We further wondered if propionic acid, the monocarboxylate with the K_i closest to the K_m for acetate was a competitive inhibitor of AcpA. The initial uptake rates of [14 C]-acetic acid were assessed in the presence of non-labelled propionic acid (Figure 12). From the results obtained we could not clearly depict the type of inhibition for propionic acid, since V_{max} decreased and K_m increased with propionate concentration increase.

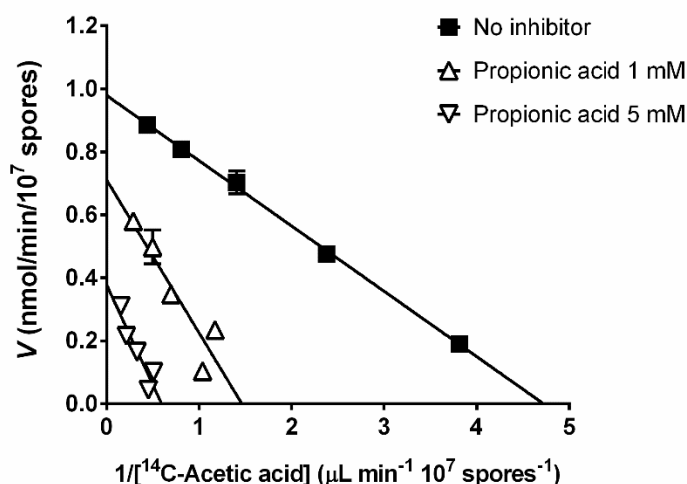


Figure 12 – Eadie-Hofstee plots of the initial uptake rates of [$1-^{14}$ C]-acetic acid, pH 6.0, in the absence (■) and in the presence (△, ▽) of non-labelled propionic acid 1 and 5 mM, respectively. The cells were grown in glucose urea and collected at the polarity maintenance stage (3-4h). Each data point represents the mean \pm SD (n=6).

In summary, our results collectively show that AcpA can be considered an acetate-propionate/ H^+ symporter. Furthermore, these results confirm that AcpA is a true

orthologue of the homologous *S. cerevisiae* Ady2 permease, which has been shown to be an acetate-propionate-formate/H⁺ symporter (Casal *et al.*, 1996; Paiva *et al.*, 2004).

AcpA is not involved in ammonium export

Ady2, the *S. cerevisiae* orthologue of AcpA, has been reported as being involved not only in acetate uptake (Paiva *et al.*, 2004), but also in ammonium export (Palková *et al.*, 2002), so we wondered about the putative role of AcpA in ammonia transport. The addition of ammonia to the reaction mixture promoted an increase in acetate uptake activity up to 200 % of acetate uptake activity with the addition of 100 mM of ammonia (Figure 13).

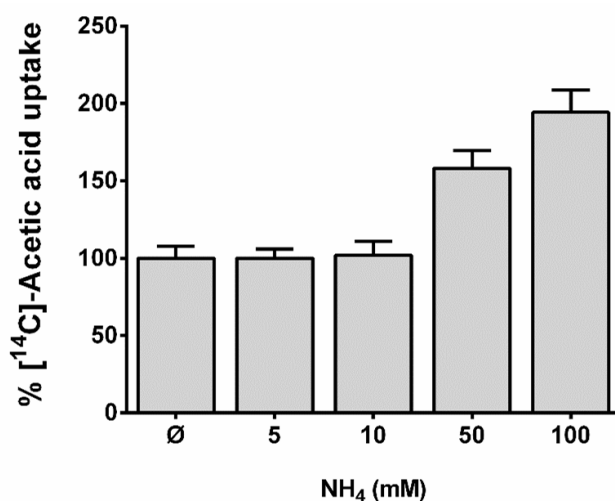


Figure 13 – Relative transport of labelled acetate (30 μM) in the presence of unlabelled ammonium tartrate at the concentrations indicated in the graph (5-100 mM). The graphic represents the percentage of acetic acid uptake of *A. nidulans acpA*⁺ considering that the uptake in the absence of ammonia was 100 %.

Furthermore, acetate transport kinetics was assessed in the presence of ammonia (50 mM) revealing no alterations in substrate affinity (K_m) for acetate, but rather an increase in the maximal apparent capacity of uptake (results not shown). To further understand the effect of ammonium on AcpA activity, we investigated whether cytoplasmically accumulated ammonia also elicits an increase in AcpA-mediated acetate transport. No differences of AcpA-mediated acetate uptake activity were recorded upon pre-loading with ammonia for 5 minutes (Figure 14), suggesting that there is no substrate acetate exchange with ammonia. These results suggest that AcpA does not seem to act as a NH₄⁺ exporter, at least in the conditions tested. How could thus the stimulating effect of external

ammonium on AcpA be explained? Given that this phenomenon is immediate (1-5 min), we should exclude any effect of ammonium on protein steady state levels or post-translational modification of AcpA. We rather favour the hypothesis that ammonium might chemically affect the protonation state of AcpA. It should be stressed, that even for Ady2, no direct evidence was found for ammonium efflux, which has been speculated on the basis of increased expression of the gene in the presence of ammonium and a correlation between ammonia production and Ady2 activity (Strachotová *et al.*, 2012).

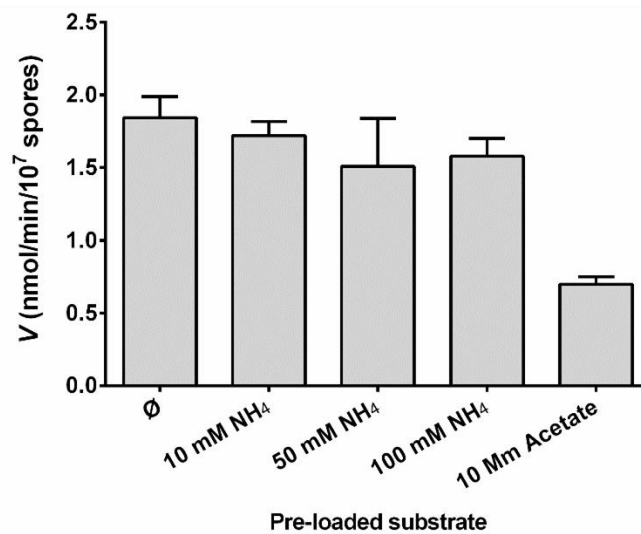


Figure 14 - Evaluation of the uptake of labelled acetate (30 μ M final concentration) in *A. nidulans* *acpA*⁺ after pre-loading with ammonium tartrate (NH₄) or acetate for 5 minutes as described in the experimental procedures.

Previous studies have shown that cells expressing the *ATO* genes (including Ady2) are more resistant to the toxic effect of methyl-ammonium (Palková *et al.*, 2002). This was another piece of indirect evidence for Ady2 involvement in ammonium/methyl-ammonium efflux. To test whether this is also the case in AcpA, cells were grown on minimal media in the presence of methyl-ammonium (Figure 15). No difference in toxicity induced by methyl ammonium was observed in the *acpA* Δ strain (Figure 15).

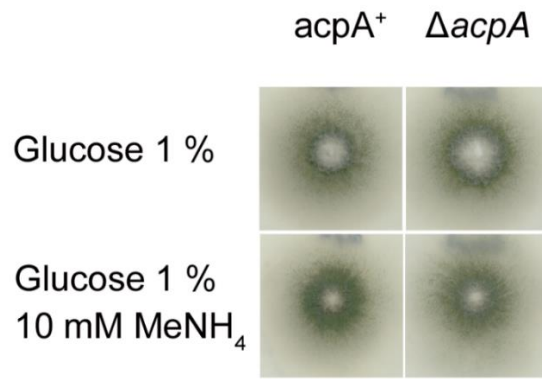


Figure 15– Growth test of *acpA*⁺ and *acpA*Δ on minimal media supplemented with urea as the nitrogen source and glucose 1 % (w/v) as the carbon source (buffered at pH 6.8). Methyl-ammonium hydrochloride was added to this media to a final concentration of 10 mM. Strains were grown for 3 days at 37 °C.

To further verify if the AcpA permease is involved in methyl ammonium efflux, experiments with labelled methyl-ammonium were performed as described in experimental procedures. No difference was observed in the amount of methyl ammonium in the supernatant or pellet (*A. nidulans* cells) between cultures of *acpA*⁺ or *acpA*Δ (Figure 16).

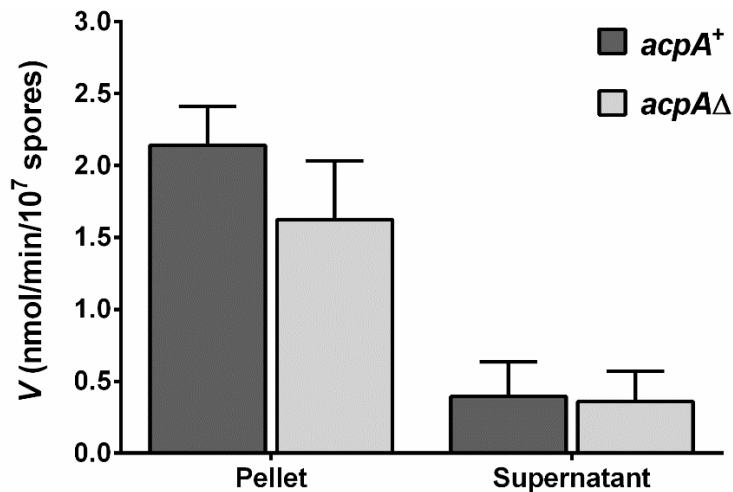


Figure 16 – Efflux assay of labelled methyl ammonium (20 μM). The graphic represents the initial uptake rates of [¹⁴C]-methyl ammonium measured in the pellet or supernatant of *acpA*⁺ or *acpA*Δ.

Although we couldn't assess this ammonium effect in a strain with no ammonium permeases (Monahan *et al.*, 2002; Monahan *et al.*, 2006), the absence of an effect in methyl ammonium efflux between the *acpA*⁺ and *acpA*Δ further suggests that this permease is not related to methyl ammonium, and probably ammonium, efflux.

Conclusions

In this work the transport activity of AcpA from *A. nidulans* was analysed in terms of specificity, regulation and putative role in ammonia export. It is demonstrated that this permease is not repressed or inactivated by carbon (glucose) or nitrogen (urea) sources, and is active from early germination stages reaching a peak of activity at a stage coincident with germ tube emergence and the onset of mycelium development. This is similar but not identical with the development expression profile of other solute transporters in *A. nidulans* (Amillis *et al.*, 2004). The main difference is that AcpA activity, unlike to what is described for other transporters (Amillis *et al.*, 2004), is already detected in resting conidiospores, suggesting a possible role in spore maintenance.

AcpA was shown to recognize and possibly transport, in addition to acetic acid, several monocarboxylic acids, such as propionic, formic or benzoic acid. These however are recognized with approximately 10- (propionate) to 100- (formate, benzoate, butyrate) fold lower affinities. At least in the case of propionate, we obtained evidence from growth tests that this acid is probably actively transported in *A. nidulans* cells (AcpA confers increased sensitivity to the toxicity of this substrate), and that it probably binds with acetate in a single substrate binding site. The observation that monocarboxylic acids, but not dicarboxylic acids, gain access to the binding site of AcpA suggests that the substrate binding site of this transporter is narrow and binds only small molecules with one carboxylate group. In the yeast *S. cerevisiae*, the Ady2 permease shares 50% identity and nearly identical specificity with AcpA, suggesting an architecturally similar binding site. On the other hand, the homologous bacterial transporter SatP from *E. coli* that shares 34% identity with AcpA, is characterised as an acetate-succinate transporter (Sá-Pessoa *et al.*, 2013). SatP accepts both mono- and dicarboxylic acids, and thus might have a slightly 'modified' substrate binding site in relation to its fungal homologues. However, we also obtained some indirect evidence that AcpA might also mediate low capacity uptake of dicarboxylic acids (a functional AcpA confers better growth on succinic and malic acids). In this case, we could not obtain any direct evidence for binding of these acids by AcpA in standard competition assays with radiolabeled acetic acid. This paradox suggests that dicarboxylic acids might indeed be recognized with low affinity by AcpA, but they follow a different trajectory for the translocation in the cells. Such cases of apparently paradoxical, non-Michaelis-Menten kinetics, have been recently reported for an MFS

mammalian glucose transporter (Jiang *et al.*, 2010) and the *A. nidulans* xanthine-uric acid transporter (Diallinas, 2013).

The similarity with the yeast Ady2 led us to investigate whether it also plays a role as a putative ammonium exporter, as hypothesised by Palková and co-workers (2002). We failed to obtain any rigorous conclusions on the AcpA-mediated ammonium efflux. Although there was a stimulation of AcpA-mediated acetate uptake activity in the presence of ammonia, growth tests and efflux assays suggest that this permease is not related to methyl ammonium, and probably ammonium, efflux. The observed results with ammonia could be caused by a decrease in the medium pH which could affect acetate uptake. We have shown that at pH 4.5 there is a decrease in the uptake of labelled acetate while no differences were observed at higher pH values (Figure 7). Uptake experiments with ammonia were performed at pH 6.8 and a drop on medium pH caused by ammonium tartrate to pH values around 4.5 would induce a reduction in maximum velocity. Instead, an increase in the velocity of acetate translocation was observed in the presence of ammonia and therefore a decrease in medium pH is unlikely. The observed difference in the velocity of acetate translocation in the presence of ammonia can also be due to changes in protonation of the permease which can induce structural transitions. An alteration in the charge of amino acid side chains can induce changes in protein conformation and function (Schönichen *et al.*, 2013).

Future perspectives

An insight on structure – homologues site-directed mutagenesis

The Acetate Uptake Transporter (AceTr) Family has three fully characterized members: Ady2, AcpA and SatP. Ady2 from *S. cerevisiae* is responsible for the uptake of acetate, propionate, formate and lactate (Casal *et al.*, 1996; Paiva *et al.*, 2004; Pacheco *et al.*, 2012); AcpA from *A. nidulans* is an acetate propionate transporter which can also recognize some dicarboxylates with very low affinities (Robellet *et al.*, 2008; this work), and SatP from *E. coli* is a succinate-acetate transporter (Sá-Pessoa *et al.*, 2013). Other members of this family have been linked to acetate utilization or sensitivity, namely MA4008 from *M. acetivorans* (Rohlin and Gunsalus, 2010) and Gpr1 from *Y. lipolytica* (Augstein *et al.*, 2003; Gentsch *et al.*, 2007). To elucidate the differences in substrate specificity among the AceTr family a rational mutagenesis approach was devised aiming at understanding the potential differences in structure responsible for substrate binding. This work is currently ongoing and only the strategy is presented here.

Fasta sequences from the characterized members of the AceTr family as well as putative fungal and bacterial homologues were obtained running a protein blast at <http://blast.ncbi.nlm.nih.gov/Blast.cgi> using SatP from *E. coli* MG1655 (NP_414551.1) as the starting sequence. A multiple protein alignment was created using the online tool Muscle at <http://www.ebi.ac.uk/Tools/msa/muscle/>. The evolutionary history was inferred by using the Maximum Likelihood method using the software MEGA5 v5.2 (Tamura *et al.*, 2011). The phylogenetic tree was then processed using FigTree v1.4.0 (<http://tree.bio.ed.ac.uk/>) and is presented in Figure 17.

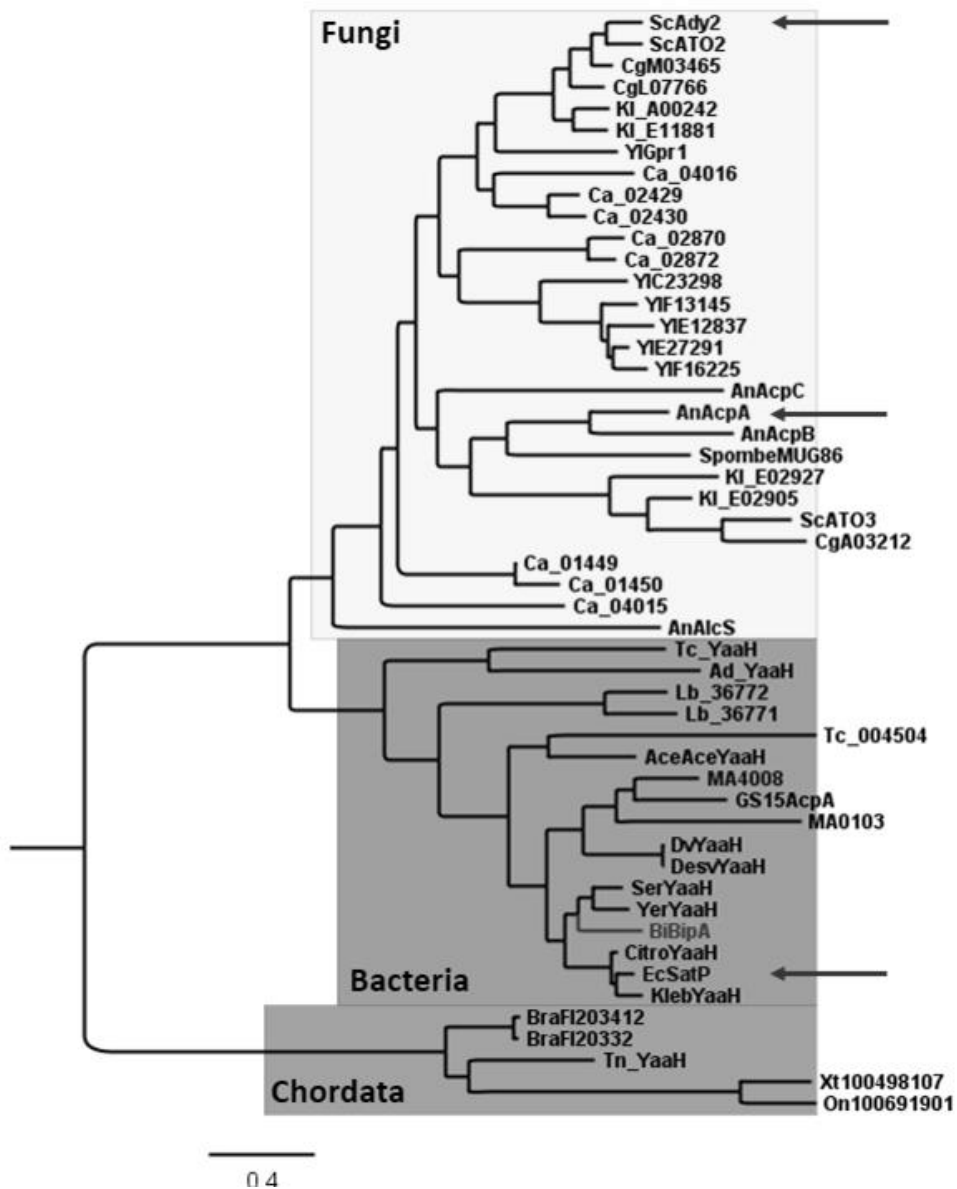


Figure 17 – Molecular Phylogenetic analysis by Maximum Likelihood method of the AceTr family. The evolutionary history was inferred by using the Maximum Likelihood method based on the JTT matrix-based model. The tree with the highest log likelihood (-23992,7299) is shown. Initial tree(s) for the heuristic search were obtained automatically by applying Neighbor-Join and BioNJ algorithms to a matrix of pairwise distances estimated using a JTT model, and then selecting the topology with superior log likelihood value. The tree is drawn to scale, with branch lengths measured in the number of substitutions per site. The analysis involved 51 amino acid sequences. There were a total of 1350 positions in the final dataset. Evolutionary analyses were conducted in MEGA5. The characterized members of the AceTr family are marked with an arrow.

The sequences analyzed were (Uniprot references): UPI00022CAD94, A4H3K7, A4H3K6, K4E2M4, K4E1L7, S9WC76, C3Z2T8, C3Z2T2, UPI0001DE783A, Q4SJU2, UPI00022B080D, Q4SJU2, Q460G9, Q5BC91, Q5BC91, B1N947, O14201, Q12359, P32907, P0AC98, Q8TUG4, Q8TIY1, Q39WL0, Q727R6, Q59LN3, HIUP63, A6T4F1, G0C2T6, F4N529, Q727R6, G9SEB0, C4YNT7, C4YNI7, C4YPM8, C4YJK0, C4YJK1, C4YPM9, C4YNT9, C4YNI8, Q6CYH9, Q6CPR3, Q6CNK2, Q6CPR2, Q6FYA8, Q6FKX9, Q6FJU7, Q6C635, Q6CAY7, P41943, Q6C4F1, Q6C1H3, Q6C1V3.

To analyse the conserved residues in the AceTr family, 15 members from bacteria, archaea and fungi were chosen and a multiple alignment was performed using Multalin (<http://multalin.toulouse.inra.fr/multalin/>). The conserved residues, including those in the AceTr family motif (N-P-[AV]-P-[LF]-G-L-x-[GSA]-F) were mutagenized for an alanine or an isofunctional or isostructural aminoacid when appropriate. These mutations will be introduced in the yeast *ADY2* gene cloned in a centromeric plasmid under the control of the *GPD* promoter (p416-GPD). The plasmids harbouring the desired mutations will be transformed in a strain with no monocarboxylic acid transport activity following a strategy devised previously for the analysis of the lactate transporter Jen1p (Soares-Silva *et al.*, 2007).

To elucidate the residues involved in defining the specificity of this transporter, a sequence alignment was carried out with *Ady2*, *AcpA* and *SatP*, members of AceTr with a characterized activity (Figure 18). Since the specificity in the bacterial member is partially different from the one found in fungi, the amino acids that are different in *E. coli* were taken into account. There are 52 such amino acids in *SatP* (*YaaH*). Among these 52, those that display a substitution involving a charged aminoacid residue were chosen for mutagenesis. These mutations will be introduced in the *yaaH* gene cloned in a high-copy plasmid (pUC18). Plasmids harbouring confirmed mutations will be transformed in a strain with no acetate transporters (Sá-Pessoa *et al.*, 2013).

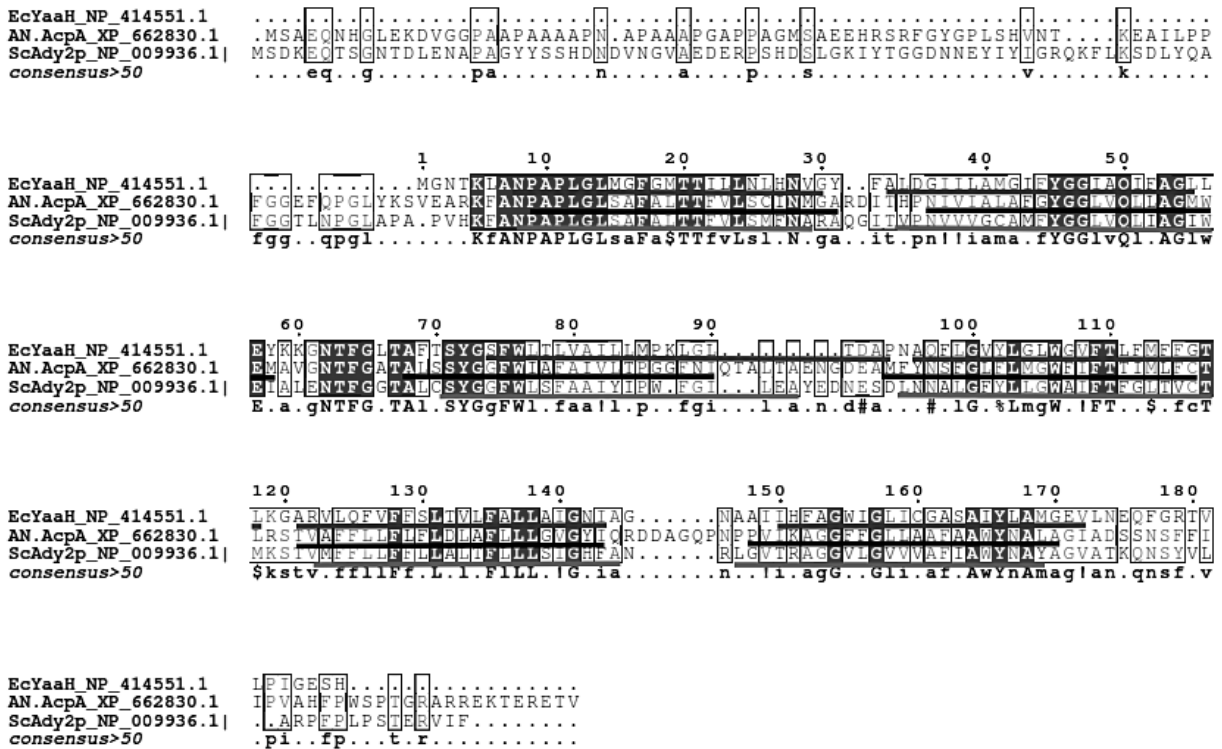


Figure 18 – Multiple sequence alignment of AceTr family members of characterized function. The protein alignment was performed using the online tool Multalin.

References

- Amillis, S., Cecchetto, G., Sophianopoulou, V., Koukaki, M., Scazzocchio, C., Diallinas, G. (2004) Transcription of purine transporter genes is activated during the isotropic growth phase of *Aspergillus nidulans* conidia. *Mol Microbiol* **52**: 205–16
- Armitt, S., McCullough, W., Roberts, C.F. (1976) Analysis of acetate non-utilizing (*acu*) mutants in *Aspergillus nidulans*. *J Gen Microbiol* **92**: 263–82
- Augstein, A., Barth, K., Gentsch, M., Kohlwein, S.D., Barth, G. (2003) Characterization, localization and functional analysis of Gpr1p, a protein affecting sensitivity to acetic acid in the yeast *Yarrowia lipolytica*. *Microbiology* **149**: 589–600
- Brock, M., Buckel, W. (2004) On the mechanism of action of the antifungal agent propionate. *Eur J Biochem* **271**: 3227–41
- Casal, M., Cardoso, H., Leão, C. (1996) Mechanisms regulating the transport of acetic acid in *Saccharomyces cerevisiae*. *Microbiology* **142** (Pt 6: 1385–90
- Casselton, L., Zolan, M. (2002) The art and design of genetic screens: filamentous fungi. *Nat Rev Genet* **3**: 683–97

- Cove, D.J. (1966) The induction and repression of nitrate reductase in the fungus *Aspergillus nidulans*. *Biochim Biophys Acta - Enzymol Biol Oxid* **113**: 51–56
- Diallinas, G. (2013) Allopurinol and xanthine use different translocation mechanisms and trajectories in the fungal UapA transporter. *Biochimie* **95**: 1755–64
- Fillinger, S., Felenbok, B. (1996) A newly identified gene cluster in *Aspergillus nidulans* comprises five novel genes localized in the alc region that are controlled both by the specific transactivator AlcR and the general carbon-catabolite repressor CreA. *Mol Microbiol* **20**: 475–88
- Flippi, M., Robellet, X., Dequier, E., Leschelle, X., Felenbok, B., Vélot, C. (2006) Functional analysis of *alcS*, a gene of the *alc* cluster in *Aspergillus nidulans*. *Fungal Genet Biol* **43**: 247–60
- Flippi, M., Sun, J., Robellet, X., Karaffa, L., Fekete, E., Zeng, A.-P., Kubicek, C.P. (2009) Biodiversity and evolution of primary carbon metabolism in *Aspergillus nidulans* and other *Aspergillus* spp. *Fungal Genet Biol* **46**: S19–S44
- Gentsch, M., Kuschel, M., Schlegel, S., Barth, G. (2007) Mutations at different sites in members of the Gpr1/Fun34/YaaH protein family cause hypersensitivity to acetic acid in *Saccharomyces cerevisiae* as well as in *Yarrowia lipolytica*. *FEMS Yeast Res* **7**: 380–90
- Georgakopoulos, P., Lockington, R. a, Kelly, J.M. (2012) SAGA complex components and acetate repression in *Aspergillus nidulans*. *G3 (Bethesda)* **2**: 1357–67
- Gournas, C., Amillis, S., Vlanti, A., Diallinas, G. (2010) Transport-dependent endocytosis and turnover of a uric acid-xanthine permease. *Mol Microbiol* **75**: 246–60
- Haguenauer-Tsapis, R., André, B. (2004) Membrane trafficking of yeast transporters: mechanisms and physiological control of downregulation. In *Molecular Mechanisms Controlling Transmembrane Transport SE* - 28. Springer Berlin Heidelberg, pp 273–323.
- Hicke, L., Dunn, R. (2003) Regulation of membrane protein transport by ubiquitin and ubiquitin-binding proteins. *Annu Rev Cell Dev Biol* **19**: 141–72
- Hynes, M.J., Murray, S.L., Andrianopoulos, A., Davis, M. a (2011) Role of carnitine acetyltransferases in acetyl coenzyme A metabolism in *Aspergillus nidulans*. *Eukaryot Cell* **10**: 547–55
- Hynes, M.J., Murray, S.L., Duncan, A., Khew, G.S., Davis, M.A. (2006) Regulatory genes controlling fatty acid catabolism and peroxisomal functions in the filamentous fungus *Aspergillus nidulans*. *Eukaryot Cell* **5**: 794–805
- Jiang, X., McDermott, J.R., Ajees, A.A., Rosen, B.P., Liu, Z. (2010) Trivalent arsenicals and glucose use different translocation pathways in mammalian *GLUT1*. *Metallomics* **2**: 211–9
- Monahan, B.J., Askin, M.C., Hynes, M.J., Davis, M.A. (2006) Differential expression of *Aspergillus nidulans* ammonium permease genes is regulated by GATA transcription factor AreA. *Eukaryot Cell* **5**: 226–37

- Monahan, B.J., Fraser, J.A., Hynes, M.J., Davis, M.A. (2002) Isolation and Characterization of Two Ammonium Permease Genes, *meaA* and *mepA*, from *Aspergillus nidulans*. *Eukaryot Cell* **1**: 85–94
- Pacheco, A., Talaia, G., Sá-Pessoa, J., Bessa, D., Gonçalves, M.J., Moreira, R., Paiva, S., Casal, M., Queirós, O. (2012) Lactic acid production in *Saccharomyces cerevisiae* is modulated by expression of the monocarboxylate transporters Jen1 and Ady2. *FEMS Yeast Res* **12**: 375–81
- Paiva, S., Devaux, F., Barbosa, S., Jacq, C., Casal, M. (2004) Ady2p is essential for the acetate permease activity in the yeast *Saccharomyces cerevisiae*. *Yeast* **21**: 201–10
- Palková, Z., Devaux, F., Icíková, M., Mináriková, L., Crom, S. Le, Jacq, C. (2002) Ammonia pulses and metabolic oscillations guide yeast colony development. *Mol Biol Cell* **13**: 3901–14
- Robellet, X., Flippi, M., Pégot, S., Maccabe, A.P., Vélot, C. (2008) AcpA, a member of the GPR1/FUN34/YaaH membrane protein family, is essential for acetate permease activity in the hyphal fungus *Aspergillus nidulans*. *Biochem J* **412**: 485–93
- Roberts, S.K., Milnes, J., Caddick, M. (2011) Characterisation of *AnBEST1*, a functional anion channel in the plasma membrane of the filamentous fungus, *Aspergillus nidulans*. *Fungal Genet Biol* **48**: 928–38
- Rohlin, L., Gunsalus, R.P. (2010) Carbon-dependent control of electron transfer and central carbon pathway genes for methane biosynthesis in the Archaeon, *Methanosarcina acetivorans* strain C2A. *BMC Microbiol* **10**: 62
- Sá-Pessoa, J., Paiva, S., Ribas, D., Silva, I.J., Viegas, S.C., Arraiano, C.M., Casal, M. (2013) SatP (YaaH), a succinate-acetate transporter protein in *Escherichia coli*. *Biochem J* **454**: 585–95
- Scazzocchio, C. (2009) *Aspergillus*: a multifaceted genus. In Schaechter M, editor(s). *Encyclopedia of Microbiology*. Amsterdam: Elsevier. Academic Press, Oxford. pp 401–421.
- Schönichen, A., Webb, B. a, Jacobson, M.P., Barber, D.L. (2013) Considering protonation as a posttranslational modification regulating protein structure and function. *Annu Rev Biophys* **42**: 289–314
- Semighini, C.P., Goldman, M.H.S., Goldman, G.H. (2004) Multi-copy suppression of an *Aspergillus nidulans* mutant sensitive to camptothecin by a putative monocarboxylate transporter. *Curr Microbiol* **49**: 229–33
- Soares-Silva, I., Paiva, S., Diallinas, G., Casal, M. (2007) The conserved sequence NXX[S/T]HX[S/T]QDXXXT of the lactate/pyruvate:H(+) symporter subfamily defines the function of the substrate translocation pathway. *Mol Membr Biol* **24**: 464–74
- Soares-Silva, I., Sá-Pessoa, J., Myrianthopoulos, V., Mikros, E., Casal, M., Diallinas, G. (2011) A substrate translocation trajectory in a cytoplasm-facing topological model of the monocarboxylate/H⁺ symporter Jen1p. *Mol Microbiol* **81**: 805–17

- Strachotová, D., Holoubek, A., Kučerová, H., Benda, A., Humpolíčková, J., Váchová, L., Palková, Z. (2012) Ato protein interactions in yeast plasma membrane revealed by fluorescence lifetime imaging (FLIM). *Biochim Biophys Acta* **1818**: 2126–34
- Tamura, K., Peterson, D., Peterson, N., Stecher, G., Nei, M., Kumar, S. (2011) MEGA5: molecular evolutionary genetics analysis using maximum likelihood, evolutionary distance, and maximum parsimony methods. *Mol Biol Evol* **28**: 2731–9
- Tazebay, U.H., Sophianopoulou, V., Scazzocchio, C., Diallinas, G. (1997) The gene encoding the major proline transporter of *Aspergillus nidulans* is upregulated during conidiospore germination and in response to proline induction and amino acid starvation. *Mol Microbiol* **24**: 105–17
- Todd, R.B., Andrianopoulos, a, Davis, M. a, Hynes, M.J. (1998) FacB, the *Aspergillus nidulans* activator of acetate utilization genes, binds dissimilar DNA sequences. *EMBO J* **17**: 2042–54
- Váchová, L., Chernyavskiy, O., Strachotová, D., Bianchini, P., Burdíková, Z., Fercíková, I., Kubínová, L., Palková, Z. (2009) Architecture of developing multicellular yeast colony: spatio-temporal expression of Ato1p ammonium exporter. *Environ Microbiol* **11**: 1866–77

Chapter VI

Final remarks and Future perspectives

Final Remarks

This thesis focused on structural-functional analysis of several carboxylate transporters. Carboxylic acids comprise a diverse group of organic compounds participating in several cellular processes and being key actors in overall cell functionality. The transport of monocarboxylates, such as lactate, pyruvate and acetate, is essential for the metabolism and homeostasis of most cells. In *Saccharomyces cerevisiae* two monocarboxylate-proton symporters have been found, one encoded by the *JEN1* gene and another by the *ADY2* gene. The main objective of the work presented in this thesis was to deepen the current knowledge on yeast carboxylate transport through structural-functional approaches.

Jen1p is a yeast lactate-pyruvate-acetate-propionate/proton symporter induced in pyruvic and lactic acid grown cells (Cássio *et al.*, 1987; Casal *et al.*, 1999). This permease also transports the micronutrient selenite (McDermott *et al.*, 2010). Structure–function relationships in Jen1p revealed that the conserved sequence ³⁷⁹NXX[S/T]HX[S/T]QDXXXT³⁹¹ in TMS-VII is part of the substrate translocation pathway of Jen1p (Soares-Silva *et al.*, 2007). In chapter II of the present work we have identified novel residues critical for the function and specificity of Jen1p (Soares-Silva *et al.*, 2011). The identification of the residues involved in specificity was obtained by two approaches: those that are shown by crystallographic and functional studies to be involved in substrate recognition in LacY and GlpT; and those that by primary amino acid sequence alignments are conserved in monocarboxylate transporters but replaced by another conserved residue in dicarboxylate transporters of the Jen2p subfamily (Casal *et al.*, 2008). These residues were substituted by isofunctional or isostructural aminoacids or by alanine. In the resulting mutants obtained, Jen1p function and specificity was accessed through growth in several mono- and dicarboxylic acids as sole carbon source as well as by lactate uptake assays. Furthermore in relevant mutants a full kinetic analysis was performed (K_m and V_{max} as well as inhibition assays). For the mutants with loss of lactate uptake activity a GFP-tagged version of the protein was generated and the localization of the protein was accessed by epifluorescence microscopy. Furthermore, a 3D model of this permease was built on the basis of its structural similarity with the GlpT permease, an antiporter of glycerol-3-phosphate/inorganic phosphate (Huang *et al.*, 2003), which by substrate docking approaches revealed a ‘sliding’ trajectory of the substrate through

critical nodal points along the substrate pore, with the polar residues genetically identified as important for function facing the pore.

Ady2p is an acetate-propionate-formate/proton symporter (Casal *et al.*, 1996; Paiva *et al.*, 2004). Ady2p plays an important role in the uptake of acetate, since its disruption abolishes the active transport of acetate (Paiva *et al.*, 2004). This gene was also described as being involved in ammonia production in *S. cerevisiae* colonies (Palková *et al.*, 2002; Váchová *et al.*, 2009). In the work described in chapter III a detailed physiological characterization of Ady2p was undertaken showing an additional role of this permease in lactate uptake. The specificity of Ady2p was also tested for a wide range of compounds, and the data obtained corroborate the role of Ady2p as a monocarboxylate transporter. The importance of these monocarboxylate transporters (Jen1 and Ady2) for the production of lactic acid on a metabolically engineered *S. cerevisiae* strain was explored (Pacheco *et al.*, 2012). *S. cerevisiae* strains constitutively expressing *LDH* gene and *JEN1* or *ADY2* genes have a higher outer lactic acid concentration, when glucose is present in the medium (Pacheco *et al.*, 2012). However, when glucose is exhausted, their consumption and uptake is more pronounced, which demonstrates that monocarboxylates permeases expression modulates lactic acid production (Pacheco *et al.*, 2012).

Ady2 is a member of the AceTr family of acetate transporters. Under the scope of this work the *Escherichia coli* member of this family, YaaH, has been described and characterized in chapter IV (Sá-Pessoa *et al.*, 2013). The *yaaH* gene as well as the gene coding for the previously described acetate transporter, *actP* (Gimenez *et al.*, 2003) were deleted in *E. coli* and the corresponding single and double mutants were evaluated for acetate uptake activity in glucose grown cells. The mutant $\Delta yaaH \Delta actP$ was used to express *yaaH* in a low and a high copy plasmid and a full kinetic profile was determined for the uptake of acetic and succinic acids by YaaH. Energetics and specificity were also accessed by uptake experiments. The physiological role of the two acetate transporters was accessed when cells were aerobically grown in glucose by following both uptake, glucose consumption, acetate formation and expression by RT-PCR. The characterization of this protein as an acetate succinate transporter performed in the scope of this thesis led to its renaming as SatP (succinate-acetate transporter protein). This work also demonstrated that SatP and Ady2 share common molecular traits regarding the substrate binding site since two specific aminoacid mutations (Leu219Val and Ala252Gly), known to promote a change in substrate specificity allowing an efficient utilization of lactic acid

in the yeast *Ady2* transporter (Kok *et al.*, 2012), fulfil the same role in *SatP* being crucial for the enhanced ability to transport lactate (Sá-Pessoa *et al.*, 2013).

AcpA, an *AceTr* member from the filamentous fungus *Aspergillus nidulans* (Robellet *et al.*, 2008) has been analysed in chapter V. This permease is expressed from the onset of spore germination being most active in the isotropic growth stage of germination and no carbon or nitrogen repression was reported. An inhibition profile was performed using non-labelled mono- and dicarboxylic acids showing inhibition by the short-chain monocarboxylic acids propionate, benzoate, formate and butyrate from which propionate was shown to be a competitive inhibitor of acetate and a substrate of this permease. The similarities with the yeast *Ady2* led us to inquire the putative role of *AcpA* as an ammonium exporter. Transport kinetic measurements and growth tests showed that although ammonia increases the acetate uptake activity of this permease, no exchange takes place, and *AcpA* is not involved in ammonia export as hypothesised for its *S. cerevisiae* homologue.

Future perspectives

In the scope of this thesis the studies performed on members of the AceTr family of transporters deepened the knowledge on acetate transport in yeast and bacteria. Despite the insights accomplished in this work other questions remain a subject of further studies. Although the knowledge on the structure of membrane proteins has increased dramatically in the last few years, still only 424 unique membrane protein structures have their structure resolved by crystallography or NMR to a resolution of less than 4-4.5 Å (<http://blanco.biomol.uci.edu/mpstruc/>). Bottlenecks in membrane protein structure determination include their low natural abundance requiring overexpression usually in heterologous systems, their hydrophobic nature that presents a barrier to its purification in a stable form and their inherent flexibility poses a problem to stability of the crystal structure as well as the appearance of artefacts in structure determination. Research in the past years has focused on developing and implementing new technologies to solve the bottlenecks in the determination of membrane protein structure with some degree of success (Bill *et al.*, 2011).

The AceTr family members are composed of 6 transmembrane span domains and no model is available for this topology as predicted by online tools. During the work presented in this thesis a prokaryotic member of this family, the *E. coli* SatP permease, was characterized and preliminary studies show high level of expression allowing to pursue for protein crystallization trials. For the production and purification of prokaryotic proteins, relatively efficient protocols are already available and the bacterial members of the AceTr family may prove stable enough to obtain a crystal structure.

The scarcity of membrane transporters structures poses a problem to the understanding of their molecular mechanisms of action and the homology modelling approach here utilized in chapter II is a good approach to obtain structural information on transporters without a crystal structure. As a first approach to the structure determinants of the members of the AceTr family a mutagenesis approach based on a holistic strategy through the study of the fungal and bacterial characterized proteins has been devised. This approach is described in the end of chapter V as future perspectives. By aligning different members of the AceTr family, conserved amino acid residues and domains, which might be structural determinants, can be identified. Proteins exhibit functional promiscuity, facilitating the divergence of new functions within existing folds. In the case of this family

of transporters different specificity profiles have been determined. The existence of these different specificity profiles among the bacterial and fungal members characterized in this thesis will enable the identification of additional residues/domains responsible for substrate recognition in this family, in a similar way to what was performed for Jen1p in this thesis and in previous work (Soares-Silva *et al.*, 2007; Soares-Silva *et al.*, 2011), accessing molecular events essential for the evolution of substrate specificity within the AceTr family.

Carboxylic acids have been used for many years in industrial settings and the demand for clean industrial alternatives leads more and more to production using microbial factories. In this work the role of carboxylate permeases as modulators of the export of carboxylic acids was investigated in *S. cerevisiae*. The yields obtained were relatively low although they are an improvement of previous reported lactic acid yields. The characterization of carboxylic acid transporters from the AceTr family in other microorganisms constitutes a first step in their use as potential modulators of acid export by expressing them in metabolically engineered *S. cerevisiae*, *E. coli* or *Aspergillus* strains. Furthermore, future mutagenesis studies can prove invaluable for enhancing secretion of carboxylic acid by improving the transporters catalytic activity or by modification of substrate specificity, yielding a plethora of possible functions to be explored in biotechnology.

References

- Bill, R.M., Henderson, P.J.F., Iwata, S., Kunji, E.R.S., Michel, H., Neutze, R., *et al.* (2011) Overcoming barriers to membrane protein structure determination. *Nat Biotechnol* **29**: 335–40
- Casal, M., Cardoso, H., and Leão, C. (1996) Mechanisms regulating the transport of acetic acid in *Saccharomyces cerevisiae*. *Microbiology* **142** (Pt 6: 1385–90
- Casal, M., Paiva, S., Andrade, R.P., Gancedo, C., and Leão, C. (1999) The lactate-proton symport of *Saccharomyces cerevisiae* is encoded by *JEN1*. *J Bacteriol* **181**: 2620–3
- Casal, M., Paiva, S., Queirós, O., and Soares-Silva, I. (2008) Transport of carboxylic acids in yeasts. *FEMS Microbiol Rev* **32**: 974–94
- Cássio, F., Leão, C., and Uden, N. van (1987) Transport of lactate and other short-chain monocarboxylates in the yeast *Saccharomyces cerevisiae*. *Appl Environ Microbiol* **53**: 509–13
- Gimenez, R., Nuñez, M.F., Badia, J., Aguilar, J., and Baldoma, L. (2003) The gene *yjcG*, cotranscribed with the gene *acs*, encodes an acetate permease in *Escherichia coli*. *J Bacteriol* **185**: 6448–55
- Huang, Y., Lemieux, M.J., Song, J., Auer, M., and Wang, D.-N. (2003) Structure and mechanism of the glycerol-3-phosphate transporter from *Escherichia coli*. *Science* **301**: 616–20
- Kok, S., Nijkamp, J.F., Oud, B., Roque, F.C., Ridder, D., Daran, J.-M., *et al.* (2012) Laboratory evolution of new lactate transporter genes in a *jen1Δ* mutant of *Saccharomyces cerevisiae* and their identification as *ADY2* alleles by whole-genome resequencing and transcriptome analysis. *FEMS Yeast Res* **12**: 359–374
- McDermott, J.R., Rosen, B.P., and Liu, Z. (2010) *Jen1p*: a high affinity selenite transporter in yeast. *Mol Biol Cell* **21**: 3934–41
- Pacheco, A., Talaia, G., Sá-Pessoa, J., Bessa, D., Gonçalves, M.J., Moreira, R., *et al.* (2012) Lactic acid production in *Saccharomyces cerevisiae* is modulated by expression of the monocarboxylate transporters *Jen1* and *Ady2*. *FEMS Yeast Res* **12**: 375–81
- Paiva, S., Devaux, F., Barbosa, S., Jacq, C., and Casal, M. (2004) *Ady2p* is essential for the acetate permease activity in the yeast *Saccharomyces cerevisiae*. *Yeast* **21**: 201–10
- Palková, Z., Devaux, F., Icíková, M., Mináriková, L., Crom, S. Le, and Jacq, C. (2002) Ammonia pulses and metabolic oscillations guide yeast colony development. *Mol Biol Cell* **13**: 3901–14
- Robellet, X., Flipphi, M., Pégot, S., Maccabe, A.P., and Vélot, C. (2008) *AcpA*, a member of the GPR1/FUN34/YaaH membrane protein family, is essential for acetate permease activity in the hyphal fungus *Aspergillus nidulans*. *Biochem J* **412**: 485–93

- Sá-Pessoa, J., Paiva, S., Ribas, D., Silva, I.J., Viegas, S.C., Arraiano, C.M., and Casal, M. (2013) SatP (YaaH), a succinate-acetate transporter protein in *Escherichia coli*. *Biochem J* **454**: 585–95
- Soares-Silva, I., Paiva, S., Dhalluin, G., and Casal, M. (2007) The conserved sequence NXX[S/T]HX[S/T]QDXXXT of the lactate/pyruvate:H(+) symporter subfamily defines the function of the substrate translocation pathway. *Mol Membr Biol* **24**: 464–74
- Soares-Silva, I., Sá-Pessoa, J., Myriantopoulos, V., Mikros, E., Casal, M., and Dhalluin, G. (2011) A substrate translocation trajectory in a cytoplasm-facing topological model of the monocarboxylate/H⁺ symporter Jen1p. *Mol Microbiol* **81**: 805–17
- Váchová, L., Chernyavskiy, O., Strachotová, D., Bianchini, P., Burdík, Z., Fercíková, I., *et al.* (2009) Architecture of developing multicellular yeast colony: spatio-temporal expression of Ato1p ammonium exporter. *Environ Microbiol* **11**: 1866–77